Temporal patterns of spiking activity in the hippocampal formation

A computational model to investigate "inheritance" of phase precession

D I S S E R T A T I O N

zur Erlangung des akademischen Grades

d o c t o r r e r u m n a t u r a l i u m
(Dr. rer. nat.)
im Fach Biologie

eingereicht an der
Lebenswissenschaftlichen Fakultät
Humboldt-Universität zu Berlin

von
M.Sc. Jorge Jaramillo

Präsident der Humboldt-Universität zu Berlin:
Prof. Dr. Jan-Hendrik Olbertz

Dekan der Lebenswissenschaftlichen Fakultät:
Prof. Dr. Richard Lucius

Gutachter:
1. Prof. Dr. Richard Kempter
2. Prof. Dr. Dietmar Schmitz
3. Dr. Matthijs van der Meer

eingereicht am: 17.10.2014
Tag der mündlichen Prüfung: 17.12.2014

Abstract

The process of faithfully retrieving episodes from our memory requires a neural mechanism capable of initially forming ordered and reliable behavioral sequences. These behavioral sequences take place on a timescale of seconds or more, whereas the timescale of neural plasticity and learning is in the order of tens of milliseconds. To shed light on this dilemma, we turn to studies of hippocampal place cells in rodents, i.e., cells that selectively increase their firing rates in locations of the environment known as the place fields. Within a field, the firing phases of a place cell precess monotonically relative to the ongoing theta rhythm. This phenomenon, termed "phase precession", leads to a temporally compressed representation of the behavioral sequences experienced by the rodent, and the compressed timescale matches the requirements of neural plasticity.

In this thesis, I study the mechanisms and functions of phase precession by proposing a framework that relies on the concept of inheritance: the simple idea that patterns of neural activity can be propagated from one region to another. Indeed, phase precession has been observed in several regions of the hippocampus and entorhinal cortex, and an important open question is whether phase precession emerges independently in each region, or conversely, whether phase precession can be "inherited" from an upstream neuronal population. The inheritance framework consists of analyzing the spiking activity of cells in feed-forward topologies, where a set of input cells project and convey excitatory input to a target cell.

First, I study the possibility that CA1 cells in the hippocampus inherit their phase precession from CA3 cells. I find that this simple hypothesis can explain the sub and suprathreshold dynamics of CA1 cells (Harvey et al., 2009; Mizuseki et al., 2012). Furthermore, I elucidate roles for excitation and inhibition in determining a CA1 place cell's response. In particular, I interpret the results of a recent experiment where interneurons from the CA1 region in the hippocampus were silenced using optogenetics (Royer et al., 2012).

An issue closely related to phase-precession inheritance, is that of place-field inheritance. Thus, I study in a computational model how place-selectivity can naturally arise in CA1 cells if CA3 inputs have distributed spatial tuning and CA3-CA1 synapses are endowed with spike-timing-dependent plasticity. I examine the conditions that allow for place-field formation in CA1 cells even if the initial distribution of CA3-CA1 synaptic weights is random. The model predicts that theta modulation and phase precession of the input CA3 cells favor the inheritance process, i.e., the time for structure formation in a CA1 cell is reduced compared to the case of no input modulation.

Next, I develop the inheritance framework further and show how the simple feed-forward topologies in the hippocampal formation assist in propagating phase precession to different regions of the hippocampus and adjacent structures. I explain how the place-selective responses of a given cell are influenced by the spatial distribution of place-field centers at the input. The inheritance framework can account for, for example, the little incidence of phase precession in interneurons (Skaggs et al., 1996), the characteristic shape of phase precession for ramp cells in the ventral striatum (van der Meer and Redish, 2011), and phase-precessing place cells that receive input from phase-precessing grid cells (Hafting et al., 2008). These results suggest that the presence of phase precession in different stages of the hippocampal circuit and other regions of the brain is indicative of a common source, a fact that can help us better understand the temporal spiking patterns in the brain.

Finally, I critically review the current evidence for a behavioral role for phase precession and suggest a roadmap for future research in this field.

Keywords: Hippocampal formation, phase precession, theta oscillations, inheritance, plasticity.

Zusammenfassung

Um eine Folge von Ereignissen aus unserem Gedächtnis abzurufen, ist zunächst ein Mechanismus erforderlich, der geordnete Sequenzen abspeichert. Hierbei stehen wir vor dem Problem, dass Ereignisse in unserem Leben auf einer Zeitskala von Sekunden oder mehr stattfinden. Auf der anderen Seite basiert das Lernen von Sequenzen auf der Plastizität von Synapsen im Gehirn, die durch die Abfolge von Aktionspotentialen von Nervenzellen im Millisekunden-Bereich gesteuert wird. Um dieses zeitliche Problem zu lösen, betrachten wir den Hippocampus, eine Struktur im Gehirn von Vertebraten, die für das explizite Gedächtnis (Fakten, Ereignisse, Sequenzen) entscheidende Bedeutung hat. In Nagetieren ist der Hippocampus sehr gut untersucht. Dort wurden Neurone gefunden, die nur dann aktiv sind, wenn das Tier innerhalb einer bestimmten Region seiner Umgebung ist: im sogenannten "Ortsfeld" des entsprechenden Neurons. Während der Bewegung durch ein Ortsfeld verschiebt sich die Phase der Nervenimpulse zu immer früheren Phasen der EEG-Oszillation. Dieses Phänomen wird als "Phasenpräzession" bezeichnet. Theoretische und experimentelle Untersuchungen zeigen, dass Phasenpräzession eine Lösung für unser Dilemma bietet: es führt zu einer zeitlich komprimierten Darstellung der Sequenz von Orten.

In der vorliegenden Arbeit untersuche ich den Mechanismus und die Funktion von Phasenpräzession im Hinblick auf die Ausbreitung neuronaler Aktivität von einer Hirnregion zu einer anderen. Phasenpräzession konnte bereits in mehreren Regionen des Gehirns beobachtet werden. Bisher war unklar, ob Phasenpräzession in jeder dieser Regionen eigenständig entsteht, oder ob die Phasenpräzession von einer vorgeschalteten Population von Neuronen "vererbt" werden kann.

Zuerst prüfe ich die Möglichkeit ob CA1-Zellen im Hippocampus ihre Phasenpräzession von CA3-Zellen "erben". Diese Hypothese kann die unter- und überschwelligen Dynamik der CA1-Zellen erklären. Darüberhinaus erläutere ich wie Exzitation und Inhibition die Aktivität einer Ortzelle bestimmen. Insbesondere interpretiere ich die Ergebnisse eines Experiments, bei dem Interneurone aus der CA1-Region des Hippocampus durch optogenetische Methoden ausgeschaltet wurden.

In engem Zusammenhang mit der Vererbung von Phasenpräzession steht die Vererbung von Ortsfeldern. Deswegen analysiere ich in einem theoretischen Modell, wie Orts-Selektivität in CA1-Zellen entstehen kann. Hierbei nehme ich an, dass die eingehenden Signale der CA3-Zellen eine räumliche Präferenz aufweisen und CA3-CA1 Synapsen einer "spike-timing-dependent plasticity"- einer besonderen Form von Plastizität- folgen. Ich untersuche die Bedingungen für die Bildung von Ortsfeldern in CA1-Zellen, auch wenn die Anfangsverteilung der synaptischen Gewichte von CA3-CA1 Verbindungen zufällig ist. Das Modell sagt voraus, dass die Theta-Modulation und Phasenpräzession der eingehenden Signale der CA3-Zellen den Vererbungsprozess begünstigen. Das bedeutet, dass in diesem Fall die Dauer für die Strukturbildung in einer CA1-Zelle kürzer ist als im Fall ohne Eingangsmodulations.

Danach zeige ich, wie "Feed-Forward" Verbindungen die Ausbreitung von Phasenpräzession in den verschiedenen Subregionen des Hippocampus und zu seinen angrenzenden Strukturen erlaubt. Das Modell erklärt damit eine Vielzahl von experimentellen Befunden. Die Ergebnisse deuten darauf hin, dass Phasenpräzession in den verschiedenen Regionen des Hippocampus auf einen gemeinsamen Ursprung zurück zuführen sein konnte. Dies würde es uns erleichtern, zeitliche Kodierung im Gehirn besser zu verstehen.

Schliesslich diskutiere ich auf Grundlage der aktuellen Literatur, ob Phasenpräzession das Verhalten beeinflusst und gebe einen Ausblick auf zukünftige Forschungsmöglichkeiten auf diesem Gebiet.

Schlagwörter: Hippocampus, Phasenpräzession, Theta-Oszillation, Plastizität.

Contents

1. Introduction

As we go about in our daily lives, our brain has the daunting task of making decisions in real time to adapt to the constantly changing features of the environment. Indeed, we are actively sensing, i.e., extracting information from, the environment to guide our behavior and maximize our possibilities of survival and reproduction. To this end, our brains have evolved the capacity to store memories: information from the past available at the present. The circuitry in our brain must somehow encode and store this information so that it's at our disposal at a later time. We are normally unaware of the connection between a dedicated brain circuitry and the formation of memories, unless we happen to study the hippocampus.

The hippocampus is a brain structure we share with all mammals. Perturbative and correlative techniques have been used to study the hippocampus and now we know, for example, that lesions in the hippocampus cause a deficit in a specific type of memory: episodic memory, or the memory of experiences in our lives (Scoville and Milner, 1957; Tulving, 1972; 2002). We also know that there are cells in the hippocampus, place cells, that have a "memory" of their own: a given cell of this type will only fire when the animal is in a restricted region of the environment, the cell's place field (O'Keefe and Dostrovsky, 1971). Is this single-cell memory related to the systems-level and behavioral concept of episodic memory?

A clue to answering this question might come from oscillations, regular fluctuations of electrical activity commonly observed in the hippocampus and other parts of the brain. Oscillations are attractive biophysically and computationally. They are biophysically attractive because they can arise from the activity of a single neuron due to the non-linear interplay of intrinsic currents, or due to an interaction of a heterogeneous group of cells in a network (Wang, 2010). They are computationally attractive because oscillations can be markers of synchrony, and synchrony has been proposed as a possible solution to the binding problem: how are the different modalities that compose a thought or a memory integrated coherently (Singer, 1993)? In the context of the hippocampus, oscillations are thought to be related to the temporal organization of assemblies: groups of cells that fire together for a period of time (Harris et al., 2003; Buzsáki and Wang, 2012). Moreover, these assemblies usually exhibit place selectivity citepDragoi2006. An underlying paradigm of current memory research and of this thesis, is that oscillations are important in organizing such place-selective assemblies with the ultimate goal of creating spatiotemporal trajectories and associations of events within those trajectories (Hasselmo et al., 2002). This is a modern view of an "episodic memory" in terms of the place-selective activity of the hippocampus.

The propagation of electrical activity through great distances in a short amount of time is one of the brain's hallmarks. As this electrical activity is routed through different stages, it is transformed and processed before it reaches its destination. This long-distance communication combined with the modular architecture of the brain is partly responsible for the brain's great computational abilities. The connectivity patterns and the intrinsic properties of cells allow for this communication to take place. For instance, a pattern of activity observed in region "A" might also be present in a region "B" downstream, so that effectively region "B" has "inherited" the pattern of activity from "A". This thesis is concerned with the

inheritance of a particular spiking pattern with relevance to memory formation. The pattern is phase precession, an oscillatory phenomenon mainly exhibited by cells in the hippocampal formation (O'Keefe and Recce, 1993; Skaggs et al., 1996; Hafting et al., 2008). During phase precession, there is a systematic advancement of spike times of place-selective cells with respect to the theta rhythm, an oscillation in the 4–12 Hz range. Importantly, phase precession is thought to be important for the formation of sequences and memory.

It is remarkable that after more than twenty years, we still do not know how phase precession is generated, or if it has a functional role. The characterization of phase precession is chiefly due to extracellular recordings, but recent advances in optogenetics and in vivo intracellular recordings have provided even more information about the phenomenon. These advances occurred almost in parallel to the development of this thesis. This was therefore a tremendous opportunity to witness firsthand two of the most impressive tools to elucidate functionality in the brain, and in particular, in the hippocampal microcircuit. Some of the most important results of the thesis are thus based on studies that integrated these techniques to address their particular questions (Harvey et al., 2009; Royer et al., 2012).

Organization of the introduction In the following, I will synthesize the literature that is relevant to the understanding of the core chapters of the thesis, namely Chapters 2, 3, 4, and 5. First, in section 1.1 ("A brief survey of the hippocampal formation"), I study general properties of the hippocampus including its proposed contribution to memory and navigation, its gross anatomy, and mechanisms and functions of plasticity. Next, in section 1.2 ("Computational role of the hippocampus"), I dwell deeper into the computational theories surrounding hippocampal function with regards to intra and extra-hippocampal dynamics. Here I present the two-stage model of memory, a model of memory formation depending on an online and an offline phase. Then, in section 1.3 ("State-dependent information processing in the hippocampus"), I define place-selective cells and the spatial representation in the hippocampus. I review theories and evidence on how such spatial representation along with oscillatory activity support the two-stage model of memory. Then, in section 1.4 ("Phase precession: a link between oscillatory activity, neural coding, and plasticity"), I formally introduce phase precession, its most important properties, and some open questions. Finally, in section 1.5 ("Scope of the thesis"), I give an overview of the contents addressed in the core chapters of the thesis.

As this introduction is intended to be a personal view of the most important developments of the field relevant to the questions I tried to answer during my thesis, it is necessarily incomplete. The references therein, however, will guide the reader in case he or she is interested in a particular topic.

1.1. A brief survey of the hippocampal formation

1.1.1. The hippocampus: a substrate for episodic memory and navigation

When we remember an event of our past along with a vivid recollection of items at a specific time and place, we are using one of the remarkable properties of our brain; we are recalling a past experience and in a certain way, re-experiencing it. These are features exclusive of episodic memories. More precisely, the term episodic memory refers to the acquisition, storage, and recall of information that can be situated in a spatiotemporal context. The original definition of episodic memory was meant to be applied for humans as it implicitly

contained the notion of consciousness. According to this view, a defining characteristic of episodic memory is that the subject can situate him or herself in the episode and mentally travel in time (Tulving, 1972; 2000).

Episodic memory is one type of declarative memory, the other being semantic which is concerned with "the general knowledge of the world" (Squire, 1992). For example, the memory of having eaten a banana for breakfast today constitutes an episodic memory, while knowing that a banana is a yellow fruit constitutes a semantic memory. For both of these memories, the process of recollection is conscious and can be "declared". The distinction is that episodic memories occur in a specific time and place, and the subject reexperiences them during recall. To study episodic memory in animals, however, the notion of episodic memory was replaced by the notion of episodic-like memory, a memory with a clear spatiotemporal component, more amenable to animal experimentation. The dynamics of memory-guided behavior in animals became important precisely because of the limitation animals have in declaring their experiences. Two popular tasks to probe memory-guided behavior are the Morris water maze task (Morris, 1984) and the delayed spatial alternation task (Dudchenko, 2004).

The first evidence of a role for the hippocampus in episodic memory was due to patient Henry Molaison, commonly referred to as patient HM in the literature (Scoville and Milner, 1957). Patient HM underwent surgery because of frequent epileptic seizures whose foci were located in the medial temporal lobe. His hippocampus as well as the amygdala and other sections of the medial temporal lobe were removed. After the surgery, patient HM could no longer form new memories, and thus suffered what is called anterograde amnesia. Notably, other types of memory were not impaired, including procedural or working memory. Furthermore, he could remember events that occurred well before the surgery, although he had also some graded retrograde amnesia, i.e., memory of the events prior to and close to the surgery were compromised. The qualitative and quantitative description of HM's behavior established two key organizational principles of memory. First, episodic memory is distinct from other memories and episodic memory can thus be compromised independently. Second, and particularly important for this thesis, is the fact that the hippocampus is an important component of the episodic memory system. These two principles gave rise to two largely independent lines of research: the study of episodic memory as a human cognitive function, and the study of animal models of the hippocampus. As this thesis is concerned with the computational function of the hippocampus in memory, I will point out some discoveries related to the study of the hippocampus that are important in understanding its role in episodic memory.

Two of the most important discoveries related to the hippocampus after the study of patient HM in the 1950's came almost simultaneously in the 1970's. In a groundbreaking paper, John O'Keefe and Jonathan Dostrovsky discovered cells in the rat hippocampal CA1 region that respond selectively to a particular portion of the environment (O'Keefe and Dostrovsky, 1971). The cells were termed place cells and the regions where they were active were termed place fields. Shortly after this remarkable discovery, Bliss and Lomo discovered long term potentiation (LTP) in the dentate gyrus of the rabbit hippocampus (Bliss and Lomo, 1973). LTP refers to a long-lasting enhancement of transmission between two neurons (details in section 1.1.3). These two concepts, that of place-selectivity and plasticity, would later lead to two of the most popular theories of hippocampal functioning: the theory of the cognitive map, and the synaptic-plasticity memory hypothesis. The basic idea behind the cognitive map theory is that there is an explicit mapping of the environment to the

brain such that space and objects embedded in space are represented in the hippocampus. The synaptic-plasticity memory hypothesis (see section 1.1.3) states that plasticity is both necessary and sufficient for the establishment of memories and learning in general. These two theories are complementary, and many current theories of hippocampal functioning (Rolls and Kesner, 2006; Hasselmo, 2012; Buzsáki, 2010) have elements of both.

An important experiment in the 1980's by Richard Morris and colleagues showed that the hippocampus is required for certain forms of spatial learning (Morris et al., 1982). This and subsequent experiments showed that space was an important high-level concept that was being represented by the hippocampus. Consistent with this idea, different types of cells were later discovered in the hippocampal formation, including grid cells (Hafting et al., 2005) and head-direction cells (Taube et al., 1990), and these cells were hypothesized to support complex navigational tasks (McNaughton et al., 2006; Moser et al., 2008) (see also section 1.3.1). Indeed, there are several lines of results in the human neuroscience literature that are consistent with the fact that the hippocampus is needed to solve a variety of spatial tasks:

- patients with hippocampal damage cannot remember the position of objects arranged on a table (Nunn et al., 1999),
- one of the prevailing symptoms of amnesics is spatial disorientation (Spiers et al., 2001),
- the volume of the hippocampi of taxi drivers in London is greater than that of controls (Maguire et al., 2000).

As I have argued in the previous paragraph, two distinct directions of research stemmed from the initial discoveries following patient HM's surgery, namely the cognitive neuroscience of episodic memory and the functional correlates of hippocampal neurons. There are current attempts to merge these two ideas by proposing that sequences of arbitrary items in episodic memory are analogous to position-dependent firing of neurons along a linear path (Buzsáki and Moser, 2013; Hasselmo, 2012). However, some researchers have made the objection that too much emphasis has been put on the "spatial navigation" correlates of the hippocampus (Eichenbaum and Cohen, 2014). Indeed, other aspects such as temporal organization are a crucial component of an episodic memory system, as the ability to remember sequential relationships among events is shared by a variety of species (Allen et al., 2014). Along these lines, episodic memories can be thought of spatiotemporal trajectories, where segments of the trajectory are associated with specific items or events (Hasselmo, 2012).

In the remainder of this chapter, I will introduce the physiology of the cells and networks in the hippocampus, and how they, to date, are hypothesized to contribute to complex cognitive tasks such as navigation and episodic memory.

1.1.2. Basic anatomy and physiology of the hippocampal formation

Here I give a brief overview of the anatomical and physiological principles that are most relevant for the results of this thesis. I kindly refer to the reader to Anderson et al. (2007) and references therein, for a more in-depth exploration of these topics and others not covered here such as the molecular aspects of hippocampal cells.

One of the reasons the hippocampal formation is a well studied system in neurobiology is because of the simple organization of its principal layers, as well as the highly organized laminar distribution of its inputs. These characteristics are also shared with many parts of the neocortex. An important difference, however, is the largely unidirectional passage

of information through intrahippocampal circuits. The hippocampal formation is divided into the hippocampus proper, the subiculum, the presubiculum, the parasubiculum, and the entorhinal cortex. The hippocampus proper is formed by two U-shaped interlocking sectors, the dentate gyrus (DG) and the cornu ammonis (CA) (Fig. 1.1 *A*). The CA region itself is divided in to regions CA3, CA2, and CA1. These features are common to the rat, mouse, monkeys, rabbits, and humans, the most studied mammals in hippocampal research (Anderson et al., 2007). There are important differences across mammals, however, in terms of volume, cell number, and ratios across the different regions. I will not address these differences, and concentrate on what is known about the rodent (mouse and rat) hippocampus and can be generalized to other mammals. As a convention, the entorhinal-hippocampal loop I will now describe begins with the entorhinal cortex. The entorhinal cortex is an important interface between several parts of the neocortex and the hippocampus. The superficial layers of the entorhinal cortex project to the hippocampus through the perforant path (Fig. 1.1 *B*): the DG and region CA3 are innervated by axons originating from layer II, while region CA1 is innervated with axons from layer III. The principal cells of the DG project to the CA3 region via the mossy fibers. The CA3 region projects to the CA1 region via the Schaffer collaterals. The CA1 field gives rise to two intrahippocampal projections. The first is to the subiculum, and the second is to the deep layers of the entorhinal cortex. The pyramidal neurons in the subiculum project to, among others, presubiculum, parasubiculum, entorhinal cortex, amygdala, prefrontal cortex, and ventral striatum. Furthermore, the return projections from subiculum and CA1 to the deep layers of entorhinal cortex are topographically organized. Thus, there is a loop of information starting at the superficial layers of the entorhinal cortex and ending at the deep layers of the same structure.

The entorhinal-hippocampal feedfoward circuitry, which will play an important role in this thesis, does not operate in isolation. The amygdala, a structure responsible for emotional components of memories (Murray, 2007), sends projections to CA3, CA1, and subiculum (Pitkänen et al., 2000). Another important connection is with the perirhinal cortex, a structure related to visual perception and memory, which is connected bidirectionally with region CA1 of the hippocampus. Other important projections to the hippocampus include those from the medial septum, which are important for pacemaking properties of interneurons (Buzsáki, 2002), and those to prefrontal cortex and ventral striatum which will be discussed in section 1.2.2.

The CA1 microcircuitry As the CA1 region of the hippocampus is an important focus of this thesis, I will discuss the circuitry and some morphological and physiological aspects of pyramidal cells and interneurons in this region. To study and distinguish the projections to and from the CA1 cells, I first briefly describe the organization of layers within CA1, which also applies to other regions in the CA and DG (Fig. 1.1 *C*). The hippocampus exhibits a laminated structure where the somata of principal cells form well-defined layers: the stratum pyramidale in CA regions and granule cell layer in DG. Lying above the stratum pyramidale (from basal to apical direction) is the stratum radiatum followed by the stratum lacunosum-moleculare, and below is the stratum oriens.

The main inputs to a CA1 cell within the hippocampal formation come from the CA3 region and the entorhinal cortex. Projections from CA3 through the Schaffer collateral system of axons arrive at the stratum radiatum, and some to the stratum oriens depending on the dorso-ventral level. No return projections have been found in the CA3-CA1 system. Superficial layer III of the entorhinal cortex projects to the dendritic tuft in stratum

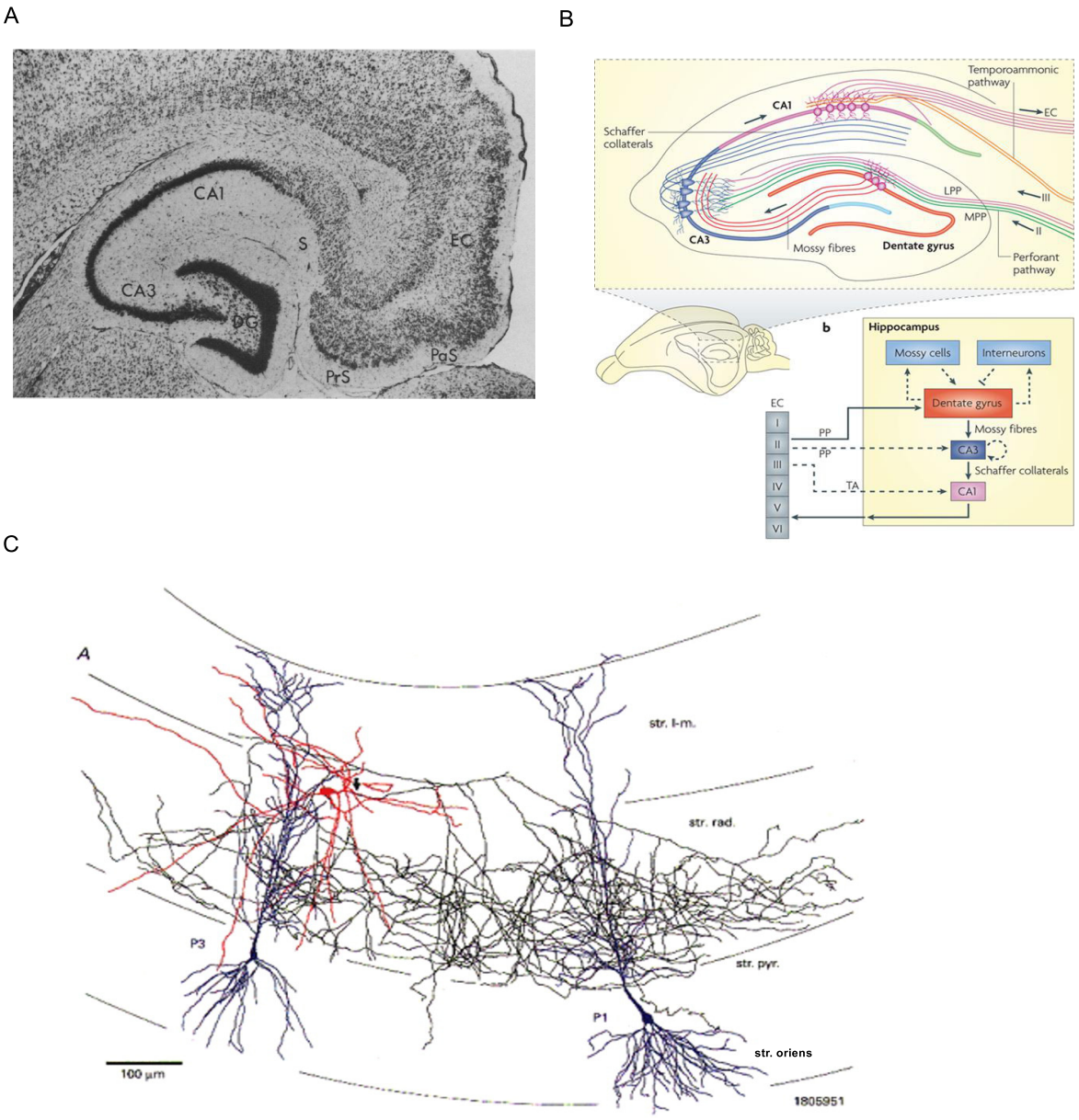

Fig. 1.1.: Anatomy of the hippocampus. ***A,*** A transverse slice of the rat hippocampus showing the hippocampal microcircuitry: entorhinal cortex (EC), the dentate gyrus (DG), CA3, CA1, the subiculum (S), presubiculum (PrS), and parasubiculum (PaS) (from Amaral and Witter 1989; reproduced with permission from Elsevier). ***B,*** Cartoon of *A* (top) and layer-specific connections in the entorhinal-hippocampal loop (bottom) (Deng et al. 2010; reproduced with permission from Nature Publishing Group). ***C,*** Reconstruction of CA1 pyramidal cells (blue) and an interneuron (red), showing the organization of layers in CA1: stratum oriens, stratum pyramidale, stratum radiatum, and stratum lacunosum moleculare (Vida et al. 1998; reproduced with permission from Wiley and Sons).

lacunosum-moleculare. The medial entorhinal cortex (MEC) projects to more proximal parts of the CA1 while the lateral entorhinal cortex projects to more distal parts.

Pyramidal cells in the CA1 region are one of the most investigated cells in the brain. These cells have a pyramidal soma, large apical dendrites that extend into the striatum

radiatum and form a dendritic tuft in stratum lacunosum moleculare, and two to eight basal dendrites that emerge from the base of the soma in stratum oriens (Cutsuridis et al., 2010). Dendrites of CA1 pyramidal cells are densely covered with spines, and the total number is estimated to be 30,000 (Megias et al., 2001). Spines serve as postsynaptic targets for glutamatergic terminals indicating excitatory input to these cells. Around 30,000 asymmetric excitatory synapses converge to a single cell (Megias et al., 2001). On the other hand, a neuron receives around 1700 inhibitory synapses in the perisomatic domain. Axon collaterals typically originate at the base of the soma in stratum oriens and innervate several cell types in an outside the hippocampus, including the interneurons which I will now discuss.

In contrast to the pyramidal cell population, interneurons are heterogeneous with respect to their morphology, physiology, and preferred targets (Klausberger et al., 2003; Cutsuridis et al., 2010). Interneurons can thus be classified according to their precise localization, anatomical features, and neurochemical properties as evidenced by their expression of a wide range of markers. Two main classes of interneurons can be distinguished with regards to their postsynaptic projections: perisomatic and dendritic inhibitory cells. A notable example from the first group are the fast-spiking parvalbumin basket cells, involved in the generation of gamma and sharp-wave ripple oscillations. Other perisomatic interneurons include the CCK-expressing basket cell and axo-axonic cells. An example of a dendritic inhibitory cell is the OLM interneuron, whose cell body lies in stratum oriens but its axons project to and inhibit apical dendrites of CA1 pyramidal cells in the stratum lacunosum moleculare. Other dendritic inhibitory neurons include the ivy cells, bistrafied cells, Schaffer collateral-associated and Perforant-path associated interneurons. I will analyze the role of inhibition within the CA1 microcircuitry in the context of phase precession in Chapter 2.

1.1.3. Synaptic plasticity and memory

Synaptic plasticity refers to the observed change of transmission properties from one neuron to another. These changes are thought to reflect learning and memory processes (Kandel, 2001). I will first review the basic mechanism of synaptic plasticity, focusing on the cellular mechanism of LTP, which is thought to be highly relevant in hippocampal processing, and in learning and memory in general (Lynch et al., 2004). Then I explore the synaptic plasticity-memory hypothesis, the possibility that synaptic plasticity is necessary and sufficient for the creation and maintenance of a memory.

To define synaptic plasticity more precisely, we must first understand the more general concept of synaptic transmission. Synaptic transmission begins with an action potential from a presynaptic cell arriving to the presynaptic cleft. The depolarized membrane causes vesicles filled with neurotransmitter to open in a process of exocytosis, and the neurotransmitter is transported to the postsynaptic cell. The neurotransmitter then binds to the receptors in the postsynaptic cell. After binding, the cell becomes permeable to positive charge entering the cell (in the case of the neurotransmitter glutamate and corresponding receptor), or negative charge (in the case of neurotransmitter such as GABA and its corresponding receptor). The resulting depolarization of the postsynaptic cell is referred to as a postsynaptic potential (PSP), excitatory or inhibitory depending on the nature of the transmitter and receptors involved. (To be precise, whether it is excitatory or inhibitory depends on the value of the membrane potential relative to the reversal potential of the receptor.) Assuming further that all incoming spikes are stereotypical (same amplitude and charge), the amplitude and slope of the PSP are determined by properties of the synapse. Synaptic plasticity then, refers to the modulation of the amplitude or slope of the PSP as a function of either the induction

protocol, or, more relevant to learning and memory, as a function of behavior or experience. The size of the PSP is also known as the strength of the synapse, a widely used concept in the neural network literature (Hopfield, 1982).

It is important to distinguish the two processes associated to synaptic plasticity: induction and expression. Induction of synaptic plasticity is the experimental protocol, i.e., stimulation of pre-synaptic and/or post-synaptic cells, used to establish a change in the strength of the synapse. Expression, on the other hand, refers to the amount of time a given synapse is strengthened or depressed before returning to a baseline value. Synaptic plasticity can thus be classified according to the time scales involved in expression (e.g., short-term vs long-term), and also according to the mechanisms and experimental protocols used to achieve this. Short term plasticity refers to the plasticity that lasts for only a few milliseconds, and important computational properties have been ascribed to it (Tsodyks and Markram, 1997). In the following paragraphs, I refer almost exclusively to the long lasting effects associated with potentiating plasticity and its connection to memory. Long term depression (LTD), the long lasting reduction in synaptic efficacy between two neurons, will not be considered here although it has an important and often overlooked contribution to learning (Kemp and Manahan-Vaughan, 2007).

Cellular mechanisms and function of LTP LTP refers to a broad class of mechanisms that allow for the long-lasting enhancement and maintenance of the synaptic strength between two cells (Fig. 1.2 *A*). It was first discovered in the rabbit hippocampus (Bliss and Lomo, 1973). Here I review the basic mechanism and function of NMDA-dependent LTP, although there are other forms of LTP that do not depend on NMDA receptors (Harris and Cotman, 1986; Gundlfinger et al., 2010).

In normal, i.e., non-plastic, excitatory transmission, a post-synaptic spike results in the release of neurotransmitter diffusing through the synaptic cleft and binding to NMDA and AMPA receptors in the postsynaptic cell. However, because of magnesium ions (Mg^+) blocking the channel, the NMDA channel remains closed. If the presynaptic cell is tetanized, i.e., stimulated at a high frequency, then the postsynaptic cell is sufficiently depolarized, which leads to expulsion of the Mg^+ block and the channel opens and becomes permeable to calcium. Calcium entering the cell initiates a cascade of events that result in an increase in the number and activity of AMPA receptors. Furthermore, via the effect of retrograde messengers the release of glutamate in the presynaptic cell is also enhanced. This process is referred to as early phase LTP, and the net effect is a stronger link between pre- and post-synaptic cells last lasting up to 2 hours. An extension of early phase LTP, late phase LTP, involves protein synthesis and is longer lasting and thus thought to be relevant for memory-related processes.

LTP is an attractive model for memory formation or information storage because of the following properties (Purves et al., 2001):
associativity: if a pathway is only weakly stimulated, and simultaneously a neighboring pathway is stimulated, then both pathways undergo LTP.
specificity: a pathway that is strongly stimulated will undergo LTP, while a neighboring pathway that is inactive will not undergo LTP.
state-dependence: the degree of depolarization of the postsynaptic cell determines whether a change occurs.
persistence: the potentiation can last from several minutes, to several months.
In the following paragraph, I will give an overview of how synaptic plasticity is connected to

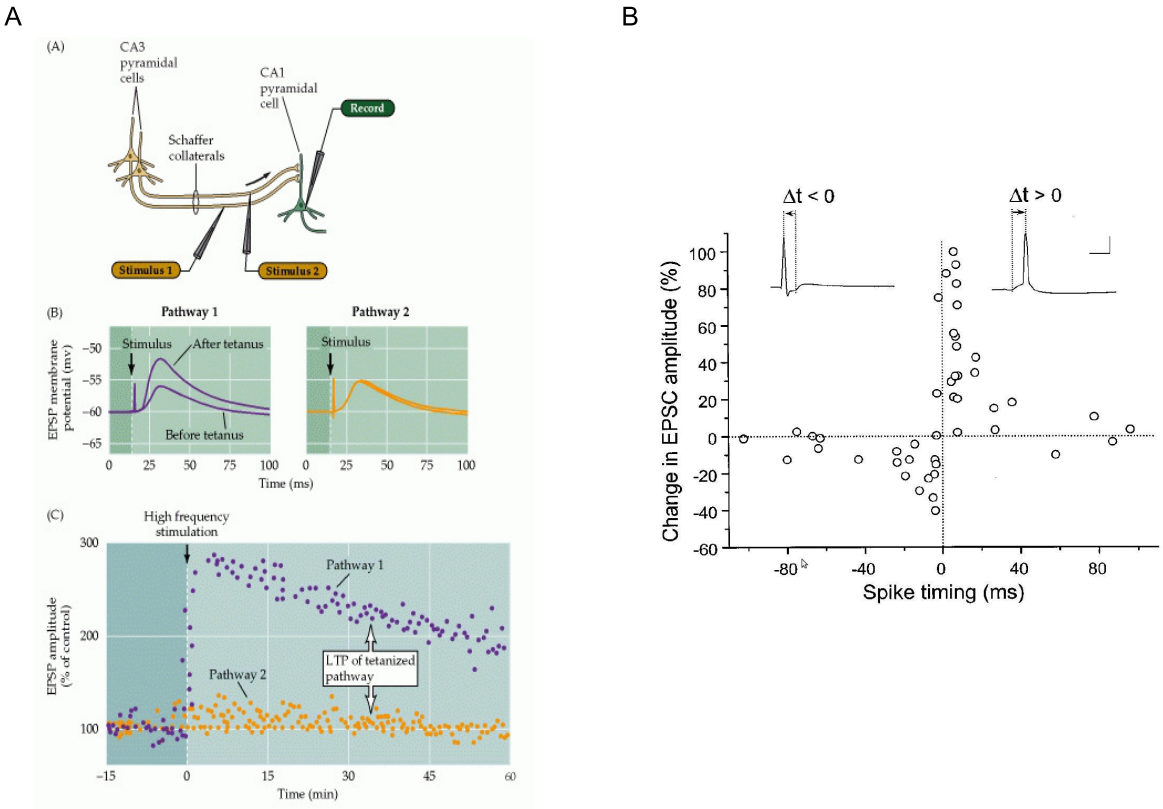

Fig. 1.2.: LTP in the hippocampus. ***A,*** Induction protocol at the Schaffer collaterals for producing LTP at the CA3-CA1 synapse (top), postsynaptic response for before and after tetanus (middle), and expression of LTP as a function of time. Reproduced from Purves et al. (2001). ***B,*** STDP window obtained from cultured hippocampal neurons. Spike timing was defined by the time interval (Δt) between the onset of the EPSP and the peak of the postsynaptic action potential during each cycle of repetitive stimulation (Bi and Poo 1998; reproduced with permission from Society for Neuroscience).

memory as observed during behavioral tasks.

The synaptic plasticity-memory hypothesis The synaptic plasticity-memory hypothesis (SPM) is an important paradigm that drives a substantial part of the research in the hippocampus and memory community. SPM states that "activity-dependent synaptic plasticity is induced at appropriate synapses during memory formation, and is both necessary and sufficient for the information storage underlying the type of memory mediated by the brain area in which that plasticity is observed." (Martin et al., 2000). In a certain sense, the SPM hypothesis is a biological realization of ideas put forward by Donald Hebb (Hebb, 1949). Does LTP equate to memory? This is indeed an oversimplification of the SPM hypothesis, but is nevertheless useful in making proper qualifications to elucidate the function of synaptic plasticity. There are many questions that would first need to be addressed. For example, in which region is LTP being investigated and what type of memory? In the definition of the SPM hypothesis, an important but difficult concept to define is memory, which can have subtle differences of meaning depending on the context. Generally, memory can be defined as changes that outlast events that trigger them. The changes might be in synaptic

strength or excitability, while the events can be external or internal to the brain region in question. The function of LTP would be to mediate encoding, but what actually is encoded and how is an emergent property of the network where plasticity is being observed (Martin et al., 2000). Thus, plasticity in hippocampus might be relevant for the encoding of places and declarative memory (Muller, 1996; Shapiro and Eichenbaum, 1999), while plasticity in other regions might mediate other types of memory, including implicit and procedural (Kandel, 2001).

Martin et al. (2000) argue that the SPM hypothesis must fulfill 4 criteria:

- Anterograde alteration: altering LTP induction should impair learning.
- Detectability: changes in synaptic strength should be observable after learning.
- Retrograde alteration: altering the pattern of synaptic weights after experience should alter the animal's memory of that experience.
- Mimicry: controlled alteration of synaptic strengths should result in an induction of a memory.

The first example of LTP being necessary for memory came from the study of rodent behavior in the Morris water maze. Infusion into the hippocampus of the selective NMDA-receptor blocker AP5 markedly impaired learning and recall in the Morris water maze (Morris et al., 1986). This is an example of anterograde alteration because the drug blocks LTP without affecting basal synaptic transmission. With the advent of genetic approaches, genetically engineered animals lacking a particular subunit of the NMDA receptor such as the GluN2A subunit, were subject to the same water-maze task. In these animals, LTP could not be induced and there were similar spatial memory impairments as in the animals infused with AP5 (Sakimura et al., 1995). Detectability has been more difficult to prove. Partial support for detectability comes from studies where, after learning, field EPSPs were increased with respect to controls (Moser et al., 1993) and where increase of glutamate release was observed (Richter-Levin et al., 1995). According to the retrograde alteration criterion of the SPM hypotesis, reversal of LTP should cause forgetting. Reversal of LTP can be achieved by the process of depotentiation, or by LTD. On the other hand, the mimicry requirement states that a memory can be created by altering the synaptic weights. These last two criteria are the most challenging and until very recently, received little evidence supporting them. The experiments by Nabavi et al. (2014) using optogenetics reperesent perhaps the most astonishing evidence of the relationship between LTP and LTD in memory (and that of retrograde alteration and mimicry described above), where the authors showed that fear conditioning can be inactivated and reactivated by LTD and LTP, respectively, and thus effectively inactivating and reactivating a memory.

In conclusion, there is accumulating evidence that supports the SPM hypothesis (but see Bannerman et al. 2014) and this hypothesis is one of the guiding principles of current memory research.

Spike-timing dependent plasticity As stated in the previous paragraphs, LTP and LTD could allow activity-dependent bidirectional modification of synaptic strengths. The protocols to establish LTP and LTD have been traditionally high (low) frequency stimulation paired with large (small) post synaptic depolarization. In biologically realistic conditions, plasticity induction in the hippocampus was found to also depend on spike timing (Levy

and Steward, 1983). Subsequent studies elucidated the importance of the relative ordering of pre- an postsynaptic spikes in inducing synaptic modification in the hippocampus and in neocortex (Bi and Poo, 1998; Markram et al., 1997; Debanne et al., 1998). This spike-timing-dependent plasticity (STDP) has now been extensively investigated in many theoretical and experimental studies. Here I briefly comment on the evidence for STDP at excitatory synapses, its basic properties, its proposed cellular mechanisms, and its suggested role in hippocampal processing.

STDP is characterized by the so-called plasticity window, which determines the amount of synaptic change as a function of the difference between presynaptic and postsynaptic times (Fig. 1.2 *B*). The plasticity window depends on many factors including dendritic location and whether the synapse in question is excitatory or inhibitory (Caporale and Dan, 2008). Bi and Poo (1998) studied STDP in dissociated hippocampal cultures. They had control over the spiking of both pre- and postsynaptic neurons and could thus characterize the timing window for the induction of STDP. It was found that if presynaptic spikes precede postsynaptic spikes by up to 30 ms, LTP was induced, whereas if the presynaptic spike occurred after the postsynaptic spike, LTD was induced. The largest changes occur when the time difference between pre- and post synaptic potentials is small. Similar results were found for monosynaptically connected neurons in cortical slices, suggesting that STDP is a general phenomenon in the brain (Markram et al., 1997; Bi and Poo, 1998; Sjöström et al., 2001).

Since STDP depends on both presynaptic and postsynaptic activities, it is a Hebbian type rule. Additionally, STDP determines the direction of synaptic modification as a function of causality and is thus distinct from other forms of correlational Hebbian plasticity. In this context, NMDA receptors can be thought of coincidence detectors, as they will open only if there is a coincidence of glutamate release due to the presynaptic spike and depolarization due to the postsynaptic spike. This means that the postsynaptic spike must arrive to the dendrites via backpropagation. The extent to which back-propagating action potentials are able to fulfill the requirements of STDP depends on many factors, including the location of the soon-to-be potentiated synapse, the distribution of active channels, the morphology of the dendritic arbor, and the neuromodulatory state (Sjöström et al., 2008). Moreover, backpropagating action potentials might not be necessary if there are local dendritic spikes that can depolarize the cell (Golding et al., 2002).

STDP has interesting functional implications when considering neural networks in general. STDP rules have been studied for temporal pattern recognition (Gerstner et al., 1993), temporal sequence learning (Abbott and Blum, 1996), navigation (Gerstner and Abbott, 1997), and coincidence detection (Gerstner et al., 1996). Furthermore, and particularly relevant for this thesis (see Chapter 3), STDP leads to competition of the weights that in turn result in a stable distribution of synaptic weights (Kempter et al., 1999; Song et al., 2000). In the hippocampus, if STDP is an accurate description for synaptic and learning dynamics, then it should account for synaptic modifications produced by complex naturalistic spike trains as those produced by place cells (Caporale and Dan, 2008). How does this actually occur in the hippocampus, e.g., which place cells become associated with each other, and via which mechanism? These are mostly open questions, but some evidence for a connection between place cells and plasticity will be given in section 1.3.1.

Computational issues surrounding synaptic plasticity and memory The SPM hypothesis is probably the best candidate theory for a cellular-functional theory of memory.

From a computational perspective, however, there are certain issues that have arisen and that have only been partly addressed. The first issue, is the stability-plasticity dilemma (Grossberg, 1980). This basically states that the ongoing storage of new memories requires a high degree of susceptibility of synapses (plasticity), while protecting older memories of being overwritten by new experiences (stability). A partial solution to this dilemma comes with the notion of a two-stage model of memory (Buzsáki 1989; McClelland et al. 1995, see also section 1.2.2). The second problem refers to the repeated application of LTP: unconstrained potentiation can lead to unbalanced levels of excitation, i.e., runaway excitation. Synaptic homeostasis might be a way to resolve this (Turrigiano and Nelson, 2000). The third problem is particularly relevant for the contents and scope of this thesis. Learning occurs over multiple time scales (Melamed et al., 2004). Is there a mechanism that allows to bridge the timescales of behavior and the time scale of neural activity?

1.2. Computational role of the hippocampus

The hippocampus is a crucial component of the episodic memory system as proven primarily by lesion experiments. The exact contribution of the hippocampus to the formation, storage, and recall of memories, is still highly debated. Notably, some researchers argue that the hippocampus is primarily used to represent physical space in a flexible manner and support navigation (O'Keefe and Nadel, 1978; McNaughton et al., 2006), while others argue of the primary importance of the hippocampus in associating elements in an abstract "relational space" (Shapiro and Eichenbaum, 1999; Eichenbaum and Cohen, 2014). These views represent of course only two popular suggestions for hippocampal function, and many researchers (myself included) would probably agree with many features of both views.

In this section I review some of the current computational ideas and experimental results associated to intrahippocampal as well as extrahippocampal dynamics. These ideas are complementary and constitute two very helpful research directions for the understanding of the computational role of the hippocampus.

1.2.1. Hippocampal subregion analysis: associative memory, pattern separation and pattern completion

Many computational studies noted the autoassociative properties of recurrent networks with memory, so that original activity is reinstated after a partial cue of the encoded memory is presented (Marr, 1971; Hopfield, 1982). In particular, Marr (1971) suggested that an important computational function of the hippocampus depends on the autoassociative properties of the recurrent networks present there. The function of the individual regions, however, was not specified. McNaughton and Morris (1987) and Rolls (1987) suggested that the CA3 region of the hippocampus, because of its recurrent collaterals (Amaral and Witter, 1989), could act as an autoassociative memory to store episodic memores, including object and place memories. For most current theories on hippocampal function, the CA3 region is the central component and others subregions are viewed as aiding CA3 in carrying out its computational function. Here I review some computational ideas for the function of the subregions of the hippocampal formations including the dentate gyrus, CA3, CA1, the entorhinal cortex, and subiculum, and evidence supporting these claims.

The dentate gyrus The dentate gyrus is composed of dentate granule cells, which are excitatory. There is now substantial evidence (e.g. Gilbert et al., 2001; Leutgeb et al., 2007; Neunuebel and Knierim, 2014) showing that the dentate granule cells are involved in an important computation called pattern separation. Pattern separation refers to the reduction of overlap of similar inputs thus enabling an output structure (e.g., CA3) to reduce interference during memory recall. The studies that assessed pattern separation typically relied on lesions to the dentate gyrus that prevent animals from detecting mismatches in spatial context. For example, the dentate gyrus would allow the encoding of distinct memories about similar places even if there is spatial overlap. The key to the operation of the dentate gyrus might come from a property of competitive networks that allows them to separate overlapping patterns (Rolls and Kesner, 2006).

Apart from pattern separation, granule cells are thought to contribute to the sparse and orthogonal representations in CA3 (Rolls and Kesner, 2006). Another notable property of the dentate gyrus, is that it is the site of most of the neurogenesis in adult brains (Drew et al., 2013).

CA3 region CA3 is believed to be the central component of the hippocampal memory system. The system of recurrent collaterals in CA3 (Li et al., 1994) allows CA3 to function as an autoassociator. An autoassociator enables arbitrary associations to be formed which could be recalled with a spatial or object cue (Marr, 1971). Furthermore, partial input of a pattern is sufficient to recall the whole pattern in a process called pattern completion. The best example of the role of CA3 in pattern completion is the study from Nakazawa et al. (2002) with NMDA receptor knock-out mice. The animals were required to perform a task where some of the familiar cues were removed. The fact that the knockout animals were impaired in this task while the controls performed normally, was an indication that CA3, and particularly intact plasticity mechanisms in CA3 (see also section 1.1.3), are critical to perform pattern completion. Other functions typically ascribed to CA3 include:

- "one shot" learning, whereby learning of an episode is possible after one presentation of the stimuli (Nakazawa et al., 2003),
- generating self-sustained reverberating activity which would contribute to short term memory (Lee and Kesner, 2002) or for path integration (Samsonovich and McNaughton, 1997), and
- learning/encoding of sequences (Hunsaker and Kesner, 2008).

During the encoding of sequences, a pattern activates a set of neurons before the next pattern, allowing STDP to strengthen the synapses between sequential patterns. During retrieval, and similar to pattern completion, partial input of the first pattern will result in sequential spiking and the sequence in full. The encoding of sequences, in particular, is an important motivation for the work in this thesis. I return to this issue when I talk about phase precession in section 1.4.

CA1 region The CA1 region is one of the most well-studied regions in the hippocampus. It is an important stage mediating transfer of information between the hippocampus and the neocortex (see also section 1.2.2) as the CA1 neurons would activate pyramidal cells in the deep layers of the entorhinal cortex (Lavenex and Amaral, 2000). For this purpose, CA1 might act as a recoding stage that would facilitate retrieval in the neocortex (Rolls

and Kesner, 2006). Indeed, the number of CA1 principal cells is greater than in any other hippocampal stage and can thus provide the first part of the expansion for the projections to neocortical cells.

The CA1 subregion plays a role in temporal pattern separation: two events that are close in time are to be "separated", i.e., remembered as two distinct events. Evidence for this role comes from trace-conditioning studies, where there is a delay period between the unconditioned and the conditioned stimulus (Weiss et al., 1999), and from delayed non-match to sample tasks (Lee and Kesner, 2002). According to Rolls and Kesner (2006), principal cells in CA1 might allow for an efficient representation of the memory that is encoded in the CA3 synapses. A memory in CA3 could consist of the different episodes allocated to distinct assemblies in CA3 (Dragoi and Buzsáki, 2006). CA1 cells receiving this input can code for larger portions of the episode. For example, a CA1 cell could code for a conjunction of an object and places, both of which have individual cells or assemblies that code for them in CA3.

Entorhinal cortex The entorhinal cortex lies at the interface between the neocortex and hippocampus. It projects to the hippocampus via the perforant path. It was found that these inputs are critical for temporal association memory (Suh et al., 2011; Kitamura et al., 2014). Furthermore, it is hypothesized that with the types of cells found in the entorhinal cortex, including head-direction cells and grid cells, the entorhinal cortex constitutes a system adept for path integration (McNaughton et al. 2006 and see section 1.3.1).

Subiculum The subiculum is an output structure of the hippocampus, situated between the hippocampus proper and the entorhinal and other cortices. Although the function of the subiculum is not very well defined, it plays a role in spatial memory and the control of the response to stress. Furthermore, it has been suggested that the dorsal subiculum is involved in spatial relations, while the ventral subiculum regulates the hypothalamic-pituitary-adrenal axis (O'Mara, 2005).

1.2.2. Hippocampus in context: the interaction of the hippocampus and other regions of the brain

The hippocampus is connected to areas associated with cognitive functions, including the basal ganglia and the neocortex. Here I discuss the role of the hippocampus in memory, decision-making, and navigation.

Hippocampal-neocortical interaction in the two stage model of memory The two-stage model (Fig. 1.3) refers to the widely accepted architecture for memory encoding, consolidation and subsequent recall involving two major structures: the hippocampus and the neocortex (Buzsáki, 1989; McClelland et al., 1995). According to the two-stage model, information is acquired during awake behavior in the hippocampus, in an encoding stage. During this stage, the hippocampus is thought to act as a memory buffer and associate elements in a spatio-temporal context (Hasselmo, 2012). The encoding stage is characterized by theta activity in the hippocampus (Buzsáki, 2002), and the activation of the feedforward circuitry in the entorhinal-hippocampal loop (Hasselmo et al., 2002). The memories that are formed and temporarily stored in the hippocampus are gradually transferred to the neocortex during the process of consolidation, i.e., the process by which newly formed

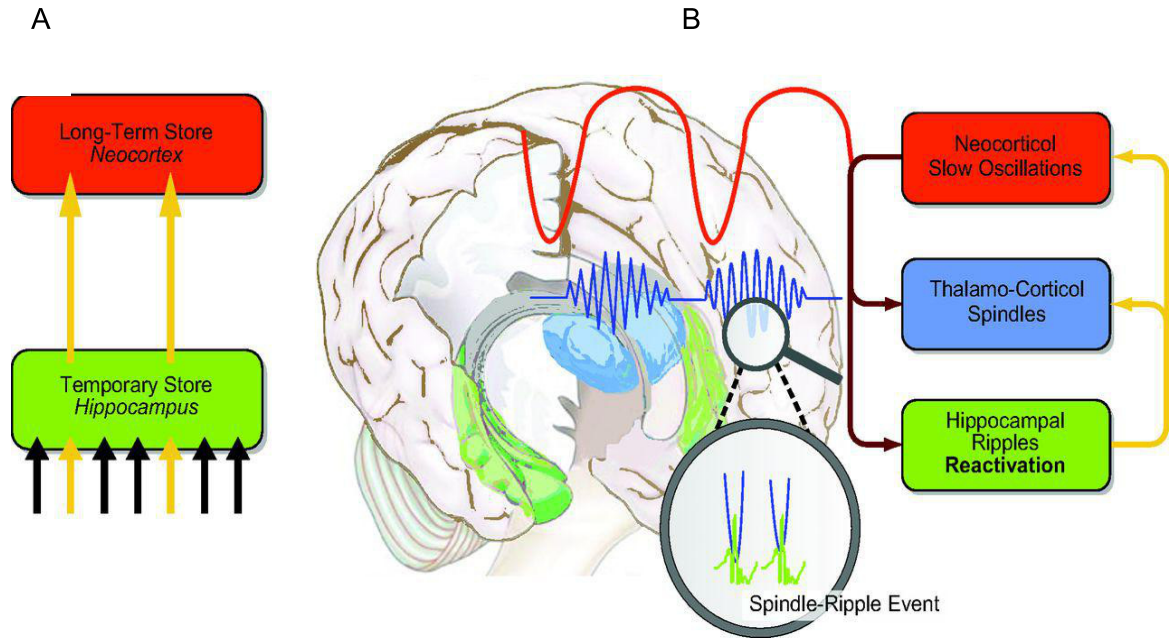

Fig. 1.3.: Two-stage model of memory. ***A,*** Schematic of the two-stage model showing the two principal regions involved. Memories are first encoded in the hippocampus and are gradually transferred to the neocortex for consolidation. ***B,*** Oscillations that are present during the process of consolidation include slow waves, sharp-wave ripples, and spindles (Rasch and Born, 2013).

traces are progressively strengthened into long-term memories and become more resistant to interference. In this consolidation stage, sharp-wave ripples (SWR) and the associated phenomenon of neural replay are believed to play an important role, particularly during sleep (see section 1.3). During the process of recall, memories are reinstated and there is a continuous bidirectional exchange of information between the hippocampus and neocortex. The hippocampus is believed to link together different components that reside in different cortical areas, and thus supporting an index representation (Teyler and Rudy, 2007). The evidence for this is usually in the form of varying degrees of coupling between hippocampus and neocortex as measured by coherence of theta or gamma oscillations during controlled behavioral tasks (Siapas et al., 2005; Jones and Wilson, 2005; Benchenane et al., 2010). For a discussion of oscillatory activity in the hippocampus, please refer to section 1.3.2.

There is evidence that supports the idea of the transfer of information from the hippocampus to the neocortex. Retrieval for remote memories become relatively independent of the hippocampus and more dependent on areas such as the prefrontal and anterior cingulate cortex (Maviel et al., 2004). Furthermore, hippocampal activity tends to precede downstream neocortical activity (Wierzynski et al., 2009), while ensemble activity in neocortical areas coincide with SWR events (Peyrache et al., 2009). Sleep is an important part of the consolidation process. During sleep, brain dynamics change radically and become dominated by sharp-wave bursts in the hippocampus, and by slow oscillations and spindles in cortex (Diekelmann and Born, 2010). Furthermore, olfactory and visual cues paired with visual stimuli during learning can strengthen memory if the stimuli is presented during subsequent slow wave sleep (Rasch et al., 2007; Rudoy et al., 2009).

Decision-making and navigation Although typically regarded as a memory system (Scoville and Milner, 1957; Shapiro and Eichenbaum, 1999; Squire et al., 2004), the hippocampus also forms part of a distributed system dedicated to decision making. Indeed, decisions result from the interaction between multiple systems to process information, some of which has to be stored and recalled (Gold and Shadlen, 2007). The hippocampus might become important when a representation of the "world" is needed to deliberate over options. This deliberation process depends on the ability of creating non-local representations at other times (van der Meer et al., 2012) and is consistent with functions ascribed to the hippocampus such as imagining the future (Maguire and Hassabis, 2011). Other structures forming part of the decision-making circuits include the prefrontal cortex, the dorsal striatum, and the ventral striatum (Niv et al., 2006) whose relative importance and recruitment depends on the type of action-selection needed to perform on a decision-making task (van der Meer et al., 2010). In particular, the ventral striatum closely interacts with the hippocampus such that reactivation of rewarded neurons occurs concurrently with hippocampal replay (Lansink et al., 2009) and ventral striatal neurons show phase precession towards a goal location, presumably inherited from the hippocampus (van der Meer and Redish, 2011; Malhotra et al., 2012). I will return to the issue of phase precession inheritance in the context of hippocampal and striatal activity in Chapter 4.

The fact that space is robustly represented in the brain by a dedicated circuitry (Moser et al., 2008), strongly suggests that the hippocampus is an important component in navigation (Morris et al., 1982; Buzsáki and Moser, 2013). There are many strategies, however, that can be used by an animal depending on the type of information required, e.g., sensory or proprioceptive, the reference frame, e.g., allocentric or egocentric, the spatial scale, and the time required to complete the task (Etienne and Jeffery, 2004). Interestingly, decision-making and navigation share much of the circuitry. Similar to decision making, strategies for navigation could be roughly divided into model-based (hippocampus-dependent) and model-free (hippocampus-independent) (Khamassi and Humphries, 2012). Thus, the hippocampus might be providing a common framework for flexibly solving both navigational and decision-making tasks.

1.3. State-dependent information-processing in the hippocampal formation

In this section, I will introduce the basic concepts that form part of the current interpretation of hippocampal dynamics, with a bias towards rodent studies on navigation and memory. First, I introduce the circuitry of place-selective cells in the entorhinal-hippocampal loop. Then, I briefly review the most important oscillations that have been observed during behavioral tasks and their interpretation. Finally, I summarize the main interactions of relevant cells that are thought to contribute to the encoding of episodes as spatiotemporal trajectories.

1.3.1. The spatial representation in the hippocampus

The study of place representations in the hippocampus came with the discovery of place cells in 1971 (O'Keefe and Dostrovsky, 1971). A place cell is a neuron that selectively increases its activity at a specific location of the environment, i.e., the place field of the cell (Fig. 1.4). Place fields represent one of the best examples of a neural correlate for a high-level cognitive concept, and inspired many theories of hippocampal function where

the hippocampus encodes the environment in a map-like manner (O'Keefe and Nadel, 1978; Muller et al., 1996). Numerous experiments have elucidated many important properties of place cells (Muller, 1996). These properties are observed at the single cell level, as well as at the level of a population.

The first question one could ask is, what are the determinants of place-cell firing? Sensory, vestibular, and path integration inputs have been found to be important and are processed in the hippocampal formation (Muller, 1996). Place-field attributes typically measured include: peak and average firing rate of the corresponding cell, size, stability, information content, and propensity to burst. All of these attributes depend on many factors including the region of the hippocampus where the place cells are recorded from, the intrinsic properties of the place cells, the shape and size of the environment that the animal explores, and whether the environment is novel or familiar. Place fields are also known to expand in the direction opposite to the direction of travel (Mehta et al., 1997; 2000; Lee et al., 2004). Finally, and very important to the work in this thesis, is the fact that the firing activity within a place field is temporally organized, such that there is a relationship between single spikes and bursts to the theta rhythm recorded simultaneously in the extracellular space (O'Keefe and Recce, 1993). This relationship is termed phase precession and will be formally introduced in section 1.4.

Due to an advancement in multi-cellular recording techniques in the 1990's (Wilson and McNaughton, 1993), it is possible to record many cells simultaneously and analyze how the firing activities are correlated in a given environment, or across environments. An interesting feature of a place-cell population, is the phenomenon of remapping: a change in firing rate and/or place field location in a novel environment (Muller and Kubie, 1987). For example, a cell that was active in one environment might change its firing properties (rate remapping) or be completely silent in the new environment (global remapping). It has been suggested that hippocampal representations in different environments represent different attractor states (Tsodyks and Sejnowski, 1995) and the phenomenon of remapping has been used as evidence that there are attractor dynamics in the hippocampus (Wills et al., 2005). Another important property of place cells at the population level, is that they are organized into assemblies, groups of cells with transient synchronous activation (Harris et al., 2002; Dragoi and Buzsáki, 2006). Some theories of hippocampal function suggest that assemblies are central to the encoding of attributes of episodes (Buzsáki and Moser, 2013). These and other features lead to the idea that hippocampal cells form a cognitive map (O'Keefe and Nadel, 1978), namely, that the hippocampus creates a representation of the environment that allows the animal to flexibly navigate through it and learn and remember the location of goals.

A circuitry for self location in the hippocampus The spatial representation in the hippocampus engages a wide brain circuitry, including grid cells, head-direction cells, and border cells (Moser et al., 2008). Grid cells were discovered in the medial entorhinal cortex (MEC) which provides input to the hippocampus (Hafting et al., 2005). Contrary to place cells, grid cells have multiple firing fields. In two dimensions, a single cell will fire in a patch-like manner across the environment creating a hexagonal structure (Fig. 1.5 *A*). A grid is characterized by its spacing (distance between firing fields), orientation, and phase relative to an external reference point. Some of the properties of grid cells are analogous to those of place cells. Similarly to place cells, the phase of the grid is non-topographic, i.e., the firing vertices of neighboring grid cells appear to be shifted randomly. Furthermore, the spacing

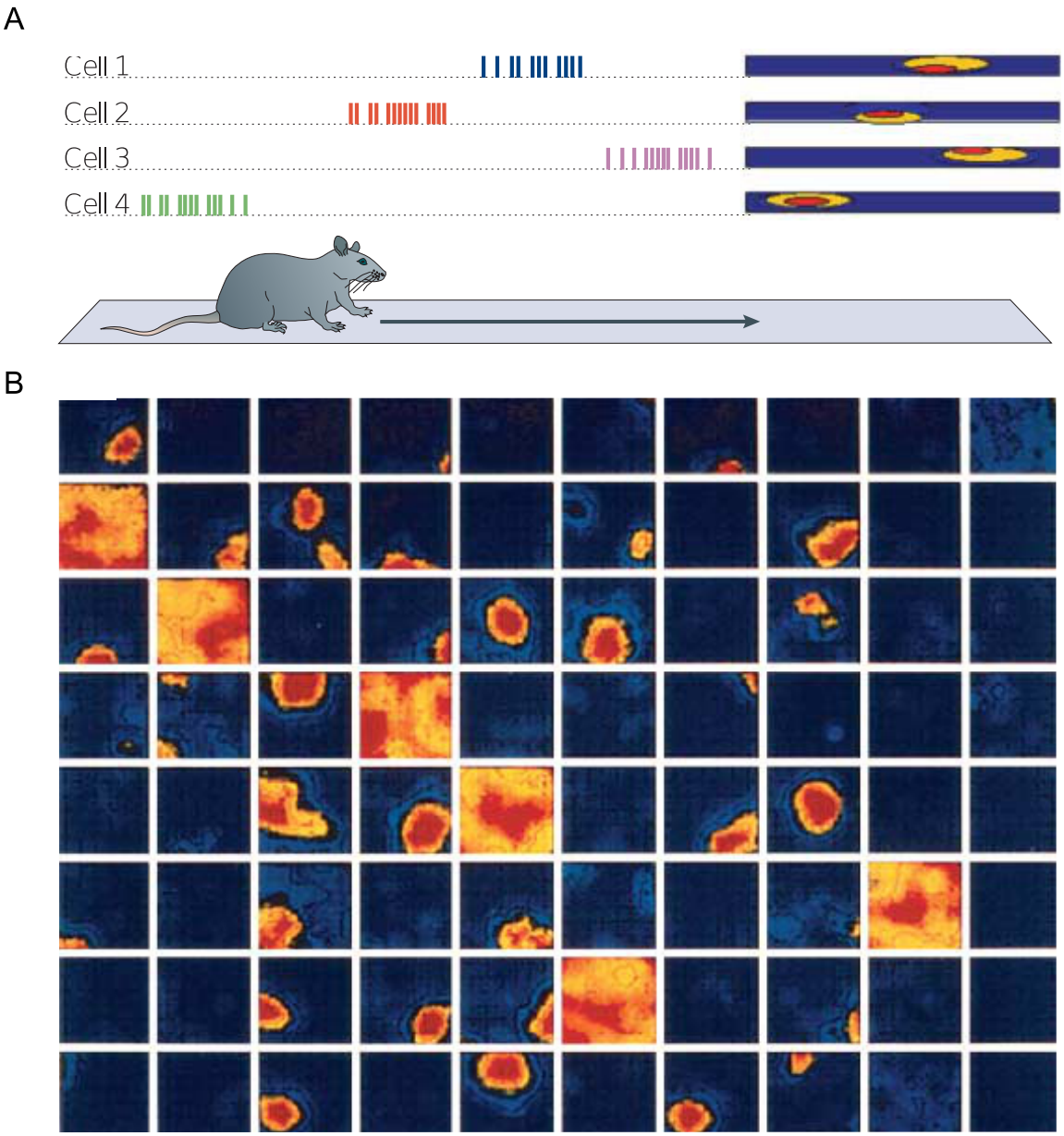

Fig. 1.4.: Place cells in the hippocampus. ***A,*** Place cells (color coded) encode specific locations through their firing rate (Nakazawa et al. 2004; reproduced with permission from Nature Publishing Group). ***B,*** Activity of place cells in the rat hippocampus while a rat navigated a two dimensional environment. Each square shows the activity of a cell that has one place field in that environment. Squares in which there is significant firing but no clear spatial selectivity show activity of putative interneurons (Wilson and McNaughton 1993; reproduced with permission from the American Association for the Advancement of Science).

increases monotonically from dorsomedial to ventrolateral locations in the MEC (Hafting et al., 2005). An important difference, however, is that unlike place cells which fire differentially across environments (Muller and Kubie, 1987), grid cells are active in all environments and observe coherent dynamics (Moser et al., 2008). The mechanisms behind grid cell formation are still not clear, although many proposals coincide in the integration of velocity signals as an essential factor in determining the grid-like structure (Giocomo et al., 2011; Barry et al., 2012).

Head-direction cells are cells that increase their firing rates above baseline levels only when the animal's head points in a specific direction (Taube et al., 1990). These cells were first discovered in the pre- and parasubiculum, but then also found in the MEC (Sargolini et al. 2006 and Fig. 1.5 *B* and *C*). Another cell type in the MEC with spatial correlates is the border cell, which has a spatial receptive field that lines up along specific geometric boundaries of the environment (Solstad et al., 2008). Thus, head-direction cells, grid cells, and border cells are suggested to constitute a circuitry specialized in the processes of path integration and navigation (McNaughton et al., 2006; Moser et al., 2008; Buzsáki and Moser, 2013), although they may also play an important role in forming an episodic memory (Hasselmo, 2012).

Are place fields formed from grid fields? Grid cells are found in the specific layers of the entorhinal cortex that project to the hippocampus. It was hypothesized that grid fields act as periodic basis functions such that the grids could be linearly combined to form place fields (McNaughton et al., 2006; Solstad et al., 2006). These models make the strong assumption of similar phases for grid cells that would be added to form the place cell, an assumption that is against the fact that phases of neighboring cells are random (Hafting et al., 2005). Subsequent theoretical studies used Hebbian learning to resolve this limitation (Rolls et al., 2006; Savelli and Knierim, 2010).

The relative importance of grid fields in creating place fields is still an open question. The hippocampus receives both spatial and non-spatial input from the entorhinal cortex (Zhang et al., 2013). Some recent results, however, have questioned the importance of grid-like inputs to determine place-field firing in a novel environment (Brandon et al., 2014). I will study this grid-to-place transformation in the context of phase precession in Chapter 4.

The place-cell representation and plasticity As argued in section 1.1.3, the normal induction and expression of plasticity in the hippocampus is important for solving spatial memory tasks. Furthermore, we know of the spatial representation afforded by place-selective cells in the hippocampal formation and their proposed role in memory. Hence, the effects of plasticity should be also observed at the level of the place-field representation of a given environment. One phenomenon that links plasticity and the place-cell representation is remapping, introduced in section 1.3.1. Because remapping has been observed when the shape of an environment (Lever et al., 2002) or cues within an environment (Bostock et al., 1991) change or because of a discrete learning event (Moita et al., 2004; Wang et al., 2012), it is believed that plasticity plays an important role so that place cells exhibit flexible environmental coding. Analysis of subfield-specific knockouts have provided evidence that remapping requires hippocampal plasticity. In CA1-specific knockouts of the NMDA receptor subunit NR1, place-cell activity is disrupted so that place fields do not retain strong location specificity and ensembles of cells with similar receptive fields are not correlated in their firing (McHugh et al., 1996). In CA3-specific knockouts of NR1, CA1 place cells have normal place

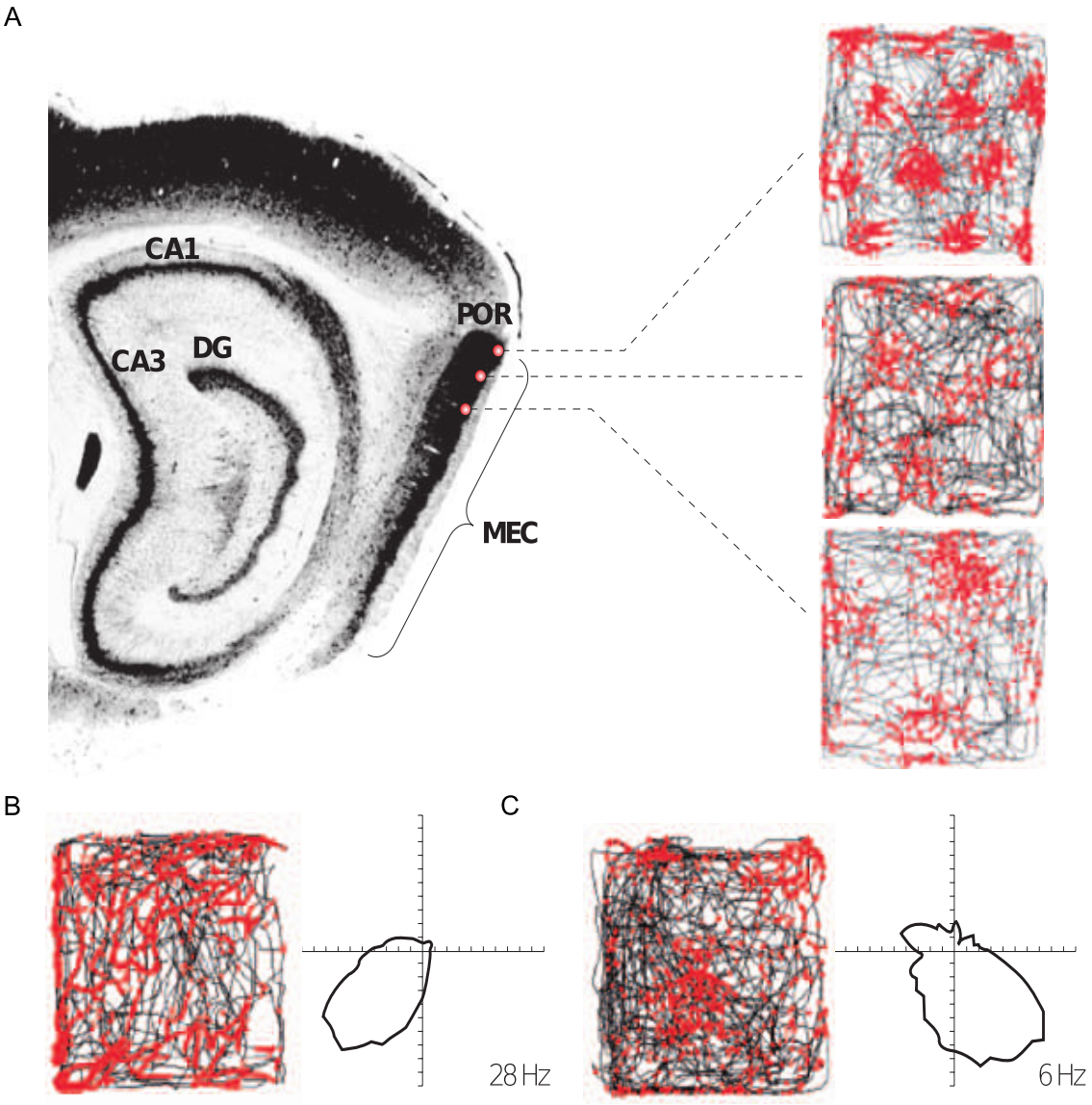

Fig. 1.5.: Path-integration circuitry in the entorhinal cortex (McNaughton et al. 2006; reproduced with permission from Nature Publishing Group). ***A,*** Spiking activity (red dots) of grid cells as the animal explores two-dimensional enclosure (black lines). Grid cells in the MEC are characterized by their spacing, i.e., the distance between the centers of any two grids. There is an increase in grid spacing corresponding to more ventral levels along the dorso-ventral axis. ***B,*** and ***C,*** Two examples of head-direction cells, cells that do not have strong spatial selectivity (left) but fire when the animal is headed in a preferred direction (right).

fields in familiar environments but enlarged, unrefined place fields in novel environments (Nakazawa et al., 2003).

The effects of plasticity can be observed at the level of single cells as well. When an animal traverses a given environment, the place fields shift in a direction opposite to the direction of motion. Backward-drifting place fields have been observed experimentally (Mehta et al., 1997; 2000; Lee et al., 2004) and theoretical studies had predicted this effect as a result of synaptic plasticity (Abbott and Blum, 1996). Indeed, blocking NMDAR-dependent plasticity abolishes this effect (Ekstrom et al., 2001). I return to this issue when I study the possibility of place-field inheritance in Chapter 3.

Finally, it has been hypothesized that features of the environment can be represented by the synaptic connectivity within the hippocampal neuronal populations (Wilson and McNaughton, 1993; Muller et al., 1996). Dragoi et al. (2003) showed that LTP of intrinsic hippocampal pathways created new place fields and produced a new correlation structure for the affected population. Although this study showed the importance of LTP in defining the population representation of an environment, it did not address directly how two place cells can become associated. A study by Isaac et al. (2009) has elucidated the role of place-cell firing patterns in the plasticity of hippocampal cells. In this in-vitro study, Isaac and colleagues injected natural spike trains to two connected CA3-CA1 cells. They could reliably induce LTP at these synapses, provided there was sufficient cholinergic tone by the application of carbachol. The studies by Dragoi et al. (2003) and Isaac et al. (2009) are indications of the role of LTP in forming associations between active assemblies.

Beyond space The investigation of cells with remarkable spatial correlates has highlighted the importance of the hippocampal formation in representing space. There are many studies, however, that have shown evidence for both strong modulation of place-cell firing by non-spatial stimuli, as well as cells that have non-spatial correlates altogether. An example of the former are cells that remap because of the presence of stimuli such as an odor or taste, or an alteration of the environment such as color (Redish, 1999; Anderson and Jeffery, 2003). An example of the latter are time cells which fire in a particular moment in time of a temporally structured event (MacDonald et al., 2011), and episode cells which fire by generating sequences in the absence of navigation (Pastalkova et al., 2008). I will review some of these non-spatial correlates in the context of phase precession and its plausible functional role in Chapter 5.

1.3.2. Oscillatory activity in the hippocampal formation

Oscillations of electrical activity recorded from neurons are believed to be important for diverse cognitive functions, including memory (Buzsáki and Draguhn, 2004; Wang, 2010). Hippocampal oscillations are usually studied through extracellular recordings, with sharp electrodes placed inside the hippocampus of the behaving rat (in vivo) or in slices (in vitro). The LFP is then obtained by filtering the recorded voltage and organizing it into frequency bands. Single-cell activity can be measured extracellularly by isolating action potentials and finding the corresponding cell that produced them in a process called clustering. Roughly speaking, action potentials represent the activity of single cells, while the LFP reflects the activity (action potentials, synaptic activity, etc.) of a population of cells surrounding the electrode. Intracellular recordings on the other hand can elucidate the rhythmic activity of single cells. These are performed with patch-clamping techniques in vitro (Sakmann and Neher, 1984) or in vivo (Lee et al., 2006).

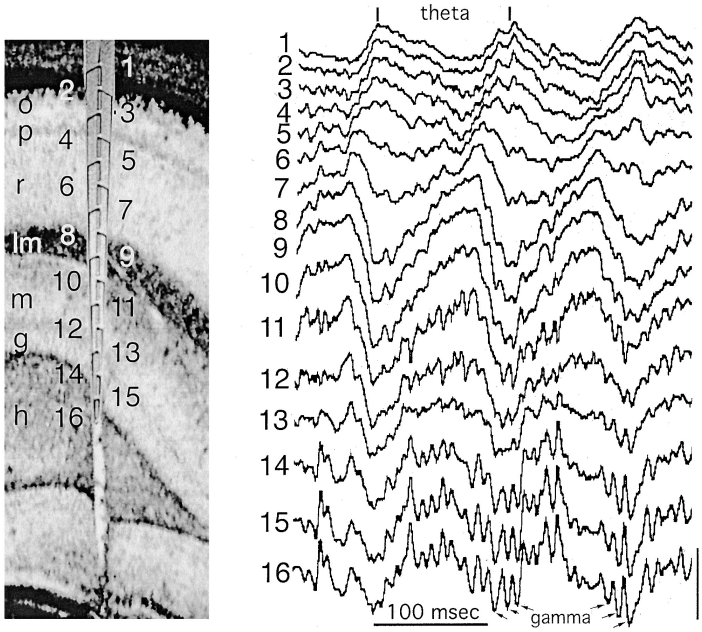

Fig. 1.6.: Theta and gamma oscillations in the hippocampus (Buzsáki 2002; reproduced with permission from Elsevier). A 16-site silicon probe in the CA1-dentate gyrus axis (left) records LFP activity during exploration (right) in different recording sites (100 μm spacing): stratum oriens (o), pyramidal layer (p), stratum radiatum (r), stratum lacunosum-moleculare (slm), granule cell layer (g), hilus (h). Gamma waves are superimposed on theta oscillation and are marked by arrows. Note that both amplitude and phase depend on the depth. Two popular recording sites are the hippocampal fissure (due to large amplitude waves) and hippocampal pyramidal layer (due to closeness to principal cell activity) and there is a 180° relative phase difference between the corresponding LFPs (Bullock et al., 1990).

I will give an overview of the theta, gamma, and SWR rhythms as observed in the hippocampus, as well as the proposed functions and underlying mechanisms.

Theta and gamma oscillations I focus on the voltage deflections observed in the local field potential (LFP) in the theta (4-12 Hz) and gamma (30-90 Hz) ranges. Both theta and gamma are observed in awake behavior and are characteristic markers of attentive states in the hippocampus, for example, during locomotion (Vanderwolf, 1969). In general, theta and gamma reflect different cognitive demands related to learning and memory (Sederberg et al., 2003; Lisman and Jensen, 2013). Concerning the hippocampus in particular, theta and gamma are thought to coordinate firing activity that play a role in the formation of cell assemblies and sequences of events (Harris et al., 2003; Lisman and Redish, 2009).

Theta oscillations are ubiquitous in the entorhinal cortex and hippocampus (Mizuseki et al., 2009). As noted in section 1.3.1, these regions contain cells whose responses code for position in the environment. The presence of both theta oscillations and place-selective neurons have motivated different roles for theta that have been amply reviewed and discussed in the literature (Hasselmo et al., 2002; Buzsáki, 2005; Lengyel et al., 2005; Colgin, 2013). Here I make a short list of some of the most popular functions ascribed to theta:

- entrainment and coordination of assemblies (Klausberger et al., 2003; Harris et al., 2003; Buzsáki, 2005),

- phasic modulation of LTP and LTD (Huerta and Lisman, 1995; Hyman et al., 2003),
- different theta phases for encoding and retrieval (Hasselmo et al., 2002), and
- generation of phase precession (O'Keefe and Recce, 1993; Skaggs et al., 1996).

Importantly, both pyramidal cells and interneurons are entrained by the theta oscillation (Skaggs et al., 1996; Csicsvari et al., 1999; Klausberger et al., 2003; Mizuseki et al., 2009; Lapray et al., 2012). The different types of interneurons found in the hippocampus can be classified according to their preferred phase of firing (Klausberger et al., 2003; Lapray et al., 2012).

The origin of theta oscillations is not well understood, and there seem to be multiple generators (Buzsáki, 2002; Montgomery et al., 2009). The amplitude and phase of theta waves change as a function of depth across the different layers (Buzsáki 2002 and Fig. 1.6). The classical theory places the medial septum as the pacemaker of the theta rhythm. Indeed, lesions of the medial septum abolish theta oscillations in downstream structures (Petsche et al., 1962). However, as there are multiple generators of the theta rhythm, it is likely that coupling and synchronization play a very important role (Colgin, 2013).

The theta rhythm can be classified on the basis of pharmacological sensitivity as type 1 theta or type 2 theta (Kramis et al., 1975). Type 1 theta refers to the theta oscillation commonly observed during active navigation which is not sensitive to atropine, a muscarinic antagonist. Conversely, the theta oscillations observed in anesthesized animals, type 2, is sensitive to atropine. This classification suggested at least two components to the theta oscillations observed in-vivo: an atropine-resistant component conveyed by the entorhinal cortex, and an atropine-sensitive component from the CA3 recurrent collaterals (Kocsis et al., 1999).

Gamma in the hippocampus has been hypothesized to act as a memory buffer for a multi-item working memory, such that the subset of cells that fire during a given cycle of the gamma oscillation represents an item (Lisman and Jensen, 2013). In the context of place-cell firing, cell assemblies are found to be dynamically organized in gamma cycles (Harris et al., 2003). Moreover, Colgin et al. (2009) showed how the frequency of gamma recorded in the CA1 region differentially routes separate streams of information: fast gamma couples the hippocampus with inputs from the MEC which convey sensory information, while slow gamma couples the CA3 and CA1 regions which might be an indication of recall. Some theoretical and experimental studies argue that gamma oscillations might also be related to the phenomenon of phase precession (Jensen and Lisman, 1996; Senior et al., 2008).

A widely accepted model of gamma rhythm generation is the pyramidal-interneuron gamma (PING), where the rhythm is generated via an interaction between a population of excitatory cells and a population of inhibitory cells (Whittington et al., 2000). Importantly, the period of the rhythm depends primarily on the decay time of the GABAa synapses (Bartos et al., 2007). The mechanisms behind gamma generation have recently been reviewed (Buzsáki and Wang, 2012).

Sometimes, gamma and theta rhythms are simultaneously present, usually interleaved (Fig. 1.6). This interleaving is referred to as nested gamma, an example of cross-frequency coupling in the hippocampus where the phase of the theta oscillation modulates the amplitude of the gamma oscillation (Belluscio et al., 2012). Such coupling is present during recall of stored information (Tort et al., 2009).

To conclude, theta and gamma oscillations seem to be important for coordinating the timing of assemblies. Research into the mechanisms behind its generation as well as its syn-

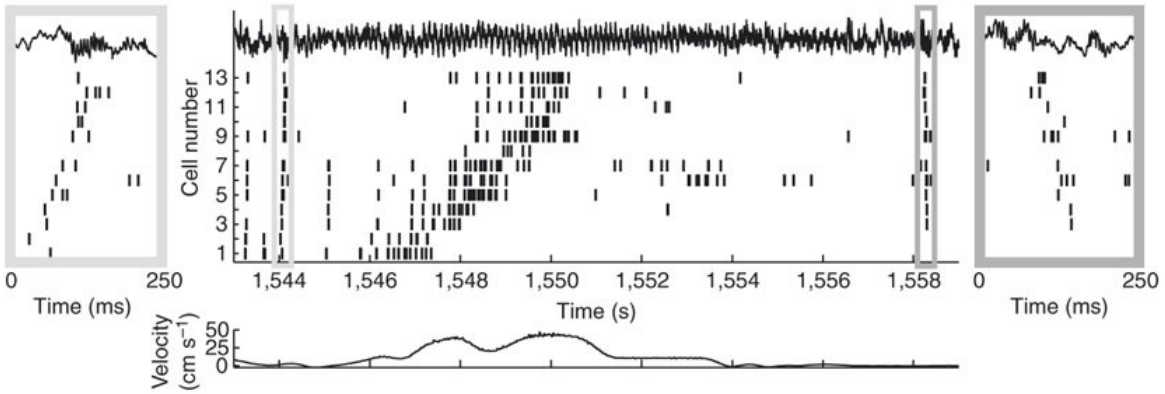

Fig. 1.7.: Sharp-wave ripples and replay of sequences in the hippocampus (Diba and Buzsáki 2008; reproduced with permission from Nature Publishing Group). Spike trains of 13 neurons before, during, and after a single lap. Also shown are the CA1 local field potential (top) and velocity of the rat (bottom). The insets show forward (left) and reverse (right) replay. Note the presence of sharp-wave ripples during the replay events.

chronization properties might help to elucidate other functions of this prominent oscillation in the hippocampal formation.

Sharp-wave ripples Sharp-wave ripples (SWR) are high frequency oscillations observed in the LFP during sleep and quite wakefulness (Fig. 1.7). I briefly review the proposed mechanisms of SWR generation and the function of SWR in consolidation.

Sharp-wave ripples can be divided into two components: a low frequency component (the sharp wave $\sim$ 10-50 Hz), and a high frequency component (the ripple $\sim$ 150-250 Hz). The sharp wave component is believed to result from synchronous bursts of a large ensemble of CA3 cells (Csicsvari et al., 2000). The dense interneuron network in the hippocampus (Klausberger et al., 2003) is believed to generate the ripple component, which in turn paces the spike timing of recruited pyramidal cells (Maier et al., 2003; Ylinen et al., 1995). Electrical communication might be also important in the generation of the high frequency component (Maier et al., 2002; Nimmrich et al., 2005). Recent experiments have provided support for the role of PV interneuron-pyramidal cell interaction in the generation of SWR (Stark et al., 2014).

Observed concurrently with SWR, is the phenomenon of neural replay which refers to the reactivation of firing patterns of place cells that were activated during behavior (Wilson and McNaughton, 1994). Such place-cell reactivation during SWR is thought to play an important role in memory consolidation (Sadowski et al., 2011; Girardeau and Zugaro, 2011). Indeed, Girardeau et al. (2009) found that selective elimination of SWR during post-training consolidation periods resulted in performance impairment in rats trained on a hippocampus-dependent spatial memory task. Interruption of awake SWR also leads to deficits in a spatial learning memory task (Jadhav et al., 2012).

1.3.3. Microcircuitry and dynamics of the hippocampus during encoding, retrieval, and consolidation

In section 1.2.2, I introduced the concept of a two-stage model which includes an online coding stage and an offline consolidation stage. On the other hand, recall or retrieval of

information is an intermediate stage that occurs during the online stage, but might depend on consolidated information in the hippocampus. The process of encoding relies on external information, i.e., outside hippocampus, while retrieval might require internal information, i.e., within hippocampus, as well (Buzsáki, 1989). Whether the hippocampus is actively participating in the encoding or retrieval of episodes may depend on the relative control of CA1 cells by their main afferents from CA3 and EC. Indeed, during learning there is a continuously changing balance between CA3 and EC drive to CA1 as a function of behavioral state (Carr and Frank, 2012). The existence of SWR (Csicsvari et al., 2000) as well as slow gamma (Colgin et al., 2009) are indicative of CA3-CA1 coupling, while fast gamma is indicative of EC-CA1 coupling (Colgin et al., 2009). The degree to which the different memory processes require extra-or intrahippocampal inputs is therefore an important open question (Carr and Frank, 2012).

The stage of online encoding is predominantly dominated by theta oscillations which are observed when the animal is actively exploring an environment (Buzsáki, 2005), and the accompanying phenomenon of phase precession (see section 1.4). It is believed that assemblies of neurons in CA3 and CA1 are actively encoding both spatial and non-spatial features that are to be flexibly combined to form an episode (Hasselmo, 2005). Cells in CA3 and CA1 have spatial receptive fields, and the firing of these spatially (and temporally) overlapping place fields could promote plasticity between sequentially active units (Dragoi and Buzsáki, 2006; Buzsáki and Moser, 2013). During online encoding, the entorhinal cortex, interface between necocortex and hippocampus, relays sensory information directly to CA1 and CA3. This transmission is enhanced by higher levels of neurotransmitters, notably acetylcholine (Hasselmo, 1999). Indeed, input from EC layer III is sufficient to sustain place-field activity in CA1 citepBrun2002 and this input is important for the encoding (but not retrieval) of a contextual memory (Suh et al., 2011). Due to the autoassociative properties of CA3 (see section 1.2.1), input from CA3 to CA1 might be more important during recall (Brun et al., 2002; Nakazawa et al., 2002; Hasselmo et al., 2002). Consistent with this idea, CA3-CA1 coupling is enhanced during memory-guided decisions in a maze (Montgomery and Buzsáki, 2007).

After online neural activity, a secondary process of consolidation and memory trace stabilization takes place during the offline epochs: quite wakefulness, rest and sleep. During these offline states, there is a reactivation of firing patterns of recent behavioral episodes (Wilson and McNaughton, 1994). Some important properties of this offline replay can be highlighted:

- Replay of place-cell activity is accompanied by sharp-wave ripples, transient high-frequency oscillations present in the local field potential (Fig. 1.7).
- The order of activation of place cell pairs during exploration is preserved and the reactivation sequence is temporally compressed relative to the original sequence (Skaggs and McNaughton, 1996).
- Hippocampal assemblies can replay sequences either in a forward (Lee and Kesner, 2002; Davidson et al., 2009) or reverse order (Foster and Wilson, 2006).
- Replay usually reflects the recent experience during encoding (O'Neill et al., 2006), unless the environment is sufficiently complex (Gupta et al., 2010).
- Replay has also been observed in the ventral striatum (Lansink et al., 2009) and prefrontal cortex (Peyrache et al., 2009).

To conclude, the processes of encoding, retrieval, and consolidation of spatial events by place-selective assemblies engage the full hippocampal circuitry. Moreover, these processes are presumably assisted by state-dependent oscillatory activity. Not all experimental results conform to this simple online encoding - offline consolidation scheme. Notably, there is the phenomenon of preplay, whereby sequences of place fields are preplayed before the actual experience takes place. This suggests that internal neuronal dynamics organize assemblies for encoding sequences that will take place in the future. A recent study has incorporated this new important result on hippocampal preplay into a theoretical framework that is in many ways different to the standard model here described (Cheng, 2013).

1.4. Phase precession: a link between oscillatory activity, neural coding, and plasticity

As discussed in the previous sections, during awake exploration there are two distinctive types of neural activity in the hippocampus: place-selective activity of single cells and LFP oscillations. In the first type, cells code for position through their firing rate within their receptive field in a restricted region of the environment whereas in the second type, the LFP reflects the synaptic and firing activity of a population of cells. Interestingly, there is a systematic relationship between the firing activity of single place-selective cells in the hippocampus and the theta rhythm observed in the LFP. When an animal enters a cell's firing field, the first spikes arrive at the so-called late phase of the theta oscillation recorded in the pyramidal cell layer. As the animal traverses the field, the spikes in subsequent cycles of the theta oscillation arrive at earlier and earlier phases. It is said that spike phases are precessing throughout the place field. Phase precession is a spiking phenomenon observed in the hippocampus (O'Keefe and Recce, 1993), and there have been many theories linking it to memory processes, particularly sequence formation (Skaggs et al., 1996; Dragoi and Buzsáki, 2006; Buzsáki and Wang, 2012). In this section I introduce phase precession, its properties, and some open questions that will be addressed in this thesis.

1.4.1. General properties of phase precession

Phase precession was first characterized by the phase-position plot, a plot of the spike phases with respect to an underlying theta oscillation as a function of position. In this plot, it is observed that during phase precession, spike phases decrease monotonically as a function of position (Fig. 1.8). This decrease is quantified by a linear correlation coefficient and a negative slope (O'Keefe and Recce, 1993). Although this is still a common way to characterize phase precession, the linear correlation analysis should be replaced by the more appropriate circular-linear correlation analysis (Kempter et al., 2012).

Phase precession as observed in the entorhinal cortex (Fig. 1.8 *A*), in the hippocampus, and subiculum have also the property of slope-size matching: the slope of phase precession is inversely related to the size of the corresponding firing field (Dragoi and Buzsáki, 2006; Maurer et al., 2006a; Kim et al., 2012; Brun et al., 2008; Kjelstrup et al., 2008). This is also equivalent to the property of constant phase-precession range, namely, that place cells tend to have a similar range independent of size or frequency. Another property typical of recordings of neural ensembles, is phase-locking at the beginning of the place field. This means that the first spikes as the animal enters the firing field occur at the "late" phase of

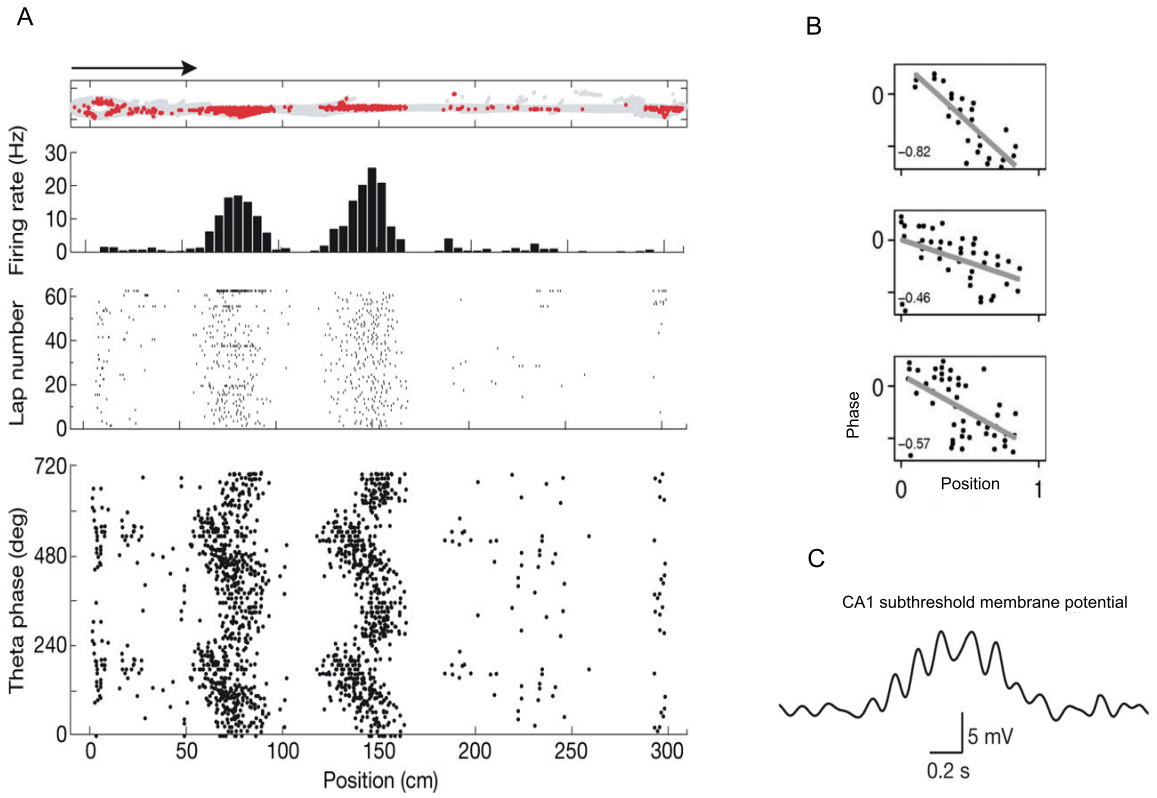

Fig. 1.8.: Phase precession in the hippocampal formation. ***A,*** Phase precession in the entorhinal cortex during running from left to right (Hafting et al. 2008; reproduced with permission from Nature Publishing Group). From top to bottom: trajectory (gray) with locations of individual spikes (red), spatial firing rate map, raster plot indicating spike positions on the track, and theta phase as a function of position (two theta cycles are shown). ***B,*** Phase precession in CA1 cells. Spike phase is plotted as a function of position within the field (y-axis, full range of 360 degrees; unlabeled tick at 180 degrees). Three different trials for the same cell are shown (Schmidt et al. 2009; reproduced with permission from Society for Neuroscience). ***C,*** In vivo subthreshold dynamics of a CA1 place cell during virtual navigation (Harvey et al. 2009; reproduced with permission from Nature Publishing Group).

the reference theta oscillation. This corresponds to the rising phase, close to the peak, of the theta LFP recorded at the pyramidal cell layer (Schmidt et al., 2009).

Another important property of phase precession is the phase-precession range which is variable, and depends on whether the analysis is based on a single trial or pooled trial basis. The first experiments showed a typical range of 360 degrees (O'Keefe and Recce, 1993), corresponding to precession over a full cycle of the theta oscillation. However, a range of 180 degrees was later found to be more typical of phase-precessing CA1 cells in single trials (Schmidt et al. 2009 and Fig.1.8 B).

Although phase precession is essentially a spiking phenomenon (O'Keefe and Recce, 1993), intracellular recordings have also contributed to our understanding of the dynamics of phase precession (Harvey et al. 2009, see Fig. 1.8 C; Domnisoru et al. 2013; Schmidt-Hieber and Häusser 2013). The subthreshold membrane potential of phase-precessing cells is characterized by an increasing and decreasing depolarization ramp and oscillatory activity

inside and outside the place field. These characteristics play a fundamental role in the validation of the inheritance model presented in Chapter 2.

Interpreting phase precession in terms of a functional role has proven challenging (Maurer and McNaughton, 2007; Robbe and Buzsaki, 2009; Lenck-Santini and Holmes, 2008). Due to the fact that phase decreases monotonically as a function of position, it was quickly recognized that phase can disambiguate entry from exit of the place field, as late phase will correspond to entry while early phase will correspond to exit (Skaggs et al., 1996). Furthermore, in subsequent studies it was shown that phase within the place field complemented the information of rate information conveyed by the average activity of the place cell (Huxter et al., 2003), and the position of the rat could be more accurately reconstructed than with rate information alone (Jensen and Lisman, 2000; Reifenstein et al., 2012). These results suggest that the hippocampus uses a phase code to represent information.

In 1996, three years after the discovery of phase precession, Skaggs and others recorded from different place cells in CA1 and dentate gyrus regions of the hippocampus. They made the important observation that the crosscorrelation of the spiking activity of two cells with overlapping place fields could be related to the important function of LTP of hippocampal synapses. The argument was that phase precession allowed for activity to be temporally compressed to fulfill the requirements of the NMDA receptor-mediated plasticity in the hippocampus. Thus, phase precession would allow for connections between co-active cells to be strengthened and consequently, sequences could be formed.

The temporal structure of crosscorrelograms of co-active cells has been investigated in many other studies afterwards (Dragoi and Buzsáki, 2006; Geisler et al., 2007; 2010; Diba and Buzsáki, 2008; Maurer et al., 2012), and will be central to the analysis of a role for phase precession in Chapter 5.

1.4.2. Mechanisms and functions underlying phase precession

Due to its proposed roles in coding and plasticity, there is an ongoing quest for understanding the significance of phase precession, and a multitude of theoretical and experimental studies tackled the question of the origin and function of phase precession. To date, both questions remain unsettled, but we have learned a great deal on how phase precession is modulated by physiological variables such as excitation, inhibition, and behavioral variables such as experience, speed, etc. In this section, I explore a few representative models of phase precession; a more complete list of published models is discussed in the introduction of Chapter 2. The function of phase precession is not yet clear, although there are some interesting suggestions that relate it to the formation of sequences (Maurer and McNaughton, 2007). Indeed, I argue in Chapter 5 that in order to elucidate the role of phase precession we must understand its mechanisms and properties so we can interfere with it.

Theoretical and experimental studies have focused on both the intrinsic properties in single cells and the connectivity patterns between different cell types in the hippocampus and entorhinal cortex to mechanistically explain phase precession (Maurer and McNaughton, 2007; Burgess and OKeefe, 2011). The most popular models, i.e., highly cited, include the oscillatory interference models (O'Keefe and Recce, 1993; Lengyel et al., 2003; Burgess et al., 2007), the somato-dendritic interference models (Kamondi et al., 1998; Harris et al., 2002; Mehta et al., 2002), and the sequence-retrieval models (Jensen and Lisman, 1996; Tsodyks et al., 1996; Wallenstein and Hasselmo, 1997; Navratilova et al., 2012) (Fig. 1.9). Oscillatory interference models explain phase precession as a beat-interference pattern between two independent oscillations of near coincident frequency, one of which is a theta oscillation and

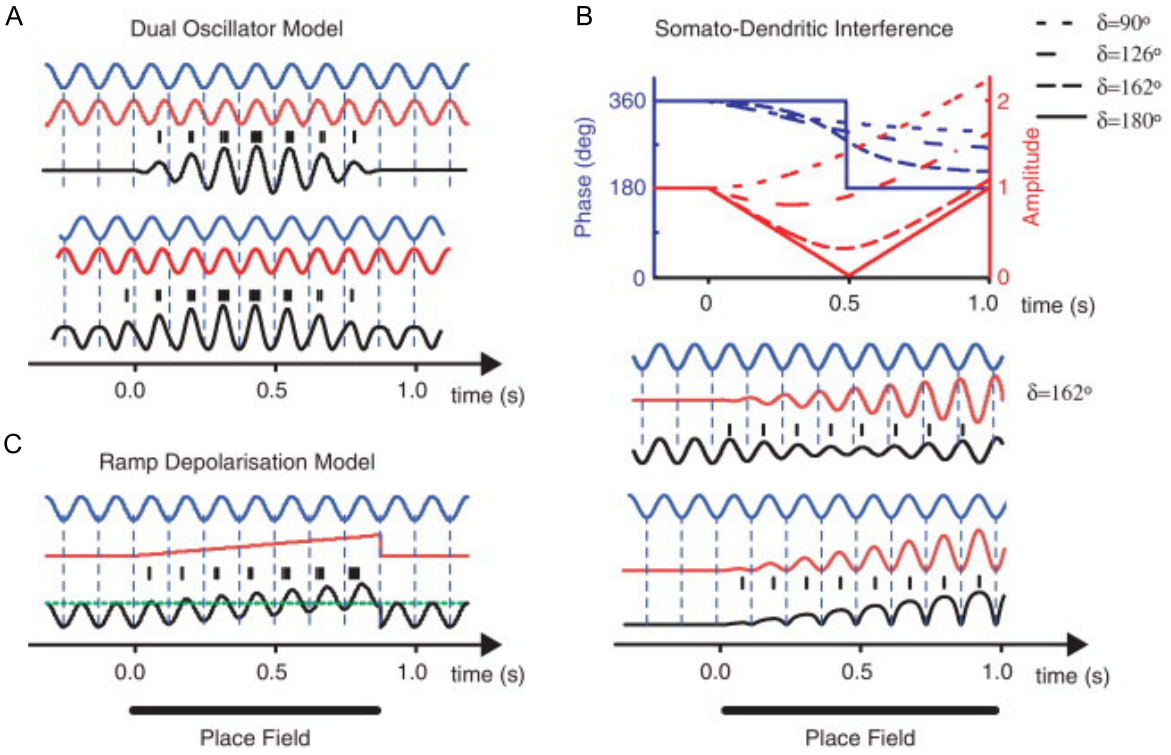

Fig. 1.9.: Cellular models of phase precession (Burgess and OKeefe 2011; reproduced with permission from Elsevier). Membrane potential dynamics (black) and inputs (blue and red) according to ***A***, the dual oscillator model (O'Keefe and Recce, 1993; Lengyel et al., 2003), ***B***, the somato-dendritic interference model (Kamondi et al., 1998; Harris et al., 2002), and ***C***, the ramp depolarization model (Mehta et al., 1997).

the other a speed or position-dependent oscillation (Fig. 1.9 *A*). This model has two basic problems. First, the model is highly susceptible to noise (Zilli et al., 2009) and second, maintaining independent oscillations in a single cell is not biophysically feasible (Remme et al., 2010). More recent implementations of the oscillatory interference model for the entorhinal cortex depend on multiple velocity-controlled oscillators (Burgess et al., 2007) and have addressed how to control noise (Burgess and Burgess, 2014). However, these models fail to reproduce the complex dependence of phase precession on trajectories in two dimensions (Reifenstein et al., 2014). Alternatively, the somato-dendritic interference (SDI) models assert that a somatic inhibitory signal interacts with an excitatory signal to produce the phenomenon. One implementation of the SDI model (Mehta et al., 2002) depends on asymmetric excitation that increases in a ramp-like manner as the animal traverses the place field, so that phase precession is generated in every theta cycle where excitation surpasses inhibition (Fig. 1.9 *B*). The strong asymmetry requirement, however, does not always hold for phase precessing cells (Schmidt et al., 2009). Furthermore, perisomatic inhibition might not be necessary for phase precession to be observed in CA1 (Royer et al., 2012). Another implementation of the SDI model (Kamondi et al., 1998; Harris et al., 2002), depends on intrinsic oscillatory activity from dendrites interfering with oscillatory activity in the soma (Fig. 1.9 *C*). A problem with this particular implementation of the SDI model is that it has difficulties reproducing the waxing and waning of the firing rate without compromising the phase-position relationship (Harris et al., 2002), as well as reproducing the relative

amplitudes of the membrane potential inside and outside the place field (Harvey et al., 2009). Finally, sequence-retrieval models suggest that firing at the end of the place field is driven by sensory, i.e., external inputs at early theta phases, while firing at the beginning is due to spread of activity from recurrently connected place cells with place fields earlier along the track (Tsodyks et al., 1996; Jensen and Lisman, 1996; Wallenstein and Hasselmo, 1997). A change of phase occurs because of a transition from internal to external inputs. A problem with this model is the assumption of asymmetric connectivity which would require Hebbian learning, i.e., experience, to develop. However, phase precession has been observed in novel environments (Cheng and Frank, 2008), and blocking NMDA receptors in the hippocampus (responsible for LTP at these synapses), does not impair phase precession (Ekstrom et al., 2001). To conclude, the mechanisms behind phase precession generation remain unsettled. For further information on the assumptions, strengths, and weaknesses of models of phase precession in general, I refer the reader to the articles by Zugaro et al. (2005), Maurer and McNaughton (2007), Harvey et al. (2009), Burgess and OKeefe (2011), Domnisoru et al. (2013), Schmidt-Hieber and Häusser (2013), Eggink et al. (2014), Jaramillo et al. (2014), and Reifenstein et al. (2014).

Open questions What is then, the origin of phase precession? A clue for answering this question might come from observing all the regions in the brain where phase precession has been described. Is phase precession generated independently in each region, or conversely, can phase precession be propagated to downstream structures by means of the propagation of excitation?

The idea that phase precession can be inherited was first put forward by Skaggs in their 1996 paper, and other authors have considered this possibility since (e.g. Cutsuridis and Hasselmo, 2012; Chance, 2012). However, to date there has been no computational study that has addressed this question systematically, and provide predictions that could be tested experimentally. A major part of this thesis aims to fill this gap in the modeling literature, by providing a simple but realistic model of neural integration and signal transmission that accounts for the presence of phase precession in the different regions of the hippocampal formation, as well as other regions of the brain where phase precession has been observed (Jaramillo et al., 2014).

1.5. Scope of the thesis

[1] In this thesis, I explore the origin and function of phase precession of pyramidal cells. I develop an argument on why phase precession can exist in different regions of the brain by characterizing phase precession as an oscillatory signal that can be propagated to different stages of the hippocampal formation, as well as to other extra-hippocampal areas such as the ventral striatum and the prefrontal cortex. The idea that excitatory oscillatory activity can be propagated through feed-forward networks constitutes the inheritance hypothesis.

In Chapter 2, I explore the inheritance hypothesis by first considering the CA3-CA1 network in the hippocampus. Based on a combined approach of computational modeling and data analysis and interpretation, I show how phase precession in CA1 can be "inherited" from CA3 by elucidating the roles of excitation and inhibition in a simple neural integration model.

[1] The work in Chapters 2, 3, and 4 of the thesis are divided into Summary, Introduction, Methods, Results, and Discussion. Importantly, the Results sections are self-contained and will occasionally reference the Methods section for further clarification of the model and equations.

A fundamental assumption of this chapter and of the phase-precession inheritance hypothesis in general, is the idea that place fields can be inherited as well. Accordingly, in Chapter 3 I consider the problem of structure formation in the hippocampus, exemplified by the CA3-CA1 feed-forward network connectivity. I tackle the question of whether an initially random distribution of synaptic strengths can evolve to a distribution that effectively represents place fields in both CA3 and CA1 via a learning rule such as spike-timing-dependent plasticity. Then, in Chapter 4, I reconsider the inheritance hypothesis in the framework of general feed-forward topologies in the hippocampal formation and adjacent structures to complement the ideas developed in Chapter 2. Some issues that are addressed include the presence of phase precession outside the hippocampus, the relatively little incidence of phase precession in interneurons, the role of spatial distributions of place-field centers, and the possibility that phase-precessing place cells can inherit their spike-timing properties from grid cells in the entorhinal cortex. To complement the mechanistic perspective of phase precession in Chapters 2, 3, and 4, I finally address the functional role of phase precession in Chapter 5. This includes a critical review of the literature that provides evidence of behavioral correlates of phase precession as well as an original framework to study phase precession in the future. Finally, I provide a summary and outlook of this thesis in Chapter 6 and a series of outstanding research questions related to the very intriguing phenomenon of phase precession in the hippocampal formation.

2. Inheritance of phase precession: from CA3 to CA1

In this chapter I pose the "inheritance of phase precession" problem in the context of the CA3-CA1 network. The results obtained here will lead to other interesting issues such as the inheritance of place fields (addressed in Chapter 3), and inheritance of phase precession in other feed-forward topologies (addressed in Chapter 4).

2.1. Summary

[1]Spatial information about the environment is encoded by the activity of place and grid cells in the hippocampal formation. As an animal traverses a cell's firing field, action potentials progressively shift to earlier phases of the theta oscillation (6–10 Hz). This "phase precession" is observed also in the prefrontal cortex and the ventral striatum, but mechanisms for its generation are unknown. However, once phase precession exists in one region, it might also propagate to downstream regions. Using a computational model, I analyze such inheritance of phase precession, for example from CA3 to CA1. I find that distinctive subthreshold and suprathreshold features of the membrane potential of CA1 pyramidal cells (Harvey et al., 2009; Mizuseki et al., 2012; Royer et al., 2012) can be explained by inheritance, and that excitatory input is essential. The model explains how inhibition modulates slope and range of phase precession, and provides two main testable predictions. First, theta-modulated inhibitory input to a CA1 pyramidal cell is not necessary for phase precession. Second, theta-modulated inhibitory input on its own generates membrane-potential peaks that are in phase with peaks of the extracellular field. The results suggest that inheritance is a plausible mechanism to explain the observed phase precession in the CA1 region of the hippocampus.

2.2. Introduction

The study of place-specific firing and local field potential (LFP) oscillations in the rodent hippocampal formation could be important to understand navigation and episodic memory (Buzsáki, 2005). Within a place field, action potentials exhibit phase precession, i.e., the firing phases relative to the LFP theta decrease as a function of position (O'Keefe and Recce, 1993). Phase precession can encode spatial information (Jensen and Lisman, 2000; Reifenstein et al., 2012) and can temporally compress behavioral sequences to match the time scales of neuronal plasticity (Skaggs et al., 1996; Bi and Poo, 1998). Mechanisms generating

[1]Part of the work presented in this chapter has been published in "Modeling inheritance of phase precession in the hippocampal formation", J Neurosci 2014. This project was a collaboration with Robert Schmidt and Richard Kempter as principal supervisor. I conceived the project, performed all simulations, analytical calculations, and interpretation of the results of this chapter.

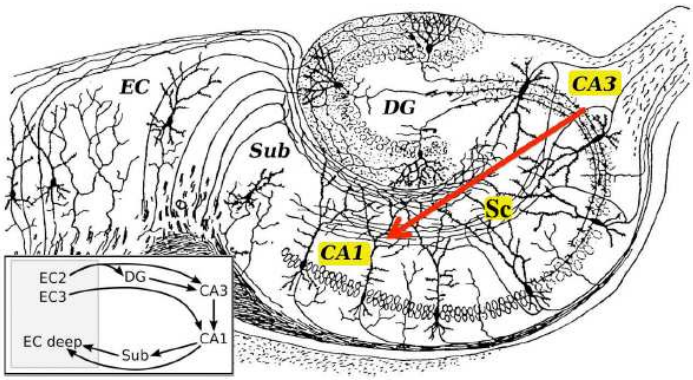

Fig. 2.1.: Transverse slice of the rat hippocampus showing the distinct regions of the hippocampal formation: the cornu Ammonis regions 3 (CA3) and 1 (CA1), the dentate gyrus (DG), the subiculum (Sub), and the entorhinal cortex (EC). Source: Adapted from Santiago Ramon y Cajal, "Histologie du Systeme nerveux de l'Homme et des Vertebres", Paris (1911). The Schaffer collateral system connects the CA3 pyramidal cells to CA1 pyramidal cells (red arrow).

phase precession, however, remain unresolved (Maurer and McNaughton, 2007; Burgess and OKeefe, 2011).

Network models of phase precession (Maurer and McNaughton, 2007) emphasize the special roles of recurrent inputs from cells with neighboring place fields (Jensen and Lisman, 1996; Tsodyks et al., 1996; Wallenstein and Hasselmo, 1997; Baker and Olds, 2007; Navratilova et al., 2012), coupled excitatory and inhibitory neurons (Bose A. et al., 2000; Castro and Aguiar, 2012; Cutsuridis and Hasselmo, 2012), and a summed-population effect (Geisler et al., 2010; Thurley et al., 2013). Alternatively, cellular models suggest that phase precession results from an interaction between a somatic and a dendritic signal within a cell (Kamondi et al., 1998; Magee, 2001; Harris et al., 2002; Mehta et al., 2002; Leung, 2011), a superposition of two oscillations with different frequencies (O'Keefe and Recce, 1993; Lengyel et al., 2003; O'Keefe and Burgess, 2005), synaptic facilitation (Thurley et al., 2008), persistent firing (Hasselmo, 2008), or excitatory inputs from two regions (Chance, 2012). The possibility of feed-forward inheritance, however, has not been studied thoroughly.

Phase precession models should be able to explain phase precession as observed in the different regions of the hippocampal formation and brain. Some problems arise, however, when the above mentioned models are applied to the CA1 region of the hippocampus. Network models, for example, assume recurrent excitatory connectivity and a particular asymmetric profile (Maurer and McNaughton, 2007). In CA3 such excitatory recurrent connectivity exists (Li et al., 1994), while the CA1 region of the hippocampus is more amply characterized by a dense inhibitory network (Klausberger et al., 2003). Furthermore, a place-cell topographic representation is assumed for these models: cells that have neighboring place fields in space are assumed to be adjacent in the hippocampus. Several studies have shown, however, that this is not necessarily the case (Redish et al., 2001; Dombeck et al., 2010). For cellular models that rely on interference between excitation and a somatic inhibitory signal, several observations can be made. In a variant of these models citepMehta2002, asymmetric excitation interferes with oscillatory somatic inhibition. This variant requires asymmetric excitation to avoid phase recession at the end of the place field. However, place cells with either symmetric or asymmetric place fields exhibit phase precession (Schmidt et al., 2009).

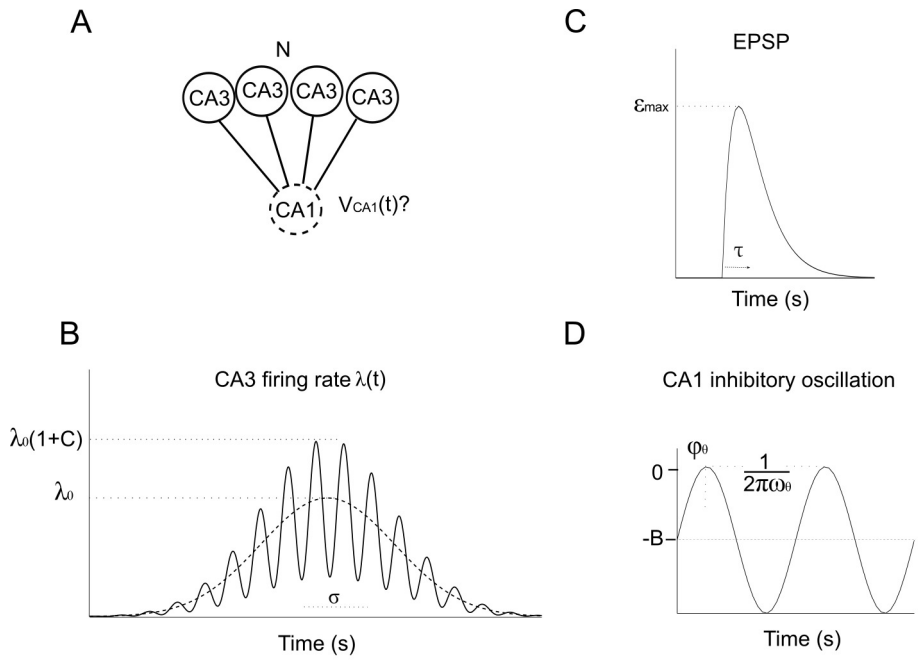

Fig. 2.2.: Model parameters for CA3-CA1 inheritance. ***A,*** Basic topology of the inheritance model, where N CA3 place cells project to a CA1 cell. ***B,*** Description of the average firing rate of the CA3 phase-precessing place cell population. ***C,*** Stereotypical EPSP in CA1 produced by an incoming spike. ***D,*** Inhibitory oscillation with angular frequency ω_θ and shifted by a phase ϕ_θ with respect to the theta local field potential recorded in the CA1 pyramidal layer.

Furthermore, the excitation does not have an oscillatory structure in this model, although most excitatory input comes from CA3 or entorhinal cells whose activities are theta modulated and phase precessing (Mizuseki et al., 2009). Thus, in principle excitation alone could suffice to explain phase precession in CA1.

In this chapter, I investigate how phase precession can be propagated from one region to another (Fig. 2.1). I first analyze how phase precession in CA3 can lead to characteristic subthreshold (Harvey et al., 2009) and suprathreshold (e.g. Mizuseki et al., 2012) features of phase precession in a CA1 place cell. This framework, however, is general and can be used as a starting point to investigate the propagation of phase precession to other regions (see Chapter 4). I also outline how inhibition modulates phase precession in CA1 (Royer et al., 2012) and make two testable predictions on the necessity of inhibition for phase precession, and on the relative phases of intracellular oscillations outside the place field and theta local field potential (LFP) recorded extracellularly in the CA1 pyramidal layer.

2.3. Methods

2.3.1. Model of the CA1 membrane potential

I model the membrane potential $V_{\mathrm{CA1}}(t)$ at the soma of a CA1 pyramidal cell (Fig. 2.2 A) by considering an inhibitory and an excitatory component. Phase-precessing excitatory input

from CA3 to CA1 is characterized by the dynamics of the CA3 population firing rate and the shape of excitatory postsynaptic potentials (EPSPs); input from the entorhinal cortex is neglected in this simplest version of the model, but the model can also account for such input (see Chapter 4). To model the excitatory component from CA3, it is assumed that the animal is traversing a place field with constant speed so that time and space are equivalent up to a constant conversion factor. The place fields of the cells of the CA3 population are assumed to be identical and completely overlapping. This assumption will be relaxed when I consider partially overlapping fields in Chapter 4.

The time course of the firing rate of a CA3 cell is described by two parts. The first part reflects the place field: the average firing rate increases when the animal enters the place field, achieves its maximum at the center of the place field, and decreases when the animal exits the place field. I describe this ramp-like behaviour of the firing rate with a Gaussian function $x(t)$ around the center t_c of the place field,

$$x(t) = \exp\left[\frac{-(t-t_c)^2}{\sigma^2}\right], \tag{2.1}$$

where σ determines the place-field width ($\sim 3\sigma$). The second part of the firing-rate model is an oscillatory modulation that accounts for CA3 phase precession. The oscillatory modulation

$$1 + C\cos(\omega_\lambda t - \phi_\lambda) \tag{2.2}$$

is characterized by the angular frequency ω_λ where $\omega_\lambda = 2\pi f_\lambda$ and f_λ is the frequency of the oscillation, the phase offset ϕ_λ with respect to the reference theta LFP, and the modulation depth C. Multiplying this oscillatory modulation with the ramp $x(t)$ in Equation 2.1, I find the firing-rate model of the input of one CA3 cell to a CA1 cell as

$$\lambda(t) = \lambda_0\left[1 + C\cos(\omega_\lambda t - \phi_\lambda)\right]x(t), \tag{2.3}$$

where λ_0 is the average firing rate in the center of the field. The combined firing rate from a population of N identical CA3 cells is then $N\lambda(t)$ (Fig. 2.2 *A* and *B*).

To ensure that the oscillating, place-field like, excitatory input rate $\lambda(t)$ to a CA1 pyramidal cell shows phase precession, I assume that f_λ is greater than the theta frequency $f_\theta = 8$ Hz (Geisler et al., 2010); furthermore, one requires several oscillation cycles within a place field, that is, $3\sigma \gg 1/f_\theta$; typically $\sigma \sim 0.3$ s corresponding to a place-field size of ~ 1 s (Fig. 2.3 *A*).

The rate $\lambda(t)$ serves as a basis to generate the spiking input to a CA1 pyramidal cell. To model the variability of spiking input, I describe the activity of a population of N CA3 cells by an inhomogeneous Poisson process with time-dependent firing rate $N\lambda(t)$. A spike at time t_f is represented as a delta function $\delta(t - t_f)$ centered at the time of firing. Combining the spikes from all N input cells, one obtains the total neural response function

$$R(t) = \sum_f \delta(t - t_f),$$

where t_f is the fth spike time. An example is shown in Figure 2.3 *B*. For the analysis and the simulations described below, it is important at what times neurons in the input population were active, but it is not important which particular CA3 neuron actually fired.

To describe how an input spike affects the membrane potential of a CA1 pyramidal cell,

I assume that each spike elicits an EPSP that is identical for all spikes and all input neurons. For simplicity, I model EPSPs by an alpha function

$$\epsilon(t) = \frac{\epsilon_{\max}}{\tau}\, t\, \exp\left(1 - \frac{t}{\tau}\right) \tag{2.4}$$

where $\epsilon_{\max}$ is the maximum amplitude obtained at $t = \tau$, and τ determines both the rise time and decay time of the EPSP (Fig. 2.2 *C*). I restrict the domain of $\epsilon(t)$ to positive time values, i.e., $t > 0$, and assume that $\epsilon(t) = 0$ for $t \leq 0$. The CA3 contribution to the CA1 excitation $v_{\text{input}}(t)$ for a Poisson spiking model is then

$$v_{\text{input}}(t) = R(t) * \epsilon(t) \tag{2.5}$$

$$= \sum_f \epsilon(t - t_f), \tag{2.6}$$

where $*$ represents the operation of convolution. An example simulation is shown in Figure 2.3 *C*. Inhibitory input is characterized by an ongoing oscillation of the membrane voltage of a CA1 pyramidal cell. The oscillation is coherent with the theta LFP (Kamondi et al., 1998; Bland et al., 2005) and is independent of place-field activity (Harvey et al., 2009; Epsztein et al., 2011). I model this intracellular theta oscillation with a sinusoidal function

$$V_\theta(t) = B\,[-1 + \cos(\omega_\theta t - \phi_\theta)] \tag{2.7}$$

where B is the amplitude of the oscillation, ω_θ is its angular frequency ($\omega_\theta = 2\pi f_\theta$, and f_θ is the frequency of the theta LFP), and ϕ_θ is the phase of the intracellular oscillation peak with respect to the theta LFP peak. Here I use the convention that 0 degrees corresponds to the peak of the theta LFP recorded in the CA1 pyramidal cell layer. Note that the DC level of the inhibitory contribution $V_\theta(t)$ is below zero, i.e., the oscillation is always hyperpolarizing.

To model the time course of the subthreshold membrane potential of a CA1 pyramidal cell during a place-field traversal, the inhibitory component in Equation 2.7 is added to the excitatory component in Equation 2.6. The total subthreshold membrane potential is

$$v_{\text{CA1}}(t) = V_\theta(t) + v_{\text{input}}(t) + V_{\text{rest}} \tag{2.8}$$

where V_{rest} is the resting membrane potential, which is -70 mV in the simulations. The example simulation in Figure 2.3 *E* shows that outside the place field, i.e. where excitatory input is negligible, the membrane potential oscillates at theta frequency f_θ with amplitude B and peaks at phase $\phi_\theta = 0$ degrees with respect to the LFP, i.e., peaks concurrently with the LFP peak. Within the place field, inhibitory and excitatory input interfere. The phases (again with respect to the LFP) of local maxima of the membrane potential are plotted against time in Figure 2.3 *F*.

Analytical expressions for the mean-field subthreshold membrane potential. To mathematically describe properties of the model of the membrane potential of a CA1 pyramidal cell, I first derive expressions for the mean-field, i.e., the trial-averaged, membrane potential. The noise due to the variable and discrete spiking activity of the CA3 neurons is characterized at a later stage.

2. Inheritance of phase precession: from CA3 to CA1

The mean-field expression for the excitatory input in Equation 2.6 is

$$V_{\text{input}}(t) = \langle v_{\text{input}}(t) \rangle \tag{2.9}$$
$$= \langle R(t) \rangle * \epsilon(t) \tag{2.10}$$
$$= N\lambda(t) * \epsilon(t), \tag{2.11}$$

where $\langle . \rangle$ indicates trial averaging. Note that I have used an upper-case V to denote a mean-field voltage. To proceed, I consider the kernel $\epsilon(t)$ as a filter $\tilde{\epsilon}(\omega) := F(\epsilon(t))(\omega)$ in the frequency domain where F denotes the Fourier transform. The filter $\tilde{\epsilon}$ has magnitude $|\tilde{\epsilon}(\omega)| = (\mathrm{e}\,\epsilon_{\max}\tau)/(1+\omega^2\tau^2)$ and phase $\phi(\omega) = \arg(\tilde{\epsilon}(\omega)) = 2\tan^{-1}(\omega\tau)$ where arg denotes the operation that yields the angle of a complex number. Using Equations 2.3 and 2.4, one can approximate $V_{\text{input}}(t)$ for $\omega = \omega_\lambda \gg 1/\sigma$,

$$V_{\text{input}}(t) \approx \mathrm{e}\,N\lambda_0\epsilon_{\max}\tau + N\lambda_0 C|\tilde{\epsilon}(\omega_\lambda)|\cos\left[\omega_\lambda(t-\tau_\phi) - \phi_\lambda\right] x(t-\tau_g), \tag{2.12}$$

where $\tau_\phi = -\frac{\partial\phi(\omega)}{\partial\omega}$ is the phase delay and $\tau_g = -\frac{\phi(\omega)}{\omega}$ is the group delay (Haykin, 2009). For the time scales involved in this integration problem ($\omega_\lambda\tau \lesssim 1$), one can approximate $\tau_\phi \approx \tau_g \approx 1.8\tau$ and rewrite the above expression as

$$V_{\text{input}}(t) \approx \mathrm{e}\,N\lambda_0\epsilon_{\max}\tau\left\{1 + \frac{C}{1+\omega_\lambda^2\tau^2}\cos\left[\omega_\lambda(t-1.8\tau) - \phi_\lambda\right]\right\} x(t-1.8\tau). \tag{2.13}$$

The excitatory contribution $V_{\text{input}}(t)$ to the CA1 membrane voltage is therefore a scaled (by $\mathrm{e}\,N\epsilon_{\max}\tau$), temporally shifted (by 1.8τ), and filtered (by $1/(1+\omega_\lambda^2\tau^2)$) version of the CA3 firing rate $\lambda(t)$ in Equation 2.3. The total mean-field membrane potential, including the ongoing theta oscillation and the resting membrane potential, is

$$\begin{aligned} V_{\text{CA1}}(t) &= V_{\text{input}}(t) + V_\theta(t) + V_{\text{rest}} \\ &\approx \mathrm{e}\,N\lambda_0\epsilon_{\max}\tau\left\{1 + \frac{C}{1+\omega_\lambda^2\tau^2}\cos[\omega_\lambda(t-1.8\tau) - \phi_\lambda]\right\} x(t-1.8\tau) + \\ &B[-1 + \cos(\omega_\theta t - \phi_\theta)] + V_{\text{rest}}. \end{aligned} \tag{2.14}$$

To further characterize the mean-field membrane potential V_{CA1} and to be able to compare its properties to experimentally accessible quantities, I assume that in the center of the place field (where $x(t) \approx 1$) the oscillation of the membrane potential is mainly due to the excitatory input from CA3, which means that the oscillation amplitude due to the ongoing inhibitory input can be neglected. In other words, I assume that $\mathrm{e}\,CN\lambda_0\epsilon_{\max}\tau \gg B$. Using this approximation, in the center of the place field the oscillation amplitude is

$$\Delta V_{\text{osc}} = \frac{\mathrm{e}\,CN\lambda_0\epsilon_{\max}\tau}{1+\omega_\lambda^2\tau^2}. \tag{2.15}$$

Furthermore, the CA1 membrane potential shows a mean depolarization ramp

$$\Delta V_{\text{ramp}} = \mathrm{e}N\lambda_0\epsilon_{\max}\tau. \tag{2.16}$$

One can readily calculate the modulation depth $C_{V_{\text{CA1}}}$ of the CA1 membrane potential by

taking the ratio of the oscillation amplitude ΔV_{osc} and the average depolarization ΔV_{ramp},

$$C_{V_{\text{CA1}}} := \frac{\Delta V_{\text{osc}}}{\Delta V_{\text{ramp}}} = \frac{C}{1+\omega_\lambda^2\tau^2} \tag{2.17}$$

where C is, as before, the modulation depth of the CA3 population activity. In other words, the modulation depth $C_{V_{\text{CA1}}}$ of the CA1 mean-field membrane potential oscillation is a filtered (by $1/(1+\omega_\lambda^2\tau^2)$) version of the modulation depth C of the CA3 firing rate.

Quantitative analysis of membrane-potential noise. The membrane potential of the CA1 model cell shows fluctuations because the input is described by discrete spikes, and spike times are generated by a Poisson process. Below I perform a quantitative analysis of this variability that is termed shot noise. The properties of this noise will then be compared to the properties of the mean-field membrane potential.

One way of quantifying the effects of shot noise on the excitatory contribution $v_{\text{input}}(t)$ is by calculating its standard deviation

$$\delta v_{\text{input}} = \sqrt{\langle \Delta v_{\text{input}}^2 \rangle} \tag{2.18}$$

where $\langle . \rangle$ denotes, again, an average of realizations, or trials, of the Poisson process. Note that this standard deviation of the membrane potential does not take into account the ongoing oscillations V_θ. The second moment of the membrane potential in Equation 2.6 is defined as

$$\langle v_{\text{input}}^2(t) \rangle = \left\langle \left[\sum_k \epsilon(t-t_k) \right]^2 \right\rangle \tag{2.19}$$

$$= \left\langle \sum_k \sum_j \epsilon(t-t_k)\epsilon(t-t_j) \right\rangle . \tag{2.20}$$

The next step in the analysis is to separate the terms dependent on the realization from those that are independent. For this, one partitions the spike-train into time intervals $I_l = [t_l\ t_{l+1})$ of infinitesimal length Δt_l. I introduce a function $\Gamma(l)$ that counts the number of events, i.e., spikes, in the interval I_l. One can thus write the second moment as

$$\langle v_{\text{input}}^2(t) \rangle = \left\langle \sum_{l' \neq l} \epsilon(t-t_l)\epsilon(t-t_{l'})\Gamma(l)\Gamma(l') + \sum_l \epsilon^2(t-t_l)\Gamma^2(l) \right\rangle \tag{2.21}$$

where I have separately considered the cases $l \neq l'$ and $l = l'$. Using the definition of an inhomogeneous Poisson process (e.g. Kempter et al., 1998), I perform an average of the functions Γ over realizations to obtain $\langle \Gamma(l)\Gamma(l') \rangle = N^2\lambda(t_l)\Delta t_l \lambda(t_{l'})\Delta t_{l'}$ and $\langle \Gamma^2(l) \rangle = N\lambda_l \Delta t_l$. With these averages, I can express Equation 2.21 as a Riemann sum that equates to two convolutions in the limit when Δt_l and $\Delta t_{l'}$ tend to zero:

$$\langle v_{\text{input}}^2(t) \rangle = [N\lambda(t) * \epsilon(t)]^2 + N\lambda(t) * \epsilon^2(t). \tag{2.22}$$

Finally, using Equations 2.11 and 2.22, one can calculate the variance of the membrane

potential,

$$\left\langle \Delta v^2_{\text{input}}(t) \right\rangle = \langle v^2_{\text{input}}(t) \rangle - \langle v_{\text{input}}(t) \rangle^2 \tag{2.23}$$

$$= N\lambda(t) * \epsilon^2(t). \tag{2.24}$$

To obtain a closed expression of the variance, I approximate the function $\epsilon^2(t) = \frac{\epsilon^2_{\max}}{\tau^2} \cdot t^2 \exp[2(1 - \frac{t}{\tau})]$ with a delta function

$$\epsilon^2(t) \approx \frac{\mathrm{e}^2}{4} \tau \epsilon^2_{\max} \delta(t - \tau) \tag{2.25}$$

where the factor $\frac{\mathrm{e}^2}{4}\tau\epsilon^2_{\max}$ equals the integral $\int_0^\infty \mathrm{d}t\, \epsilon^2(t)$. Now the convolution is easy to perform, and the variance is

$$\left\langle \Delta v^2_{\text{input}}(t) \right\rangle \approx \frac{N\mathrm{e}^2}{4} \tau \epsilon^2_{\max} \lambda(t - \tau). \tag{2.26}$$

The input firing rate $\lambda(t - \tau)$ depends on time t, and so does the variance $\langle \Delta v^2_{\text{input}} \rangle$. To obtain a time-independent estimate of the variance that characterizes the noise within the place field, I replace the time-dependent rate $\lambda(t - \tau)$ by the average firing rate λ_0 in the center of the place field. A typical value of the standard deviation δv_{input} of the membrane potential then is

$$\delta v_{\text{input}} = \frac{\mathrm{e}\, \epsilon_{\max}}{2} \sqrt{N\lambda_0 \tau}. \tag{2.27}$$

I can now construct a "quality parameter" ρ of the membrane potential that characterizes the relative strength of the oscillation amplitude ΔV_{osc} with respect to the noise amplitude δv_{input}:

$$\rho := \frac{\mathrm{e}}{2} \frac{\Delta V_{\text{osc}}}{\delta v_{\text{input}}}$$

$$= \frac{C}{1 + \omega^2_\lambda \tau^2} \sqrt{N\lambda_0 \tau}. \tag{2.28}$$

The prefactor e/2, which is close to 1, was introduced to arrive at a simple expression devoid of an irrelevant numerical prefactor. The contributions to the quality parameter ρ are therefore: the number N of active CA3 cells projecting to a single CA1 cell, the time constant τ of the EPSP, the modulation depth C of the population rate oscillation at angular frequency ω_λ, and the mean firing rate λ_0 in the center of the place field. Using Equations 2.15 and 2.16, one can rewrite the above expression of the quality parameter ρ in terms of experimentally measurable voltages ΔV_{ramp}, and ΔV_{osc} as

$$\rho = \frac{\Delta V_{\text{osc}}}{\sqrt{\mathrm{e}\, \epsilon_{\max} \Delta V_{\text{ramp}}}}. \tag{2.29}$$

Furthermore, using Equation 2.15 for ΔV_{osc}, Equation 2.16 for ΔV_{ramp}, and Equation 2.28 for ρ one can determine C, N, and $\epsilon_{\max}$. To obtain an explicit expression for C, I use the

ratio of ΔV_{osc} and ΔV_{ramp} and rearrange the terms:

$$C = \frac{\Delta V_{\text{osc}}}{\Delta V_{\text{ramp}}} \left[1 + (2\pi\, f_\lambda\, \tau)^2\right] \ . \tag{2.30}$$

Using this result for C in Equation 2.28, I find

$$N = \left(\frac{\Delta V_{\text{ramp}}}{\Delta V_{\text{osc}}}\right)^2 \frac{\rho^2}{\lambda_0\, \tau} \ . \tag{2.31}$$

Inserting this result for N in Equation 2.16, I obtain

$$\epsilon_{\text{max}} = \frac{\Delta V_{\text{osc}}}{\rho^2} \left(\frac{\Delta V_{\text{osc}}}{\Delta V_{\text{ramp}}}\right) \ . \tag{2.32}$$

I am thus able to derive and predict values of the model parameters C, N and ϵ_{max}. To provide an estimate of the error of the prediction, for example of N, based on known and measurable parameters as in Equation 2.31, one can use a rule of propagation of errors as

$$\delta N = \sqrt{\left(\frac{\partial N}{\partial V_{\text{ramp}}}\right)^2 (\delta \Delta V_{\text{ramp}})^2 + \left(\frac{\partial N}{\partial V_{\text{osc}}}\right)^2 (\delta \Delta V_{\text{osc}})^2 + \left(\frac{\partial N}{\partial \lambda_0}\right)^2 (\delta \lambda_0)^2 + \left(\frac{\partial N}{\partial \tau}\right)^2 (\delta \tau)^2}, \tag{2.33}$$

where δN is the (predicted) error of the estimate of N, and $\delta \Delta V_{\text{ramp}}, \delta \Delta V_{\text{osc}}$, $\delta \lambda_0$, and $\delta \tau$ are standard errors of the mean, obtained from the literature (Harvey et al., 2009; Magee and Cook, 2000; Mizuseki et al., 2009; 2012).

Estimation of the CA3 firing rate from a phase precession recording. Here I estimate the shape of the firing rate of a population of CA3 cells based on a plot of phase vs. normalized position for phase-precessing CA3 cells (Fig. 2.5 *A*). As the phase-position plot contains data from many different trials, one can expect to obtain only an approximate version of the true firing rate of a population of CA3 cells in one trial. To calculate the firing rate, I recreated a trajectory that an animal possibly followed to produce such a phase-position plot. The trajectory is shown as a set of diagonal blue lines in Figure 2.5 *A*. The trajectory of the virtual animal was determined by its position (the x axis of the plot) and phase (the y axis of the plot). Note that both spike phase and time are represented by the y axis of the plot, the difference being a conversion factor modulo 360 degrees. The movement of the animal was followed along each diagonal line. The slope of each line is the same and was determined by a constant speed which I assumed. I counted the spikes within a predefined time window along the trajectory. Because phase is a circular variable whereas time is always monotonously increasing, the diagonal line along which the trajectory of the animal is followed (and hence the spike count) continues until it reaches 360 degrees in the y axis, and then starts again from 0. One obtains a spike count for each window until the animal exits the place field. Thus, a spike histogram over cells and trials was effectively extracted from the phase-position plot and in this way, I obtained a grand-average population firing rate. The resulting firing rate along the track was then linearly scaled so that the extracted peak firing rate from the phase-position plot corresponded to an a priori known maximum firing rate of a CA3 cell. I used 20 Hz for the peak firing rate (e.g. Mizuseki et al., 2012).

2.3.2. Suprathreshold model of phase precession

To account for phase precession of spikes of CA1 cells, I used the two-compartment model that was developed by Pinsky and Rinzel (1994) for CA3 cells and adapted to the CA1 region by Kamondi et al. (1998). This particular model reproduces bursting in CA1 pyramidal neurons. The voltages V_s and V_d are described by the following differential equations,

$$C_m \frac{\mathrm{d}V_s}{\mathrm{d}t} = -I_L - I_{Na} - I_K - \frac{g_c}{p}(V_s - V_d) + I_s/p \tag{2.34}$$

$$C_m \frac{\mathrm{d}V_d}{\mathrm{d}t} = -I_L - I_{Na_p} - I_{K_s} - \frac{g_c}{1-p}(V_d - V_s) + I_d/(1-p) \tag{2.35}$$

where s and d stand for somatic and dendritic compartment, respectively, C_m is the membrane capacitance per unit area, I_L is a (ohmic) leak current density, I_{Na} is a sodium current density, I_K is a potassium current density, I_{Na_p} is a persistent sodium current density, I_{K_s} is a slow potassium current density, g_c is the coupling conductance between the two compartments (s and d), p is the ratio of the somatic area to the total area, I_s is the synaptic current density applied to the soma, and I_d is the synaptic current density applied to the dendrite. The current densities I_{Na}, I_{Na_p}, I_K, and I_{K_s} are described by the Hodgkin-Huxley formalism (Pinsky and Rinzel, 1994). The values for the intrinsic conductances are taken from Kamondi et al. (1998).

The synaptic current density I_d in the model represents the phase-precessing activity of the presynaptic CA3 cells and is modeled as a sum of excitatory postsynaptic currents (EPSCs) in a similar fashion as for the subthreshold model, where the CA3 input was modeled as a sum of EPSPs. As for the subthreshold model, I assume that spikes are generated via an inhomogeneous Poisson process, and convolve the respective neural response function with an EPSC. A single EPSC kernel is represented by an alpha function (as in Equation 2.4), i.e.,

$$\epsilon_I(t) = \frac{\epsilon_{I_{\max}}}{\tau_I} t \exp\left[1 - \frac{t}{\tau_I}\right] \tag{2.36}$$

where the subscript I indicates a current kernel. The convolution of the EPSC kernel ϵ_I with the neural response function $R(t)$, i.e., the CA3 spike train generated via a Poisson process, is precisely the current density I_d that is fed onto the dendrite:

$$I_d = \frac{1}{A_d}\epsilon_I(t) * R(t) = \frac{1}{A_d}\epsilon_I(t) * \sum_f \delta(t - t_f) = \frac{1}{A_d}\sum_f \epsilon_I(t - t_f), \tag{2.37}$$

where A_d is the area of the dendritic compartment. The synaptic current density I_s, which is fed onto the soma, models the effect of the ongoing theta oscillation that is coherent with the extracellular LFP,

$$I_s = I_{s_{\max}} \cos(\omega_\theta t - \phi_I) \tag{2.38}$$

where ϕ_I is a phase offset with respect to the theta LFP. Values of the model parameters used for the simulations are specified in the caption of Figure 2.6. The output firing rate λ_{CA1} of a CA1 cell is obtained by calculating the spike count within the place field divided by the size (in seconds) of the place field.

2.4. Results

Using a minimal computational model, I investigate inheritance of phase precession, i.e., the unidirectional transmission of phase precession from one region to another, for example in the hippocampal formation. To this end, I consider a population of phase-precessing neurons in one region projecting to a single output cell in another region.

2.4.1. Phase precession in a CA3-CA1 network model

I first focus on the CA3-CA1 network of the rodent hippocampus. Can phase precession in a CA1 cell be explained by phase precession observed in a population of CA3 cells? To study this case, I consider N CA3 place cells with identical place fields that project to a single CA1 cell, and I model the average firing rate of the CA3 pyramidal cells during the traversal of a place field (Fig. 2.3*A*).

This population firing rate, here as a function of time, reflects the activity of cells that phase precess because this rate oscillates at a frequency (here 8.5 Hz) that is slightly larger than the theta frequency (here 8 Hz). Peak firing rates are about 15 spikes/s in the center of the simulated place field, and rates decay to zero outside the field. With such a firing-rate profile, spike times are generated by means of an inhomogeneous Poisson process. The spike times of $N = 200$ statistically independent, but otherwise identical, simulated CA3 pyramidal cells are shown in the raster plot in Fig. 2.3*B*. Furthermore, each input spike is assumed to elicit an excitatory postsynaptic potential (EPSP; Fig. 2.3*C*, inset) in a target CA1 cell. The depolarization received by a CA1 cell is thus the sum of many EPSPs reflecting a transient excitatory CA3 input (Fig. 2.3*C*). This contribution to the membrane potential of the simulated CA1 cell is noisy (due to the Poisson process), and is delayed and scaled (due to filtering by the EPSP) with respect to the firing rate of the CA3 cell shown in Fig. 2.3*A*.

To simulate the full subthreshold membrane potential of a CA1 cell that receives transient excitatory phase-precessing input from CA3 place cells, I add an ongoing intracellular oscillation at theta frequency, and this oscillation rides on top of a resting membrane potential at -70 mV (Fig. 2.3*D*). This ongoing intracellular oscillation is assumed to be (1) typically smaller in amplitude than the maximum amplitude of the excitatory component, (2) present independent of any place-field activity, and (3) phase locked to the extracellularly recorded local field potential (LFP) in the theta band. This ongoing intracellular oscillation could be generated by inhibitory input.

By summing the ongoing inhibitory and the transient excitatory input, one obtains the oscillatory membrane potential of the CA1 model neuron as shown in Figure 2.3*E*. To test whether this subthreshold membrane potential reflects phase precession, I study local maxima and assign an LFP phase to each peak. The peak phases are plotted as a function of time in Figure. 2.3*F*. Within the place field, there is clear phase precession, i.e., there is a strong correlation between phase and time, and the slope is negative because the peak phases are mainly determined by the phase-precessing excitatory input from CA3. Outside the place field, the phase of the peaks is constant at about 360 degrees because peaks are determined by the inhibitory input that is locked to the LFP theta oscillation.

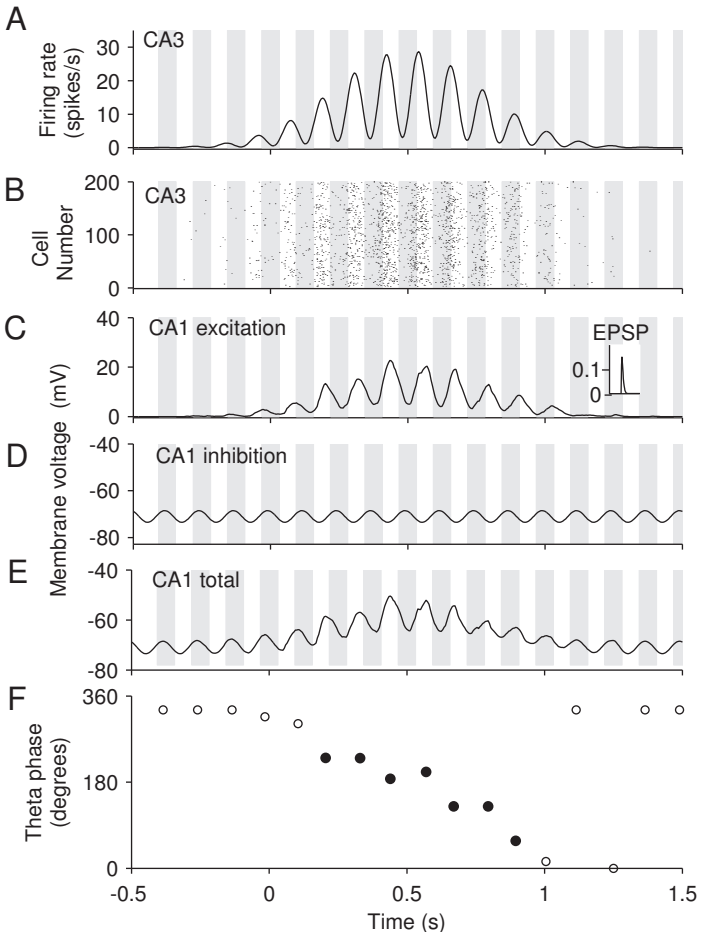

Fig. 2.3.: Computational model for inheritance of phase precession from CA3 to CA1. ***A***, Model of the firing rate of a CA3 cell during the traversal of a place field between 0 and 1 s time. The vertical gray shaded bars indicate half theta periods ($1/(2f_\theta) = 62.5$ ms), and the middle of each gray bar corresponds to 0 ($\equiv 360$) degrees. Peaks of the firing rate occur at earlier and earlier theta phases, which indicates phase precession. ***B***, Raster plot of spike times of $N = 200$ CA3 cells. Spikes are generated by an inhomogeneous Poisson process using the rate in *A*. ***C***, Contribution of 200 CA3 cells to the voltage in a CA1 cell. Each spike in *B* elicits an EPSP (inset), and EPSPs are summed. ***D***, The intracellular theta oscillation of a CA1 cell is phase locked to the extracellular LFP and is independent of place-field activity. ***E***, Membrane potential of a CA1 cell obtained by adding the CA3 input in *C* to the intracellular theta oscillation in *D*. ***F***, Theta phase of peaks of the CA1 membrane voltage in *E*. Open dots: outside the place field; filled dots: inside the place field. Further model parameters (see 2.3 for details): $C = 0.7$, $\sigma = 0.35$ s, $f_\lambda = 8.5$ Hz, $\phi_\lambda = 200$ degrees, $\lambda_0 = 10$ spikes/s, $\tau = 10$ ms, $\epsilon_{\max} = 0.15$ mV, $B = 1$ mV, $\phi_\theta = 0$ degrees.

2.4.2. Subthreshold signatures of phase precession in CA1 pyramidal cells can be explained by inheritance

The simulated subthreshold membrane potential of a CA1 pyramidal cell (Fig. 2.3, *E* and *F*) exhibits three key features as observed in *in-vivo* whole-cell recordings in awake animals

that cross a place field (Fig. 1.8 *C*): (1) The mean membrane potential rises and falls in a ramp-like manner, which is reminiscent of the CA1 (subthreshold) place field (Lee et al., 2006; Harvey et al., 2009; Epsztein et al., 2011). In the model, the subthreshold place field in CA1 is a result of the CA3 place-field mean activity, which depolarizes the membrane potential. The place field in CA1 is thus inherited from a population of CA3 cells that have overlapping place fields. (2) The amplitude and the frequency of the oscillations of the membrane potential are larger within the place field than outside (Harvey et al., 2009). To explain the larger amplitude using the model, I assumed that the amplitude of the oscillatory contribution of the excitatory input from CA3 is larger than the amplitude of the ongoing inhibitory oscillation, a constraint that I will later use to estimate parameters of the model. To explain the higher frequency, I note that the excitatory contribution originates from CA3 phase-precessing cells that are oscillating at a frequency higher than LFP theta oscillations, hence higher than the ongoing inhibitory oscillation, which was assumed to have the same frequency as the theta LFP. (3) Peaks of the subthreshold membrane potential show phase precession (Harvey et al., 2009). In the computational model, phase precession in the CA1 membrane potential is inherited from phase precession of the inputs from CA3. Overall, the simulation results suggest that CA3 excitatory input and an ongoing inhibitory oscillation are sufficient to explain the main subthreshold features of the membrane potential of CA1 pyramidal cells that show phase precession (Harvey et al., 2009).

Parametrization of the computational model. How are the subthreshold features of phase precession related to the parameters of the computational model of a CA3-CA1 network? I first briefly describe the model in mathematical terms (for details see the Methods in section 2.3). The input from CA3 is described by the time-dependent firing rate $\lambda(t) = \lambda_0 \cdot [1 + C\,\cos(2\pi\, f_\lambda\, t - \phi_\lambda)]\; x(t)$ (see also Equation 2.3) with mean firing rate λ_0 in the center of the place field, modulation depth C of the oscillatory component of the firing-rate oscillation at frequency f_λ and phase ϕ_λ. The Gaussian function $x(t)$ with maximum value 1 and size σ describes the temporal extent of a CA3 place field (Fig. 2.3*A*). This firing-rate model is used to generate spikes, each spike evokes an EPSP, and EPSPs are linearly integrated. An EPSP is described by an alpha function with amplitude $\epsilon_{\max}$ and time constant τ (Fig. 2.3*C*, inset). A further important model parameter is the number N of CA3 cells that provide input to a single CA1 cell. The ongoing theta oscillation of the CA1 membrane voltage (Fig. 2.3*D*) is quantified by the amplitude B, the theta frequency f_θ, and the phase ϕ_θ (with respect to the extracellular theta LFP): $V_\theta(t) = B \cdot [\cos(2\pi\, f_\theta\, t - \phi_\theta) - 1]$ (see also Equation 2.7).

Some model parameters are constrained by experimental data (mean ± standard error): $\lambda_0 = 12.4 \pm 4$ spikes/s (estimated from main text and Figure 7*H* in Mizuseki et al., 2012), $f_\lambda = 8.6 \pm 0.3$ Hz (estimated from Figure 14*A* in Mizuseki et al., 2012), $\phi_\lambda = 190 \pm 30$ degrees (estimated from Figure 2*D* in Harris et al., 2002), $f_\theta = 8.1 \pm 0.2$ Hz (estimated from Figures 1-5 in Geisler et al., 2010), $B = 0.7 \pm 0.1$ mV (estimated from Figure 5*C* in Harvey et al., 2009), and $\tau = 10 \pm 3$ ms (estimated from Figure 3*D* in Magee and Cook, 2000). Note that $\tau \approx \tau_d/2$ where τ_d is the decay constant in Magee and Cook (2000). However, other parameters are not easily accessible. In particular, the phase ϕ_θ of ongoing intracellular theta oscillations outside the place field (with respect to theta LFP recorded in the CA1 pyramidal layer) is unclear in awake behaving animals. Furthermore, for the input from CA3 to CA1, the modulation depth C of the population firing rate is not available. Finally, the number N of CA3 cells that drive one CA1 cell as well as the *in-vivo* EPSP amplitude

$\epsilon_{\max}$ are, so far, free parameters of the model. In what follows, I constrain these parameters by comparing the computational model to available data on properties of place fields and phase precession, including an analysis of the noise in the membrane potential.

2.4.3. Subthreshold features of phase precession constrain model parameters

While an animal traverses a place field, CA3 neurons fire sequences of spikes, and the spikes evoke EPSPs that contribute to the membrane voltage of a CA1 neuron. This sum of EPSPs is variable in each run because the activity of CA3 neurons is variable. To account for such variability in the inheritance model, spikes are generated in each CA3 neuron by means of an inhomogeneous Poisson process. The variability of the membrane voltage due to such "shot noise" critically depends on the number N of CA3 cells that generate the place-field response in the CA1 cell. Intuitively, one expects a more faithful representation of the CA3 population activity for an increasing number N of CA3 neurons. In Figure 2.4 results of numerical simulations of CA1 membrane-potential traces are shown for values of N between 30 and 260. Note that here I only consider the phase-precessing, i.e., excitatory, contribution to the membrane potential. To allow for an easy comparison of membrane-potential traces associated with values of N that span one order of magnitude, EPSP amplitudes are scaled proportional to $1/N$. The appearance of a simulated CA1 membrane-voltage trace also depends on the modulation depth C of the oscillatory firing rate of the simulated CA3 cells. Figure 2.4 shows that increasing C from 0.3 to 0.7 (for fixed N) enhances the oscillatory component of voltage traces.

The simulated voltage traces in Figure 2.4 show that the model parameters N and C have a major impact on the shape of the CA1 membrane potential. However, there is a trade-off between N and C. Indeed, the oscillations of voltage traces on the diagonal from top-left to bottom-right in Figure 2.4 are similar. To quantify differences and similarities in the appearance of voltage traces, which is essential to constrain the ranges of the model parameters N and C, I introduce a signal-to-noise ratio. The signal-to-noise ratio ρ is defined as the average amplitude of the membrane-potential oscillation divided by the average amplitude of the shot noise in the center of the place field (see Equation 2.28):

$$\rho = \frac{C\sqrt{N\,\lambda_0\,\tau}}{1+(2\pi\,f_\lambda\,\tau)^2}\ . \tag{2.39}$$

Note that ρ is independent of the EPSP amplitude, which justifies the voltage scaling of the traces in Fig. 2.4. The larger ρ the greater is the amplitude of the oscillations compared to the shot noise, or, more qualitatively, the clearer is the oscillatory structure of the CA1 voltage trace. For example, the voltage trace for $N = 30$ and $C = 0.3$ shows a membrane-potential trace for which the oscillations are barely distinguishable from the noise, which is described by a rather low value $\rho = 0.7$. In Fig. 2.4, the signal-to-noise ratio ρ increases from bottom-left ($\rho = 0.7$) to top-right ($\rho = 6.5$) because both N and C are increased. On the diagonal from top-left to bottom-right the signal-to-noise ratio is constant ($\rho = 2.2$) because of the particular choices of N and C. These traces are most similar to the CA1 voltage traces recorded by Harvey et al. (2009) in awake behaving mice.

So far, the signal-to-noise ratio suggested by experimental data (for example $\rho = 2.2$) constrains the model parameters N and C but does not lead to particular values. Moreover, the EPSP amplitude $\epsilon_{\max}$ cannot yet be determined. Therefore further properties of

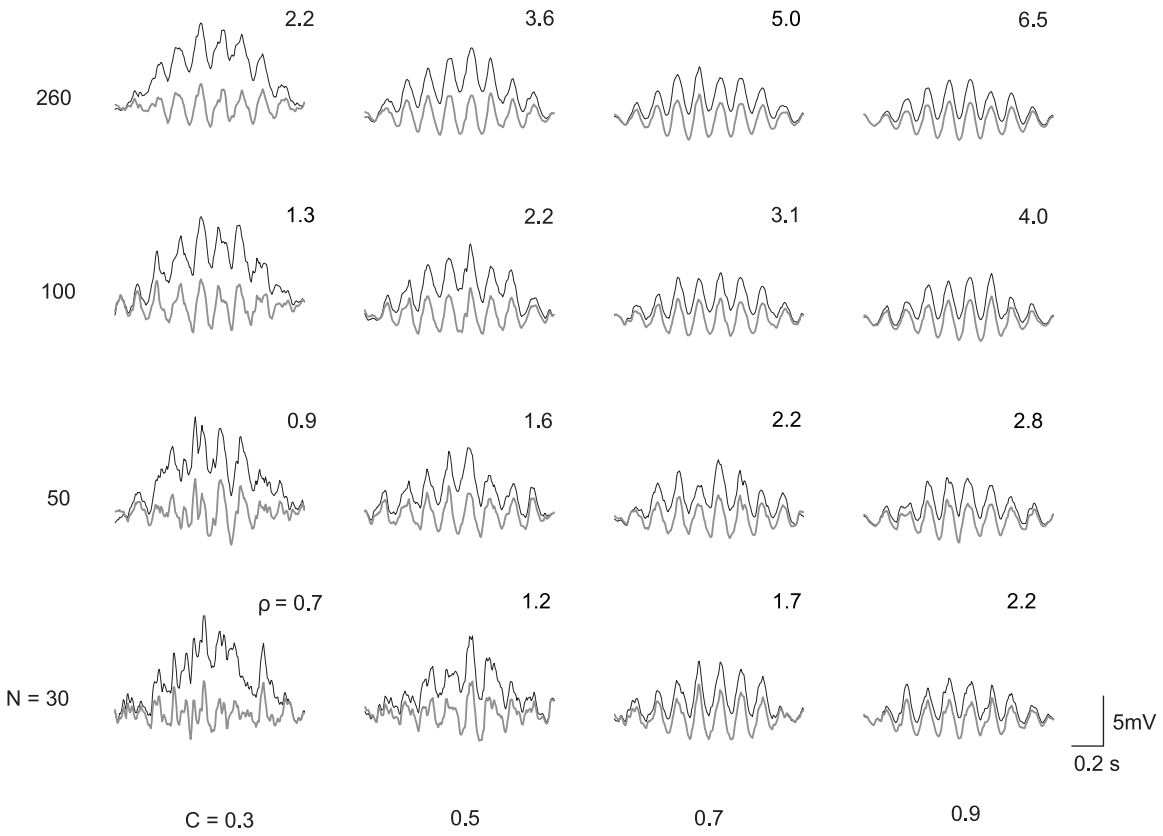

Fig. 2.4.: Signal-to-noise ratio ρ of simulated CA1 membrane voltage traces during place-field traversals. Voltage traces (black) depict the contribution of the excitatory input from CA3 to the CA1 membrane potential; gray traces are high-pass filtered (> 4 Hz) to suppress the slow depolarization ramp. Each voltage trace provides an example for some number $N = \{30, 50, 100, 260\}$ of CA3 neurons and for some firing-rate modulation depth $C = \{0.3, 0.5, 0.7, 0.9\}$. The number at the upper right side of each trace denotes the corresponding quality parameter ρ from Equation 2.39. Voltage traces along the diagonal from top-left to bottom-right all have the same quality parameter $\rho = 2.2$, and the oscillatory components as well as the noise are similar. Further model parameters: $\sigma = 0.35$ s, $\lambda_0 = 10$ spikes/s, $f_\lambda = 8.5$ Hz, and $\tau = 10$ ms. The EPSP amplitude $\epsilon_{\max}$ is varied between 0.1 mV and 2.6 mV across voltage traces such that the expected oscillation amplitudes (Equation 2.15) are similar, which allows for an easy comparison of shapes across a large range of model parameters N and C.

experimental subthreshold membrane-voltage traces must be related to the computational model. Characteristic quantities that can be extracted from the data are, for example, the oscillation amplitude ΔV_{osc} and the mean depolarization ramp ΔV_{ramp} in the center of the field. Harvey et al. (2009) found $\Delta V_{\text{osc}} = 1.3 \pm 0.4$ mV and $\Delta V_{\text{ramp}} = 2.7 \pm 0.4$ mV.

A thorough theoretical analysis of the inheritance model reveals a direct relationship between model parameters and the oscillation amplitude ΔV_{osc} and the mean depolarization

ramp ΔV_{ramp} (for details see Equations 2.15 and 2.16):

$$\Delta V_{\text{osc}} \approx \frac{\mathrm{e}\, C\, N\, \lambda_0\, \tau\, \epsilon_{\max}}{1 + (2\pi\, f_\lambda\, \tau)^2} \tag{2.40}$$

and

$$\Delta V_{\text{ramp}} \approx \mathrm{e}\, N\, \lambda_0\, \tau\, \epsilon_{\max} \tag{2.41}$$

where $\mathrm{e} = \exp(1) \approx 2.71828$ is Euler's number. Both equations are excellent approximations if the amplitude B of ongoing oscillations is smaller than the oscillation amplitude ΔV_{osc} of the transient component in the center of the field.

Equation 2.39 for ρ, Equation 2.40 for ΔV_{osc}, and Equation 2.41 for ΔV_{ramp} are sufficient to determine the three free model parameters C, N, and $\epsilon_{\max}$ (for details see Materials and Methods, Equations 2.30, 2.31, and 2.32):

$$C = \frac{\Delta V_{\text{osc}}}{\Delta V_{\text{ramp}}} \left[1 + (2\pi\, f_\lambda\, \tau)^2\right] , \tag{2.42}$$

$$N = \left(\frac{\Delta V_{\text{ramp}}}{\Delta V_{\text{osc}}}\right)^2 \frac{\rho^2}{\lambda_0\, \tau} , \tag{2.43}$$

$$\epsilon_{\max} = \frac{\Delta V_{\text{osc}}}{\rho^2} \left(\frac{\Delta V_{\text{osc}}}{\Delta V_{\text{ramp}}}\right) . \tag{2.44}$$

To summarize, using the computational model and salient features of subthreshold voltage data, I am able to explicitly predict values for the model parameters C, N, and $\epsilon_{\max}$.

Furthermore, I use standard rules of error propagation applied to Equations 2.42, 2.43, and 2.44 and the experimental values for τ, ΔV_{osc}, ΔV_{ramp}, f_λ, λ_0, and ρ to estimate the mean and error (i.e., standard error of the mean) of model parameters N, C, and $\epsilon_{\max}$ as

$$C = 0.6 \pm 0.1, \tag{2.45}$$

$$N = 208 \pm 120, \text{ and} \tag{2.46}$$

$$\epsilon_{\max} = 0.13 \pm 0.035 \text{ mV}. \tag{2.47}$$

The value for $\epsilon_{\max}$ is comparable to the values of EPSPs (≈ 0.2 mV) recorded *in-vitro* (Magee and Cook, 2000). The estimation of the modulation depth C from the literature would depend on recordings of the activity of a population of CA3 cells during a single place-field traversal, which are not available. A preliminary estimate, however, can be obtained from the averaged firing rates across multiple traversals for CA1 cells (e.g. Skaggs et al., 1996). Thus, the values for the CA3 firing-rate modulation depth C and number of presynaptic CA3 cells N are to date unknown, and are therefore predictions of the inheritance model.

2.4.4. Analysis of a CA3 place cell recording validates model parameters

From a plot of phase vs. normalized position of CA3 cells exhibiting phase precession, I extracted an approximate time-dependent firing rate for the CA3 cell population (Fig. 2.5). The procedure to extract the firing rate is described in section 2.3. This firing rate gives insight into how a typical CA3 cell spikes through out a place field and could validate or falsify the initial assumption on the form of $\lambda(t)$ of the inheritance model.

The extracted firing rate shown in Figure 2.5 B is oscillatory with a high modulation

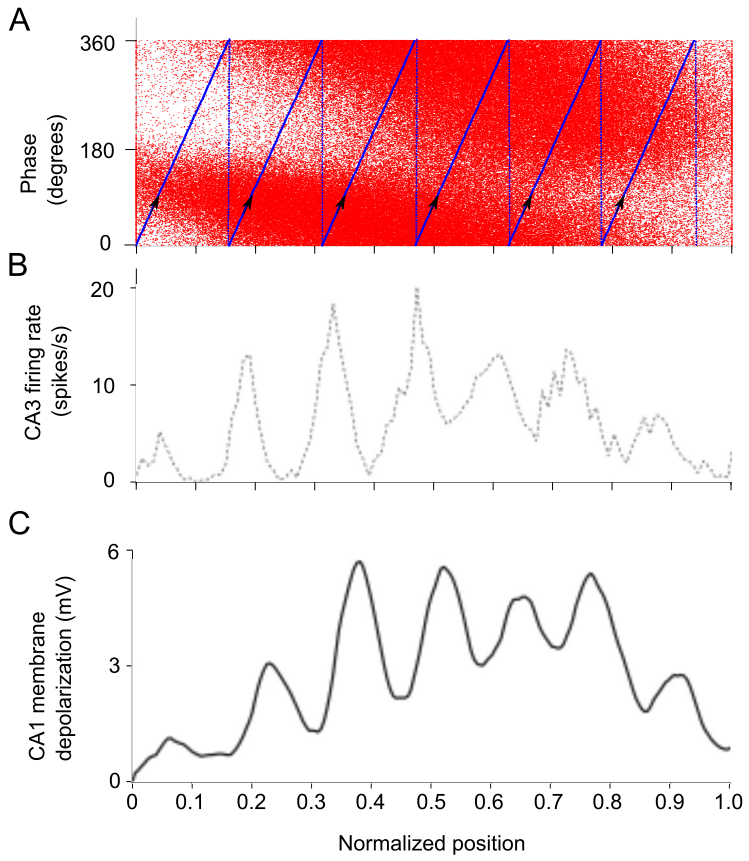

Fig. 2.5.: Firing rate extracted from active CA3 cells in multiple trials (data courtesy of Kamran Diba and Gyorgy Buszaki, unpublished). ***A***, Phase-position plot of pooled trials of simultaneously recorded CA3 place cells. Each dot represents a spike from a CA3 cell. ***B***, Firing rate of a population of CA3 cells, extracted from *A*. Blue lines and arrow heads depict a trajectory of a virtual rat at a constant speed v across the place field (details in section 2.3). ***C***, Membrane potential of a CA1 cell receiving input from 200 CA3 cells whose firing rate is shown in *B*. Further model parameters: $v = 0.5$ m/s, $\sigma = 0.4$ m.

and there is an increasing and decreasing ramp of excitation. The average modulation depth $C \approx 0.7$ found in the extracted firing rate is even greater than the range of predicted minimal values in Equation 2.47. Furthermore, a strong modulation in general is a sign that the phase precessing cells are firing with a high degree of synchrony within the place field. The firing rate shown in Figure 2.5 thus displayed relevant features which validate the earlier assumption of the model firing rate $\lambda(t)$.

The scaled CA3 firing rate I extracted was used to drive a Poisson spike train, and the resulting voltage trace (Fig. 2.5 *C*) exhibits subthreshold features that agree with both the theoretical model and intracellular recordings (Harvey et al., 2009).

2.4.5. Phase precession in a bursting model neuron.

I have shown that the inheritance model can account for subthreshold features of phase precession. Phase precession, however, is also a suprathreshold phenomenon where spikes of place cells shift to earlier phases relative to theta LFP. Therefore, in the context of a spiking

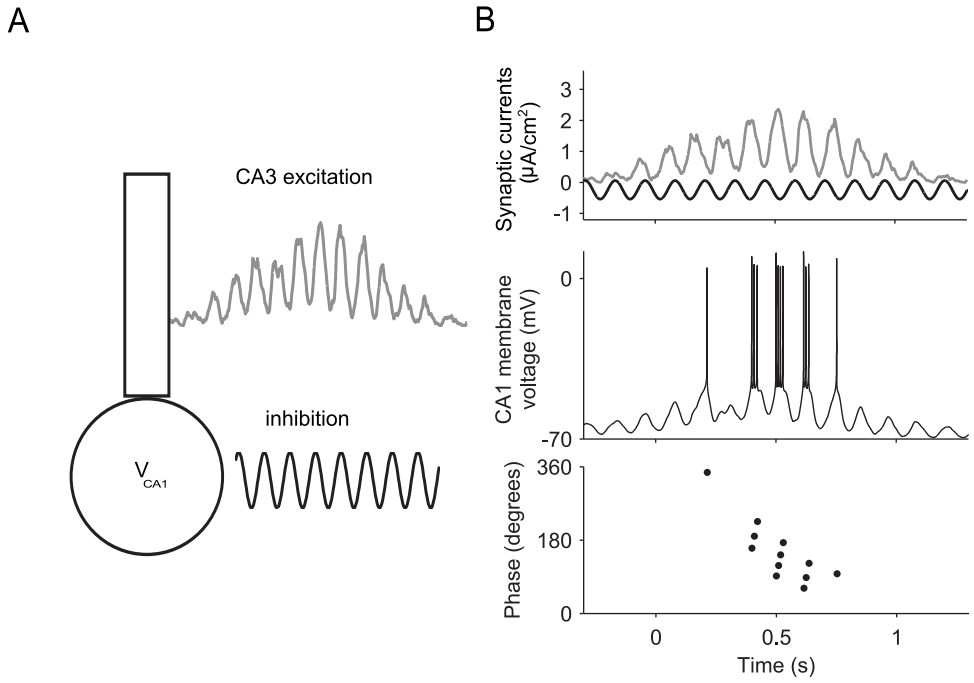

Fig. 2.6.: A two-compartment spiking model reproduces phase precession in a CA1 cell as predicted by inheritance. ***A***, Structure of the two-compartment model (Pinsky and Rinzel, 1994; Kamondi et al., 1998) where V_{CA1} is the membrane potential of the somatic compartment. ***B***, Top, Dendritic input current (gray, from CA3) and somatic input current (black, reflecting ongoing theta oscillations) contribute to the CA1 voltage. Dendritic input is generated as a sum of EPSCs of amplitude $\epsilon_{I_{\max}} = 15$ pA and time constant $\tau_I = 4$ ms. Somatic input is characterized by an amplitude $I_{s_{\max}} = 0.3$ μA/cm^2 and $\phi_I = 0$ degrees. Middle, membrane-voltage V_{CA1} during the traversal of a virtual CA1 place field. Bottom, theta phase of V_{CA1} spikes as a function of time.

model neuron, I examine whether the input from CA3 cells that exhibit phase precession is sufficient to produce phase precession of spikes of a CA1 cell. For this purpose, I use a two-compartment model to segregate the inhibitory contribution arriving at the perisomatic compartment from the excitatory contribution arriving at the dendritic compartment. Particularly, I use a two-compartment model that accounts for bursting, which was developed by Pinsky and Rinzel (1994) for CA3 neurons and adapted for CA1 neurons (Kamondi et al., 1998). A schematic is shown in Fig. 2.6*A* (details in section 2.3).

The two inputs to the CA1 model neuron are dendritic (I_d) and somatic (I_s) current densities ($[\frac{\mu A}{cm^2}]$), referred to below simply as currents. The dendritic current I_d represents the total phase-precessing signal coming from CA3. More precisely, each input spike elicits an excitatory post-synaptic current (EPSC). The current I_d is thus a sum of EPSCs, and this summed current is applied to the dendritic compartment of the model neuron. The somatic current I_s represents an inhibitory oscillation that is phase locked to the LFP (Kamondi et al., 1998) and is applied to the somatic compartment.

Figure 2.6*B* shows an example of the time courses of both currents as well as the CA1 membrane potential for one traversal of the place field. The two-compartment model generates isolated action potentials and bursts, and the spiking activity shows phase precession,

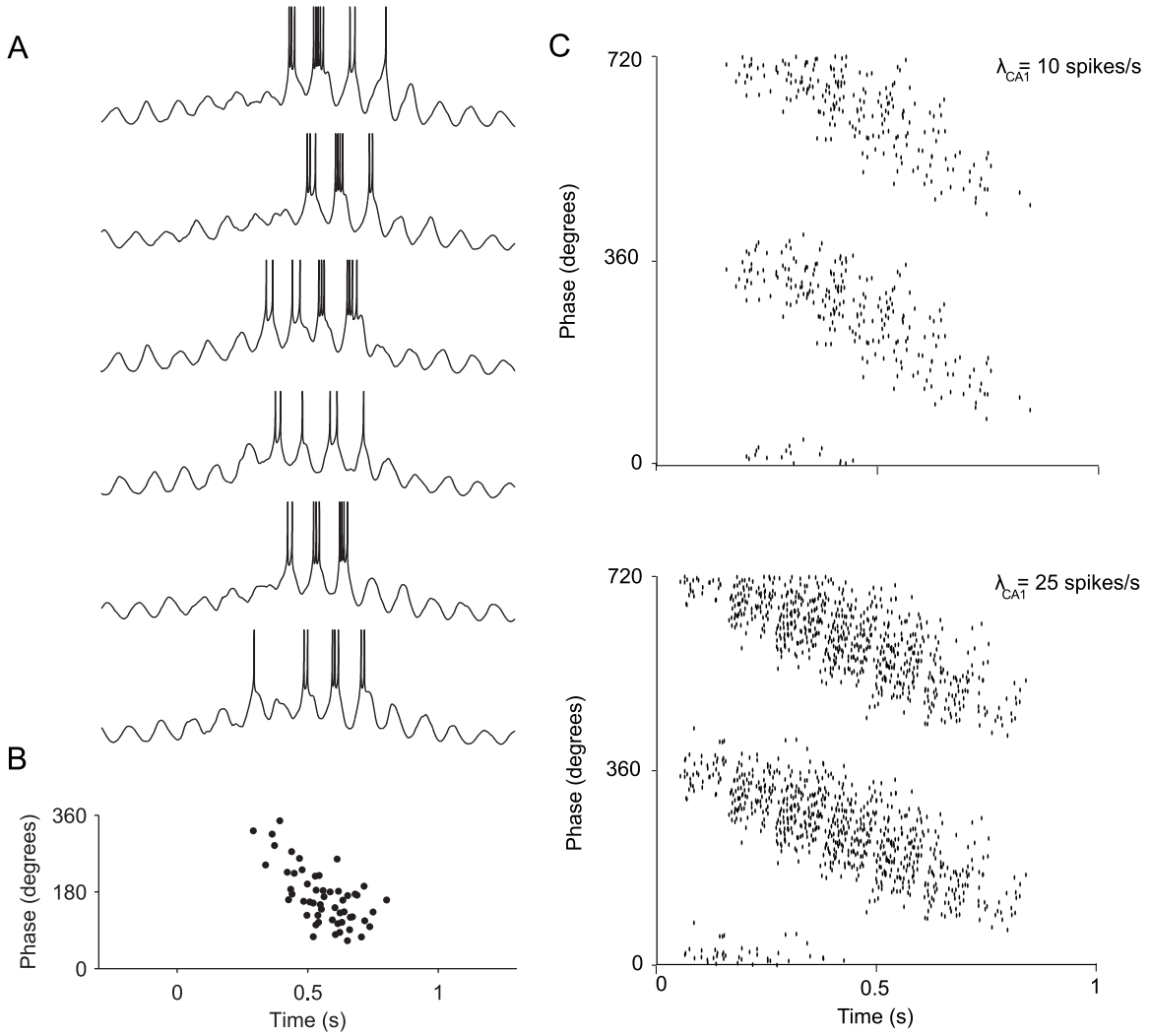

Fig. 2.7.: Pooled trials of phase precession. ***A***, Six membrane-potential traces for different traversals through the place field. The phase at field entry is random. Note that the spikes lie on top of the peaks of the subthreshold oscillations. ***B***, Phase-time plot for 12 traversals of the place field, including those in *A*. Further model parameters are as in Figure 2.6. ***C***, Phase-time plots for 30 traversals and average firing rate (per traversal) of 10 spikes/s (top) and 25 spikes/s (bottom).

here with respect to time, similar to CA1 pyramidal cells *in vivo* (O'Keefe and Recce, 1993; Pastalkova et al., 2008; Schmidt et al., 2009). Simulated membrane potentials for several traversals through the CA1 virtual place field are shown in Figure 2.7*A*, and the pooled

spike phase vs. time plot in Fig. 2.7*B* again demonstrates phase precession. Furthermore, the model reproduces a similar phase precession profile for low, as well as for high rates (Fig. 2.7*C*, top and bottom). This results are in line with studies that have shown that phase precession occurs for high and low rates (Huxter et al., 2003), and in general, that phase information complements rate information (Jensen and Lisman, 2000; Reifenstein et al., 2012)

In the spiking model, the intrinsic ionic currents in the dendrite and soma are responsible for the bursting dynamics. However, the phase precession in the CA1 model cell is essentially due to the input from CA3 phase-precessing cells. Indeed, the spikes and bursts occur at the maxima of the underlying oscillations of the membrane potential, as shown in Fig. 2.7*A*. This means that the subthreshold membrane-potential peaks are a good predictor of suprathreshold behavior, which is in line with data from Harvey et al. (2009), Domnisoru et al. (2013), and Schmidt-Hieber and Häusser (2013). Because of this tight link between sub- and supra-threshold phase precession in the model, in the following section I restrict the analyses to the subthreshold dynamics only.

2.4.6. Intracellular theta oscillations modulate phase precession of CA1 model cells

In the previous sections I examined in detail the role of excitatory input from CA3 phase-precessing cells but largely neglected the influence of the ongoing intracellular theta oscillations in CA1, which are phase locked to the extracellular theta LFP. Now I elucidate the role of these ongoing oscillations, which may be mediated by somatic inhibitory input into CA1 pyramidal cells. To this end, the phase ϕ_θ and the amplitude B of the ongoing theta oscillations are varied in the model while the excitatory input is kept fixed (Fig. 2.8). I restrict the analysis to a mean-field model, i.e., the shot noise is neglected. The excitatory input is therefore the firing rate of a population of CA3 cells convolved with an EPSP.

To evaluate the influence of an ongoing, putatively inhibitory, theta oscillation of the membrane potential on phase precession in CA1, I compare this more involved case to the simpler case without such ongoing oscillations (red color in Fig. 2.8); note that there is clear phase precession in CA1 in the case without ongoing oscillations. I begin by studying the impact of the phase ϕ_θ on phase precession while the amplitude $B = 1$ mV is fixed (Fig. 2.8, *A* and *B*). To demonstrate how the range and the overall shape of phase precession depends on the phase ϕ_θ of ongoing somatic inhibitory input, I first consider the case of $\phi_\theta \approx 0 = 360$ degrees. In this case, the peak phases of the ongoing somatic oscillation are in phase with the peaks of the extracellular LFP. Interestingly, for $\phi_\theta \approx 0$ degrees, slope, range, and entry phase of phase precession are larger than for the standard case with no ongoing theta oscillations. For $\phi_\theta \approx 0$ degrees, the phases of the CA1 membrane voltage peaks at field entry are ≈ 300 degrees (Skaggs et al., 1996; Mizuseki et al., 2009; 2012), which can be explained by the entrance phase of CA3 firing (≈ 200 degrees, Harris et al., 2002), a subsequent phase delay due to synaptic filtering of the EPSP (≈ 50 degrees $= 1.8\tau \cdot f_\theta \cdot 360$ degrees, see Equation 2.13), and a delay due to the inhibitory oscillation (≈ 50 degrees, estimated from Fig. 2.8*B*). Overall, the case $\phi_\theta \approx 0$ degrees matches *in-vivo* data well. In contrast, for other phases of the ongoing somatic oscillation, for example $\phi_\theta \approx 120$ degrees and $\phi_\theta \approx 240$ degrees, phase precession does not match *in-vivo* data: the slope and the range of phase precession are reduced, and at field entry the phase is smaller compared to the standard case of pure CA3 excitatory input.

To study the influence of the amplitude of the ongoing intracellular theta oscillations on

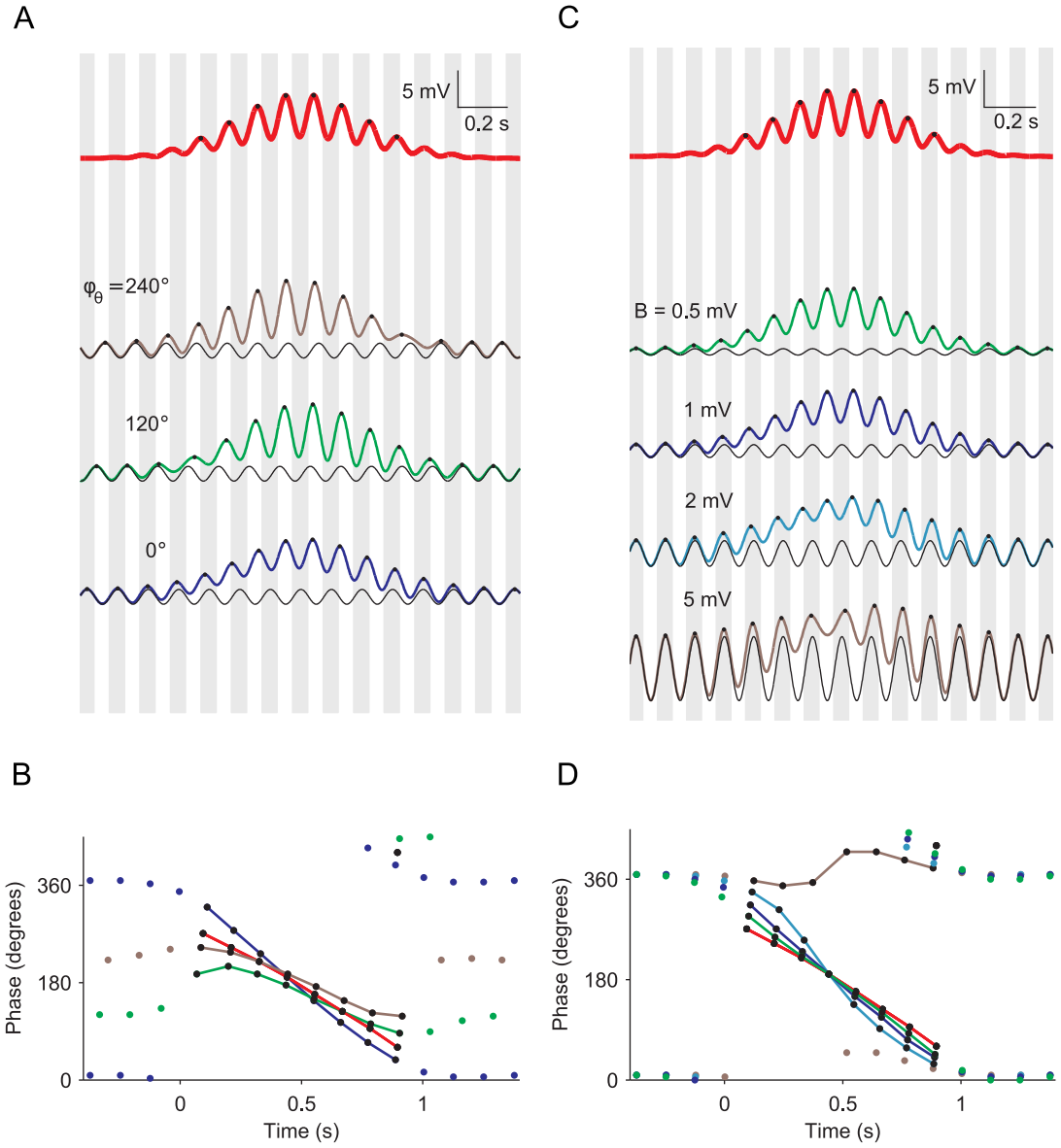

Fig. 2.8.: Amplitude and phase of intracellular theta oscillations modulate phase precession. ***A***, Membrane-potential traces for different phases of inhibition. The vertical gray shaded bars indicate half theta periods ($1/(2f_\theta) = 62.5$ ms), and the middle of each gray bar corresponds to 0 ($\equiv 360$) degrees. The phase and amplitude of excitation (red, top) are fixed, and they correspond to the mean-field version of Fig. 2.3 *C*. Three different phases of inhibition (black lines) are used to calculate corresponding CA1 voltage traces: 240 (top, brown), 120 (middle, green), and 0 (bottom, blue) degrees. The amplitude of inhibition is fixed at 1 mV (black lines). ***B***, Theta phase of peaks in *A* as a function of time since field entry. Peaks of the colored voltage traces are marked by circles. Colored lines connect the dots within the place field. ***C***, Membrane-potential traces for varying amplitudes of inhibition. The phase and amplitude of excitation (red, top) are fixed as in *A*. The phase of inhibition is fixed at 0 degrees while the amplitude is variable: 0.5 (green), 1 (blue), 2 (cyan), and 5 (brown) mV. ***D***, Theta phase of peaks in *C* as a function of time since field entry. Peaks of the colored voltage traces are marked by circles. Colored lines connect the dots within the place field.

phase precession, phase is fixed at the value $\phi_\theta \approx 0$ degrees, which matches *in-vivo* data best, and the amplitude B is varied (Fig. 2.8, C and D). Phase precession strongly depends on the amplitude B of ongoing somatic inhibitory input. The range of phase precession is largest for moderate values of B, for example $B = 1$ mV (as in Fig. 2.8, A and B) and $B = 2$ mV. In contrast, for $B = 5$ mV, phase precession practically disappears because the ongoing intracellular oscillation at theta frequency dominates the transient excitatory component. On the other hand, for $B = 0$, i.e., excitation only, and 0.5 mV, the range of phase precession is reduced compared to the case $B = 1$ mV. The detailed phase relation of the traces for $B = 0$ and $B = 1$ mV in Fig. 2.8D is even consistent with data from Royer et al. (2012): for $\phi_\theta \approx 0$ degrees, a reduction of the amplitude of inhibition leads to smaller phases near field entry (phase advance) whereas towards field exit phases are larger (phase delay).

In Figure 2.9, I examine more closely the experimental result from Royer et al. (2012). In this experimental paradigm, mice were head fixed while running on a treadmill, and place-cell activity was recorded in the CA1 region of the hippocampus (Fig. 2.9 A). Inhibition was reduced locally by using optogenetics to silence parvalbumin-expressing (PV) interneurons in CA1. The effects on neighboring CA1 pyramidal cells were subsequently analyzed. Royer et al. (2012) found changes in the firing rate of CA1 pyramidal cells, but most notably, also changes in spike timing and phase precession for the place cells. Figure 2.9 C (top right) shows the mean theta phases for spikes within five different segments of the place field for "control" CA1 cells (blue, normal interneuron firing) and "light" CA1 cells (red, silenced interneurons). After interneuron silencing, there was a clear phase shift towards early phases at the beginning of the place field, and an opposite shift towards the second half of the place field. Note that phase precession persisted after silencing. I interpret the experimental results as follows: CA3 excitation interacts with oscillatory inhibition at a phase $\phi_\theta \approx 0$ degrees to generate the CA1 membrane potential (Fig. 2.9 B) and corresponding phase-position plot (Fig. 2.9 C, bottom right). The predicted phase-position plot qualitatively matches the experimental phase-position plot (Fig. 2.9 C, top right), if the activity of CA1 "light" cells is interpreted as essentially due to CA3 excitation. Moreover, the phase histograms in different segments of the place field (Fig. 2.9 D, top) can be qualitatively reproduced with the subthreshold model (2.9 D, bottom). This analysis leads to an important result: inhibitory oscillations are not needed for phase precession as observed in CA1, but can characteristically affect the range and entry phase of CA1 place cells. In particular, the results from the Royer et al. (2012) experiment can be explained by the simple model of excitation plus inhibition, if it is assumed that $\phi_\theta \approx 0$ degrees. Thus, I predict that the inhibitory oscillations are almost in phase with the extracellularly recorded LFP.

In summary, the inheritance model of phase precession predicts that the ongoing intracellular theta oscillation in CA1 pyramidal cells is not necessary for phase precession. Phase precession remains without such intracellular theta oscillations because phase precession is inherited from the excitatory input from CA3. However, the interaction of a specific ongoing oscillation, possibly due to inhibitory interneurons, and transient excitatory oscillations from CA3 pyramidal cells can modulate phase precession in CA1 in a characteristic way. For $\phi_\theta \approx 0$ degrees, the range and entry phase of phase precession are reduced if inhibitory input is suppressed, which is supported by data from Royer et al. (2012). Therefore, the inheritance model of phase precession predicts that the ongoing intracellular theta oscillation in CA1 pyramidal cells is in phase with the extracellular LFP theta oscillation, i.e., $\phi_\theta \approx 0$ degrees.

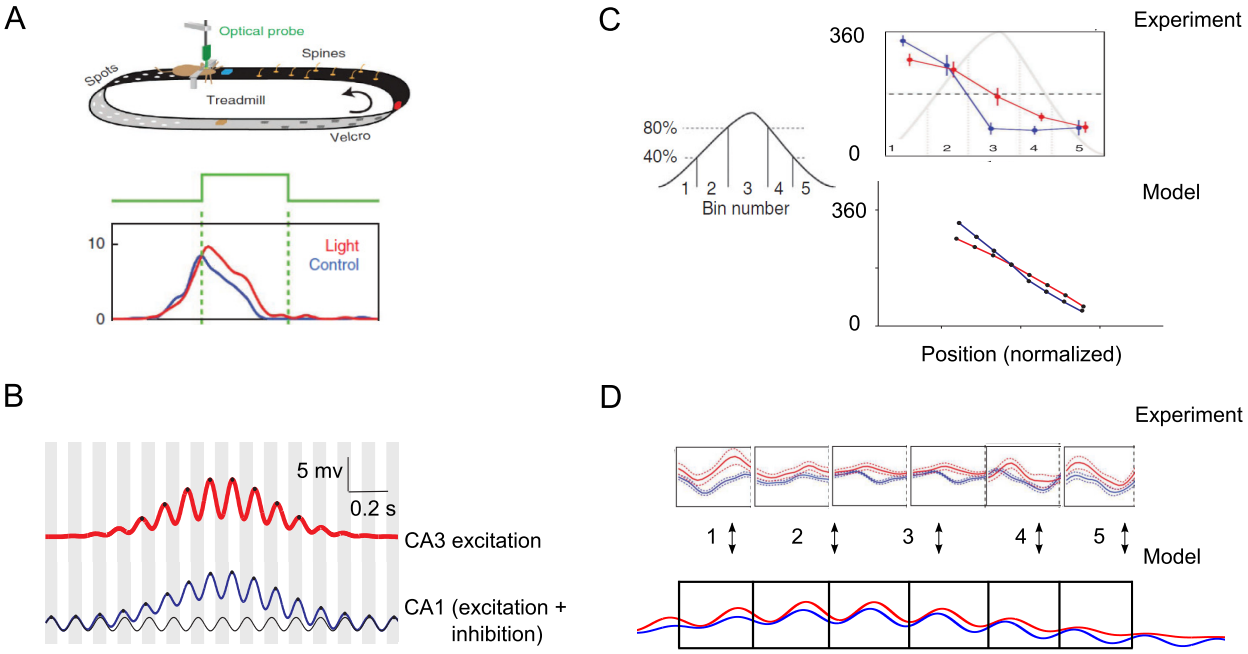

Fig. 2.9.: Interpretation of interneuron-silencing experiment from Royer et al. (2012). ***A***, A mouse navigates on a treadmill with its head fixed while an optical probe delivers pulses at a fixed point in the track to selectively silence interneurons in the CA1 region (top). Firing-rate and spike-timing properties of place cells in the CA1 region are affected by the light-induced silencing of inhibition ("light" vs. "control", bottom). ***B***, The CA1 membrane potential (blue) is the sum of CA3 excitation (red) and oscillatory inhibition (black), see also Figure 2.8 *A*. ***C***, In Royer et al. (2012), the place field was divided into five segments (left). Mean theta phases within the segments of the place field for their experiment (top right) and for the model (bottom right). ***D***, Phase histograms, denoted by "Experiment", were constructed for each segment of the place field for "light" (red) and "control" (blue) conditions. By overlaying CA3 excitation (red) with CA1 membrane potential (blue), the computational model qualitatively reproduces the phase preferences of "light" and "control". (Figures in *A*, *C*, and *D* were reproduced from Royer et al. 2012 with permission from Elsevier).

2.5. Discussion

I developed a computational model that explains how hippocampal phase precession in one region can be propagated to another. Main findings are: (1) Phase precession in a small subset of CA3 pyramidal cells is sufficient to explain phase precession in a CA1 pyramidal cell. (2) Inhibitory input to the CA1 cell is not necessary to generate phase precession, but inhibition can increase the slope and enlarge the range of phase precession.

2.5.1. Subthreshold dynamics of CA1 place cells

According to this inheritance model, the subthreshold signatures of phase precession in a CA1 cell (Harvey et al., 2009) reflect the firing-rate characteristics of phase-precessing place cells, for example in CA3. Particularly, the mean depolarization of a CA1 cell in the center of a place field ($\approx$ 4 mV), i.e., the subthreshold place field, is the result of increased excitatory drive; the oscillatory component of the CA1 membrane potential, which has $\approx$ 2 mV amplitude in the center of the place field, is due to phase-precessing feed-forward input; and subthreshold voltage traces oscillating in the theta frequency-range are noisy due to variable spiking input, but the oscillation amplitude is larger than the standard deviation of the noise in single runs through a place field. These experimental constraints imply that one needs $N \gtrsim 200$ active place cells in the CA3 region, whose population firing rate has a modulation depth $C \gtrsim 0.6$. To arrive at the above predictions, uniform synaptic weights and transmission probabilities were assumed for the individual CA3-CA1 projections, as well as small variations of the individual CA3 cells' firing rate (but see Leutgeb et al. 2006). Furthermore, the CA3 firing-rate model did not include pair-wise correlations that arise, for example, from task-dependent switching of reference frames (Jackson and Redish, 2007), or assembly-level organization (Foster and Wilson, 2007). Such correlations hint at the importance of network-level interactions during phase precession (e.g. Lisman and Redish, 2009). The assumptions on the single-cell and network level can understimate the predictions for N and C, which should be better interpreted as lower bounds. Finally, I showed that peaks of the modeled subthreshold oscillations show phase precession (Harvey et al., 2009; Schmidt-Hieber and Häusser, 2013; Domnisoru et al., 2013), and, using a spiking model neuron, I confirmed that the peaks predict phase precession of action potentials of CA1 pyramidal cells.

2.5.2. Inhibitory contribution to phase precession

I characterized the inhibitory input to a CA1 cell by an ongoing oscillation of the membrane potential that is coherent with the theta LFP but is independent of place-specific activity (Harvey et al., 2009; Epsztein et al., 2011). This oscillation was parametrized by the phase ϕ_θ of peaks with respect to the theta-LFP peaks and by its amplitude B. Only for $\phi_\theta \approx 0$ and amplitudes $B \lesssim 1$ mV that are smaller but comparable in magnitude to the maximum oscillation amplitude ($\approx$ 2 mV) due to the incoming CA3 excitation, the inhibition increases the range and the slope of phase precession of a CA1 cell, compared to the case where the CA1 cell receives excitation only. Oscillatory inhibitory input therefore can explain why the range of phase precession in CA1 is larger than in CA3 (Harris et al., 2002; Mizuseki et al., 2009; 2012). That inhibition only modulates phase precession but is not necessary for its generation receives support from Royer et al. (2012) who showed that transiently silencing PV interneurons reduced range and slope of phase precession of neighboring pyramidal cells in a

characteristic way, which is reproduced in detail by the inheritance model. The inheritance model thus predicts $\phi_\theta \approx 0$ degrees. The assertion that $\phi_\theta \approx 0$ degrees is in line with the following data. In awake animals during the theta state, PV interneurons preferentially fire before the trough of the theta LFP, at about 130 degrees (Royer et al., 2012; Varga et al., 2012), and project to the perisomatic region of CA1 pyramidal neurons. Because of the inhibitory nature of this projection and a small delay mainly due to synaptic filtering, the evoked oscillation of the membrane potential in CA1 pyramidal cells can be assumed to have minima at about 180 degrees and, therefore, maxima at about 0 degrees, as predicted.

The specific prediction $\phi_\theta \approx 0$ of the inheritance model distinguishes it, for example, from the somatodendritic-interference model (SDI) of phase precession (Kamondi et al., 1998; Magee, 2001; Mehta et al., 2002; Harris et al., 2002), which requires maxima of the inhibition at $\phi_\theta \approx 180$ degrees. In the SDI model, phase precession within a single neuron arises as a result of the interference between a slowly varying, ramp-like excitatory input to dendrites and an oscillating, inhibitory input to the soma. Phases of spikes of a CA1 pyramidal cell at the entrance of a place field then occur at about 0 degrees because at this phase the excitation just exceeds the minima of the inhibitory oscillation. Spike phases then precess because of increasing excitatory input. For decreasing excitatory input towards the end of the place field, some additional adaptation of CA1 cells or asymmetric excitation may avoid phase "recession". The SDI model is therefore in stark contrast to the inheritance model. Experiments that determine the theta phase of oscillations evoked by inhibitory input could reject one of them.

2.5.3. Inheritance of phase precession in the entorhino-hippocampal loop

In general, a difference between the inheritance model and previous models of phase precession is that the latter can explain how phase precession is generated ab initio. Network models, for example, require considerable recurrent connectivity within the local network (Jensen and Lisman, 1996; Tsodyks et al., 1996; Wallenstein and Hasselmo, 1997). These models are therefore more consistent with the denser recurrent connectivity of CA3 or EC than that of CA1 (Amaral and Witter, 1989). However, even in CA3 recurrent connectivity may not be necessary to explain phase precession, which could alternatively arise from facilitation of the mossy fiber synapse (Thurley et al., 2008) or inheritance from the dentate gyrus and/or EC (Molter and Yamaguchi, 2008).

I showed that CA3 input is sufficient to generate phase precession in CA1 but the CA1 region receives excitatory input also from layer III of the MEC, which can generate place-specific activity in CA1 (Brun et al., 2002; Nakashiba et al., 2008) and exhibits phase precession (Hafting et al., 2008; Climer et al., 2013; Reifenstein et al., 2014). As reviewed by Ahmed and Mehta (2009), either of these two inputs seems to be sufficient to generate CA1 place fields, but both are required for a sharp spatial tuning. The contribution of the entorhinal cortex will be analyzed in detail in Chapter 4. Here I advocate that once mechanisms for phase precession in the CA3 region and the MEC are established, they will be sufficient to explain phase precession in CA1 through inheritance (Skaggs et al., 1996; Yamaguchi and McNaughton, 1998; Yamaguchi et al., 2007).

To conclude, the hypothesis that phase precession in CA1 is inherited from CA3 is consistent with both intracellular and extracellular recordings. Understanding the mechanisms behind phase precession, including the inheritance contribution described in this chapter, might help us understand how intrahippocampal dynamics are related to complex cognitive processes in the brain.

The inheritance model presented in this chapter made some very important assumptions regarding place-selectivity in the CA3 input population and of the target CA1 cell receiving that input. First of all, the model required that the CA1 cell is active at the same place as the CA3 cells that provide excitatory inputs to it. It is not clear, however, how this place-selectivity might arise in a CA1 cell given random connectivity in the CA3-CA1 network. Second, the place fields in the CA3 input population were highly overlapping. What can the inheritance model say when the place fields are allowed to be partially overlapping? In Chapters 3 and 4, I will study these two questions by developing further the inheritance framework proposed here.

3. A model of place-field inheritance through Hebbian learning

In the previous chapter, I outlined how the inheritance of phase precession in the hippocampal formation might take place. Particularly, I focused on the CA3-CA1 network and showed how a population of CA3 cells can propagate phase precession to a single CA1 cell receiving this input. An important assumption of this model was that the place fields of the upstream CA3 assembly are highly overlapping with the place field of the target CA1 cell. In the scenario I considered, it was implied that not only the phase precession was inherited but also the place selectivity. It is not clear, however, how the right CA3-CA1 synaptic weights are selected to form a place cell in CA1 so that a CA1 cell responds in a limited region of the environment. In this chapter, I explore how a CA1 place field can emerge from the activity of a population of CA3 neurons tuned to different places given that (1) the CA3-CA1 weights are initially random and (2) the CA3-CA1 synapses are endowed with a spike-timing-dependent-plasticity rule.

3.1. Summary

[1] Place selectivity is ubiquitous throughout the hippocampal formation. It is not clear, however, how a cell can develop spatial tuning. If the inputs to a given cell are spatially tuned to different places but the weights of the synapses that connect the inputs to the target cell are random, there is no structure and hence no place-selectivity in the output cell. Here I explore how spatial tuning emerges via a symmetry-breaking process whereby a few synapses become strengthened while others become weakened through Hebbian learning. This scenario is explored at the CA3-CA1 collateral system where the synapses that connect CA3 place cells to a CA1 cell have been shown to be plastic. It is shown, both analytically and numerically, that a structure emerges if there is sufficient overlap amongst the place fields of the input cells. Furthermore, I show how and why theta modulation and/or phase precession of the upstream cells aids in the structure formation process.

3.2. Introduction

Place cells in the hippocampal formation have been well characterized since their discovery in 1971. Although it is known that path integration mechanisms, sensory input, other spatially tuned cells, and previous experience play an important role, there is to date no widely accepted theory on the formation of place fields (Moser et al., 2008).

[1] The work presented in this chapter is the result of a collaboration with Richard Kempter, Henning Sprekeler, and, notably, Tiziano D'Albis who worked on this project in the context of his thesis for the Bernstein Center for Computational Neuroscience Berlin master program. I conceived the project, supervised Tiziano D'Albis in all stages of the development of the project, and interpreted the results. Tiziano performed the numerical simulations for Figures 3.3 and 3.4, and carried out the analytical derivations in Appendix A.

Place fields have been observed throughout the hippocampal formation, including the dentate gyrus, regions CA3 and CA1, and the subiculum. Most recordings on place fields come from pyramidal cells in regions CA3 and CA1 (Mizuseki et al., 2012). The CA1 pyramidal cells receive excitatory inputs from the CA3 pyramidal cells through the Schaffer collaterals and from layer III of entorhinal cortex (EC) through the perforant path (Anderson et al., 2007). The CA3 region contains place cells (e.g. Mizuseki et al., 2012) while EC consists of a mix of grid cells, head-direction cells, band cells, and non spatially-tuned cells (Hafting et al., 2005; Sargolini et al., 2006). Thus, some of the inputs to a CA1 cell have some degree of spatial tuning (Zhang et al., 2013). Indeed, the possibility of place-field formation from entorhinal grid-field input has been proposed in several studies (McNaughton et al., 2006; Solstad et al., 2006). In this chapter, I focus on the CA3 inputs to CA1 and propose that a CA1 place field can spontaneously emerge from the activity of spatially-tuned CA3 neurons if synapses obey a Hebbian synaptic plasticity rule. The study of place-field inheritance at the CA3-CA1 synapses is mainly motivated by the following:

- The inheritance of phase precession as explored in the previous chapter requires inheritance of place-field tuning as well.
- Intact CA3-CA1 synaptic plasticity mechanisms have been found to be important for the formation of sharp CA1 place fields: McHugh et al. (1996) observed diffuse CA1 place fields in CA1-specific NMDAR1 knockout mice, and more generally, NMDA receptors are heavily involved in synaptic plasticity and learning (Nakazawa et al., 2004).
- Both regions show high place-selective activity during navigation in linear and open environments (Harris et al., 2002; Mizuseki et al., 2009; 2012; Kjelstrup et al., 2008).
- CA3 represents the largest source of excitatory input to a CA1 pyramidal cell (Megias et al., 2001) and excitatory projections from the CA3 region to the CA1 region through the Schaffer collaterals are unidirectional (Megias et al., 2001; Kajiwara et al., 2008).

The Hebbian learning rule adopted here is spike-timing dependent plasticity (STDP) (e.g. Gerstner et al., 1996; Markram et al., 1997; Kempter et al., 1999; Song et al., 2000), where a change of the synaptic weights depends on the ordering of pre- and post-synaptic activation (see also Chapter 1). Although no clear evidence exists for STDP at the CA3-CA1 connection (Wittenberg and Wang, 2006), STDP has been shown to be a valid model to explain synaptic changes of hippocampal neurons in dissociated cultures and in slices (Markram et al., 1997; Bi and Poo, 1998). Furthermore, from a theoretical perspective, STDP has some properties that are relevant for the study: the learning rule can induce competition between the inputs for the control of the post-synaptic output, enabling a neuron to learn input correlations in an unsupervised manner (Kempter et al., 1999; Abbott and Nelson, 2000). Indeed, STDP has been successfully adopted in several computational studies modelling the activity-based emergence of neural functions, including learning the precise temporal delays in a model of the auditory system of the barn-owl (Gerstner et al., 1996) and to model the development of a stimulus-selective cortical column (Song and Abbott, 2001). Is STDP sufficient to explain the emergence of a CA1 place field if CA3-CA1 synaptic strengths are initially randomly distributed?

In Chapter 2, I considered phase precession in the CA3 population. How does phase precession affect the place-field inheritance process? More generally, how does theta modulation of the spiking activity interact with the STDP rule? Using a mathematical model

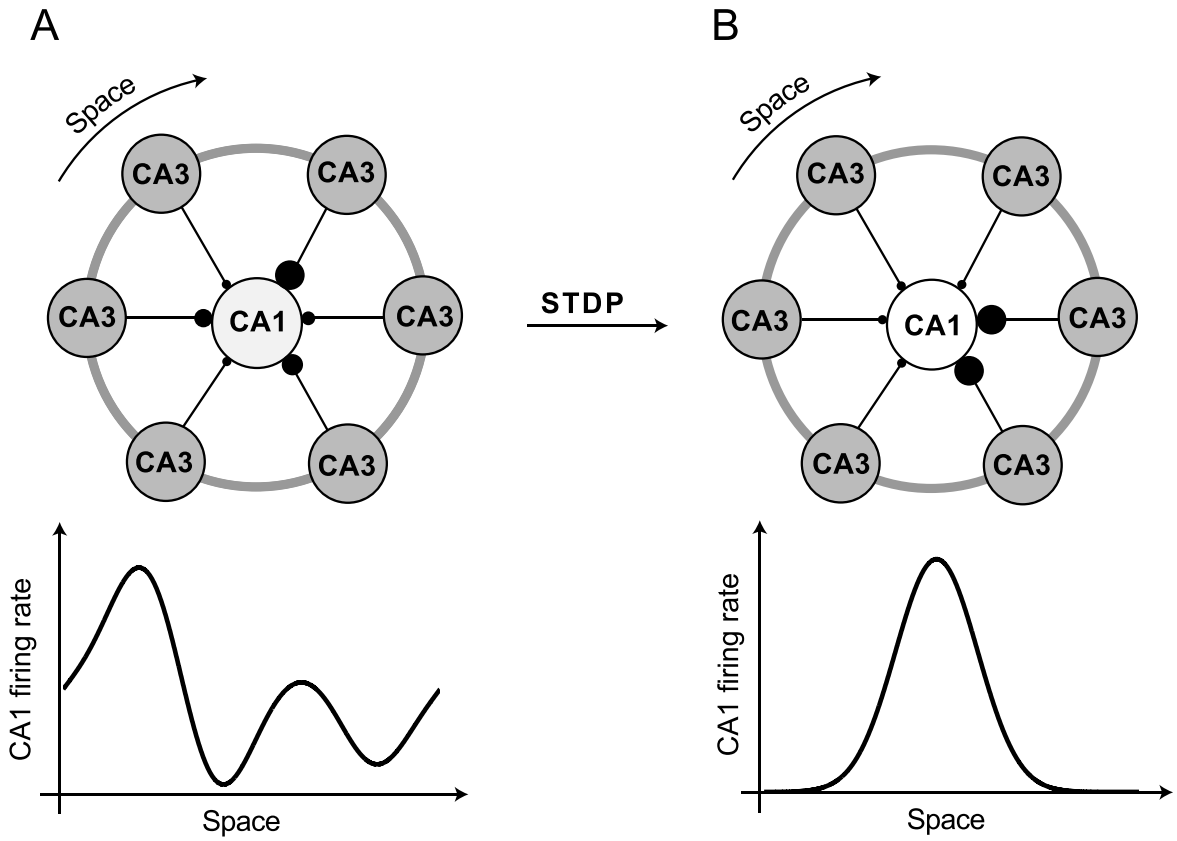

Fig. 3.1.: Model of place-field inheritance through STDP. A single CA1 cell receives synaptic inputs from many CA3 place cells arranged in a ring topographically where neighboring cells have neighboring place fields on the track. ***A,*** Initially, the CA3-CA1 synaptic connections are randomly distributed and no place field is present in CA1. ***B,*** I hypothesize that, after experience, a structure emerges in the space of CA3-CA1 synaptic weights which corresponds to a place field in CA1.

of the neural activity in CA3 and CA1, I propose a model for the CA3-CA1 inheritance of hippocampal place fields based on STDP. I consider a hypothetical experiment where a rat is running around a circular track, and a pool of active CA3 cells project to a single CA1 cell. The model assumes that place fields are already formed in CA3 and that the CA3-CA1 connections are plastic according to STDP. I test the hypothesis of CA3-CA1 place-field inheritance by studying both analytically and numerically the dynamics of the CA3-CA1 synaptic efficacies. Finally, I investigate the roles of the hippocampal theta modulation and phase precession in the model.

3.3. Methods

3.3.1. Model topology

I model the activity of a population of N CA3 cells projecting to a CA1 cell, assuming that place fields are already formed in CA3 and that the CA3-CA1 synaptic efficacies are plastic according to STDP. The possibility of CA3-CA1 place-field inheritance is examined considering an hypothetical experiment of a rat running at constant speed on a circular

track. The hypothesis is that, starting from random connectivity, the activity of the CA3 place cells, combined with the STDP learning rule, can induce structure formation in the distribution of the CA1 input synapses giving rise to a CA1 place field (Figure 3.1).

3.3.2. Dynamics of the synaptic weights endowed with a Hebbian learning rule: spike-timing dependent plasticity

Consider N pre-synaptic input neurons that project to one post-synaptic output neuron. Furthermore, these N synapses obey an STDP rule as proposed by Kempter et al. (1999) where:

(1) an input spike at synapse i increases J_i for $i = 0, \ldots, N-1$ by an amount $\eta\, w^{\text{in}}$;

(2) an output spike increases the weights of all input synapses by an amount $\eta\, w^{\text{out}}$;

(3) an input-output pair of spikes at synapse i increases J_i by an amount $\eta\, W(\Delta t)$ (Hebbian term);

where η is the learning rate ($0 < \eta \ll 1$), w^{in} and w^{out} are constant parameters ($w^{\text{in}} > 0, w^{\text{out}} < 0$) and $W(\Delta t)$ is the learning window as a function of the time difference $\Delta t = t_{\text{pre}} - t_{\text{post}}$ between input and output spikes. Additionally, hard-bounds are imposed to individual synapses within the limits 0 and $J_{\max} > 0$. To understand the effect of bounds, the unbounded case is studied analytically.
To model the dynamics of the learning rule for the N CA3-CA1 synapses, four assumptions are made. First, the learning rate η is such that the time scale of learning is much slower than the neural spiking dynamics. Second, the pre-synaptic inputs are inhomogeneous Poisson processes with rates $\lambda_i^{\text{in}}(t)$. Third, the post-synaptic output is an inhomogeneous Poisson process with rate

$$\lambda^{\text{out}}(t) = v_0 + \sum_{i=0}^{N-1} \sum_k J_i(t_i^k)\epsilon(t - t_i^k) \tag{3.1}$$

where v_0 is the spontaneous output-rate, $\epsilon(t)$ is the excitatory post-synaptic potential (EPSP), and t_i^k is the arrival time of the k^{th} input spike at synapse i. For convenience, the EPSP function is normalized to unit integral: $\int_{-\infty}^{\infty} \mathrm{d}t\, \epsilon(t) = 1$. Fourth, the input firing rates averaged over a time interval $\mathcal{T}$, are identical and constant: $\frac{1}{\mathcal{T}} \int_t^{t+\mathcal{T}} \mathrm{d}t\, \lambda_i^{\text{in}}(t) = \lambda^{\text{in}} \quad \forall t, i$, where $\mathcal{T}$ is much larger than typical inter-spike intervals. Kempter et al. (1999) showed that, under the above assumptions, the dynamics of the synaptic efficacies $\{J_i\}$, averaged over the time interval $\mathcal{T}$, obey the following differential equation:

$$\frac{\mathrm{d}}{\mathrm{d}t} J_i(t) = k_1 + k_2 \sum_{j=0}^{N-1} J_j(t) + \sum_{j=0}^{N-1} Q_{ij}(t)\, J_j(t) + k_3 J_i(t). \tag{3.2}$$

Absorbing the learning rate η in w^{in}, w^{out}, and W, and denoting $\widehat{W}(0)$ as the integral of the learning window, the three constants k_1, k_2, and k_3 are

$$\begin{aligned} k_1 &= [w^{\text{out}} + \widehat{W}(0)\lambda^{\text{in}}]v_0 + w^{\text{in}}\lambda^{\text{in}}, \\ k_2 &= [w^{\text{out}} + \widehat{W}(0)\lambda^{\text{in}}]\lambda^{\text{in}}, \\ k_3 &= \lambda^{\text{in}} \int_{-\infty}^{\infty} \mathrm{d}s\, W(s)\epsilon(-s), \end{aligned} \tag{3.3}$$

and the matrix $Q_{ij}(t)$ is given by

$$Q_{ij}(t) = \frac{\eta}{\mathcal{T}} \int_{t}^{t+\mathcal{T}} \mathrm{d}\tau \int_{-\infty}^{\infty} \mathrm{d}s\, W(s) \left[\lambda_i^{\mathrm{in}}(\tau + s) - \lambda^{\mathrm{in}}\right] \left[\Lambda_j^{\mathrm{in}}(\tau) - \lambda^{\mathrm{in}}\right] \tag{3.4}$$

where $\Lambda_j^{\mathrm{in}}(t)$ are the EPSP-filtered input intensities: $\Lambda_j^{\mathrm{in}}(t) = \int_{-\infty}^{\infty} \mathrm{d}\tau\, \epsilon(\tau)\, \lambda_j^{\mathrm{in}}(t-\tau)$. Under the assumptions above, I use Equation 3.2 to model the dynamics of the CA3-CA1 synaptic efficacies, choosing an averaging time window of length $\mathcal{T} = T_{\mathrm{tot}}$, where T_{tot} is the time taken by the rat to complete one round of the track. This choice is reasonable because, considering a rat running at constant speed, the spatially-tuned CA3 input intensities are periodic with fundamental period T_{tot}. Therefore, averaging over T_{tot} is equivalent to averaging over any larger interval multiple of T_{tot}. In this setting, one can eliminate the time dependence from the expression of $Q_{ij}(t)$ in Equation 3.4,

$$Q_{ij} = \frac{\eta}{T_{\mathrm{tot}}} \int_{0}^{T_{\mathrm{tot}}} \mathrm{d}\tau \int_{-\infty}^{\infty} \mathrm{d}s\, W(s) \left[\lambda_i^{\mathrm{in}}(\tau + s) - \lambda^{\mathrm{in}}\right] \left[\Lambda_j^{\mathrm{in}}(\tau) - \lambda^{\mathrm{in}}\right], \tag{3.5}$$

and one can re-write the learning dynamics as a linear dynamical system with constant coefficients:

$$\frac{\mathrm{d}}{\mathrm{d}t} J_i(t) = k_1 + k_2 \sum_{j=1}^{N} J_j(t) + \sum_{j=1}^{N} Q_{ij}\, J_j(t) + k_3\, J_i(t). \tag{3.6}$$

As STDP learning window double-exponential function is adopted (Song et al., 2000),

$$W(\Delta t) = \begin{cases} A^+ \exp(\Delta t/\tau_+) & \text{if } \Delta t < 0 \\ -A^- \exp(-\Delta t/\tau_-) & \text{if } \Delta t \geq 0, \end{cases} \tag{3.7}$$

where $\Delta t = t_{\mathrm{pre}} - t_{\mathrm{post}}$ is the time difference between a pair of pre- and post-synaptic spikes, τ_+ and τ_- define the intervals over which synaptic strengthening and weakening occur, and A_+ and A_- determine the maximum amount of synaptic modification ($A_+ > 0, A_- > 0$). The parameters A_+, A_-, τ_+ and τ_- are chosen such that the integral of the learning window is positive: $\widehat{W}(0) = A_+\tau_+ - A_-\tau_- > 0$. Furthermore, assuming $w^{\mathrm{in}} > 0$ and $w^{\mathrm{out}} < 0$ the learning rule leads both to a normalization of the output rate and to a competition between the inputs such that input correlations can be learned (Kempter et al., 1999). Additionally, the constraints $k_2 < 0$ and $-k_2 \gg k_3$ are imposed, and weak input correlations are assumed, i.e., $Q^{\mathrm{av}} \ll -k_2$, where $Q^{\mathrm{av}} = N^{-2} \sum_{ij} Q_{ij}$ is the average value of the correlation matrix $mathbf{Q}$.

In this case, the learning rule leads to an intrinsic normalization of the average synaptic efficacy $J^{\mathrm{av}} = N^{-1} \sum_i J_i$ to the fixed-point (Kempter et al., 1999)

$$J_*^{\mathrm{av}} = -\frac{k_1}{N(k_2 + Q^{\mathrm{av}}) + k_3} \approx -\frac{k_1}{N k_2}\,. \tag{3.8}$$

For convenience, I further impose $1 - k_1/k_2 \ll 1$ such that J_*^{av} is close to $1/N$.Finally, the EPSP is modeled as an alpha function normalized to unit integral:

$$\epsilon(t) = t/\tau_{\mathrm{EPSP}}^2 \exp(-t/\tau_{\mathrm{EPSP}})\mathcal{H}(t),$$

where $\mathcal{H}(t)$ is the Heaviside step function and τ_{EPSP} is the decay time constant.

3.3.3. Description of the CA3 input dynamics

I model the activity of a population of N CA3 place cells projecting to a single CA1 cell considering a rat running at constant speed v on a circular track of length L ($v = 0.5$ m/s, $L = 1$ m). Therefore, the activity $\lambda_i^{\text{in}}(t)$ of a CA3 place cell is periodic with period $T_{\text{tot}} = L/v = 2$ s, and it can be expressed with an infinite periodic summation,

$$\lambda_i^{\text{in}}(t) = \sum_{n=-\infty}^{\infty} \lambda_i^L(t - n\,T_{\text{tot}}) \quad \forall n \in \mathbb{Z}, \tag{3.9}$$

where $\lambda_i^L(t)$ is the time-dependent Poisson firing rate of cell i for an infinite linear track. The summation starts from $n = -\infty$ rather than from $n = 0$ to avoid boundary effects at $t = 0$.

The activity of the CA3 neurons is modeled in four different scenarios: (1) no theta modulation, (2) in-phase theta modulation, (3) phase precession, and phase recession. Hippocampal recordings (O'Keefe and Recce, 1993; Skaggs et al., 1996; Harris et al., 2002; Mizuseki et al., 2012) are more consistent with the phase-precession scenario. The other scenarios are interesting from a theoretical point of view, allowing to disentangle different aspects of the neural activity in CA3 and to better understand the roles of theta modulation and phase precession. The function $\lambda_i^L(t)$ takes a different form for each of the four scenarios considered.

In the first scenario, the firing rate of a CA3 cell is modeled as a Gaussian function G (Figure 3.2A):

$$\lambda_i^L(t) = T_{\text{tot}}\lambda^{\text{in}} \underbrace{\frac{1}{\sigma\sqrt{2\pi}} \exp\left(-\frac{(t - T_i)^2}{2\,\sigma^2}\right)}_{G(t - T_i)}, \tag{3.10}$$

where $T_i \in [0, T_{\text{tot}})$ is the time taken by the virtual rat to reach the center of place field i in the first round of the track, and σ determines the size of the place field. Here, as in all the remaining cases, place fields are regularly spaced on the track and in time:

$$T_{i+1} - T_i = \Delta T = \frac{T_{\text{tot}}}{N} \quad \forall i. \tag{3.11}$$

The normalization factor $T_{\text{tot}}\lambda^{\text{in}}$ in Equation 3.10 is chosen such that the activity of the CA3 inputs, averaged over the period T_{tot}, is equal to λ^{in}:

$$\frac{1}{T_{\text{tot}}} \int_0^{T_{\text{tot}}} \mathrm{d}t\, \lambda_i^{\text{in}}(t) = \frac{1}{T_{\text{tot}}} \int_{-\infty}^{\infty} \mathrm{d}t\, \lambda_i^L(t) = \lambda^{\text{in}} \quad \forall i, \tag{3.12}$$

as it is assumed by the STDP model (Section 3.3.2, assumption 4).

In the second scenario, the hippocampal theta rhythm imposes a common modulation to the inputs (Mizuseki et al., 2009; 2012) so that the input-modulating frequency f_λ matches the frequency f_θ of the theta oscillation (Figure 3.2B). As a consequence, the input intensities of different CA3 inputs peak always at the same phase of the theta rhythm, i.e., neither phase precession nor phase recession are modeled. For convenience, the input oscillations peak at the peaks of the theta rhythm. In this scenario, CA3 place field is modeled as

$$\lambda_i^L(t) = T_{\text{tot}}\lambda^{\text{in}}\,[1 + \cos(\omega_\lambda\, t)]\, G(t - T_i) \tag{3.13}$$

where $\omega_\lambda = 2\pi f_\lambda$ is the angular velocity of the modulating sinusoid. The time-averaged input intensity is

$$\frac{1}{T_{\text{tot}}} \int_0^{T_{\text{tot}}} \mathrm{d}t\, \lambda_i^{\text{in}}(t) = \lambda^{\text{in}} + \lambda^{\text{in}}\, \cos(\omega_\lambda T_i)\, \widehat{G}(\omega_\lambda) \tag{3.14}$$

where $\widehat{G}(\omega) = \int_{-\infty}^{\infty} \mathrm{d}t\, G(t) \exp(-j\omega t)$ is the Fourier transform of $G(t)$ and j is the imaginary unit. If the width σ of the Gaussian is large enough compared to the fundamental period of the modulating sinusoid, i.e., $\pi\sigma \gg 1/f_\lambda$, then $\widehat{G}(\omega_\lambda) = \exp(-\omega_\lambda^2\sigma^2/2) \ll 1$, and the integral in Equation 3.14 can be approximated by λ^{in}. Finally, to maintain the circularity of the system, I impose $f_\lambda = k/T_{\text{tot}}$ with $k \in \mathbb{N}$.

In the third scenario, I consider modulated CA3 inputs that show phase precession: as the animal moves across a place field, the associated place cell spikes preferentially at earlier and earlier phases of successive theta cycles (Figure 3.2C) (O'Keefe and Recce, 1993). To generate such phase precession in a firing rate model, the input-modulating frequency f_λ is slightly higher than the frequency of the theta oscillation f_θ. I assume $f_\theta = (1-c)f_\lambda$ where c is the so-called compression factor $(0<c\ll 1)$ (Geisler et al., 2010). Additionally, following Geisler et al. (2010), I assume that, at the center of each firing field ($t = T_i$ for cell i), the phase of the input oscillation $\omega_\lambda t + \phi_i$ equals the phase of the theta rhythm $\omega_\theta t$, meaning that high discharge probability occurs at a preferred theta phase (Huxter et al., 2003; Dragoi and Buzsáki, 2006). For convenience, and in line with the in-phase-modulation scenario, I assume this phase to be zero (in Figure 3.2C high firing rate-peaks occur around the peak of the theta cycle). Mathematically, this requires input i to be modulated with a phase offset $\phi_i = -c\,\omega_\lambda T_i$, which leads to the following time-dependent firing rates:

$$\lambda_i^L(t) = T_{\text{tot}}\lambda^{\text{in}} \left[\, 1 + \cos(\omega_\lambda\, (t - c\, T_i)) \,\right] G(t - T_i). \tag{3.15}$$

In this case, the distance ΔT between two place fields is related to the compressed distance $c\Delta T$ between the spike timings within a theta cycle, that is, the order of spiking within a theta cycle encodes the sequence of place fields traversed (Skaggs et al., 1996). In other words, if the rat takes a time ΔT to move from one place-field center to another, the corresponding place cells spike, within a theta cycle, with an average time lag $c\Delta T$ (Figure 3.2C). Note that by setting $c = 0$ in Equation 3.15 one recovers the case of modulation without phase precession in Equation 3.13. Similarly to this previous case, the time-averaged input intensities can be approximated by λ^{in} because

$$\frac{1}{T_{\text{tot}}} \int_0^{T_{\text{tot}}} \mathrm{d}t\, \lambda_i^{\text{in}}(t) = \lambda^{\text{in}} + \lambda^{\text{in}}\, \cos\left(\omega_\lambda T_i\, (1-c)\right)\, \widehat{G}(\omega_\lambda) \approx \lambda^{\text{in}} \quad \forall t_0, i. \tag{3.16}$$

Finally, to maintain the circularity of the system, I impose $f_\lambda = k/T_{\text{tot}}$ and $f_\theta = h/T_{\text{tot}}$ with $k, h \in \mathbb{N}$, which implies $c = (k-h)/k$.

In the fourth scenario, I consider the hypothetical case in which the CA3 inputs would show phase recession: as the animal moves across a place field, the associated place cell spikes at later and later phases of successive theta cycles, and the order of spiking within a theta cycle encodes the sequence of place fields traversed in reverse order (Figure 3.2D). In this scenario, the CA3 input intensities are modeled in the same way as in the phase-precession case, but inverting the direction of the phase shifts in the modulating sinusoid:

$$\lambda_i^L(t) = T_{\text{tot}}\lambda^{\text{in}} \left[\, 1 + \cos(\omega_\lambda\, (t + c\, T_i)) \,\right] G(t - T_i). \tag{3.17}$$

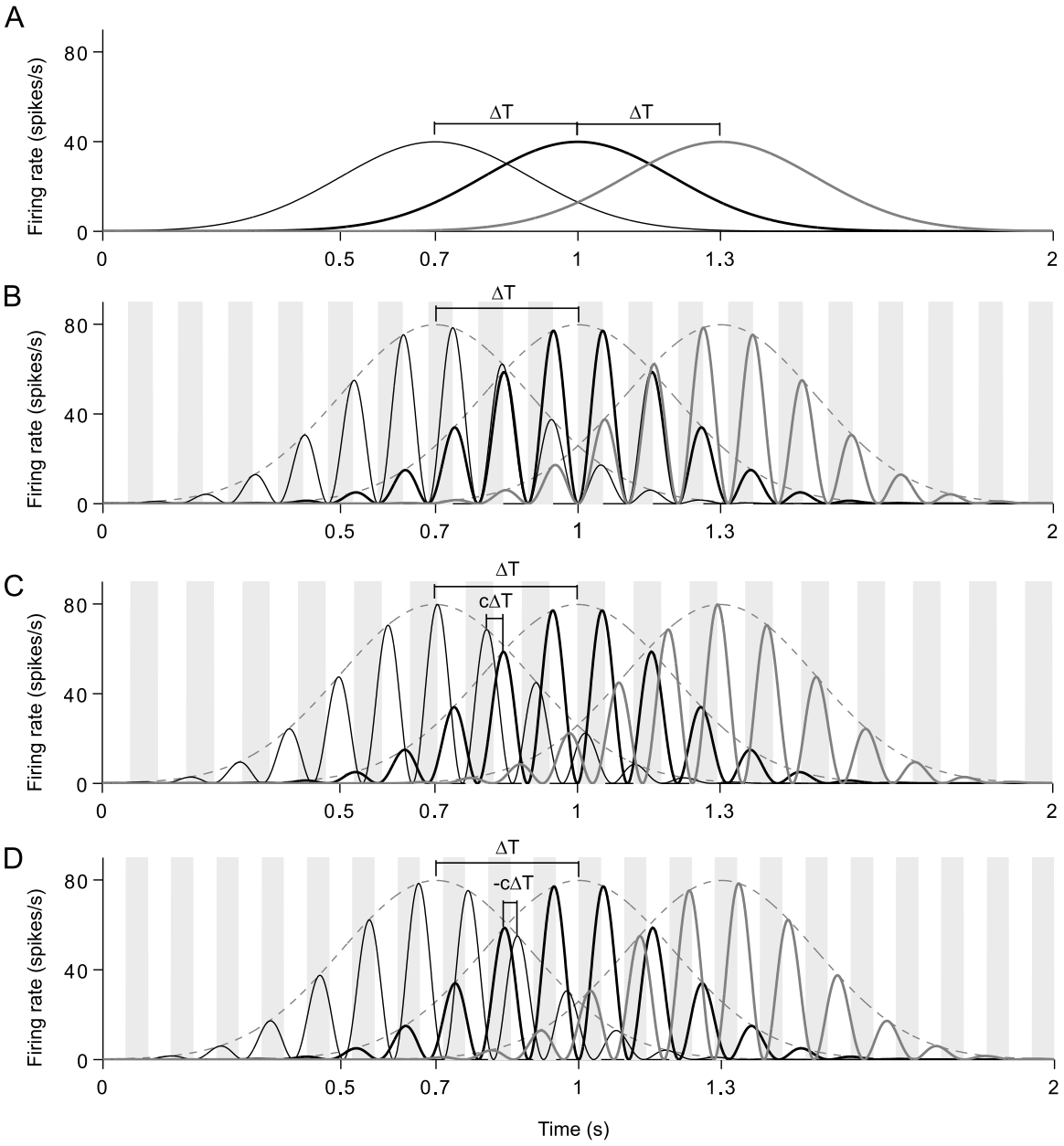

Fig. 3.2.: Model of the CA3 input dynamics for four different input rates $\lambda_i^{\text{in}}(t)$: ***A,*** no modulation, ***B,*** in-phase theta modulation, ***C,*** phase precession, ***D,*** and phase recession. In *B*-*D*, the input-modulation frequency f_λ is kept constant ($f_\lambda = 9.5$ Hz), while the theta-oscillation frequency f_θ is $f_\theta = f_\lambda = 9.5$ Hz in *B*, $f_\theta = (1-c)f_\lambda = 8.5$ Hz in *C*, and $f_\theta = (1+c)f_\lambda = 10.5$ Hz in *D*. Here $c = 0.105$ is the compression factor and gray shades indicate rising phases of the theta cycle. In *B*, the inputs peak in phase with the theta cycle, while in *C* (*D*), the inputs peak at earlier and earlier (later and later) phases in successive theta cycles. ΔT is the time taken by the virtual rat to move between two neighboring place-field centers. Within a theta cycle, neighboring inputs peak with an average time lag that is zero in *B*, $c\Delta T$ in *A*, and $-c\Delta T$ in *D*. Note that in *D* the inputs peak in reverse order compared to the direction of place- field traversal.

Thus, theta frequency f_θ is obtained that is slightly higher than the frequency f_λ of the input oscillations ($f_\theta = (1+c)f_\lambda$ for $0 < c \ll 1$). Similarly to the previous case, the time-averaged input intensities are approximated by λ^{in}, and I impose $f_\lambda = k/T_{\text{tot}}$ and $f_\theta = h/T_{\text{tot}}$ with $k, h \in \mathbb{N}$ to maintain the circularity of the system.

3.3.4. Initial conditions and bounds of the synaptic weights

It is assumed that there is no structure in the synaptic weights before learning takes place. Therefore, the evolution of the synaptic weights (Equation 3.6) is started with random initial conditions, i.e., from a random vector $\mathbf{J}(0)$. More formally, $\mathbf{J}(0)$ is a random vector whose components are uniformly distributed with mean $J_{\text{norm}} = 1/N$ and range Γ where $\Gamma \ll J_{\text{norm}}$. The biophysical interpretation of $\mathbf{J}(0)$ is that of random synaptic wiring where the synaptic efficacies are normalized, i.e., the sum of the efficacies is a constant. Furthermore, it is assumed that synaptic weights are bounded between two saturation levels 0 and $J_{\max}$ ($J_{\max} \gg 1/N$).

3.4. Results

I study whether a place field in CA1 can be inherited from the CA3 region. More precisely, I examine whether a structure can emerge in the synaptic weights connecting CA3 cells to a CA1 cell if the CA3 cells are spatially tuned and the CA3-CA1 synaptic weights are initially randomly distributed but endowed with an STDP rule. For this, I assume that a virtual rat is running on a circular track and place fields on the track are arranged topographically in a ring (see Figure 3.1). In this scenario, CA3 cells are arranged in a ring and each project to the same target CA1 cell. I simulate the dynamics of the CA3-CA1 synaptic efficacies according to the STDP rule describing their evolution. To this end, the differential equation describing the dynamics of the synaptic efficacies $\mathbf{J}$, i.e., Equation 3.6, is solved numerically. Moreover, $\mathbf{Q}$ in Equation 3.6 is calculated using the input intensities $\{\lambda_i^{\text{in}}(t)\}$ introduced in Section 3.3.3 for the four cases considered. The parameter values used for the simulations are given in Appendix A.2.

3.4.1. Emergence of a CA1 place field: case of non-modulated inputs

I begin studying the development of the synaptic efficacies for the simplest case where inputs are not modulated. Figure 3.3 shows the results obtained for a random initial condition. We notice that the synaptic efficacies diverge towards the two saturation levels until, at the end of the simulation, they are bimodally distributed at 0 and $J_{\max}$ (Figure 3.3A). This symmetry breaking derives from the competitive dynamics that is intrinsic to the additive STDP learning rule. Additionally, the synaptic efficacies cluster in a way that only synapses corresponding to neighboring CA3 inputs are potentiated while all the others are depressed (Figure 3.3B,C), such that a place field emerges in CA1 (Figure 3.3D).

The location where a CA1 place field emerges depends only on the initial condition, which is random. The size of a CA1 place field is proportional to the number of potentiated CA3-CA1 synapses, which, in turn, depends on the upper saturation boundary $J_{\max}$. The STDP learning rule tends to keep the average synaptic efficacy normalized and, as a consequence, the number of potentiated synapses decreases as the upper saturation boundary increases. I choose $J_{\max} = 0.4$ to avoid the trivial case where only a single synapse survives; this case is obtained numerically for $J_{\max} \geq 1.2$ because the number of synapses is discrete and the

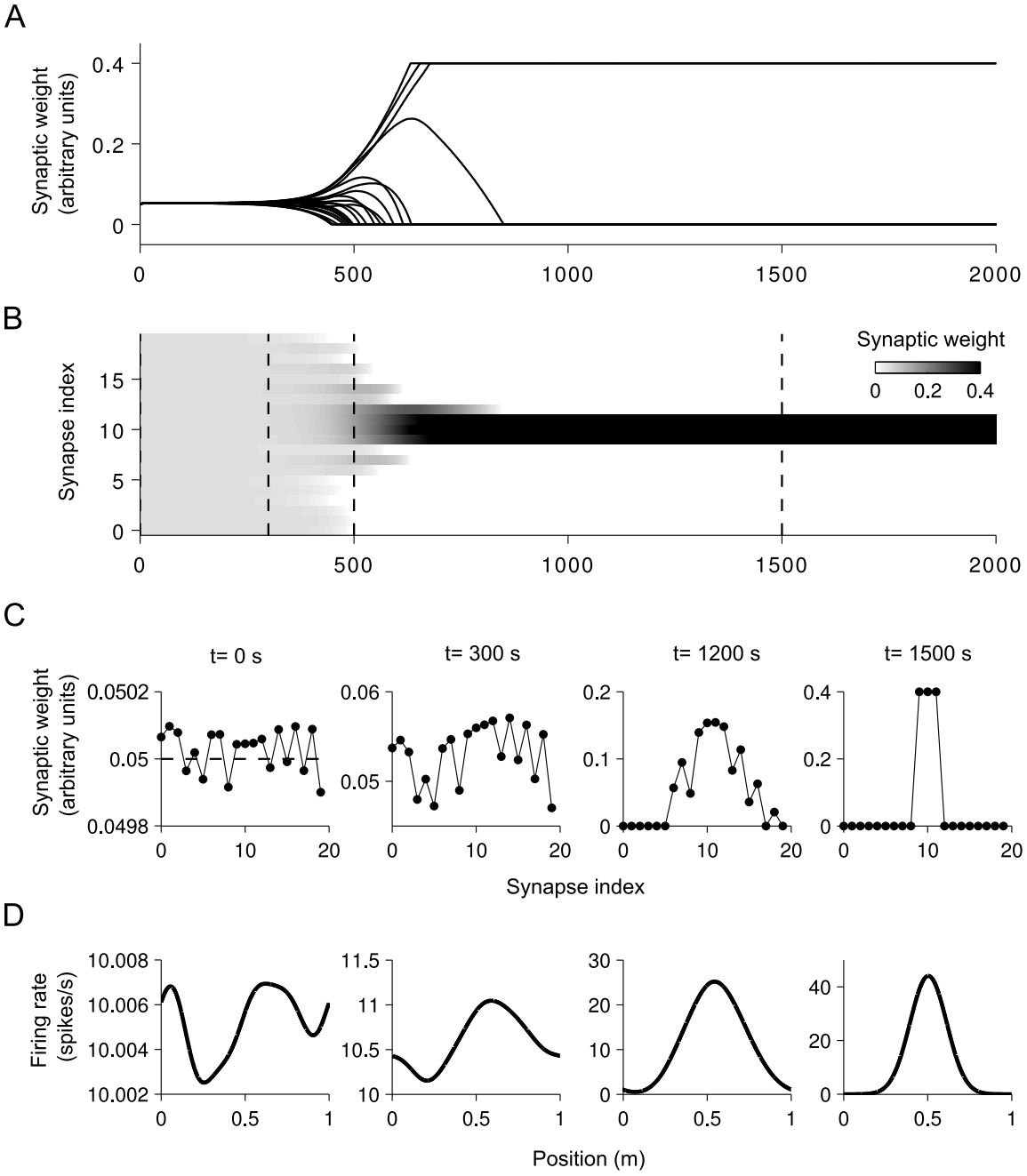

Fig. 3.3.: Emergence of a CA1 place field for non-modulated inputs and bounded synapses. ***A,*** Efficacies of individual synapses as a function of time. ***B,*** Synaptic efficacy vector, coded on a gray-scale, and plotted over time. The components of the synaptic efficacy vector are ordered according to the topography of the associated CA3 place fields, i.e, similar indexes in the efficacy vector correspond to neighboring CA3 place fields. ***C,*** Snapshots of the synaptic efficacies at the four time points indicated (vertical dashed lines in B). In the first panel ($t = 0$), the horizontal dashed line corresponds to the normalization level J_{norm}. ***D,*** Ensemble-averaged rate of the CA1 output neuron $r^{\mathrm{out}}(t) = v_0 + \sum_{i=0}^{N-1} J_i(t)\Lambda_i(t)$, computed at the same time points as in C.

learning rule normalizes the average synaptic efficacy to $J^* \approx -k_1/(Nk_2 + N^{-2}\sum_{ij}^{N} Q_{ij})$, which is slightly higher than $1/N$ (Kempter et al., 1999).

3.4.2. Emergence of a CA1 place field: cases of in-phase theta modulation, phase precession, and phase recession

To investigate the roles of theta modulation and phase precession in the inheritance process, I study the development of the CA3-CA1 synaptic efficacies in the three remaining scenarios: in-phase theta modulation, phase precession, and phase recession. For better comparison, in all scenarios the same initial condition and the same parameter values are adopted (Appendix A.2). The simulations are performed both without and with imposing the saturation boundaries to the synaptic efficacies. The case of unbounded synapses, although less biologically realistic, is easier to study analytically and allows to disentangle the fundamental system dynamics from the boundary effects (see Appendix A). In the three scenarios with theta-modulated inputs, the input-modulation frequency f_λ was kept constant while the frequency f_θ of the theta rhythm changed accordingly, i.e., $f_\theta = f_\lambda$ for in-phase theta modulation, $f_\theta = (1-c)f_\lambda$ for phase precession and $f_\theta = (1+c)f_\lambda$ for phase recession (Section 3.3.3).

Example simulations for all cases are reported in Figure 3.4. First, we notice that in all cases a place field emerges in CA1: a dark stripe in a plot indicates a cluster of CA3-CA1 potentiated synapses associated to neighboring CA3 input place fields (Figure 3.3). Additionally, the four scenarios show interesting differences concerning two main points: (1) the time taken for a CA1 place field to emerge and (2) the tendency of a CA1 place field to drift over time.

The fact that a place field emerges faster in the case of in-phase theta modulation and phase precession cases compared to no-modulation can be understood as follows. Since in all scenarios the time-averaged input rates are normalized at the same value λ^{in}, the effect of the theta modulation is to re-distribute the input spikes in time windows with the length of a theta period (Fig. 3.2 A and B). This re-distribution increases the probability for a pair of input-output spikes to be separated by a time-lag that is effective for the plasticity rule and thus favors structure formation. A similar redistribution of spikes is produced also in the phase-precession and phase-recession scenarios (Fig. 3.2 C and D), leading to faster structure formation with respect to the base case. However, as a result of the phase shifts, the overlap between the inputs is now reduced with respect to the in-phase theta modulation case (Fig. 3.2 $B-D$), and less pairs of input-output spikes interact with the learning window, leading to structure formation on a slower time scale.

With unbounded synapses, a CA1 place field drifts over time in all cases (Fig. 3.4 A and Fig. A.1B in the Appendix, left panel). The drift of a CA1 place field is backward with respect to the direction of movement in the first three cases, and forward in the fourth one (phase recession). This can be intuitively understood as follows. Suppose a virtual rat traverses the CA3 input place fields from left to right. The output place field is roughly given by the sum (average) of the input place fields that, for simplicity, can be divided into "early" i.e., fire on average before the output place cell, and "late", i.e., fire on average after the output place cell. Due to the STDP learning rule, the synapses of the "early" input cells develop LTP while the synapses corresponding to the "late" cells develop LTD. Thus, the position of the output place field tends to drift towards the potentiated synapses, i.e., towards the left or in the backwards direction. In the case of phase precession, this effect is exacerbated because of the separation of LTP and LTD due to the phase shift with respect

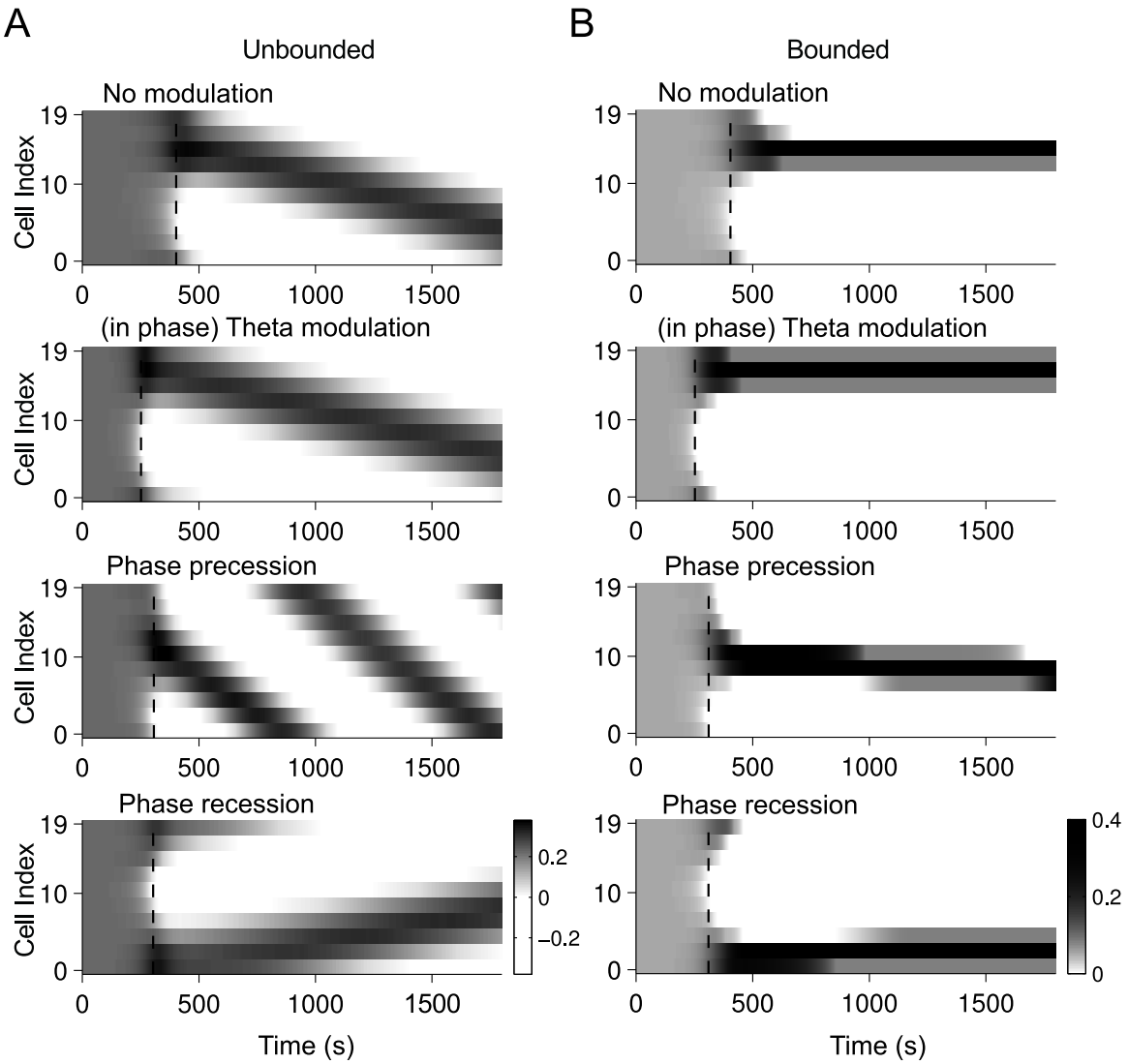

Fig. 3.4.: Emergence of a CA1 place field in the four scenarios: no modulation, in-phase theta modulation, phase precession and phase recession (from top to bottom). The simulations are presented without (***A***) and with (***B***) the two saturation boundaries 0 and $J_{\max}$. Each panel shows the vector of synaptic weights $\mathbf{J}$ coded on a gray-scale and plotted over time. In *A*, the efficacy vector was normalized to unit norm at each time point for visualization purposes (the actual values diverge). The dashed vertical lines denote the time points when a CA1 place field is formed ($\|\psi\| = 0.5$, see main text).

to the input. In the case of phase recession, late inputs peak before early inputs within one theta cycle, leading to a drift in the forward direction. The saturation boundaries have a stabilizing effect on the tendency of a CA1 place field to drift over time (Figure 3.4*B* and Figure A.1*B* in the Apppendix, right panel). Indeed, with bounded synapses, one obtains a stable CA1 place field in three scenarios out of the four considered: no-modulation, in-phase-modulation, and phase-recession. Nevertheless, with phase precession, where the drifting speed with unbounded synapses was considerably higher, the bounds are not able to stabilize the place field and a slow backward drift of the CA1 place field is observed. Interestingly, backward drifting place fields have been also reported experimentally (Mehta et al., 1997; 2000; Lee et al., 2004). Theoretical studies have proposed synaptic plasticity as an explanation for this phenomenon (Abbott and Blum, 1996; Mehta et al., 2000), and the blockage of NMDAR-dependent synaptic plasticity was found to abolish the effect (Ekstrom et al., 2001).

3.5. Discussion

In this chapter I have studied whether it is possible for a CA1 place field to emerge if the inputs are spatially tuned to different places but the synaptic weights are initially random. I studied a simple topology where CA3 cells are arranged in a ring and project to a single CA1 cell. The main findings are that (1) overlapping CA3 place fields along with an additive STDP rule lead to a symmetry breaking of the CA3-CA1 weights such that initially random synaptic wiring is sufficient to explain the emergence of a CA1 place field, (2) theta modulation, both in-phase or the case of phase precession, favors the inheritance process, i.e., the time to form a structure is decreased, and (3) phase precession leads to a drift of the emerging CA1 place field.

3.5.1. Spatial tuning and synaptic plasticity

In the model, spatially-tuned CA1 firing fields were produced by spatially-tuned synaptic inputs. This is assumption is in agreement with a subthreshold ramp-like depolarization of the membrane potential observed within the firing fields of CA1 place cells (Harvey et al., 2009; Epsztein et al., 2011). Moreover, since a CA1 place field emerged from the integration of neighboring CA3 input place fields, place fields will be larger in CA1 than in CA3, which is consistent with experimental findings (Mizuseki et al., 2012). Additionally, the location of a CA1 place field depended only on the initial configuration of the CA3-CA1 synaptic efficacies, which was random, meaning that random synaptic wiring between CA3 and CA1 is sufficient to explain the spatial distribution of CA1 place fields. According to the model, place fields in CA1 would be disrupted if synaptic plasticity mechanisms are blocked or inhibited. Indeed, McHugh et al. (1996) observed larger and less-structured CA1 place fields in CA1-specific NMDAR1 knockout mice. More generally, several studies revealed the importance of NMDAR-dependent plasticity for spatial memory in the hippocampus (Nakazawa et al., 2004). Additionally, I found that synaptic plasticity causes CA1 place fields to drift over time, where the drift is backwards with respect to the direction of movement. This result is consistent with backward-drifting place fields observed experimentally (Mehta et al., 1997; 2000; Lee et al., 2004), and with the fact that blocking NMDAR-dependent plasticity abolishes the effect (Ekstrom et al., 2001).

Structure formation is an important consequence of unsupervised learning rules such as

STDP. The fact that a place field can emerge from a intially random synaptic weight distribution can explain the tuning of spatial receptive fields, but also more generally, other cells with receptive fields as those found in the visual cortex. Other ways to obtain sharp tuning in receptive fields include balanced excitation and inhibition (Hansel and van Vreeswijk, 2012) and attractor networks (Tsodyks et al., 1996). However, it is plausible that a rule such as a STDP exists at the CA3-CA1 synapse and thus the emergence of a spatially-tuned receptive field is a natural consequence of this rule along with the place-selective activity observed at the CA3 region of the hippocampus.

3.5.2. Effects of theta modulation and phase precession

It was shown how theta modulation of the spikes affects the process of place-field formation. Particularly, the cases of in-phase theta modulation and phase precession lead to a faster place field formation than without any modulation. This elucidates a plausible property of phase precession, namely that it favors structure formation (Molter and Yamaguchi, 2008). In Chapter 2 I explored how phase precession in CA3 can be transmitted through feed-forward propagation. The fact that phase precession can lead to faster place field formation of a downstream cell receiving these inputs might be an important function of phase precession. Most functions hypothetically abscribed to phase precession refer to sequence formation (see Chapter 5), so the work developed in the present chapter adds to the list of plausible functions of phase precession. I also found that phase-precessing CA3 place cells cause CA1 place fields to drift faster. Therefore, it is predicted that if phase precession is abolished in the CA3 region, place fields will drift slower in CA1.

3.5.3. Model assumptions and conflicting studies

There are two main lines of results that would argue against the learning of place fields. First of all, place fields can emerge in CA1 even without previous spiking activity as required by a learning rule such as STDP (Lee et al., 2012). This seems in contrast with versions of the STDP rule that rely on post-synaptic firing. Interestingly, Lee et al. (2012) showed that a spatially-tuned subthreshold depolarization appears also in non-spiking CA1 cells, i.e., silent cells, when the soma is slightly depolarized with a spatially-uniform current. The authors suggested that silent cells, like place cells, receive spatially-tuned input, but that this input may not propagate to the soma because of a non-linear gating mechanism dependent on the somatic potential. This observation is in line with the hypothesis that spatial-tuning may be learned within the dendritic tree of place cells, as well as of silent cells, without the need of somatic activation. Indeed, Hebbian learning mechanisms exist even in the absence of post-synaptic firing: Golding et al. (2002) showed that, when somatic spiking was blocked, large amplitude EPSPs (2-4 mV) and locally generated dendritic spikes were sufficient to induce LTP at both distal and proximal synapses of a CA1 pyramidal neuron. Additionally, Remy and Spruston (2007) showed that even a single burst of Schaffer-collateral activation was sufficient for this type of plasticity to occur. Since large-amplitude EPSPs can result from the spatio-temporal integration of correlated synaptic inputs, this was proposed as a Hebbian learning mechanism independent of action-potential firing and back-propagation. We suggest that such a mechanism could induce spatial tuning in a CA1 pyramidal neuron in the same way as Hebbian STDP did in the model.

The second line of results refers to the time for the learning process to take place. The model, although too abstract to predict the actual time needed for learning (the learning-

rate parameter η is not directly related to any measurable biological quantity), suggests that learning is a slow process requiring multiple traversals of the same place to be effective. This might seem in contrast with place fields being observed early after exposure to a novel environment, sometimes even at the very first traversal of a new place (Hill, 1978). In this respect, spatially-tuned CA3-CA1 connections may not need to be re-learned in each environment, but are rather shaped and refined throughout the entire life of an animal exploring different environments. This remains compatible with an environmental-specific remapping of the place-cell activity in CA1 (Leutgeb et al., 2005) that could result from a similar remapping of the activity in CA3.

I now discuss other limitations of the model. First, the entorhinal input to CA1 was not considered although experiments suggest that CA1 place fields are maintained by this input alone (Brun et al., 2002). I hypothesize that a Hebbian learning mechanism can also lead to CA1 place fields from spatially-tuned grid-like entorhinal input. Indeed, grid-to-place models based on Hebbian learning exist (Rolls et al., 2006; Savelli and Knierim, 2010; Cheng S and Frank, 2011), and it cannot be excluded that CA3 and entorhinal inputs interact such that associations are learned between the two. I will return to this issue in Chapter 4 where I study the grid-to-place transformation in the context of phase precession inheritance. Second, only excitatory connections have been considered in the model, while a dense network of interneurons provides strong inhibitory input to hippocampal pyramidal cells (Klausberger et al., 2003). This strong inhibition may indeed explain the low firing rate of CA1 pyramidal cells. Finally, several simplifications have been made in the model: the number of modeled CA3 inputs ($N = 20$) was much lower than the actual number of Schaffer-collateral synapses, $\approx$30 000 (Megias et al., 2001), hippocampal pyramidal cells were assumed to be simple linear Poisson units, synaptic efficacies were modeled as continuous variables ignoring the quantal nature of synaptic transmission (Anderson et al., 2007), and the synaptic saturation boundaries, as well as the parameters of the STDP learning window, were not directly related to measurable biophysical quantities. Nevertheless, with the minimal model presented in this chapter one can study the place-field inheritance hypothesis, and understand, with both analytical and numerical means, how particular properties of the hippocampal neural activity may affect this inheritance.

To conclude, while the mechanisms underlying place-field formation remain unclear, it was shown that the place-field activity in one hippocampal region can be propagated to a downstream region by simple Hebbian learning. Additionally, phase precession was found to favor this inheritance, although it leads to a backward drift of the inherited place fields.

4. Coordination of phase precession through feedforward topologies in the hippocampal formation

In Chapters 2 and 3 I studied the CA3-CA1 network. First, in Chapter 2 I showed that CA3 phase precession can explain the phase precession observed in a CA1 cell and how this is consistent in both sub- and suprathreshold regimes. Next, in Chapter 3 I showed that even with initial random connectivity between these two regions, a place field can emerge in CA1 if CA3 cells already show place-selective activity. In this chapter I now consider a general topology where many cells (input) project to a target cell (output), and the input cells have partially overlapping fields and exhibit phase precession.

4.1. Summary

[1] Phase precession is present throughout the hippocampal formation as well as in the prefrontal cortex and ventral striatum. It is not known whether phase precession is generated independently in each of these regions or conversely, phase precession can be inherited from upstream regions. Here I study the possibility that phase precession can be inherited via feed-forward topologies inside and outside the hippocampus. I find that excitatory input is essential, and that the spatial distribution of place-field centers determine both the place selectivity as well as the phase-precession characteristics of an output cell. Within these framework, I am able to explain why phase precession in the ventral striatum has a particular shape, why interneurons do not phase precess even if they receive inputs from phase precessing cells, and how entorhinal phase precessing cells can form a phase precessing cell in the hippocampus. The results suggest that phase precession is coordinated, a fact that could help explain the ultimate origin of phase precession and shed light on its function.

4.2. Introduction

Phase precession is a spiking phenomenon that was first discovered in the CA1 region of the hippocampus (O'Keefe and Recce, 1993). Afterwards, phase precession was observed throughout the hippocampus (e.g. Skaggs et al., 1996), the entorhinal cortex (Hafting et al., 2008), the prefrontal cortex (Jones and Wilson, 2005), the subiculum (Kim et al., 2012), and the ventral striatum (van der Meer and Redish, 2011). Interestingly, principal cells in these regions receive feed-forward projections from regions that also show phase precession.

[1] Part of the work presented in this chapter has been published in "Modeling inheritance of phase precession in the hippocampal formation", J Neurosci 2014. This project was a collaboration with Robert Schmidt and Richard Kempter as principal supervisor. I conceived the project, performed all simulations, analytical calculations, and interpretation of the results of this chapter.

Can phase precession observed in a cell be simply inherited from a population of cells upstream? What are the main determinants of place-selectivity and phase precession of a downstream cell that receives excitatory input from a set of input cells? In Chapter 2, I had explored the case of the CA3-CA1 network where I showed that an assembly of CA3 cells can propagate phase precession to CA1 given constraints on the size, as well as on the modulation depth of the population firing rate of the assembly. I now analyze a more general feed-forward topology and focus on spatial distributions of place-field centers of excitatory phase-precessing input cells to determine the resulting place selectivity and the phase-precession characteristics of a target cell. I consider, for example, how distributions of place fields in the hippocampal formation give rise to the phase precession observed in areas outside the hippocampus, such as the prefrontal cortex or the ventral striatum (Malhotra et al., 2012). Furthermore, I address the question of why phase precession in hippocampal interneurons is weaker than in principal neurons (Maurer et al., 2006b; Ego-Stengel and Wilson, 2007; Geisler et al., 2007). Finally, I consider entorhinal phase precession which is known to persist after hippocampal activation (Hafting et al., 2008), and how it could lead to phase precession of place cells in the hippocampus. The proposed inheritance mechanism may thus account for phase precession in various cell types in the hippocampus proper, subiculum, prefrontal cortex, and ventral striatum.

4.3. Methods

Here I develop a formalism to study inheritance of phase precession in a general feed-forward topology. In section 2.4.1, I considered inheritance in the CA3-CA1 network of the hippocampus and assumed that the place fields of the cells of the CA3 population that project to a single CA1 cell are identical. I now relax this assumption and consider the case where the place fields of the input population are spatially distributed and partially overlapping. Furthermore, the topology need not be limited to the CA3-CA1 network.

4.3.1. Model for place-selective responses in a feed-forward network.

Consider a virtual rat running on a linear track of length L at a constant speed v, so that the time to complete a run is $T_{\text{tot}} = L/v$. I assume that, along a particular direction (e.g., from left to right), there are N active place cells whose place fields overlap on the track. Furthermore, it is assumed that these cells exhibit phase precession within their place fields. These N input cells project to a single output cell that linearly integrates the inputs to produce a somatic voltage. I wish to characterize the behavior of this output cell in terms of place-field selectivity and phase precession.

The rate $\lambda(t, T_i)$ of a place cell that is active on the linear track is

$$\lambda(t, T_i) = \lambda_0 \left[1 + C \cos\left(2\pi f_\lambda (t - \tau_i)\right)\right] \exp\left[\frac{-(t - T_i)^2}{\sigma^2}\right] \tag{4.1}$$

where T_i is the center of the place field, f_λ is the frequency of the oscillation modulating each cell, C is the firing-rate modulation depth, τ_i is the theta-time scale shift of the oscillation, and σ is proportional to the place field's size. Since phase precession is assumed at the input, the frequency of each single-cell oscillation is greater than the frequency of the theta LFP ($f_\lambda > f_\theta$). As shown in previous studies, the variables T_i and τ_i are correlated so that one

can write $\tau_i = kT_i$, where k is a constant, the compression factor (Skaggs et al., 1996; Dragoi and Buzsáki, 2006; Geisler et al., 2010).

The population firing rate $\lambda(t)$ is obtained through a sum over the N cells,

$$\lambda(t) = \sum_{i=1}^{N} \lambda(t, T_i). \tag{4.2}$$

For $N \gg 1$ and if $T_{i+1} - T_i \ll \sigma \ \forall i$, I can introduce the density p of place field centers such that the population input rate is

$$\lambda(t) \approx \int p(T)\lambda(t, T)\ \mathrm{d}T. \tag{4.3}$$

For place-field centers within the interval $[-\frac{T_{\mathrm{tot}}}{2},\ \frac{T_{\mathrm{tot}}}{2}]$, the normalization condition is

$$\int_{-T_{\mathrm{tot}}/2}^{T_{\mathrm{tot}}/2} p(T)\ \mathrm{d}T = N. \tag{4.4}$$

Thus, I can analytically calculate the population activity $\lambda(t)$ once the density p of place-field centers is defined at the input. Here I consider four distributions, namely p_D (delta), p_G (Gaussian), p_U (uniform), and p_R (ramp) defined by

$$p_D(T) = N\delta\left(T\right), \tag{4.5}$$

$$p_G(T) = \frac{N}{\sqrt{\pi}\sigma_d} \exp\left[\frac{-T^2}{{\sigma_d}^2}\right], \tag{4.6}$$

$$p_U(T) = \frac{N}{T_{\mathrm{tot}}} \quad \text{for } -\frac{T_{\mathrm{tot}}}{2} \le T \le \frac{T_{\mathrm{tot}}}{2} \text{ and 0 otherwise,} \tag{4.7}$$

$$p_R(T) = \frac{2N}{T_{\mathrm{tot}}^2}\left(T + \frac{T_{\mathrm{tot}}}{2}\right) \quad \text{for} -\frac{T_{\mathrm{tot}}}{2} \le T \le \frac{T_{\mathrm{tot}}}{2} \text{ and 0 otherwise,} \tag{4.8}$$

where $\sigma_d \ll T_{\mathrm{tot}}$ is the width of the Gaussian distribution. Finally, the cell's output activity, i.e., somatic voltage $V_{\mathrm{out}}(t)$ is

$$V_{\mathrm{out}}(t) = \lambda(t) * \epsilon(t) \tag{4.9}$$

where $\epsilon(t)$ is as before, a kernel representing an EPSP. I have simulated the results for $V_{\mathrm{out}}(t)$ for each of the above distributions in Figures 4.1 and 4.2. Here I analytically derive $\lambda(t)$ for the case of $p = p_G$. In this case, the integral for the population rate, Equation 4.3, becomes

$$\lambda(t) \approx \frac{N\lambda_0}{\sqrt{\pi}\sigma_d} \int_{-\infty}^{\infty} \left[1 + C\cos\left(2\pi f_\lambda(t - kT)\right)\right] \exp\left[\frac{-(t-T)^2}{\sigma^2}\right] \exp\left[\frac{-T^2}{{\sigma_d}^2}\right] \mathrm{d}T, \tag{4.10}$$

where the limits at infinity are taken provided the size σ_d of the place-field center distribution p_G is much smaller than T_{tot}. Solving the above integral, one obtains

$$\lambda(t) = \frac{N\lambda_0}{\sqrt{\pi(\sigma_d^2 + \sigma^2)}} \exp\left[\frac{-t^2}{\sigma_d^2 + \sigma^2}\right] \left\{1 + C\exp\left[\frac{-(\pi f_\lambda k\sigma_d\sigma)^2}{\sigma_d^2 + \sigma^2}\right] \cos\left[2\pi f_\lambda t\left(1 - \frac{k{\sigma_d}^2}{\sigma_d^2 + \sigma^2}\right)\right]\right\}. \tag{4.11}$$

The above expression represents an output place field with width (proportional to) σ_R and

modulated with a frequency f_R given by

$$\sigma_R = \sqrt{\sigma_d^2 + \sigma^2} \tag{4.12}$$

$$f_R = f_\lambda \left(1 - \frac{k{\sigma_d}^2}{\sigma_d^2 + \sigma^2}\right). \tag{4.13}$$

Furthermore, the modulation depth C_{out} of the output cell is

$$C_{\text{out}} = C \exp\left[\frac{-(\pi f_\lambda k \sigma_d \sigma)^2}{\sigma_d^2 + \sigma^2}\right]. \tag{4.14}$$

Now I calculate the phase-precession range for this output place field. The range $\Delta\phi$ is given by

$$\Delta\phi = 2\pi(f_R - f_\theta)3\sigma_R \tag{4.15}$$

$$= 2\pi \left[f_\lambda \left(1 - \frac{k\sigma_d^2}{\sigma_d^2 + \sigma^2}\right) - f_\lambda(1-k)\right] 3\sqrt{\sigma_d^2 + \sigma^2} \tag{4.16}$$

$$= 6\pi f_\lambda k \frac{\sigma^2}{\sqrt{\sigma^2 + \sigma_d^2}} \tag{4.17}$$

where I have used the fact that $f_\theta = f_\lambda(1-k)$ (Geisler et al., 2010). In the limit of a large place field distribution ($\sigma_d \gg \sigma$), I recover the results predicted for a uniform distribution $p = p_U$ at the input, i.e., a theta oscillation at the output with no place selectivity.

Grid-to-place phase-precession inheritance model. To study inheritance from grid cells to place cells in the hippocampus, I consider the case of phase precession in grid cells of the MEC, which project to pyramidal cells in the hippocampus via the perforant path. Solstad et al. (2006) modeled the grid-to-place transformation as a sum of periodic modes, corresponding to the spacings of the grids, to produce a non-periodic place field. I extend these results and include an oscillatory modulation of the input grid fields as to account for phase precession.

To model the periodic modes, I focus on the 1-dimensional case such that the grid-field activity G is periodic along the x-axis,

$$G(s, x) = \frac{G_{\max}}{2}\left[\cos\left(\frac{2\pi}{s}x\right) + 1\right], \tag{4.18}$$

where $G_{\max}$ is the maximum firing rate within the field and s is the grid-field spacing, i.e., distance between two consecutive grid maxima. By linearly combining grid fields with different spacings s, I wish to obtain a target function $P(x)$ that represents the activity of a place field and is parametrized as

$$P(x) = P_{\max} \exp\left[\frac{-x^2}{\sigma^2}\right] \tag{4.19}$$

where $P_{\max}$ is the maximum firing rate and σ determines the size of the place field. The

even function $P(x)$ can be decomposed into Fourier modes as

$$P(x) = \frac{1}{\sqrt{2\pi}} \int_{-\infty}^{\infty} \tilde{P}(k) \cos(kx)\, \mathrm{d}k \tag{4.20}$$

where $k = 2\pi/s$ is the spatial frequency and

$$\tilde{P}(k) = P_{\max} \frac{\sigma}{\sqrt{2}} \exp\left[\frac{-k^2\sigma^2}{4}\right] \tag{4.21}$$

is the Fourier transform of $P(x)$. In general, $\tilde{P}(k) := \frac{1}{\sqrt{2\pi}} \int P(x) e^{ikx} \mathrm{d}x$.

To relate the place-field activity $P(x)$ to the grid-field activity $G(s, x)$ in Equation 4.18, I express the cosine term in Equation 4.20 in terms of the grid functions as

$$\cos\left(\frac{2\pi}{s}x\right) = \frac{2}{G_{\max}} G(s, x) - 1. \tag{4.22}$$

The expression for $P(x)$ in Equation 4.20 then reads

$$P(x) = \int_{-\infty}^{\infty} \frac{2\sqrt{\pi} P_{\max}\sigma}{G_{\max}\ s^2} \exp\left[\frac{-\pi^2\sigma^2}{s^2}\right] \left[G(s, x) - \frac{G_{\max}}{2}\right] \mathrm{d}s \tag{4.23}$$

where $s = 2\pi/k$ and $\mathrm{d}s = (-2\pi/k^2)\, \mathrm{d}k$. One can express the above expression as a Riemann sum by considering $N \gg 1$ grid fields and by discretizing s as

$$s_n = s_{\min} + (n-1) \cdot \frac{s_{\max} - s_{\min}}{(N-1)} \tag{4.24}$$

where $n \in \{1, 2, .., N\}$ and $s_{\min}$ and $s_{\max}$ are the minimum and maximum spacings, respectively. Equation 4.23 can be approximated as (including a factor 2 to account for both positive and negative spatial frequencies)

$$P(x) \approx \sum_{n=1}^{N} \underbrace{\left(\frac{s_{\max} - s_{\min}}{N-1}\right) \frac{4\sqrt{\pi} P_{\max}\sigma}{G_{\max} s_n^2} \exp\left[\frac{-\pi^2\sigma^2}{s_n^2}\right]}_{= A(s_n, \sigma)} \left[G(s_n, x) - \frac{G_{\max}}{2}\right] \tag{4.25}$$

where $A(s_n, \sigma)$ is the synaptic weight connecting a grid cell with grid field activity $G(s_n, x)$ to the target place cell. Note that the weight $A(s_n, \sigma)$ depends on both the spacing s_n of the input grid functions and the size σ of the target place field; see Figure 4.4 *E* for an example of $A(s_n, \sigma)$ for $\sigma = 0.2$ m, $N = 50$, $s_{\min} = 0.1$ m, and $s_{\max} = 4$ m.

To account for phase precession, I introduce an oscillatory modulation M_n of the grid-cell firing rates $G(s_n, x)$ in a similar manner as done for CA3 cells in Equation 2.2. The time-dependent modulation M_n for a grid cell with spacing s_n is

$$M_n(t) = C \cos(\omega_n t - \phi) + 1 \tag{4.26}$$

where $C \in (0,\ 1]$ is the modulation depth, ω_n is the angular frequency, and ϕ is a phase

offset. The modulated grid activities $G_M(s_n, x)$ are then

$$G_M(s_n, x) = G(s_n, x) M_n \left(\frac{x}{v}\right) \tag{4.27}$$

where, as in Chapter 2, I assume that the virtual animal is running at a constant speed v such that $t = x/v$.

The requirements for choosing ω_n and ϕ are such that (1) there is phase precession per se (Hafting et al., 2008), (2) that the phase-precession slope is inversely proportional to the size of the firing field (Brun et al., 2008), and (3) that there is phase-locking of the first spike(s) within the field (Mizuseki et al., 2009). The first requirement is fulfilled if one takes $\omega_n \gtrsim \omega_\theta \ \forall n$, where ω_θ is the angular frequency of the theta LFP. The second requirement is equivalent to demanding that the phase-precession range Ω is constant and the same for all grid fields, i.e., the range is independent of the grid spacing. For this, I must first define the size of a single grid firing field, which in the model is closely related to the spacing s_n. A firing rate above 20% of the peak rate delineates the extent of a firing field (Kjelstrup et al., 2008; Brun et al., 2008). Using this criterion and Equation 4.18, one can deduce that the size of a grid firing field is $\approx 0.7 s_n$, and therefore $0.7 s_n / v$ is the time spent traversing a grid field. Thus, the phase-precession range Ω can be expressed as

$$\Omega = (\omega_n - \omega_\theta) \cdot \frac{0.7 s_n}{v}, \tag{4.28}$$

which implies

$$\omega_n = \frac{\Omega \ v}{0.7 s_n} + \omega_\theta. \tag{4.29}$$

The simplest way to model phase-locking of the first spike within a grid field, and to fulfill the third requirement, is to ensure that the theta phase at entry ϕ_{entry} is the same for two neighboring firing fields, which are separated by the spacing s_n. The difference between the entry phases (with respect to theta LFP) of the two consecutive grid fields should be 2π. This condition is equivalent to

$$(\omega_n - \omega_\theta) \cdot \frac{s_n}{v} = 2\pi. \tag{4.30}$$

The phase offset ϕ in Equation 4.26 can be expressed in terms of the experimentally measured entrance phase ϕ_{entry}. Because of the phase-locking condition, the entry phase ϕ_{entry} is the same for neighboring grid fields. Therefore, the relationship between the entrance phase ϕ_{entry} and the phase offset ϕ can be determined for any firing field. Focusing on, for example, the central grid field, the phase offset ϕ is approximately the phase measured at the center of the field, i.e., near the origin at $x = 0$ (or $t = 0$); see Equation 4.26. Since the central grid field is symmetric about the origin, and the phase decreases linearly with position, the phase at grid-field entrance ϕ_{entry} is related to ϕ (for any spacing s_n) as

$$\phi \approx \phi_{\text{entry}} - \frac{\Omega}{2}. \tag{4.31}$$

With these requirements for ω_n and ϕ in Equations 4.29, and 4.31 respectively, I can write

M_n in Equation 4.26 as

$$M_n\left(\frac{x}{v}\right) = C\cos\left(\frac{\Omega x}{0.7s_n} + \omega_\theta\frac{x}{v} - \phi_{\text{entry}} + \frac{\Omega}{2}\right) + 1. \tag{4.32}$$

Extending Equation 4.25, the final expression for the modulated place field $P_M(x)$ is

$$P_M(x) \approx \sum_{n=1}^{N} A(s_n,\sigma)\left[G(s_n,x)M_n\left(\frac{x}{v}\right) - \frac{G_{\max}}{2}\right]. \tag{4.33}$$

Note that I have used the same synaptic-weight function $A(s_n,\sigma)$ as for the non-modulated case in Equation 4.25. To obtain the membrane potential of the output cell, I perform the convolution between $P_M(x)$ and an EPSP kernel $\epsilon(t) \equiv \epsilon\left(\frac{x}{v}\right)$,

$$V_{\text{out}}(x) = P_M(x) * \epsilon\left(\frac{x}{v}\right), \tag{4.34}$$

which is plotted in Figure 4.4 *D* (top panel, normalized). The peaks of $V_{\text{out}}(x)$, which are shown in Figure 4.4 *D* (bottom panel), exhibit phase precession.

To derive an approximation for the phase-precession range of the output place field, I focus on the fast oscillatory component, which is determined by M_n in Equations 4.32 and 4.33. The (angular) spatial frequency of the modulation (coefficient of x in Equation 4.32) is

$$\frac{\Omega}{0.7s_n} + \frac{\omega_\theta}{v}, \tag{4.35}$$

where the term $\Omega/0.7s_n$ denotes the spatial slope of phase recession of a grid cell with spacing s_n. Note that because phase decreases with position, the true slope is negative, i.e. $-\Omega/0.7s_n$.

The slope of the output place field can be obtained from the mean modulation $\langle M_n\rangle$ with respect to the synaptic-weight distribution $A(s_n,\sigma)$. One can also estimate the phase-precession slope of the output place field by simply considering the mean spatial slope $\langle s_n\rangle$ at the input. This approximation corresponds to the first term of a Taylor expansion of $\langle M_n\rangle$. The phase-precession slope of the output place field is thus $\Omega/(0.7\cdot\langle s_n\rangle)$ where the mean spacing is

$$\langle s_n\rangle = \frac{\sum_{n=1}^{N} s_n A(s_n,\sigma)}{\sum_{n=1}^{N} A(s_n,\sigma)} \approx 6.5\ \sigma. \tag{4.36}$$

The mean slope of phase precession at the output is then $\Omega/(0.7\cdot 6.5\sigma)$. With the size 3σ of the output place field and the corresponding slope $\Omega/(0.7\cdot 6.5\sigma)$, I can calculate the phase-precession range $\Delta\phi$ at the output:

$$\Delta\phi = \frac{\Omega}{0.7\cdot 6.5\sigma}\cdot 3\sigma \approx 0.66\ \Omega. \tag{4.37}$$

Note that the output range $\Delta\phi \approx 0.66\ \Omega$ is (1) smaller than the input range Ω, which means that range is reduced in the grid-to-place transformation, and that $\Delta\phi$ is (2) independent of the size σ of the output place field, which means that slope-size matching is conserved from the MEC grid fields to the hippocampal place fields. For an input range of $\Omega = 250$ degrees (see Figure 4.4 $A-C$), the value of the phase-precession range at the output is $\Delta\phi \approx 0.66\cdot 250$ degrees $\approx$ 165 degrees, and this value matches the numerically obtained

phase-position plot in Figure 4.4 D (bottom panel).

4.4. Results

In Chapter 2 I studied a CA1 place cell that inherits phase precession from a subset of CA3 cells that share a common place field, i.e., the input corresponded to identical place fields of many different CA3 cells. I now relax this strong assumption and study a more general case of inheritance where the place fields at the input are allowed to be spatially distributed.

4.4.1. Inheritance explains phase precession for a variety of place-selective responses.

To study spatially distributed inputs in the inheritance model, I still assume that each input cell shows phase precession within its place field, i.e., input place fields are characterized by a common frequency f_λ of modulatory activity ($f_\lambda > f_\theta$). Moreover, input place fields all have the same size, which is parameterized by the width σ. Furthermore, pairs of overlapping input place fields are aligned such that the theta-time scale delay between firing-rate peaks is correlated to the distance between place-field centers (Dragoi and Buzsáki, 2006; Geisler et al., 2010); for details see the Methods in section 4.3). Furthermore, I assume that an output neuron linearly integrates the excitatory input, producing a somatic voltage as a response.

To connect the analysis of phase precession for spatially distributed place-field centers to the analysis of the CA3-CA1 network in Chapter 2, I first consider again the case of identical input place-field centers (Fig. 4.1A, top), i.e., all input place fields are perfectly overlapping. This simplified scenario corresponds to the topology of my previous results regarding the CA3-CA1 system and serves as a reference for the other distributions of input fields in Figs. 4.1 and 4.2. By summing the depolarization provided by the identical input place fields, one obtains an output place field (Fig. 4.1A, middle) that is essentially the same as the input place field. As expected, there is phase precession throughout the output place field as evidenced by the negative slope of the corresponding phase-position plot (Fig. 4.1A, bottom).

Next, I consider a Gaussian distribution of the centers of input place fields, and the width of this distribution is characterized by σ_d (Fig. 4.1B). Adding such distributed input place fields, one obtains an output place field that is larger than each individual input place field (as in Fig. 4.1A), and the size $\sigma_R = \sqrt{\sigma_d^2 + \sigma^2}$ of the output place field is determined by both the size σ of the input place fields as well as by the width σ_d of the distribution of field centers (Equation 4.12). This scenario can explain why, on average, the size of place fields increases from CA3 to CA1 (Fig. 4.1 C) and to the subiculum (Mizuseki et al., 2012; Kim et al., 2012). Moreover, the slope of the phase-position plot at the output is shallower than at the input, although the range of phase precession is similar. Thus, the inheritance model can explain why the slope is inversely proportional to the field size (Huxter et al., 2003; Terrazas et al., 2005; Dragoi and Buzsáki, 2006; Kim et al., 2012; and Fig. 4.1 D).

Another interesting case is a spatially uniform distribution of the place-field centers (Fig. 4.2C). This case might correspond, for example, to the input of a basket cell in CA1. Adding such uniformly distributed inputs, one observes an oscillation of the membrane potential of the output cell, but there is no spatial preference. The corresponding phase-position plot indicates that peaks of the membrane potential do not show phase precession. The phase of the membrane-potential oscillation is at about 130 degrees, and the membrane potential

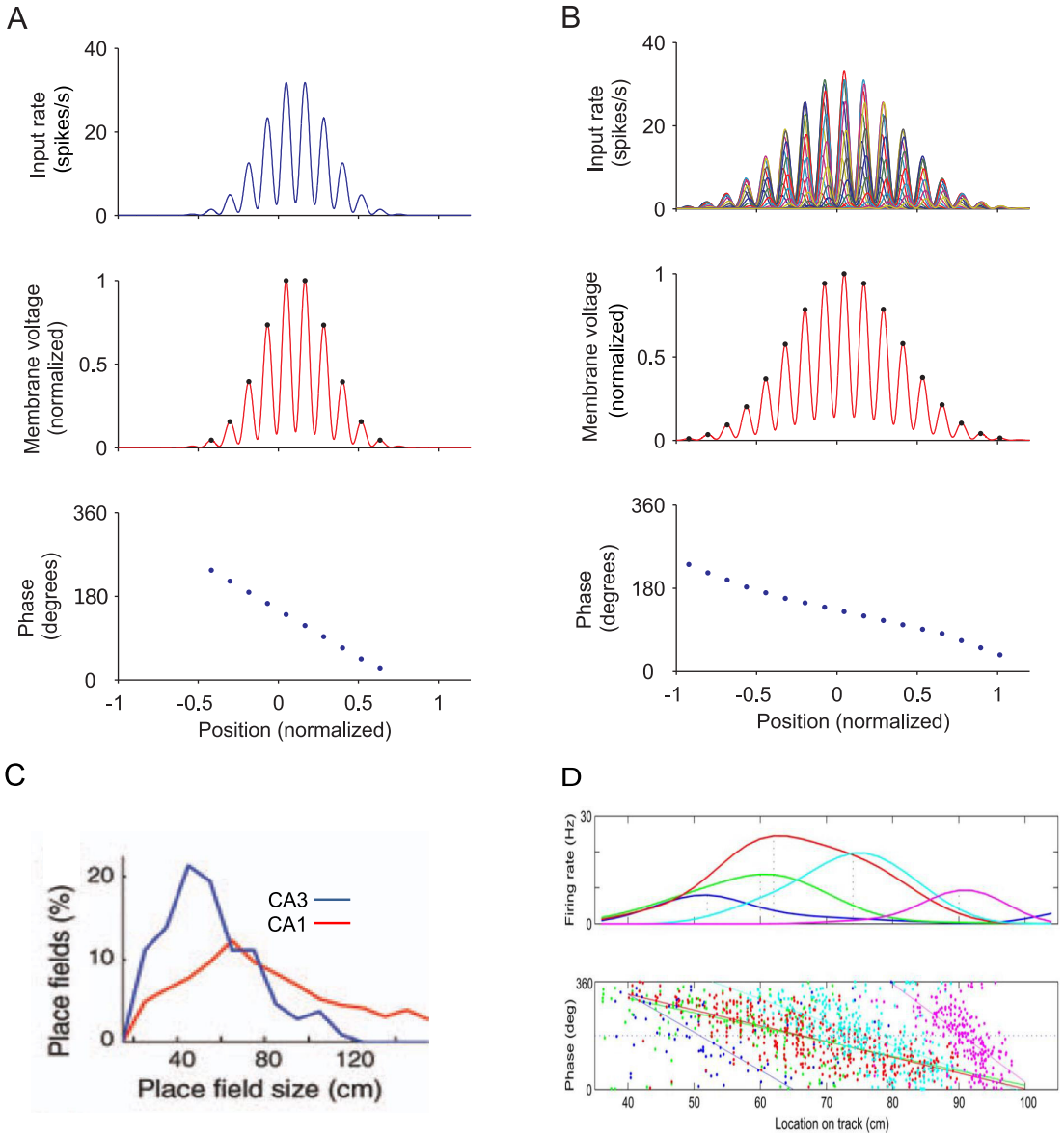

Fig. 4.1.: Phase precession for different distributions of place-field centers in the input: delta (***A***) and Gaussian (***B***) distribution of width $\sigma_d = 0.45$. *A* and *B* show the spatially distributed firing rates of $N = 20$ identical place fields ($\sigma = 0.3$) at the input (top), the normalized membrane voltage of the output cell (middle), and the phase-position plot of the output cell (bottom). ***C,*** Distribution of place-field sizes in regions CA3 and CA1 (adapted from Mizuseki et al. (2012); reproduced with permission from Wiley and Sons) ***D,*** Firing rate (top) and phase-position plot (bottom) for five example cells with overlapping place fields in the hippocampus (Dragoi and Buzsáki 2006; reproduced with permission from Elsevier).

is oscillating precisely at theta frequency f_θ although the phase-precessing input cells were oscillating at a frequency $f_\lambda > f_\theta$ (see also Geisler et al., 2010). This behavior of the output cell is reminiscent of the activity of basket cells in the hippocampus, which receive excitatory input from place cells. Basket cells fire phase locked to theta, the preferred firing phase is

about 130 degrees (Varga et al., 2012; Royer et al., 2012; see Figure 4.2 C), and there is little spatial preference (Frank et al., 2001).

Now, I consider a ramp-like distribution of place-field centers (Fig. 4.2B). This means that the density of place fields at the input increases linearly along a specified axis. The resulting output place field is, not surprisingly, also ramp-like: the mean depolarization increases steadily, but then falls off abruptly. Furthermore, this ramp-like depolarization is modulated by an oscillation, which shows a characteristic shape of phase precession: an initially shallow phase-precession slope, some plateau below 180 degrees and, finally, some steeper phase precession. Such ramp-like neurons are found in the ventral striatum (van der Meer and Redish, 2011), and, remarkably, the observed shape of the phase precession resembles the shape generated by the model (compare Figures 4.2 B and D).

The inheritance model can also explain the presence of "double" phase precession within a place field (Maurer et al., 2006a). Indeed, CA1 place cells can have more than one place field in a given environment, and these place fields could overlap so strongly, that the firing-rate map would appear to be unimodal. However, within such a place field, there can be two or more independent cycles of phase precession. This is illustrated in Figure 4.3. The interpretation of this result in terms of inheritance is as follows: two distinct overlapping CA3 assemblies that are sufficiently synchronous (Fig. 4.3 A) can produce two independent cycles of phase precession in an output cell within the same field (Fig. 4.3 B-D).

4.4.2. Phase precession and the grid-to-place transformation

Finally, I test whether hippocampal phase precession can be inherited from the MEC. Principal cells in the MEC fire in a grid-like manner in open environments (Hafting et al., 2005) and exhibit phase precession, even after inactivation of the hippocampus (Hafting et al., 2008). Furthermore, grid cells project to the hippocampus (Zhang et al., 2013). Is it possible to obtain a phase-precessing place cell from a population of phase-precessing grid cells? Analogous to the derivations concerning place-field distributions, I assume an input layer of phase-precessing grid cells projecting to a single output hippocampal cell. In the context of my previous results regarding inheritance of phase precession to CA1 (Chapter 2), the input grid cells could correspond to cells from MEC layer III that project to a cell in CA1.

In the one-dimensional case I study here, the grid-field activity is periodic along the axis where the virtual rat is running (Brun et al., 2008). Following my previous approach for CA3-CA1 inheritance (Fig. 2.3), I implemented phase precession within grid fields through a time-dependent firing-rate modulation (Fig. 4.4 $A-C$). In the simulations, grid cells have different field spacings, and the size of the firing field, which is defined by a 20% threshold (e.g. Brun et al., 2008), is about 0.7 times the grid spacing. Grid cells also have phase-precession slopes that are inversely proportional to the field size, with a constant phase-precession range of ~ 250 degrees (Hafting et al., 2008; Reifenstein et al., 2012), and the spike phase at field entry is ~ 200 degrees (Reifenstein et al., 2013; Climer et al., 2013).

The synaptic weights of the projection from MEC layer III to CA1 are calculated such that a linear combination of periodic grid fields produces a non-periodic place field at the output; see Methods in section 4.3 for details and Solstad et al. (2006) for the original derivation in two dimensions. The resulting synaptic-weight distribution in Fig. 4.4 E is asymmetric with a steeper rise and shallower decay. For the inheritance model, I used a uniform distribution of grid spacings, although recent studies have highlighted the existence of discrete modules or clusters in the MEC that reflect a degree of anatomical spatial organization (Stensola et al., 2012; Kitamura et al., 2014; Ray et al., 2014). Including the effect

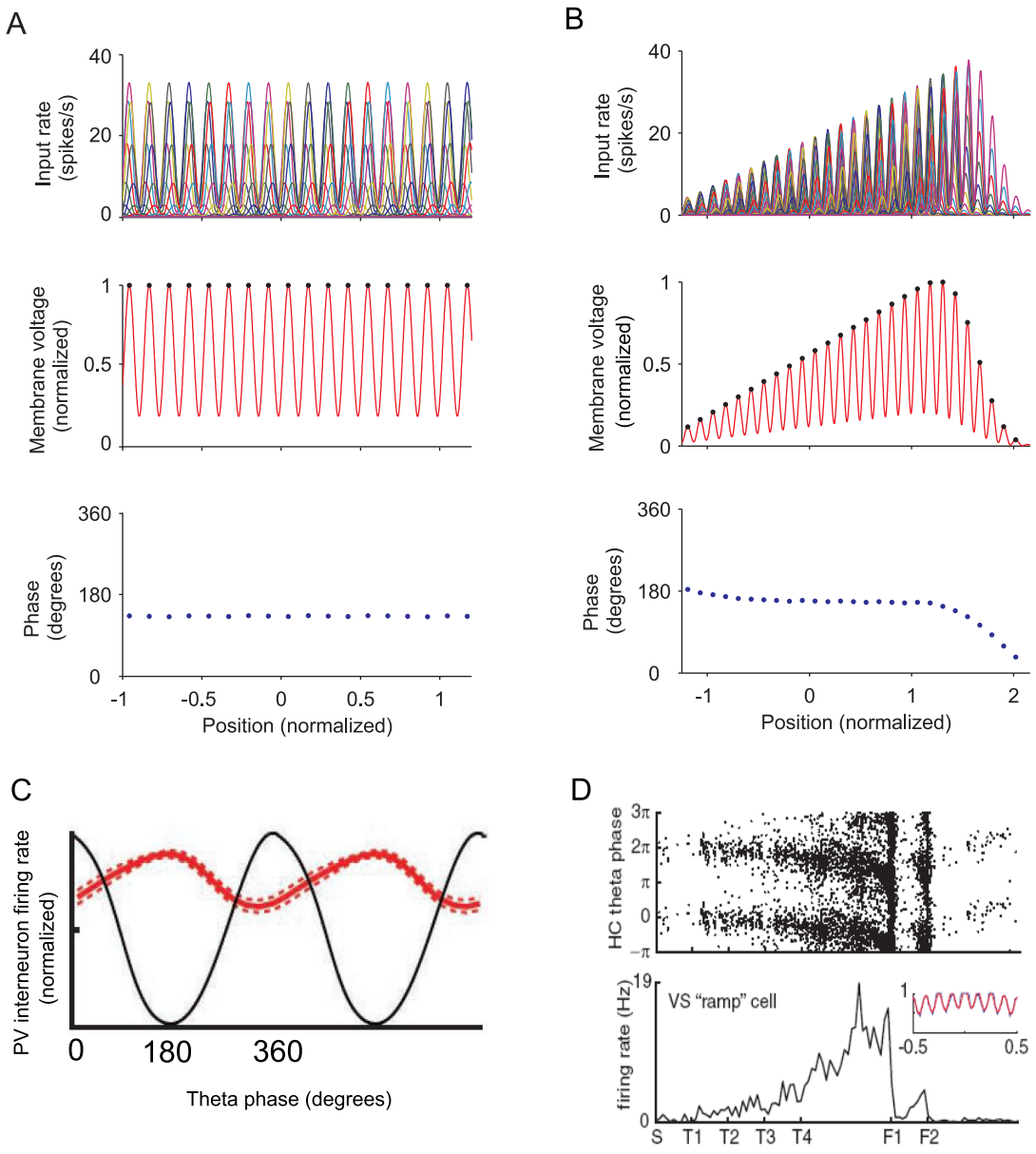

Fig. 4.2.: Phase precession for different distributions of place-field centers in the input: uniform (***A***) and ramp (***B***) distribution. *A* and *B* show the spatially distributed firing rates of $N = 20$ identical place fields ($\sigma = 0.3$) at the input (top), the normalized membrane voltage of the output cell (middle), and the phase-position plot of the output cell (bottom). ***C***, Histogram of preferred firing phases for PV interneurons in vivo (Royer et al. 2012, reproduced with permission from Elsevier). ***D***, Phase plot (top) and firing rate (bottom) of "ramp" neurons in the ventral striatum (van der Meer and Redish 2011; reproduced with permission from Society for Neuroscience).

of such clusters into my model would result in a coarser discretization of the grid-spacing of the synaptic-weight distribution without affecting the main results.

The membrane-potential of the output cell reflects a single place field of width $3\sigma = 0.66$

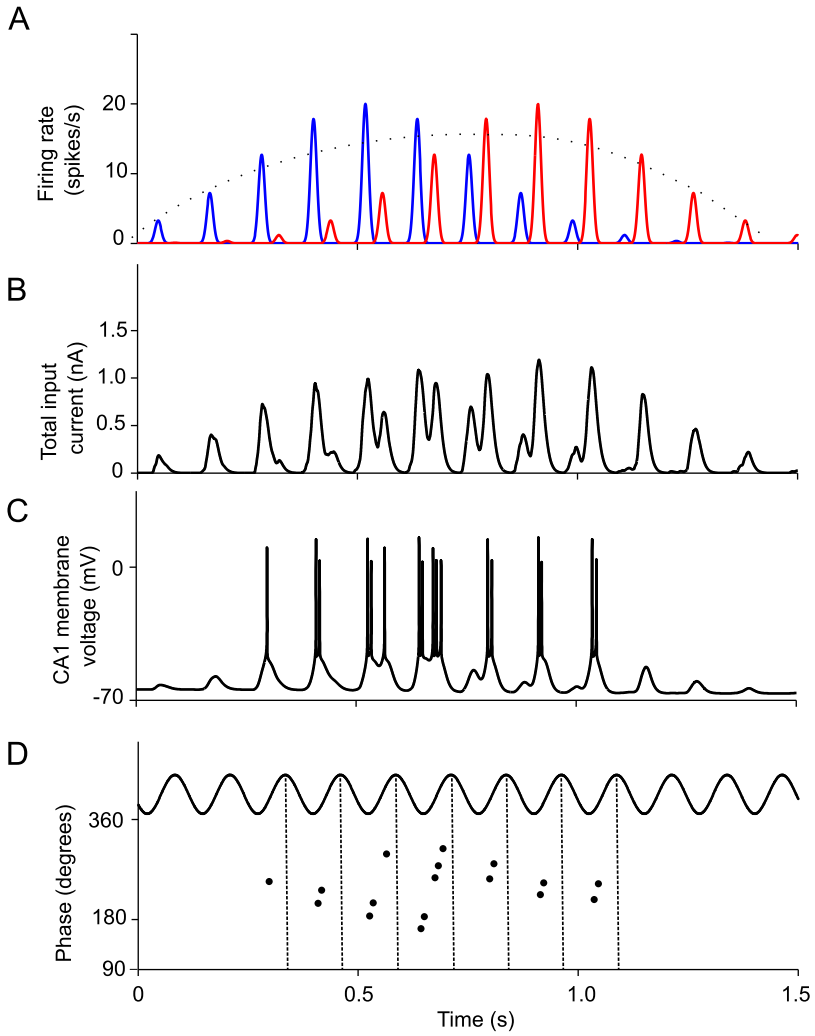

Fig. 4.3.: Double phase precession for CA1 place fields (Maurer et al., 2006a). ***A***, Firing rate of two overlapping active assemblies from CA3 (red and blue) that project to a CA1 cell. Dotted lines show the extent of the place field where the CA1 cell is active. ***B***, Total input current received by a CA1 cell. ***C***, Spikes within the CA1 place field as produced by the two compartment spiking model in Figure 2.6. ***D***, Phase-time plot showing two overlapping and independent cycles of phase precession within one place field for one CA1 cell (single trial). For reference, a theta oscillation is plotted above and dotted lines mark the theta cycles.

m (Fig. 4.4 *D*), a value that is close to the smallest grid spacing s with a considerable synaptic weight (Fig. 4.4 *E*). The membrane-potential peaks of the output place field exhibit phase precession (Fig. 4.4 *D*, bottom panel); however, the range of phase precession is only ~ 145 degrees. This small range, which is the product of the size and the phase-precession slope of the output field, can be explained by the grid-to-place inheritance. The size $\sim 3\sigma$ of the output field is related to the shape (e.g., the steep rise) of the synaptic-weight distribution in Figure 4.4 *E* (solid arrow). The phase-precession slope of the output field, however, is largely determined by the mean phase-precession slope of the input grid activity, and this mean slope is related to the mean grid spacing of the input population. Figure 4.4 *E* (dashed arrow)

indicates that the mean grid spacing of the input population is $\sim 6.5\ \sigma = 1.4$ m (Equation 4.36), and therefore the mean grid-field size is $\sim 0.7 \cdot 1.4$ m $=$ 1 m. Accordingly, the mean slope of phase precession in the input is ~ 250 degrees / 1 m $= 250$ degrees/m. Using this slope and the obtained size of the output place field ($3\sigma = 0.66$ m), I estimated the range of phase precession as 250 degrees/m $\cdot 0.66$ m $= 165$ degrees; see also Equation 4.37. This estimation assumed a linear phase-position relation, although the phase-position relation in Figure 4.4 *D* is actually sigmoidal. Thus, the phase range of ~ 145 degrees estimated from the simulation is smaller. The saturation of the phase at the borders of the field indicates the transition to a constant phase of membrane-voltage peaks outside the place field, a behavior that is similar to Figure 4.2 *C*.

The phase of the first spike (entry phase) in the modeled output place field in Figure 4.4 *D* is ~ 200 degrees, which is equal to the entry phase 200 degrees of the input grid fields. This seemingly paradoxical zero phase difference, however, must not be interpreted as a zero transmission delay between the two regions, but can be explained by the cancellation of two effects. On the one hand, the ~ 100-degree reduction of the phase range from input to output leads to a ~ 50 degrees advance of the onset phase because of the symmetry of the place field around its center. On the other hand, there is a phase shift due to synaptic filtering of the EPSP and axonal transmission delay, which is also ~ 50 degrees ($\approx 1.8\tau \cdot f_\theta \cdot 360$ degrees; see Equation 2.13).

Phase precession could thus be propagated from MEC layer III to CA1. Interestingly, the resulting phase-position relations due to input from MEC or from CA3 significantly overlap within a theta cycle (compare Fig. 4.1 *A* for CA3 and Fig. 4.4 *D* for the MEC layer III). Thus, the model predicts that both MEC layer III and CA3 can contribute to the phase precession observed in CA1. These results could apply also to the connection from MEC layer II to CA3. More generally, a grid-to-place transformation is sufficient to account for inheritance of phase precession from entorhinal cortex to the hippocampus, and it can explain the observed reduction of the range of phase precession (Harris et al., 2002; Mizuseki et al., 2009; Schmidt et al., 2009; Reifenstein et al., 2012).

Overall, inheritance of phase precession can explain a variety of sub- and supra-threshold responses in the hippocampus and related structures in terms of place-selectivity and presence of phase precession.

4.5. Discussion

In this chapter I have formalized the notion of inheritance as applied to general feed-forward topologies in the hippocampal formation. The input can be characterized by the spatial distribution of centers of phase-precessing place cells. This characterization of the input determines both the place-field selectivity and the phase-precession slope of a target cell receiving such input.

The conclusions of the CA3-CA1 inheritance model developed in Chapter 2 also hold for more general feed-forward projections. Particularly, I showed that CA3 input is sufficient to generate phase precession in CA1. However, CA1 receives excitatory input also from layer III of the MEC, which can generate place-specific activity in CA1 (Brun et al., 2002; Nakashiba et al., 2008). Furthermore, cells in MEC layer III exhibit phase precession (Hafting et al. 2008; Climer et al. 2013; Reifenstein et al. 2013; but see Mizuseki et al. 2009). I showed that the contributions from CA3 and from MEC layer III generate similar phase-position relations, and thus both pathways can contribute to the phase precession observed in CA1.

Once the mechanism(s) for phase precession in CA3 and MEC are established, they will be sufficient to explain phase precession in CA1 through inheritance (Skaggs et al., 1996; Yamaguchi and McNaughton, 1998; Yamaguchi et al., 2007).

The inheritance model can account for several further features of phase precession (see also Figs. 4.1, 4.2, and 4.3): (1) The slope of phase precession matches the size of the place field so that the range remains about constant (Huxter et al., 2003; Dragoi and Buzsáki, 2006). (2) Place-field sizes in the input population are smaller than those downstream (Jung and McNaughton 1993; Mizuseki et al. 2012; Kim et al. 2012; but see Lee et al. 2004). (3) Putative basket cells show little spatial preference and have a preferred firing phase of about 130 degrees (Lapray et al. 2012; Varga et al. 2012; Royer et al. 2012; see also Skaggs et al. 1996), which can be explained by inputs from place cells with place-field centers that are evenly distributed in space (Geisler et al., 2010). Some weak phase precession in interneurons (Maurer et al., 2006b; Ego-Stengel and Wilson, 2007; Geisler et al., 2007) may be due to spatially uneven excitatory input. (4) Phase precession in the ventral striatum (van der Meer and Redish, 2011) has a characteristic shape and there is ramp-like activity of neurons. These observations can be explained by inheritance from hippocampal place fields when there is an increasing density of fields towards a location, for example when an animal is approaching a goal (Hetherington and Shapiro, 1997). (5) CA1 cells can have two or more overlapping place fields, and in each subfield there is phase precession (Maurer et al., 2006a). This spatial overlap of phase precession in a single CA1 cell can be explained by two or more sufficiently synchronously phase-precessing input assemblies; see also Jones and Wilson (2005) for phase precession in the prefrontal-cortex. Indeed, the presence of two or more bursts within a theta cycle poses a challenge for cellular models, because it is not clear how two different burst frequencies can be independently controlled within one theta cycle (Maurer and McNaughton, 2007). (6) The "grid-to-place" transformation (McNaughton et al., 2006; Solstad et al., 2006; de Almeida et al., 2009; Cheng S and Frank, 2011) along with a firing-rate modulation of the input can also account for the inheritance of phase precession from grid cells to place cells.

In summary, the results of the inheritance model predict that the distributions of place-field centers (or equivalently, a corresponding distribution of synaptic weights (Malhotra et al., 2012)) and field-widths of a population of phase-precessing cells determine the phase precession of a downstream cell that receives this input. Such synaptic-weight distributions may be shaped through synaptic plasticity, which is an interesting topic for future theoretical and experimental work.

To conclude, phase precession can be a result of network, cellular, and inheritance effects combined. Inheritance in particular, might help explain why phase precession is observed in many parts of the brain. The results suggest that the entorhinal cortex might be the generator of phase precession. Simultaneous recordings of cells in different regions (e.g. Mizuseki et al., 2009) are needed to establish the existence of assemblies as predicted in Chapter 2 as well as the place-field center distributions predicted in this chapter.

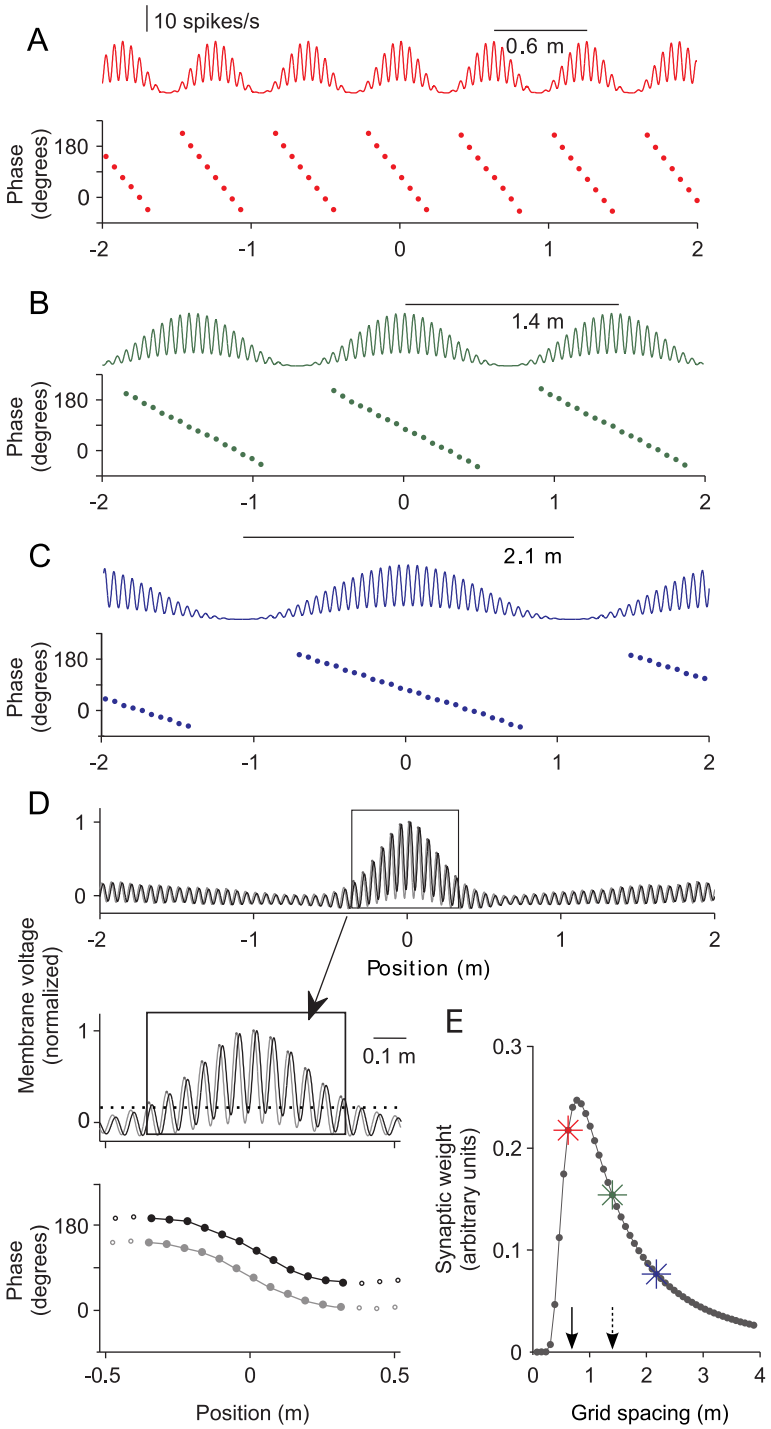

Fig. 4.4.: Phase-precessing grid cells can generate a phase-precessing place cell. ***A***, ***B***, ***C***, Firing rate as a function of position of three example grid cells with different spacings ($s = 0.6$ m, 1.4 m, 2.1 m) on a linear track (top) and theta phase of firing-rate peaks (bottom). The phase-precession slope is inversely proportional to the grid-field size while the range (≈ 250 degrees) and entry phase (≈ 200 degrees) are constant. ***D***, The sum of the firing rates of 50 grid fields with equi-distant spacings $s \in [0.1\text{ m},\ 4\text{ m}]$ (gray trace) is filtered by an EPSP kernel, which results in the membrane voltage (black trace). The box around the resulting place field (width $3\sigma \approx 0.66$ m) is enlarged below (arrow). Peaks of the voltage trace inside the place field show phase precession (bottom, black dots). An unfiltered trace with the corresponding phase-position plot is shown in gray. A threshold of 20% (dashed line) delineates the extent of the place field. ***E***, Weights of 50 synapses between the grid cells and the place cell in *D* as a function of the grid spacing s. Arrows indicate the width 3 σ of the output place field (solid) and the mean grid spacing 6.5 σ (dashed). Colored asterisks indicate the example grid cells in *A*, *B*, and *C*.

5. Towards an understanding of the behavioral relevance of phase precession

[1] In the previous chapters, I studied the phenomenon of phase-precession and place-field inheritance from a mechanistic point of view. In this chapter, I will address the question of whether phase precession has a computational role or whether it is epiphenomenal. For this, I have synthesized and critiqued the literature that points to behavioral correlates for phase precession. I also suggest a framework on how to study phase precession and what relevant questions should be asked to advance our understanding of this interesting phenomenon.

Summary

Hippocampal place cells and their sequential activation represent an important conceptual model to explain navigation and episodic memory. Spikes fired within a given place field show a relationship to the theta rhythm recorded extracellularly: neurons change their preferred firing phase, i.e., "precess" across theta cycles, as a function of the relative position within the firing field. First observed in the hippocampus and then in other parts of the brain, phase precession is thought to be related to the encoding of sequences of visited places. Although the evidence so far does not contradict this claim, it is not clear whether phase precession plays an active role by enabling sequence learning, whether phase precession merely reflects encoding and/or retrieval dynamics, or whether phase precession is purely epiphenomenal. Here I synthesize the literature to investigate the function of phase precession in terms of behavioral correlates. I examine these observed behaviors in the context of proposed computational roles, some of which are tied to the hypothesized underlying mechanisms of phase-precession generation. Importantly, to elucidate functionality, we need to understand how to interfere with phase precession. Thus, here I also review how phase precession has been altered via deliberate manipulation of the circuitry or by controlling the behavioral tasks. I claim that a better understanding of, first, the behavioral correlates of phase precession and, second, the means to interfere with phase precession will help guide future research on hippocampal dynamics and more generally, sequential activity in the brain.

Phase precession, sequences, and coding

The hippocampus is a notable structure in the brain implicated in both episodic memory and navigation in mammals (Squire et al., 2004; Buzsáki, 2005; Buzsáki and Moser, 2013). More precisely, it is believed that neural assemblies in the hippocampus are coordinated to represent spatio-temporal trajectories in the brain (Hasselmo, 2012). These functions have been investigated via a combination of behavioral and neurophysiological studies (Martin et al., 2000; Rolls and Kesner, 2006; Squire and Wixted, 2011).

[1] The contents of this chapter are planned to appear in review form.

There are cells in the hippocampal formation that fire in particular regions of the environment while an animal is navigating (O'Keefe and Dostrovsky, 1971). These cells thus have spatial receptive fields and code for position in the environment via their firing rate (Ahmed and Mehta, 2009). Two major classes of place-specific firing have been found (Moser et al., 2008). First, there are cells that fire in one restricted region of the environment. They were originally observed in the CA1 region of the hippocampus (O'Keefe and Dostrovsky, 1971), and later observed in diverse regions such as CA3, the dentate gyrus, and the subiculum. These cells were termed place cells and the region of the environment where the place cell is active is referred to as its place field. This major discovery motivated the "cognitive map theory" of the brain (O'Keefe and Nadel, 1978; McNaughton et al., 2006) that states that the environment is represented as maps in the brain, a physiological realization of earlier cognitive theories put forward by Tolman and others (Tolman, 1948). The other major class of place-specific cells are the grid cells (Hafting et al., 2005). When an animal is navigating a two dimensional environment, e.g., a square enclosure, a grid cell will fire action potentials such that they form a pattern in space, reminiscent of a hexagonal structure. Grid cells were initially discovered in the medial entorhinal cortex, but are also known to exist in pre- and parasubiculum (Boccara et al., 2010). There are also cells that have non-spatial correlates altogether. An example of these are time cells, which fire in a particular moment in time of a temporally structured event (MacDonald et al., 2011), and episode cells which fire by generating sequences in the absence of navigation (Pastalkova et al., 2008).

Within a given firing field, the spikes of the corresponding place-specific cell undergo phase precession: the systematic advancement of the phase of the spikes relative to an ongoing theta oscillation (4–12 Hz) (Fig. 5.1 *A*). Phase precession is a typical property of place-cell firing (Mizuseki et al., 2009; Maurer et al., 2006a), and it is present in different stages of the hippocampal formation (Skaggs et al., 1996; Harris et al., 2002), as well as the entorhinal cortex (Hafting et al., 2008), ventral striatum (van der Meer and Redish, 2011), the subiculum (Kim et al., 2012), and prefrontal cortex (Jones and Wilson, 2005). Although phase precession is mostly prevalent in principal cells, phase precession has been occasionally observed also in interneurons (Ego-Stengel and Wilson, 2007; Geisler et al., 2007; Maurer et al., 2006b).

Phase precession has been suggested as a notable example of phase coding in the brain (Dayan and Abbott, 2001). Individual phases convey information about the relative position of the animal within its firing field; late phases indicate that the animal is entering the place field, while early phases indicate that the animal is exiting the place field. Thus, phases code for relative position within the place field during phase precession. Furthermore, phase precession is an ideal candidate to solve the problem of coding of behavioral sequences by bridging the time scales of behavior and neural plasticity (Skaggs et al., 1996; Melamed et al., 2004).

Despite considerable efforts in modeling and analyzing phase precession, there is to date no clear answer to whether and how the brain uses the information encoded in the phases of spiking. Under the assumption that phase precession is an important code in the hippocampus, corrupting phase precession should lead to specific behavioral deficits. As phase precession is predominantly a entorhinal-hippocampal phenomenon, these behavioral deficits are expected to be related to episodic memory and/or navigation. Phase precession, however, has been elusive to experimental work linking it to behavior. Here I argue that one important reason why there is little evidence linking behavior to phase precession, is our lack of understanding of the mechanisms of phase precession generation. Indeed, if we do not

know the neural mechanisms underlying phase precession, it is difficult to interfere with it experimentally and observe how this alteration affects behavior. Another reason is that the existing literature on behavioral correlates of phase precession has not yet been adequately synthesized.

In the following paragraphs, I review evidence for behavioral correlates of phase precession, including studies that have reported phase precession in non-navigational tasks. First, I define phase precession and its main features as well as other observed dynamics at the theta time scale such as temporal compression and theta sequences. After briefly commenting on some representative models of phase-precession generation, I collect ideas on the function of phase precession that can in principle be tested experimentally. Next, I examine the literature for a connection between normal (abnormal) phase precession and normal (abnormal) behavior as quantified by performance in a spatial memory task. Finally, I suggest some key questions that could be addressed with the techniques available today and can hopefully serve as a roadmap for future research in this field.

The distinctive properties of phase precession

I now introduce some important ideas related to the definition of phase precession, its main properties, its relationship to a broader class of theta-timescale dynamics that includes temporal compression and theta sequences, and a brief overview of the proposed mechanisms of phase precession.

As stated in the previous section, the defining feature of phase precession is that spikes from a cell within its firing field, arrive earlier in subsequent cycles of the theta oscillation. The initial characterization of phase precession was in terms of the relationship between the firing phases of CA1 pyramidal cells and the position of the animal as it navigated through a linear track (O'Keefe and Recce, 1993). According to these first observations, a cell exhibits phase precession if the theta phase decreases monotonically as the animal crosses the place field of the corresponding cell. This relationship is quantified by 1) a correlation coefficient, that captures the extent of a linear relationship between the two variables theta phase and position, and 2) the slope of the linear fit, which informs whether the phase decreases (negative slope) or increases (positive slope) as a function of position. Note, however, that since phase is a circular variable and place is a linear variable, circular-linear statistical methods are appropriate (Kempter et al., 2012).

Phase precession is in line with the observation that the spiking frequency of the cell is slightly higher than the frequency of the extracellularly recorded theta oscillations (Geisler et al., 2007; Mizuseki et al., 2009). This turns out to be also true for the intracellular oscillations of a place cell or grid cell observed within its firing field (Harvey et al., 2009; Domnisoru et al., 2013; Schmidt-Hieber and Häusser, 2013). Other salient properties include slope-size matching (Dragoi and Buzsáki, 2006; Maurer et al., 2006a) and that the range of phase precession in CA1 is approximately 180 degrees in single trials (Schmidt et al., 2009) (Fig. 5.1 *B*).

Most of what we know about phase precession comes from studies involving linear tracks. From these experiments, we have learned how phase precession is modulated by factors such as speed (O'Keefe and Recce, 1993; Geisler et al., 2007; Maurer et al., 2012), age (Shen et al., 1997), experience (Mehta et al., 2002; Ekstrom et al., 2001; Cheng and Frank, 2008), geometric alterations of the environment (Mizuseki et al., 2009; 2012; Harris et al., 2002; Diba and Buzsáki, 2008; Kjelstrup et al., 2008; Brun et al., 2008), and network oscillations (Senior et al., 2008; Belluscio et al., 2012). In the following sections, I will review other

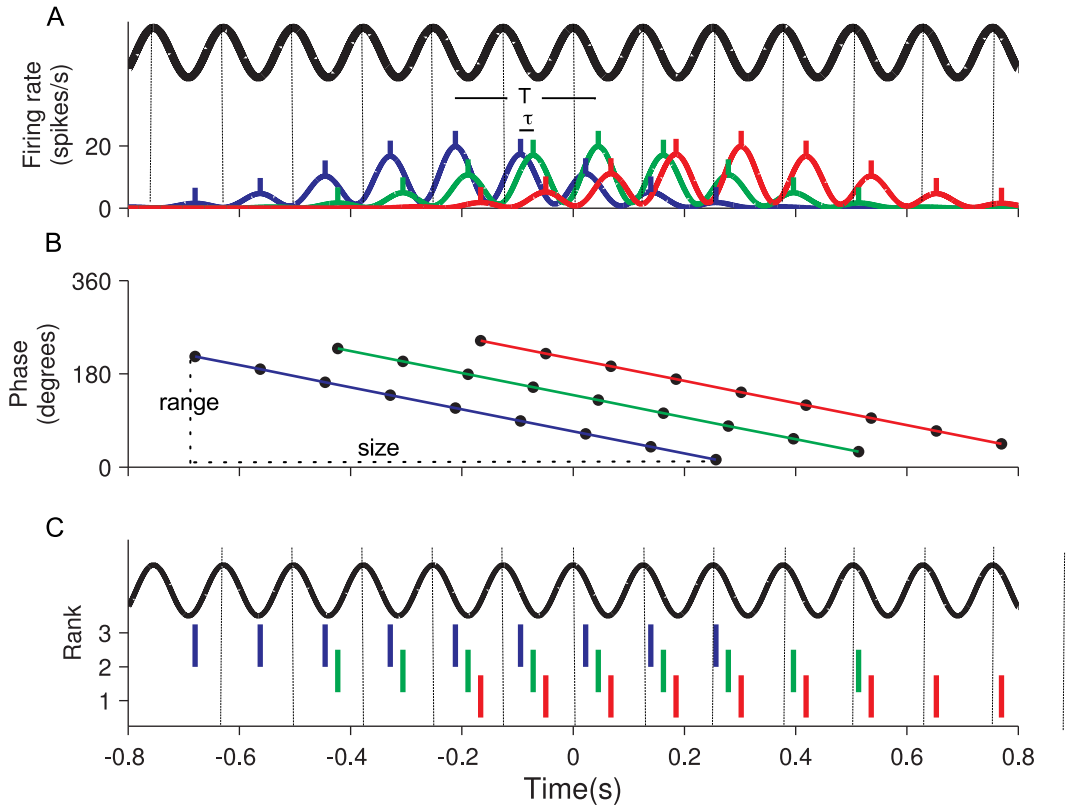

Fig. 5.1.: Phase precession and theta-time-scale dynamics in the hippocampal formation. ***A,*** Activity of three place cells (blue, green, and red) within their overlapping place fields. For clarity, a single spike is shown to occur preferentially at the peaks of the firing activity. Across theta cycles, spikes arrive at earlier phases with respect to the theta oscillation (black). T is the separation in time between two consecutive place-field centers, while τ is the theta-time-scale separation between two spikes corresponding to two consecutive place fields within a theta cycle. ***B,*** Phase-position plot for the three place cells in A. ***C,*** Theta sequences allow the representation of traversed place fields at a theta time scale. Here, rank is correlated with spike time within a theta cycle, the defining feature of a theta sequence (Foster and Wilson, 2007).

properties of phase precession, particularly those properties that are related to behaviors beyond the linear track.

Theta-time scale dynamics: a general framework

As mentioned before, during phase precession the firing frequency of spikes, as measured by their autocorrelation function, is slightly higher than the frequency of the theta local field potential (LFP) oscillations. This specific relationship between the spikes of single cells and the LFP during phase precession affords the title "theta-time scale dynamics" for this phenomenon. There are, at least, two other examples of theta-time scale dynamics that have been observed in the hippocampal formation: temporal compression and theta sequences. It is not clear to which extent these three examples of theta-scale dynamics are related, or whether they are three different characterizations of the same phenomenon. In this section, I define the concepts of temporal compression and theta sequences and the

relevant experimental findings associated to them.

It has become customary to record the LFP and several cells simultaneously from the hippocampus while a rodent is actively exploring the environment (Wilson and McNaughton, 1993; Skaggs et al., 1996). To understand how their firing activities are related at a theta time scale (Harris et al., 2003; Maurer et al., 2006a; Dragoi and Buzsáki, 2006), one basic possibility is to analyse the phase precession of each place cell individually and compare phase-precession features across cells. A more advanced option is to calculate the cross-correlation function between the activity of two active place cells. If these two cells have overlapping place fields, the correlation function reflects the coactivity of the place cells across theta cycles. The crosscorrelation function between the spiking activity of two phase-precessing cells is oscillatory, which reflects the intrinsic theta-oscillatory activity of each cell during phase precession. From the crosscorrelogram, one can calculate the underlying envelope by means of an adequate filter and obtain the time T at which the maximum of the envelope occurs. This time T is essentially the separation in time of the two place-field peaks. If one assumes that the animal is traversing a linear track with a constant speed, then T (in seconds) should correlate with the distance x (in meters) between the two place field peaks. This is indeed the case, and the time T is referred to as the "behavioral" time lag (Skaggs et al., 1996; Dragoi and Buzsáki, 2006; Geisler et al., 2010). The crosscorrelogram, however, has also a structure at the theta time scale. The time of the first peak, with respect to a reference at 0, corresponds to the theta time lag τ. Thus, while T represents a behavioral time scale, τ represents a neural (or theta) time scale. Note that both T and τ are extracted from a single crosscorrelogram, i.e., they are defined for a given pair of cells with overlapping place fields. In the case of place fields of equal size, τ is simply the time lag between the spikes of a place cell and a neighboring place cell within one theta cycle (Fig. 5.1 *A* and Geisler et al. (2010)). It turns out that, for a given population of cells with overlapping place fields, the quantities T and τ are linearly correlated (Skaggs et al., 1996; Dragoi and Buzsáki, 2006; Diba and Buzsáki, 2008; Geisler et al., 2010; Maurer et al., 2012). From the T vs. τ relationship, one can define the sequence compression index k as the correlation coefficient, and the compression factor c as its slope. Intuitively, if T and τ are highly (linearly) correlated, this implies that c is approximately constant for the population, i.e., $c = \tau/T$. The compression factor c thus characterizes the population. These observations are collectively referred to as temporal compression. Importantly, temporal compression is believed to be crucial for the induction of synaptic plasticity between cells with overlapping place fields (Skaggs et al., 1996; Dragoi and Buzsáki, 2006).

Several studies have shown that the place-cell activity in the hippocampus is highly overlapping and can cover one or two dimensional environments (Wilson and McNaughton, 1993). The place cells are activated sequentially in order to cover the environments and therefore one can establish an order of place-cell firing. Foster and Wilson (2007) realized that not only is the place cell activity sequential, but also its representation at a theta time scale (Foster and Wilson, 2007). They introduced the concept of theta sequences, which formally refers to the correlation between cell order or "rank", and spike timing within one theta cycle (Fig. 5.1 *C*). Intuitively, this means that the behavioral sequences are also observed on a faster time scale, in a manner reminiscent of temporal compression. Thus, phase precession, temporal compression, and theta sequences, can be thought of as different characterizations of theta time scale dynamics, although the relationship might be complex (Dragoi and Buzsáki, 2006; Foster and Wilson, 2007; Itskov et al., 2008).

In the following section, I will summarize the proposed functions of phase precession,

their plausibility, and their relationship to existing models of phase precession.

Proposed functions of phase precession and relationship to mechanism of generation

To elucidate the function of phase precession, we must understand the underlying mechanisms that may allow us to interfere with it. Although we have learned a lot about phase precession ever since its discovery in 1993, unraveling the mechanisms has been challenging and there is to date no consensus on how it is generated. In this section, I explore the relationship between a few representative models and their hypothesized functions. For further information on the assumptions, strengths, and weaknesses of models of phase precession in general, I refer the reader to the articles by Zugaro et al. (2005), Maurer and McNaughton (2007), Harvey et al. (2009), Burgess and OKeefe (2011), Domnisoru et al. (2013), Schmidt-Hieber and Häusser (2013), Eggink et al. (2014), Jaramillo et al. (2014), Reifenstein et al. (2014).

After the first report on phase precession in 1993 (O'Keefe and Recce, 1993), Skaggs and colleagues outlined an important property of phase precession, namely the temporal compression of sequences within one theta cycle (Skaggs et al., 1996). This observation started a series of publications that addressed not only the generation of phase precession, but also aimed at explaining functional roles of phase precession (Wagatsuma and Yamaguchi, 2007; Yamaguchi et al., 2007; Maurer and McNaughton, 2007). Here I summarize three popular hypotheses about the role of phase precession as 1) a phase code, 2) an indicator of sequence retrieval and prediction, 3) an enabler of synaptic plasticity. Note that these three functions are not necessarily independent. I describe the hypotheses in some detail and explain how they relate to proposed generation mechanisms. In a later section, I analyze the evidence in favor or against these hypotheses.

Let me first summarize the phase-code hypothesis. It was already mentioned several times that during phase precession, the firing phases advance systematically with respect to the theta rhythm. In CA1 cells, for example, the first spikes occur during the late phase, while the last spikes occur at an early phase. Thus, the phase contains information about where the animal is, and this interpretation is independent of how phase precession was generated, although how this phase information is actually used is currently not clear. Because of phase precession, it is possible to disambiguate entry and exit through the place field. Furthermore, if an animal is traversing the overlapping region between two neighboring place fields, the phase disambiguates the two corresponding cells as the late-phase spike is associated to the field the animal is entering while the early-phase spike is associated to the field the animal is exiting. In addition, Bose A. et al. (2000) proposed that a cell receiving input from phase- precessing cells can distinguish whether the upstream cell was in fact within its place field based on phase information alone, since phases within a place field occur for a particular range. Thus, the phase-coding hypothesis states that theta phase complements the information provided by the coarse place-selectivity at the level of the trial-averaged firing rate (Huxter et al., 2003; Wu and Yamaguchi, 2010).

I now comment on sequence retrieval and models of phase precession based on this proposed function (Tsodyks et al., 1996; Jensen and Lisman, 1996; Wallenstein and Hasselmo, 1997; Navratilova et al., 2012). The basic premise for these models is the concept of look-ahead, here explained in the context of a traversal through a linear track: if the animal

is located at some position x in the environment, place cells corresponding to upcoming places, i.e., ahead of x, will be activated in a sequence after the activation of the place cell corresponding to that position x. Since the sequential activation of the place cells occurs at a much faster time scale than through the movement of the animal, this implies that while the animal is still at position x, place cells whose place fields lie ahead of the animal will all be active. Supposing that the animal has already been trained in this particular environment, the look-ahead property can be interpreted as the animal predicting locations on the basis of its previous experience. In other words, the sequence of firing fields is being retrieved as the animal traverses the track (Lisman and Redish, 2009). I now make the connection to phase precession. An important assumption in the above model is that cells are recurrently connected by asymmetric synaptic weights that allow the propagation of activity in a particular direction (Jensen and Lisman, 1996; Tsodyks et al., 1996), and that the beginning of a theta cycle (or the first gamma cycle (Jensen and Lisman, 1996; Lisman and Redish, 2009)) is a cue for initiating the look-ahead, also called a "sweep" (Johnson and Redish, 2007). I take a simple four-cell $ABCD$ network as an example, where A connects to B, B to C, and C to D, and I assume that the corresponding place fields overlap and are located in space in the same order from left (place field of A) to right (place field of D). In such a network, each cell receives excitation from basically two sources: an external source containing place-selective information, and an internal source from the cells within the recurrent network. When the animal enters the place field corresponding to place cell A, place cell A fires because it is receiving external excitatory input. Because of the connectivity within the network of place cells, cells B and C fire due to a chaining mechanism so that the first spike(s) of B and C occur later in the theta cycle. In the next theta cycle, the animal is within the place field of B, place cell B fires because it is receiving external excitatory input, and now C and D fire because of the chaining process brought about by the recurrent connections. In the next cycle, the chain repeats itself. The firing phases of cell D changes from one theta cycle to another, precessing from a late to an early phase. Basically, phase precession is observed because of a transition from internal dynamics from the lateral connections to driven dynamics from the feed-forward excitation. When entering the field, the first spikes occur because of the internal dynamics, i.e., excitation from neighboring fields. This way of obtaining phase precession is related to the concept of prospective coding: prospective, because a cell fires due to internal processes, even before it has received its place-selective external input.

The sequence-retrieval model of phase precession is intimately related to the function it proposes, as the sequence-retrieval or prediction is the essential idea behind the mechanism. This is also true for other network models, where the architecture to produce phase precession is consistent with a multistep autoassociative memory model, i.e., it allows for multiple memory recall processes (Bose A. et al., 2000), or there is a balance between encoding and retrieval (Cutsuridis and Hasselmo, 2012; Baker and Olds, 2007). Thus, for these models and the sequence-retrieval model I discussed, phase precession follows from, or at least is consistent with, a more global computation in the hippocampal formation such as pattern completion (Rolls and Kesner, 2006; Rolls, 2013; Nakazawa et al., 2002), which requires the participation of recurrently connected cells.

Other phase precession models are mostly concerned with the physiological characterization of phase precession as observed in experiments (O'Keefe and Recce, 1993; Skaggs et al., 1996). In these, usually cellular models (Kamondi et al., 1998; Magee, 2001; Harris et al., 2002; Mehta et al., 2002; Lengyel et al., 2003; Burgess et al., 2007; Hasselmo, 2008; Mau-

rer and McNaughton, 2007), the function (if any) follows from some emergent property of phase precession related to temporal compression (Skaggs et al., 1996; Dragoi and Buzsáki, 2006). These functions include binding sequences together for episodic memory formation (Mehta et al., 2002; Yamaguchi, 2003; Dragoi and Buzsáki, 2006), conserving sequential firing patterns across regions (Skaggs et al., 1996; Jones and Wilson, 2005; van der Meer and Redish, 2011; Malhotra et al., 2012) and cognitive map formation (Wagatsuma and Yamaguchi, 2007). The common idea behind these emergent functions of phase precession is the relationship between temporal compression and Hebbian learning rules such as STDP, a relationship which was not explicit in previous models of temporal sequences (Levy, 1996; Abbott and Blum, 1996). Through temporal compression, behavioral sequences experienced by the animal, i.e., place-field sequences, are compressed within a theta cycle. Because of the temporal compression, place cells from two overlapping place fields are brought together in a time scale of tens of milliseconds which is the appropriate time scale for the induction of STDP (Markram et al., 1997; Bi and Poo, 1998; Kempter et al., 1999; Song et al., 2000). STDP is a type of plasticity between cells whose direction (whether it is potentiating or depressing) depends on the relative ordering between presynaptic and postsynaptic spikes (Gerstner et al., 1996; Bi and Poo, 1998). In particular, and considering a system composed of two cells, if a presynaptic spike arrives before and hence causes a postsynaptic spike, then LTP is produced. Conversely, if the postsynaptic spike arrives before a presynaptic spike long term depotentiation (LTD) is induced. Suppose that two cells are connected synaptically. A popular computational assumption put forward by Donald Hebb, is that if a cell (or assembly) A fires before B, then the synapse from A to B is strengthened. Hippocampal cells fire sparsely, usually within their restricted spatial receptive fields. It is not clear how a unidirectional strengthening is possible based on the spike timings of the participating cells A and B if the cells are firing randomly, e.g., the spike times are Poisson-distributed, within their fields. However, phase precession overcomes this by bringing the spikes within two or more overlapping cells together in the tens of milliseconds time scale of the NMDA receptor, and hence of STDP at the hippocampal synapses. In the example above, "A then B" would be encoded in the corresponding synaptic weight. Thus, through phase precession, asymmetric connections between place cells can be formed that allow for rapid encoding and subsequent retrieval of sequences.

In the following sections, I examine the evidence for a functional role for phase precession and in particular, how it relates to some of the proposed theories developed above.

Phase precession as a neural code: spatial and event coding

In this section I focus on the phase code implied by the phase precession phenomenon. It is important to note that phase coding is in principle more general than phase precession, as it encompasses any relationship between behavior/computation or environmental information and a particular phase of theta oscillation at a theta time scale. In this review, I will not consider some interesting theories about the role of separate phases for encoding and retrieval (Hasselmo et al., 2002), phase locking between structures during cognitive tasks (Jones and Wilson, 2005), theta "flickering" between maps (Jezek et al., 2011), cross-frequency coupling (Colgin et al., 2009; Belluscio et al., 2012), theta-phase modulation of plasticity (Huerta and Lisman, 1995; Hyman et al., 2003), or any other study that does not address phase precession implicitly or explicitly.

The place-cell representation in the hippocampus allows for the reconstruction of the animal's trajectory, and the maximum firing rate of an assembly codes for the current po-

sition of the animal (Wilson and McNaughton, 1993). By complementing the rate, phase information has been used to reconstruct more precisely the current location of an animal (Jensen and Lisman, 2000; Reifenstein et al., 2012). Furthermore, information within one theta cycle has been used to reconstruct trajectories of the rat representing past, current, and future positions with a Bayesian decoder in a one-dimensional environment (Gupta et al., 2012; Bieri et al., 2014; Cei et al., 2014) or a dynamic time offset algorithm in a two-dimensional environment (Itskov et al., 2008). It is not clear, however, whether the animal itself can implement similar types of decoding to guide its behavior.

As argued before, phase information can disambiguate entry to a place field (late phase) from exit (early phase). This is true, even if the animal engages in backward travel (Cei et al., 2014): the animal was transported by a train and entered the place field backwards with its head facing opposite to the travel direction; nevertheless phase precession commences with a late spike phase. Thus, phase no longer coded for absolute position but phase instead reflected travelled distance through the field (see also the two-dimensional phase precession in Skaggs et al. 1996).

An important question that arises with respect to the existence of phase coding is whether the phase code in the hippocampus is independent from the rate code. One possibility is that phase precession can be explained on the basis of the firing rate of the cell, for example, based on the spike train dynamics (Harris et al., 2002) or the coupling of the excitation to an oscillation (McLelland and Paulsen, 2009; Mehta et al., 2002). Another possibility, arguably more interesting, is that phase precession carries complementary information and is independent of the firing rate of a cell (Wu and Yamaguchi, 2010). The presence of similar phase precession for both high and low firing rates argues for independence between the two variables (Huxter et al., 2003; Kim et al., 2012). Ultimately, phase might have a complex relationship with rate and position (Cei et al., 2014).

Phase precession can also anticipate a goal location or landmark. This was the case for striatal cells in the nucleus accumbens, which are known to exhibit anticipatory reward-related firing (van der Meer and Redish, 2009). As animals navigated a T- maze during a spatial alternation task, cells in the ventral striatum ramped their firing activity towards reward locations. These "ramp" cells (van der Meer and Redish, 2009) also exhibited phase precession (van der Meer and Redish, 2011), and the precession was found to be biased towards the reward locations. The spiking phase of these neurons could provide information about the distance to the reward or, more generally, the anticipatory activity of the phase-precessing ramp cells could underlie the learning of place-reward associations (Malhotra et al., 2012). Along these lines, it is thus possible that the phase precession present in the ventral striatum is in fact inherited from the hippocampus (van der Meer and Redish, 2011; Malhotra et al., 2012; Jaramillo et al., 2014).

The observed relationship between phase precession and signaling of events is not restricted to spatial receptive fields. In a combined behavioral and electrophysiological study, Lenck-Santini and colleagues (2008) elucidated the discharge properties of hippocampal neurons during a jump-avoidance task. In a jump-avoidance task, rats are first dropped into a box. This signals the event of “drop”. Then, after 15 seconds, a shock is delivered to the rat. After subsequent trials, the rat tries to avoid shocking by jumping onto the rim of the box. This signals the event of “jump”. Single cells in the CA1 region of the hippocampus showed tuning, i.e., event-related firing, to either or both “drop” and “jump”. A cell was said to be tuned to the event if the firing rate of the cell at the time of the event was at least 3 SD greater than the firing rate averaged during 1 s after the drop and before the jump.

There were "drop", "jump", and "drop+jump" cells, i.e., cells that exhibited activity during both drop and jump. Importantly, the firing activity of event-related cells showed phase precession, in this case with respect to time. Indeed, a significant circular-linear correlation coefficient was observed for 89% of the cells. For jump-event cells, the phase precession plot is approximately centered on the time of jump, whereas for "drop" cells the phase precession goes until the time of drop.

Since the jump-avoidance task is a non-spatial task, phase precession in this task is indicative that hippocampal processing is related to the encoding of a succesion of events, not only positions (Eichenbaum, 2004). Indeed, phase precession often occurs within an event field, not necessary a spatial firing field (Pastalkova et al., 2008; Itskov et al., 2008; Takahashi et al., 2014), and in single trials during traversal of linear tracks, phase correlates equally well with position and time (Schmidt et al., 2009). Thus, the concept of firing field should be extended to include events or episodes (MacDonald et al., 2011) and the definition of phase precession should be extended to include time as an equally important correlate of theta phase.

Does phase precession enable plasticity?

As discussed above, phase precession is hypothesized to facilitate STDP between active cells. Here I discuss the evidence linking phase precession to plasticity, related studies, and open questions. The synaptic plasticity-memory hypothesis posits that learning and memory are mediated by changes in the strength of synaptic connections between cells as a function of experience (Martin et al., 2000). Recent studies have made a strong case for this relationship, particularly the role of long term potentiation (LTP) and depression (LTD) in fear conditioning (Nabavi et al., 2014). However, although there are some notions of the relationship between LTP and place-selective activity in the hippocampal formation (Dragoi et al., 2003), there is still no accepted mechanism on how sequences of place fields, possibly relevant for navigation or memory, are generated starting from plasticity.

One of the successes of theoretical neuroscience was to predict the effects of synaptic plasticity on the firing of hippocampal place cells. Particularly, it was predicted that due to experience-mediated synaptic plasticity, the membrane potential and firing rate of CA1 cells should increase and furthermore, the shape of the receptive field should become more skewed such that place fields shift backwards relative to the direction of motion (Abbott and Blum, 1996). Experiments were explicitly designed to test this hypothesis, and indeed, the shape of the hippocampal place fields were found to be asymmetric and the level of asymmetry was dependent on experience (Mehta et al., 1997; 2000). Furthermore, these effects are abolished if the NMDA receptors in CA1 cells are blocked, pointing to a causal role for NMDA-dependent plasticity in the asymmetric expansion of place fields (Ekstrom et al., 2001). These results suggest that asymmetric changes in place fields are brought about by experience, and presumably STDP played an important role. However, there is no causal evidence that this place-cell plasticity was in fact enabled by phase precession. Notably, the experiments from Ekstrom et al. (2001) showed that phase precession persisted while NMDA receptors were blocked.

Another study has explored the role of place-cell firing patterns in the plasticity of hippocampal cells. In this in-vitro study, Isaac and colleagues injected natural, i.e., physiological spike trains to two connected CA3-CA1 cells (Isaac et al., 2009). They could reliably induce LTP at these synapses, provided that there was sufficient cholinergic tone by the application of carbachol. The degree of LTP was dependent on the degree of temporal overlap between

the two spike trains, which mimics the spatial overlap during place-field traversals. This provides evidence that synaptic plasticity between place cells could be used to encode spatial distance (Muller et al., 1996). An important finding was that LTD was never observed in response to the spike patterns, suggesting that near coincident firing generates LTP regardless of the relative order between presynaptic spikes and postsynaptic spikes. Phase precession was not analyzed in this study, as this was an in vitro model. However, the presence of strong theta modulation in the crosscorrelograms of the cells that were injected with spike trains suggests that these spikes corresponded to phase-precessing spikes in vivo. An interesting control in this study would have been to inject a Poisson-modulated spike train with a rate equal to the average rate over the place field. If phase precession enables plasticity, it is expected that spike trains without a temporal structure should be less effective in inducing LTP. Isaac and colleagues (2009) removed short interval spike pairs from place-cell activity, which prevented LTP induction. This study accounts for NMDA-dependent, i.e., Hebbian, forms of plasticity but non-Hebbian forms of plasticity have also been induced at the mossy fiber synapse with naturalistic spike trains (Gundlfinger et al., 2010; Mistry et al., 2011).

The studies described above, i.e., Isaac et al. (2009) and Mehta et al. (1997; 2000), suggest that plasticity comes from experience as well as from the typical firing patterns found in the hippocampus in vivo during place-field traversals. The Mehta et al. studies provided evidence of plasticity by the emergent properties of spatial receptive fields as a function of experience. In the case of the study by Isaac et al., the evidence for LTP was more direct and as a function of natural place-cell activity. However, two important questions remain: how does single-cell plasticity transform into sequence learning, and what properties of naturalistic spiking patterns, particularly phase-precessing patterns, are required for the optimal induction of plasticity?

Behavioral sequences: "look ahead", "look behind", and spatial memory

Look ahead and look behind

I have introduced the concept of theta sequences within a theta cycle as the compressed activity of different cells representing a path through the environment (Fig. 5.1 *C*). Up to the study of Foster and Wilson (2007) (Fig. 5.2 *A*), it was not clear what parts of the environment were represented by theta sequences, or more generally, what their behavioral significance was. The importance of theta sequences was assessed by Gupta and colleagues in a spatial alternation task (Gupta et al., 2012) where rats navigated a T-maze and they had to remember on which side (i.e., left or right) the food reward was. Interestingly, Gupta et al. found that theta sequences represented paths ahead of the animal (look ahead) and paths behind (look behind), and these representations occurred mostly at landmarks or points of special interest such as decision points (Fig. 5.2 *B*). Thus, the paths represented were usually between landmarks and not across. It would have been ideal to correlate these findings with phase precession features, e.g., slope, sequence compression index, or degree of overlap between neighboring place fields; however, phase precession was not quantified.

The computational process just described was referred to by Gupta et al. (2012) as behavioral chunking or segmentation, because distinct portions of the journey, mostly between landmarks, were represented at a theta time scale. Furthermore, using a Bayesian decoder, they concluded that theta sequences represent more information about spatial paths as ex-

pected solely from the place-field density distribution. Similar conclusions were reached in a study where rats were placed on a train and were carried through a maze (Cei et al. 2014, see Fig. 5.2 *C*). In this study, phase precession was reported in the forward and in the backward direction of travel through a given place field. Sweeps for forward travel were observed that started behind the actual position of the rat. Using a Bayesian decoder, it was found that the sequences represented the ongoing trajectory independent of direction of travel, and phase precession was consistently observed.

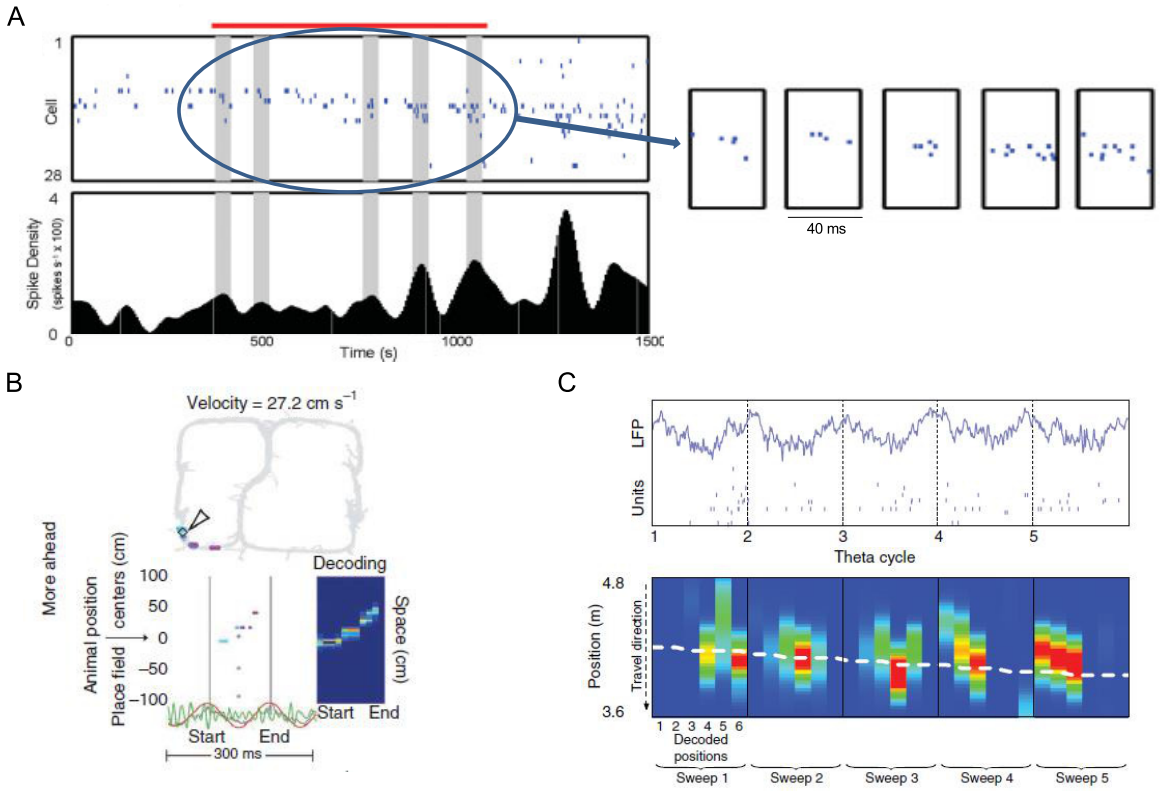

Fig. 5.2.: Theta sequences and the representation of trajectories. ***A,*** Place-field activity represented by sequences of spikes within a theta cycle (Foster and Wilson 2007; reproduced with permission from Wiley and Sons). On the left, CA1 cells are ordered according to the position of the place field center in a linear environment. The serial position of the cells is referred to as rank. Gray bars denote 40 ms windows and are selected on the basis of the maximum of spike-density plots (left, bottom). Blue oval and magnification denote the theta sequences (right) defined on the basis of the correlation of rank with spike-time within the 40 ms window. ***B,*** Spikes within a theta cycle represent trajectories ahead of the animal (Gupta et al. 2012; reproduced with permission from Nature Publishing Group). Arrow shows current position of a rat that traverses a T-maze (above) and colored dots correspond to cells active at points ahead of the arrow on the track. The order of the dots on the track corresponds to the order of the spikes within a cycle. ***C,*** Theta sequences during backward travel (Cei et al. 2014; reproduced with permission from Nature Publishing Group). LFP theta oscillations and spikes of CA1 pyramidal cells (top) and the reconstruction of trajectories (blue denotes minimum and red denotes maximum probability) using a Bayesian decoder (bottom).

Until now, I have discussed prospective (look ahead) and retrospective (look behind)

coding from a multi-cell perspective: the activity of multiple cells was organized within a theta cycle to represent past or upcoming trajectories. However, single cells can also display prospective and retrospective properties (Mehta et al., 1997; Frank et al., 2001; Lee et al., 2004; Battaglia et al., 2004; Lisman and Redish, 2009). Operationally, one can define a cell to exhibit prospective coding if its peak firing rate lies within the first half of its place field, whereas it exhibits retrospective coding if its peak firing rate lies within the second half of its place field (Bieri et al., 2014). In the study by Bieri et al. (2014), rats ran on a linear track for food reward, and place cells in CA1 were prospective and retrospective on different trials. Prospective coding was preferentially present when fast gamma was present, and retrospective coding when slow gamma was present. Importantly, phase precession was present in both types of cells, but was stronger for retrospective coding cells.

Theta sequences were characterized by estimating the spatial trajectory from the activity of cells and calculating prediction errors based on the current position of the animal: positive prediction errors would correspond to ahead sequences, and negative correspond to behind sequences as those reported by Gupta et al. (2012).

Overall, theta sequences indeed represent paths ahead of the animal, or "sweeps" (Johnson and Redish, 2007) as proposed by phase-precession sequence-retrieval models. This is evidence in favor of the predictive nature of the phase precession. However, in the studies by Gupta et al. (2012) and Bieri et al. (2014), not only paths ahead of the animal were represented, but also paths behind. Thus, it is not clear if the sequence-retrieval models as they were originally formulated can account for these findings.

Spatial memory and sensitivity to sequential activity

I now focus on studies where a relationship has been found, usually in the form of a correlation, between features of phase precession and performance in a behavioral task. As described previously, these tasks usually take the form of spatial memory tasks, such as the delayed-spatial T-maze alternation task.

Episodic memory might depend on self-generated sequential neuronal activity, that is, neural activity that is not directly controlled by environmental stimuli (Buzsáki, 2005). In the experimental paradigm from Pastalkova et al. (2008), rats generated sequential activity of neuronal firing while they were actively moving in a running wheel (Harris et al., 2002). Importantly, this sequential activity occurred during the delay period of a delayed alternation task while the animal was on the running wheel, but its spatial position was fixed. This assembly activity, characterized by sequential firing and phase precession, contained useful information to predict the future choice of the rat in the maze, left or right (Pastalkova et al., 2008). In the Pastalkova et al. (2008) study, hippocampal cells in the CA1 region were recorded during wheel and maze running. A subset of the recorded CA1 cells showed place-field activity in the maze, and corresponding phase precession. Interestingly, a subset of the CA1 putative pyramidal cells also fired transiently at specific times of wheel running. The epochs when the neurons fired, also referred to as episode fields, remained stable in successive trials, reminiscent of place-specific firing. Within the episode fields, there was clear phase precession that had similar properties as phase precession for place-cell firing, e.g., the slope of phase precession was inversely related to the temporal length of the episode field, unit firing oscillated at a higher frequency than LFP, and similar mean slopes for individual cells were observed. Phase precession was linked to sequential activity, in the sense that phase precession was only present for trials for which there was a memory demand, i.e., if the rat runs on the wheel during a delay period between trials. The authors devised control

tasks where the animal was allowed to run on the wheel but was not immerse in any task, for example, if the animal ran on the wheel for a water reward next to the wheel. There was no consistent sequential activity in this control case and, interestingly, the theta-related dynamics were markedly different: firing phases did not decrease as a function of time, i.e., there was no phase precession, but spikes instead were phase-locked to the theta LFP.

Phase precession has been observed in animals that remain at the same place, but are nevertheless moving, as in the aforementioned study by Pastalkova et al. (2008). However, even movement does not seem to be necessary for phase precession to be observed. In the study by Takahashi (2014), rats were trained in a spatial memory alternation task. The apparatus consisted of a box whose front wall contained two holes, left and right, while the back wall had another "fixation" hole. A new trial begins when the rat pokes its nose in the fixation hole for 1 second. After a subsequent delay of 1.5 s, the rat could visit the front wall and had to alternate between choosing the right and left hole, and was rewarded for each correct choice (Takahashi et al., 2014). A subset of cells from the hippocampal CA1 region showed fixation-related activity: the firing rate selectively increased and decreased within the fixation period. Furthermore, these "fixation" cells showed phase precession, from the CA1 pyramidal layer theta peak at the beginning of fixation, to the trough at the end. This is the first reported example of theta phase precession without movement or locomotion, and phase precession thus reflects solely internal memory processes. Interestingly, the neurons that exhibited phase precession were sensitive to the alternation sequence during behavior before fixation. This means that the shift in spike timing was stronger for trials with the preferred sequence (right-left, or left-right). The sensitivity to sequences was more readily observed at the level of the population.

The studies examined in this section related memory processes to hippocampal dynamics. However, there was no attempt to alter phase precession. In the next section, I discuss the interesting case of altered phase precession and how it affects behavior.

Altered phase precession and behavior: towards interfering with phase precession

As stated in this review, the mechanisms underlying phase precession are not clear. We have nevertheless learned about some aspects of the mechanisms involved through several means, including pharmacology (Robbe and Buzsaki, 2009; Lenck-Santini and Holmes, 2008), optogenetics (Royer et al., 2012), knockout studies (Allen et al., 2011), lesion/inactivation (Zugaro et al., 2005; Hafting et al., 2008; Schlesiger et al., 2013), intracellular recordings (Harvey et al., 2009; Domnisoru et al., 2013; Schmidt-Hieber and Häusser, 2013), network state (Senior et al., 2008; Bieri et al., 2014), and behavioral modulation, i.e., how certain tasks elicit particular phase precession patterns (Cei et al., 2014; Ravassard et al., 2013). In this section, I focus on those studies where phase precession was altered with respect to normal behaving animals (controls) and behavioral differences were concurrently observed. I also comment on those studies where different behavioral demands resulted in particular phase precession patterns, and therefore give insight into the mechanisms of phase precession.

Correlates of abnormal theta-time scale dynamics

Robbe and Buzsaki (2009) examined the effect of cannabinoids on the spatial coding properties of place cells in the hippocampus, as well as on memory and navigation on a spatial alternation task (Robbe and Buzsaki 2009 and Fig. 5.3). The effects of cannabinoid agonists on memory are well documented (Ranganathan and D'Souza, 2006; Hampson and Deadwyler, 1999), but there are open questions regarding the relationship between (1) neural activity and cannabinoids and (2) theta-scale dynamics and spatial memory. The authors found that the administration of a cannabinoid agonist impaired rats in performing the delayed spatial alternation task while leaving the place-field (i.e., rate) representation essentially intact. However, on a theta time scale, the time scale relevant for phase precession, there were alterations of the dynamics as measured by phase precession correlation coefficients and the sequence compression index introduced in the previous section.

In the Robbe et al. (2009) study, a group of rats were injected with CP55940, a cannabinoid receptor 1 (CB1) agonist that is known to impair memories in humans as well as interfere with synchrony of hippocampal network activity. The rats belonging to the control group were injected with a vehicle of saline solution that was later shown to not affect neuronal activity or behavioral performance on controls. Rats were trained to perform on a delayed-spatial T-maze alternation task (Fig. 5.3 *A*). Place-cell activity was recorded from the CA1 region of the hippocampus for both groups as the rats traversed the T-maze. I first describe the effects of the cannabinoid agonist on the neural activity, particularly the effects on place-field activity and phase precession with respect to controls. Interestingly, the place-cell activity of the cannabinoid group was similar to controls, in that the place-cell representation was not affected in terms of either spatial information, which quantifies spatial tuning, or spatial correlation, which quantifies the degree of remapping. There were some significant effects, however, on the average firing rate and peak-firing rate of place cells. These differences in firing rate were shown to be a consequence of the cannabinoid decreasing running speed. In general, the effects on place-cell firing were mild. The most striking effects were documented after observing the theta-time scale dynamics, which included the combined analysis of theta modulation, phase precession, and temporal compression. The power and frequency of the single-unit autocorrelograms and the phase-position correlation coefficient and slope were reduced under the influence of the cannabinoid (Fig. 5.3 *B*). Furthermore, the correlation between theta time lag and place-field distance was strongly reduced after cannabinoid injection. These effects were reversible, i.e., after animals recovered from the effects of the drug, the neural activity of the injected animals were similar to controls.

Apart from the differences in neural activity outlined before, the rats under effects of the cannabinoid were impaired in the delayed spatial alternation task. Choice accuracy was reduced for drug-infused animals and performance was close to chance level, whereas control animals made few errors: 92% (averaged over rats) of the trials were correct (Fig. 5.3 *A*). Particularly interesting was the relationship between the choice accuracy and the recorded neural activity in one of their datasets. There was a strong correlation between the percentage of correct trials and the theta-scale sequence compression index (Fig. 5.3 *C*). As the place-cell representation was relatively unaffected, the correlation between the compression index and the percentage of correct trials suggest that the theta-scale coding was necessary to perform the task (Robbe and Buzsaki, 2009). This is one of the few accounts of a link between theta-time scale spike coordination (or lack thereof) and cognitive impairment. Overall, the results suggest that spatial memory depends not only on a spatial code, but also on the temporal coordination between neurons.

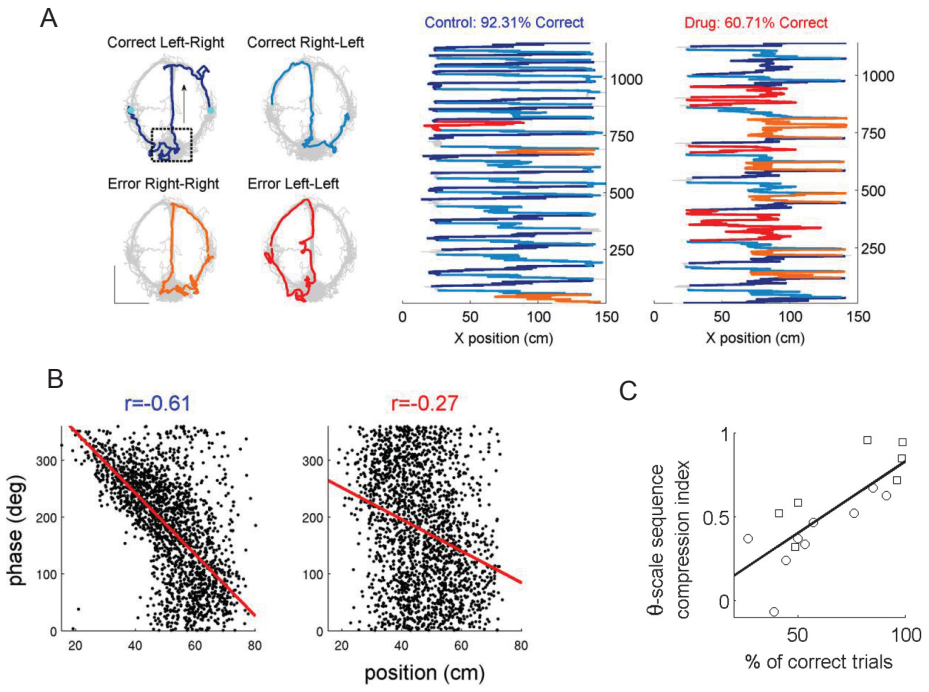

Fig. 5.3.: Abnormal phase precession correlates with deficits in a spatial memory task (Robbe and Buzsaki 2009; reproduced with permission from Society for Neuroscience). ***A,*** Spatial alternation maze. Rats were trained to run around the T-maze, alternating direction on each trial. Only correct alternations were rewarded (left). Systemic injection of a cannabinoid results in learning deficits for the spatial alternation task (middle and right). **B,** Phase position plots for a place cell for control (left) and drug-infused (right) conditions. ***C,*** Theta sequence compression index (Dragoi and Buzsáki, 2006) as a function of percentage of correct trials in the spatial alternation task (circles and squares represent two different experiments).

A relationship between abnormal phase precession and theta time scale dynamics was also observed for animals undergoing epilepitic seizures (Lenck-Santini and Holmes, 2008). As in the Robbe et al. (2009) study, there were two groups of animals that were compared in the Lenck-Santini and Holmes (2008) study: control and drug-infused. The drug-infused group was given pilocarpine and lithium chloride, compounds that induced seizures in this group. Both control and epileptic animals were trained to perform on a linear track for a food reward, and place cells were recorded from both groups during the traversal of the linear track. Some mild differences were found regarding place-cell statistics: both mean firing rate and peak firing rate were slightly higher in epileptic animals, while coherence and information content were slightly lower. These measures suggest a mild alteration of the place-cell representation. Phase precession and theta-time scale dynamics were assessed and important differences were found between the epileptic and control groups. In controls, the

percentage of cells with significant phase precession with negative slope was higher (96%) than in epileptic rats (65%). Only in the epileptic rats, a group of cells had a positive slope. To quantify temporal compression, crosscorrelograms were calculated at the theta-time scale and the running time scale. The compression factor, i.e., the ratio between theta-time scale lag and running lag between cells, was more constant in the population of control cells than in the epileptic group. As discussed previously, the constancy of the compression factor for a population implies a high sequence compression index. For the cells recorded from the epileptic group, theta lag was still correlated with running time lag, but the variance was significantly higher, i.e., some groups of cells had a disproportional relationship between the two time lags.

After the experiments in the linear track that determined the characteristics of phase precession in both groups, the animals performed a Morris water maze task (Morris, 1984). There was a clear deficit in learning for epilepitic rats. Controls could achieve an escape latency of 15 s while epileptic animals never learned the task. On the sixth day, the platform was removed and only controls showed preference for the quadrant where the platform was. The authors suggest that the abnormality in temporal coding could be the cause of the deficits in learning. It should be noted, however, that the abnormal phase precession and temporal compression were detected in the recordings during traversal of the linear track. Only afterwards, the animals were trained on the Morris water maze, where the spatial memory deficits were observed. I elucidate some important similarities and differences of the two aforementioned studies:

In both the Robbe et al. and Lenck-Santini et al. studies, there was a clear disturbance of temporal coding while the place coding was relatively unaffected. However, only in the cannabinoid study could the behavior be correlated with the abnormalities in phase precession. Moreover, in the cannabinoid study the abnormalities in phase precession were present in most cells compared to the epilepsy study, where the percentage of phase precessing cells decreased from 95% to 65% for epileptic animals. From a mechanistic point of view, the effects of the cannabinoids and the seizures might also be different. While the effect of epileptic seizures might include cell loss, up/down regulation of intrinsic channels, and long lasting changes in excitability (Lenck-Santini and Holmes, 2008), the effects of the cannabinoids are believed to be mostly related to network synchrony (Robbe et al., 2006; Maier et al., 2012).

In another study that relates abnormalities in coding to behavior, gap junctions in interneurons were found to be important for normal spatial and temporal coding (Allen et al., 2011). In animals lacking the connexin 36 gene responsible for gap junctions in interneurons, there were abnormalities in both spatial and temporal coding: the stability of spatial representations decreased with respect to control, and theta phase was different in the later portion of place fields in a zig-zag maze. Furthermore, these animals had deficits in the rewarded spatial alternation task that measures short term spatial memory (Allen et al., 2011). Although this is another example of a correlation between abnormal phase precession and behavior, the deficits in phase precession were rather subtle compared to the Robbe et al. (2009) and Lenck Santini et al. (2008) studies, and it is thus difficult to make any strong conclusions about the role of spike timing for this study.

Altered circuits and altered phase precession

Although phase precession and normal hippocampal dynamics likely depend on appropriate levels of excitation and inhibition (Ahmed and Mehta, 2009), it is not clear which features are

necessary nor which is the minimal circuit required to produce phase precession as observed in the hippocampus. Extrahippocampal sources might be important (Zugaro et al., 2005; Hafting et al., 2008; Schlesiger et al., 2013). Zugaro and colleagues transiently electrically perturbed the hippocampus, resulting in the effective silencing of place cells in the CA1 region for 100-300 ms (Zugaro et al., 2005). Surprisingly, after the perturbation place cells resume firing at a phase similar to that of controls without perturbation, i.e., as if there was no perturbation at all. Thus, this suggest that the phase information is updated outside the hippocampus. This is also consistent with the fact that inactivating the hippocampus only midly affects the phase precession observed in the entorhinal cortex (Hafting et al., 2008).

Inhibition is an important factor in modulating spatial tuning (Couey et al., 2013; Pastoll et al., 2013; Wilent and Nitz, 2007; Ego-Stengel and Wilson, 2007; Geisler et al., 2007; Maurer and McNaughton, 2007), but its precise role during phase precession is not yet established. An important step in this direction was taken by Royer and colleagues, who silenced parvalbumin-expressing interneurons in the hippocampal CA1 region (Royer et al., 2012). They found that after silencing the interneurons, neighboring CA1 pyramidal cells continued to phase precess, suggesting that perisomatic inhibition is not necessary to explain the phase precession as observed in CA1. However, spike phases shifted at entry and towards the end of the place field (Royer et al., 2012), suggesting a modulatory role for the inhibition (Jaramillo et al., 2014). Other alterations of the parvalbumin-expressing interneurons including NMDA ablation, have altered the spike-timing properties of hippocampal pyramidal cells at a theta time scale (Korotkova et al., 2010). Although these changes in spike timing suggest an alteration in phase precession, this was not quantified. To conclude, although there is no consensus on the mechanisms generating phase precession, it has been possible to alter the entorhinal-hippocampal circuitry in specific ways that resulted in altered phase precession.

Behavioral modulation of phase precession

Understanding the mechanism behind phase precession might gives us insight into its behavioral role. Conversely, behavioral tasks can probe predictions of different models of phase precession. In a task where animals experienced backward travel on a train (Cei et al., 2014), phase precession and theta sequences were observed for both forward and backward travel. Importantly, the phase precession during the backward traversal was not replaying the forward trajectory, i.e., point of entry to the field was marked always by late phase, as would have been predicted by sequence-retrieval models. Bearing in mind that for both forward and backward travel the animal was facing the same direction, the asymmetry that allows for phase precession as "look ahead" can not be attributable to the head direction signals. These observations place a difficulty on sequence retrieval models, as asymmetry is a crucial requirement.

In another experiment, animals were trained to navigate in a virtual reality setting, and the effects of being in a virtual reality setting were compared to a “real-world” setting (Ravassard et al., 2013). In particular, the environmental inputs were different because during virtual reality the animal had less access to distal visual and vestibular cues. In turn, there were differences in place-cell representation and theta dynamics. Theta frequency was lower in virtual reality and the dependence on speed was abolished. Phase precession, on the contrary, was very similar in both virtual reality and real world tasks, for any speed. These observations might be difficult to explain via cellular interference-type models of phase precession, which depend on speed and precise values of the theta frequency (O’Keefe and

Recce, 1993; Burgess et al., 2007; Lengyel et al., 2003). Properties of neural dynamics during navigation in two-dimensional environments can also be informative with regards to phase precession mechanism (Climer et al., 2013; Jeewajee et al., 2014; Reifenstein et al., 2014). During two-dimensional foraging, a grid field can be entered through multiple paths. In one extreme, a firing field can be entered tangentially and another, it can be entered direct through its center. Tangential traversals are accompanied by a steeper phase precession slope than for a direct traversal through a firing field center (Reifenstein et al., 2014). Phase precession models for grid fields that rely on oscillatory interference (Burgess et al., 2007; Jeewajee et al., 2008) cannot explain this complex dependence of phase precession on trajectories in a two dimensional environment.

Thus, in these experiments, phase precession was not altered per se, but nevertheless was useful in comparing model predictions to actual measured dynamics.

Concluding remarks

The study of phase precession and theta-time scale dynamics in general has shed light not only on hippocampal dynamics, but also on memory-related behaviors as outlined in this review. There are many open questions regarding phase precession in the hippocampal formation in terms of both functions and mechanisms (Maurer and McNaughton, 2007). In particular, I would highlight the role of phase precession in synaptic plasticity, which is currently not understood. If there is enough evidence to reasonably unify phase precession and synaptic plasticity, we can test the synaptic plasticity memory hypothesis more closely (Martin et al., 2000) as we have added an important functional and mechanistic element to these efforts. More generally, it would be very interesting to find evidence linking place-selective activity and plasticity in general, and study not only theta-time scale dynamics but also gamma (Lisman and Jensen, 2013), and sharp-wave ripples (Sadowski et al., 2011) in connection with plasticity. Importantly, phase precession is observed also in novel environments (Ekstrom et al., 2001; Cheng and Frank, 2008), while sequence-retrieval models of phase precession require an initial, i.e., without experience, specific connectivity. It would be interesting to investigate further properties of phase precession in trained vs. naive animals.

The future steps of phase precession research will probably involve tools such as genetics, including optogenetics, combined intracellular and extracellular recordings, and virtual reality. The electrophysiological study of phase precession should occur in the context of a behavioral task that assesses memory, the so-called hippocampus dependent tasks. Thus, it is likely that what we learn about phase precession in the near future will come concurrently with what we learn about its role in behavior. The relationship between mechanism and behavior is not necessarily one-directional, but more like a loop (Fig. 5.4): interfering with the mechanism allows us to learn about its functional role, but at the same time, understanding phase precession in the context of an appropriate behavioral task can help us test theories on how theta-time scale dynamics can change as a function of behavior and thus constrain models. We have learned, for example, that cannabinoids can be used as a tool that selectively impairs the spike-timing properties of pyramidal cells without affecting the place code (Robbe and Buzsaki, 2009). Furthermore, we have learned that phase precession can be studied in connection to internally generated sequences in behavioral paradigms as those used by (Takahashi et al., 2014) and (Pastalkova et al., 2008) that allow for the isolation of internal memory processes from other processes such as sensory-motor feedback or

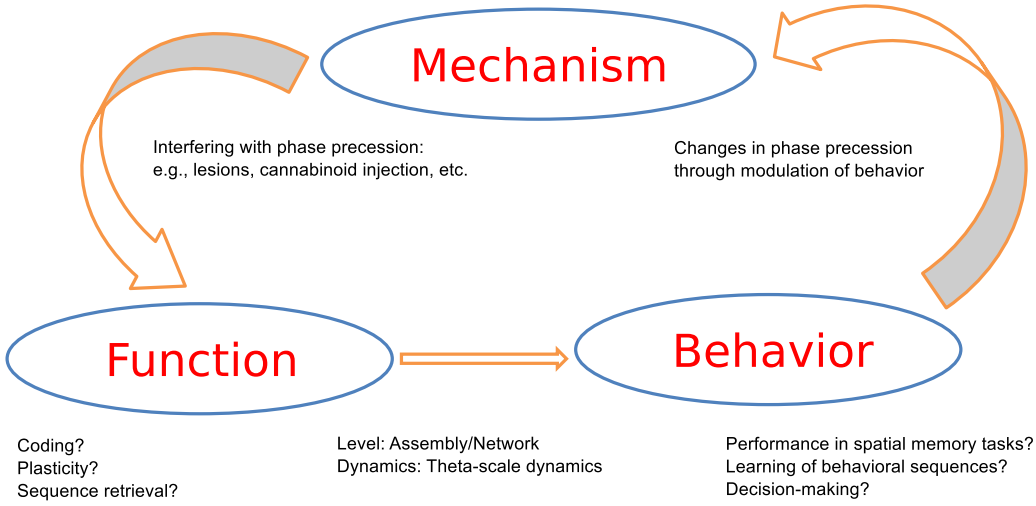

Fig. 5.4.: Next steps: understanding mechanism, function, and behavior concurrently.

path integration.

In the course of these new investigations, we may find that there is no functional role attributable to phase precession, although this review should at least cast a doubt on this possibility. Even if phase precession turns out to be epiphenomenal, we will have learned a lot about connectivity, dynamics of different cell types, and new ways of analyzing spatio-temporal receptive fields (see also Malhotra et al. 2012). The question of how behavorial sequences are learned is still open for debate, particularly how to connect the "slow" time scale of behavior with the "fast" time scale of plasticity (Melamed et al., 2004; Leibold et al., 2008). Taking into account the current and future theoretical and experimental caveats, phase precession is the best theory we have underlying the formation of sequences starting from place fields and synaptic plasticity.

6. Summary and outlook

In this thesis I have explored the inheritance mechanism as an important contribution to the phase precession observed in the different regions of the hippocampal formation as well as other parts of the brain. Inheritance in this thesis refers to the propagation of a signal through feed-forward topologies, such that a downstream region will exhibit a signal with some of the characteristics of the original upstream signal. The signal is characterized in relationship to the theta LFP by important parameters such as frequency, slope, range, and entrance phase. I have formalized the notion of inheritance and used this concept to explain a wide variety of experimental results, in the sub- and suprathreshold regimes: (1) Phase precession in a small subset of CA3 or MEC principal cells is sufficient to explain phase precession in a CA1 pyramidal cell. (2) Inhibitory input to the CA1 cell is not necessary to generate phase precession, but inhibition can increase the slope and enlarge the range of phase precession. (3) Theta modulation and phase precession present in CA3 cells aid in the place-field development of a downstream CA1 cell receiving this input. (4) The spatial distribution of field centers and the width of fields of the input population determine not only the spatial selectivity but also the phase-precession characteristics of the target cell.

6.1. Interpretation of the results

Testing the inheritance hypothesis Inheritance was made explicit in terms of its requirements and implications throughout the thesis. How can the inheritance hypothesis be tested? First of all, I review some of the main predictions outlined in Chapters 2, 3, and 4.

1. The first prediction concerns perisomatic inhibition in CA1 cells. I predict that such inhibition is not strictly necessary for the generation of phase precession as observed in CA1, as such phase precession will be inherited from CA3. Particularly, I predict that the somatic oscillations of CA1 cells in vivo as measured outside the place field are mediated by inhibition and are approximately in phase with the theta rhythm recorded in the pyramidal cell layer.

2. Another prediction concerns the existence of CA3 assemblies that project to a single CA1 cell. These assemblies were characterized by a modulation depth $C \approx 0.6$ and size $N \approx 200$.

3. The inheritance model also predicts the existence of particular spatial distributions of place-field centers, and that these distributions shape the phase precession of a target cell receiving input from these cells. In particular, the little incidence of phase precession in interneurons might be the result of spatially uniform input arriving to those cells. The spatial distributions described above could be shaped through synaptic plasticity.

4. Blocking phase precession in CA3 might lead to slower place field formation in CA1.

The data from Harvey et al. (2009) could in principle address prediction (1). The data set from Harvey et al. (2009) includes oscillations in and outside the place field, but the phase relationship between the oscillations of a CA1 cell outside its place field and theta LFP was not analyzed in the study. To test prediction (2), multi-cellular recordings could be performed that would quantify the firing rate of a population of CA3 cells at a single trial level. From these estimates one can extract a modulation depth for the firing rate of an assembly within a place field. Determining the size of the assembly projecting to a single CA1 cell is challenging and would require retrograde tracing. Prediction (3) is more difficult to test. Further experimental studies might elucidate a functional relationship between place-selectivity in the hippocampus and, for example, place and reward-related behavior in other areas such as the ventral striatum (van der Meer and Redish, 2011; Malhotra et al., 2012). Theoretical studies that address the role of plasticity in place-field formation (see also Chapter 3) could help us understand the origin of these distributions, and whether they are present in physical or in synaptic space. Finally, prediction (4) relies on selectively interfering with phase precession which is, as stated in Chapter 5, very difficult.

Although not predictions per se, it would be also interesting to check existing literature for relationships not yet reported in the data that could support the inheritance hypothesis. For example, in the Brun et al. (2002) study inputs from the CA3 area to CA1 were removed and the authors reported that place-selectivity in CA1 principal cells did not disappear. However, Brun et al. (2002) did not report on the presence of phase precession. The work I developed in Chapter 2 suggests that both CA3 and MEC layer III inputs could contribute to the phase precession observed in CA1 place cells. Nevertheless, it would be interesting to study phase precession (or lack thereof) in animals where a set of inputs has been removed as in the Brun et al. (2002) study (see also Brun et al. 2008), and compare this phase precession to normal phase precession, i.e., phase precession in animals with no alteration of their inputs. Another study to note is that of Mizuseki et al. (2009), who reported delays of activity between the different regions of the hippocampus. These delays were interpreted as a signature of independent internal computations. Some of the methods used in the Mizuseki et al. (2009) article, such as mean circular phases to characterize the spiking behavior of a cell, might have overestimated the phase preferences and thus biased the delays and their interpretation. Furthermore, the study could have classified cells into "phase-precessing" and "non-phase precessing" to draw stronger conclusions about phase preferences and firing rate. Finally, interneuron activity which they also recorded might have contributed, through inhibition, to the delays they observed. The Mizuseki et al. (2009) data set is now available online for anyone who would like to persue these and other questions.

Does phase-precession inheritance serve a computational role? As reviewed in Chapter 5, the function of phase precession in general is not clear. Thus, to comment on the even more restricted function of inheritance of phase precession is speculative. The fact that different subregions of the hippocampus subserve different purposes (Kesner et al., 2004), might point to a region-dependent role for phase precession. Indeed, if phase precession helps in the association of place cells with overlapping place fieds (e.g. Skaggs et al., 1996; Muller et al., 1996) through STDP, then the role for phase precession will be dependent on the emergent role of plasticity for that particular region (Martin et al., 2000). Along these lines, phase precession in the dentate gyrus would be related to pattern separation while phase precession in CA3 would be related to pattern completion and sequence formation. There is no indication yet that this is the case, but with what we have learned about phase

precession and how to interfere with it (see Chapter 5) together with concurrent analyses of the functions of different regions (Neunuebel and Knierim, 2014), it might be possible to start answering these questions related to specific functions of phase precession.

Skaggs et al. (1996) suggested that along with phase precession, sequences could also be inherited. The process would be roughly as follows: Let A, B, C, D represent four patterns of activity corresponding to a sequence of places that are traversed from left (A) to right (D). Due to phase precession of the corresponding assemblies within their fields and the associated phenomenon of temporal compression (Skaggs et al., 1996; Dragoi and Buzsáki, 2006), the following partial sequences, i.e., patterns of activities, are activated: AB, ABC, BC, BCD, CD. If A' represents the pattern of activity of an assembly downstream inheriting phase precession from A (and similarly for B', C' and D'), then the sequence in the downstream region $A'B'$, $A'B'C'$, $B'C'$, $B'C'D'$, $C'D'$ would follow directly from inheritance. There are many questions that must be addressed about plasticity in general, before accepting this simple picture. What characteristics, apart from timing, allows for the association of place cells through plasticity? One important aspect, is the role of neuromodulators such as acetylcholine or dopamine in mediating place-cell related plasticity. Another aspect relates to the salience or overrepresentation of a particular place or particular object-place association (Anderson and Jeffery, 2003). Are some places privileged because of being close to goal or a reward? Indeed, the hippocampus projects to ventral striatum and prefrontal cortex, regions involved in reward-learning, and the work in this thesis has shown that phase precession in these regions can be inherited from the hippocampus (see also van der Meer and Redish, 2011; Malhotra et al., 2012). Perhaps phase precession in these regions helps to form associations between places and rewards for decision-making (van der Meer and Redish, 2011; van der Meer et al., 2012).

An interesting paradigm to study inheritance is that of theta sequences (Foster and Wilson, 2006; Gupta et al., 2010). This paradigm must be combined with existing techniques that allow for the recording of multiple interacting assemblies from, for example, CA3 and CA1 (Buzsáki and Wang, 2012) to study more deeply the connection between the coherent activation of assemblies and sequences.

Here I suggest other possible functions of inheritance:

- In the context of CA3-CA1 inheritance, CA1 may assist the general process of recoding of information previously coded in CA3 (Rolls and Kesner, 2006). In particular, CA1 could serve as a layer to bind contextual elements coded in CA3.

- Patterns that are transferred from CA3 to CA1 might lead to a sparser representation that facilitates recall (Kesner et al., 2004).

- Due to effectively averaging over many input cells by a downstream neuron (see section 2.4.1), inheritance is a mechanism that might reduce noise and facilitate read-out.

- If phase precession in general is related to plasticity, inheritance of phase precession might facilitate the induction of plasticity in downstream regions.

As outlined above, inheritance might serve a computational role in the context of coding and plasticity. Even if this is not the case, the study of phase precession in different areas of the brain might lead to interesting insights regarding both anatomical and functional connectivity, which set of afferents controls the output of a cell, and which region is more likely to "lead" another. These insights could help in the quest of understanding how memories

are transferred to the neocortex, how the hippocampus is involved in decision-making circuits, and what the physiological and cellular requirements are to sustain theta and gamma rhythmicity in a given area.

What is the "ultimate" origin of phase precession? Phase precession has been observed in different regions of the hippocampal formation, as well as the prefrontal cortex and ventral striatum. Notably, this thesis did not address the de novo generation of phase precession. The fact that phase precession could be inherited from the entorhinal cortex as proposed in this thesis, and that phase precession in entorhinal cortex persists after inactivation of the hippocampus (Hafting et al., 2008), makes the entorhinal cortex an interesting candidate as primary generator of phase precession. This doesn't prevent, for example, the possibility that entorhinal cortex inherits its phase precession from other structures upstream. I make the important claim that if mechanisms for phase precession in the entorhinal cortex are elucidated, then through inheritance of phase precession and place-selectivity as explored in this thesis, we will have understood why phase precession is present in the regions where it has been observed to date. In the next section, I comment on what a new phase precession model should address.

6.2. Future work

I now informally propose a few projects that are related to the topics presented in this thesis and could be addressed through computational models. Other more general questions are presented separately.

Experimentally-constrained de novo phase precession model As argued above, it is still not clear what the origin of phase precession is. Due to studies emphasizing the importance of extrahippocampal inputs during phase precession (Zugaro et al., 2005; Hafting et al., 2008), the focus of research in phase precession might shift to the entorhinal cortex. Most phase-precession models, however, (Maurer and McNaughton, 2007; Burgess and OKeefe, 2011) were meant to be applied for the hippocampus. A systematic evaluation of these and more recent models (e.g. Hasselmo, 2012; Navratilova et al., 2012) is missing with respect to what I believe represent the most important properties of phase precession:

1. negative correlation between the spike phases relative to theta and position (or time) within a firing field (O'Keefe and Recce, 1993; Schmidt et al., 2009; Pastalkova et al., 2008),

2. slope-size matching across cells and for individual firing fields (e.g. Dragoi and Buzsáki, 2006; Reifenstein et al., 2012),

3. phase locking at the beginning of a firing field (e.g. Skaggs et al., 1996; Hafting et al., 2008),

4. phase-precession range of 180 degrees in CA1 cells for single trials (Schmidt et al., 2009),

5. peaks of membrane potential oscillations co-occur with spikes and also display phase precession (Harvey et al., 2009; Domnisoru et al., 2013; Schmidt-Hieber and Häusser,

2013), while frequency of membrane potential oscillations outside place field have the same frequency as theta LFP (Harvey et al., 2009),

6. rhythmic firing at a frequency close to theta (Geisler et al., 2007; Mizuseki et al., 2009; 2012),

7. covariance of single-cell frequency and theta frequency (e.g. Geisler et al., 2010),

8. firing rate increases and decreases, while phase always advances (Huxter et al., 2003),

9. prevalence of phase precession in principal cells and not interneurons (e.g. Mizuseki et al., 2009),

10. presence of phase precession in different stages of the hippocampal formation as well as ventral striatum and prefrontal cortex (Skaggs et al., 1996; Harris et al., 2002; Jones and Wilson, 2005; van der Meer and Redish, 2011; Mizuseki et al., 2012; Kim et al., 2012),

11. complex dependence on trajectories in two dimensions (Reifenstein et al., 2014).

This list is probably not exhaustive, but note how much we have learned from the phase precession mechanism. Do these constraints point to a specific class of models? In particular, can a theoretical relationship between theta phase and position or time be derived solely from these constraints? This is not an easy task, and it may be that only a combination of cellular, network, and inheritance mechanisms can account for these findings (Jaramillo et al., 2014).

Theta-time-scale dynamics As outlined in Chapter 5, it's not clear how phase precession is related to other theta-time-scale phenomena, including theta sequences, and temporal compression. It would be interesting to compare characteristic features of one phenomenon to those of another. For example, how does phase-locking of cells influence the temporal compression correlation, i.e., the sequence compression index (Dragoi and Buzsáki, 2006)?

Another issue is that some studies (e.g. Foster and Wilson, 2007) have indicated that phase precession is not sufficient to account for the existence of theta sequences. For this, Foster and Wilson (2007) shuffled phase precession data and, based on the set of phases corresponding to a given position, they created surrogate spike times and constructed new theta sequences. This was done while leaving the phase-position relationship intact. The surrogate theta sequences obtained after the shuffling were weaker than the original sequences as expressed by a lower rank-time correlation. They concluded that a phase-position correlation is not sufficient to account for the tight temporal correlations observed during theta sequences. I claim that this argument is flawed, because phase correlates equally well with time, especially in single trials (Schmidt et al., 2009). Thus, any alteration in the phase-time correlation (as with shuffling) will necessarily affect the theta sequence temporal correlations. Along these lines, I suggest that a phenomenological model of phase precession, e.g., an inhomogeneous Poisson process, is able to capture many essential features of theta-time-scale dynamics, including phase-position correlation, temporal compression, and theta sequences. Notably, the Poisson process won't be able to reproduce correlations as observed in experiments (Foster and Wilson, 2007; Jackson and Redish, 2007), but the phenomenological model could unify these possibly different characterizations of theta-time-scale dynamics and potentially explain the shuffling experiment by Foster and Wilson (2007).

Subthreshold dynamics vs. spiking during phase precession Although phase precession is essentially a spiking phenomenon (O'Keefe and Recce, 1993), intracellular recordings (Domnisoru et al., 2013; Schmidt-Hieber and Häusser, 2013; Harvey et al., 2009) have provided us with an informative subthreshold perspective. A consistent finding in these studies is that spikes occur at the subthreshold peaks of the underlying oscillatory membrane potential. This has the important implication that the intracellular oscillations, like spikes, are precessing with respect to the extracellular theta rhythm. It is not clear, however, why the spikes actually occur on top of the membrane potential peaks. Simple (e.g., leaky) integrate-and-fire models predict that spikes occur at a fixed threshold and thus spikes would not necessarily have to occur at the peaks. Thus, is there a specific class of spiking models that actually do spike on top of the peaks? Are there special conductances involved that allow for this particular dynamic behavior? Furthermore, can one use this fact as a constraint to evaluate different phase-precession candidate mechanisms?

Phase-precession enhancement An interesting possibility, is that phase precession could be enhanced, i.e., phase-precession features such as correlation coefficient and slope could be increased as a function of experience or of the architecture where phase precession is observed. Indeed, an important parameter of the firing rate of a place-cell assembly is C, the modulation depth at a particular frequency f_λ (see Chapter 2), and this quantity is related to the phase precession of a downstream cell receiving this input. The modulation depth C is perhaps a dynamical variable that could increase as a function of experience. It would be interesting to study how synchronization or plasticity affect the evolution of C and thus of phase precession.

Other open questions and related issues I will now pose some outstanding questions, i.e., important questions that will require thorough theoretical and experimental investigation, that either stem from the analysis of the mechanisms of phase precession or are closely related:

1. What is the precise relationship between the temporal compression mediated by sharp-wave ripples during replay and the temporal compression mediated by phase precession?
2. Does the overlap between two fields promote Hebbian plasticity between the corresponding cells, and does phase precession facilitate this process?
3. To which extent does phase precession contribute to the theta rhythm (Geisler et al., 2010), and vice versa?

If we are able to answer these three questions, we will have solved an important part of the phase-precession riddle.

6.3. Final remarks

Phase precession and its associated temporal compression represent the best theory we have underlying the formation of sequences starting from place fields and synaptic plasticity. The phenomenon of phase precession is observed in many parts of the brain, and this phase precession might be partly inherited from other regions that already exhibit phase precession (Jaramillo et al., 2014).

As I am writing the last pages of this thesis, I hear that Profs. John O'Keefe, Edvard Moser, and Mary-Britt Moser have won the Nobel Prize for Medicine or Physiology for the discovery of a "positioning system in the brain". This is indeed a remarkable achievement, and many of us who are pursuing an academic career in this field owe these pioneers a debt of gratitude. Some might criticize this selection on the basis of it being too soon, or too incidental, or not applicable enough to deserve such a mention. Although I might agree with some of these objections, the fact still remains that the discovery of place cells and grid cells represent one of the major breakthroughs in systems neuroscience, and one of the few discoveries that link behavior to the activity of single cells. Moreover, it has had a major impact on all levels of research, from molecules all the way to behavior. The dynamics of cognitive circuits, i.e., the circuits responsible for memory, navigation, and/or decision making, are complex. Nevertheless, we know the remarkable fact that a single cell, a place cell, can represent the abstract concept of space. Similar arguments hold for grid cells, with the added value of the beauty and symmetry of the pattern they evoke. Perhaps place cells and grid cells turn out being epiphemenonal, a possibility I also suggested for phase precession. But maybe not, and this possibility has driven research in this field for the last 30 years, with the hope that one day in the not so distant future, another Nobel prize recipient will begin his or her acceptance speech with the exclamation, "I now know what place cells and grid cells are actually doing!".

A. Appendix: Mathematical analysis of place-field inheritance and model parameters

A.1. Mathematical analysis of place-field inheritance

In this section I study the place-field inheritance model proposed in Section 3.3.1. In particular, I define and study the tuning index, a measure to interpret the results shown in Figure 3.4.

A.1.1. The tuning index

To characterize and quantify the behavior of the evolution of the synaptic weights, I define the CA1 tuning index

$$\psi(t) := \tilde{J}_1(t)/\tilde{J}_0(t) \tag{A.1}$$

where $\tilde{J}_k := \sum_{n=0}^{N-1} J_n \exp(-2\pi njk/N)$ is the k^{th} component of the Discrete Fourier Transform (DFT) of $\mathbf{J}$. To obtain the Fourier components of $\mathbf{J}$, one must solve the differential equation for $\mathbf{J}$. Before calculating the Fourier components in section A.1.2, I first give an interpretation of the tuning index.

The tuning index ψ is a complex number that can be interpreted as follows: its modulus $\|\psi\|$, i.e., the vector strength of $\mathbf{J}$, indicates the degree of spatial tuning of a CA1 neuron; its phase indicates the position of a CA1 place field on the track. Indeed, since $\|\psi\|$ is proportional to the modulus of the first Fourier component of the efficacy vector $\mathbf{J}$, a high value of $\|\psi\|$ corresponds to synaptic efficacies that vary slowly over synapse index, which is the case for potentiated synapses associated to neighboring CA3 place fields, resulting in a CA1 place field. Additionally, the phase of ψ equals the phase of the first Fourier component of $\mathbf{J}$. Therefore, it indicates which synapses are potentiated or depressed and, as a result, the location of a CA1 place field on the track.

In Figure A.1, I show the dynamics of the tuning index ψ for the simulations in Figure 3.4. In all cases, the vector strength $\|\psi\|$ increases exponentially and, for bounded synapses, it saturates at about $\|\psi\| = 1$ (Figure A.1A). Comparing the vector strengths in the four scenarios, we notice that for theta-modulated CA3 inputs a CA1 place field emerges faster than for no modulation. This is true for both bounded and unbounded synapses, and the presence of the synaptic saturation boundaries does not considerably affect the time of place-field formation (Figure A.1A, insets). Among the three scenarios with theta-modulated inputs, the in-phase modulation is the one where a CA1 place field is formed fastest while phase precession and phase recession lead to slower place-field formation.

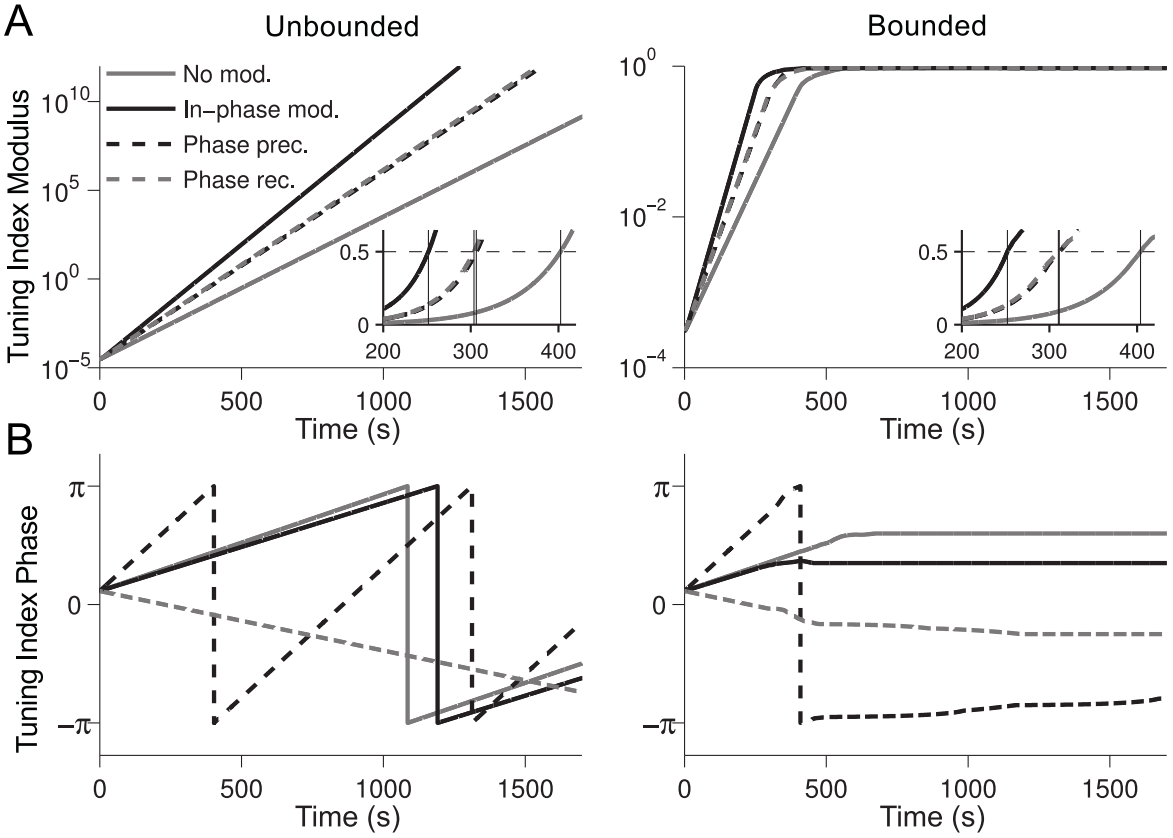

Fig. A.1.: Modulus (***A***) and phase (***B***) of the tuning index ψ for the simulations in Figure 3.4. The modulus of ψ (logarithmic scale) indicates the tuning strength of the CA1 neuron while its phase indicates the position of a CA1 place field on the circular track. The insets in A (linear scale) show the time points at which a CA1 place field emerges ($\|\psi\| = 0.5$).

A.1.2. Analysis of the dynamics of the synaptic learning rule

Equation 3.6 describes the dynamics of the synaptic weights. This equation is solved by first ignoring the boundary conditions ($0 \leq J_i \leq J_{\max}$). I first rewrite Equation 3.2 in matrix form to obtain

$$\frac{\mathrm{d}}{\mathrm{d}t}\mathbf{J}(t) = \underbrace{(\mathbf{Q} + \mathbf{M}k_2 + \mathbf{I}k_3)}_{\mathbf{A}}\,\mathbf{J}(t) + \underbrace{\mathbf{m}k_1}_{\mathbf{b}} \tag{A.2}$$

where $\mathbf{M}$ is the NxN matrix $M_{i,j} = 1\,\forall i,j$, $\mathbf{I}$ is the identity matrix of size N, and $\mathbf{m}$ is the constant vector $m_i = 1\,\forall i$. Since the system matrix $\mathbf{A}$ is circulant, it has a set of N independent eigenvectors $\{\mathbf{v}_k\}$ and N distinct eigenvalues $\{\lambda_k\}$ such that $\mathbf{v}_k = (\omega_k^0, \omega_k^1, \ldots, \omega_k^{N-1})^T$ and $\lambda_k = \sum_{n=0}^{N-1} a_n (w_k)^{-n}$ where $\{\omega_k\}$ are the N^{th} roots of unity ($\omega_k = \exp(2\pi jk/N)$, $j = \sqrt{-1}$), and the vector $\mathbf{a} = \{a_n\}$ is the first column of $\mathbf{A}$. Therefore, all the solutions of the dynamical system can be expressed in the eigenvectors' basis:

$$\mathbf{J}(t) = \sum_{k=0}^{N-1} c_k \mathbf{v}_k \exp(\lambda_k t) + \mathbf{h} \tag{A.3}$$

where the coefficients $\{c_k\}$ depend on the initial condition, and $\mathbf{h}$ is the steady-state solution of the dynamical system given by $h_n = J_*^{\mathrm{av}}\,\forall n$ (Equation 3.8). Substituting the eigenvectors

$\{\mathbf{v}_k\}$ one obtains

$$J_n(t) = \sum_{k=0}^{N-1} c_k \exp\left(\frac{2\pi jnk}{N}\right) \exp(\lambda_k t) + J_*^{\text{av}} \quad \text{for } n = 0, \ldots, N-1. \tag{A.4}$$

From Equation A.4, rewriting in polar form the coefficients $c_k = \|c_k\| \exp(j \arg(c_k))$, and expanding in their real and imaginary parts the eigenvalues $\lambda_k = \lambda_k^R + j\lambda_k^I$, one obtains

$$J_n(t) = \sum_{k=0}^{N-1} \|c_k\| \exp(\lambda_k^R t) \cos\left(\lambda_k^I t + \arg(c_k) + \frac{2\pi nk}{N}\right) + J_*^{\text{av}}. \tag{A.5}$$

It shall be noticed that the imaginary part of $J_n(t)$ vanishes, i.e.,

$$\sum_{k=0}^{N-1} \|c_k\| \exp(\lambda_k^R t)\, j \sin\left(\lambda_k^I t + \arg(c_k) + \frac{2\pi nk}{N}\right) = 0, \tag{A.6}$$

because, within the sum in Equation A.6, term k cancels out with term $N-k$, and the $k=0$ term equals 0. Equation A.5 shows that the solutions $J_n(t)$ of the dynamical system are linear combinations of exponentially modulated sinusoids. The real parts of the eigenvalues $\{\lambda_k^R\}$ determine the exponential growth or decay while the imaginary parts $\{\lambda_k^I\}$ determine the frequency of the oscillations.

As shown in Section 3.4, a CA1 place field emerges when the synaptic efficacies vary slowly over synaptic index, i.e., when the lowest-frequency component of the efficacy vector dominates: $\|\tilde{J}_1\| \gg \|\tilde{J}_n\|$ for $n > 1$ where $\tilde{J}_n = \sum_{k=0}^{N-1} \exp(-j2\pi nk/N) J_k$ is the n^{th} component of the DFT of $\mathbf{J}$. Additionally, the modulus of $\tilde{J}_1$ indicates how fast a place field is formed whereas its phase indicates the place-field position on the track. From Equation A.4, the DFT of the efficacy vector is computed as

$$\tilde{J}_k(t) = N\, c_k\, \exp(\lambda_k t) + N J_*^{\text{av}} \delta_{k0} \tag{A.7}$$

where δ_{ij} is the Kronecker delta.

Using Equation A.7 into Equation A.1 and noticing that $\tilde{J}_0$ is real one obtains:

$$|\psi| = \frac{|c_1| \exp(\lambda_1^{\text{R}} t)}{|c_0| \exp(\lambda_0^{\text{R}} t) + J_*^{\text{av}}}, \tag{A.8}$$

$$\arg(\psi) = \arg(c_1) + \lambda_1^{\text{I}} t. \tag{A.9}$$

meaning that λ_1^R and λ_1^I determine the time of formation and the drifting speed of a CA1 place field, respectively. In the following, the system eigenvalues are analytically estimated from three basic functions defined in the inheritance model: the CA3 place-fields' Gaussian function G, the STDP learning window W and the EPSP ϵ.

A.1.3. Analytical calculation of the eigenvalues

The eigenvalues $\{\lambda_k\}$ of the circulant matrix $\mathbf{A}$ can be computed from the DFT of its first column $\mathbf{a}$:

$$\lambda_k = \sum_{n=0}^{N-1} a_n (w_k)^{-n} = \sum_{n=0}^{N-1} a_n \exp\left(-\frac{2\pi jnk}{N}\right) := \tilde{a}_k, \tag{A.10}$$

and using the definition of $\mathbf{A}$ in Equation A.2 I obtain

$$\lambda_k = \tilde{q}_k + k_3 + \delta_{k0}\, N k_2 \tag{A.11}$$

where $\tilde{\mathbf{q}}$ is the DFT of the first column $\mathbf{q}$ of the correlation matrix $\mathbf{Q}$.

To calculate $\tilde{\mathbf{q}}$, I first show that each element of the matrix $\mathbf{Q}$ is obtained by sampling a continuous function $F^L(d)$ that depends only on the distance d between two place fields. From Equation 3.5 and Equation 3.9, one derives

$$Q_{ij} = \frac{\eta}{T_{\text{tot}}} \sum_{n=-\infty}^{\infty} \int_{-\infty}^{\infty} \mathrm{d}s\, W(s) \int_{-\infty}^{\infty} \mathrm{d}\tau\, \epsilon(\tau) \int_{-\infty}^{\infty} \mathrm{d}t\, \lambda_i^L(t) \lambda_j^L(t - s - \tau - nT_{\text{tot}}) + K \tag{A.12}$$

where $K := -(\lambda^{\text{in}})^2 \int_{-\infty}^{\infty} \mathrm{d}s W(s)$. To substitute the definition of the input intensity $\lambda_i^L(t)$, one needs to distinguish the four scenarios considered: no modulation, in-phase theta modulation, phase precession and phase recession.

In case of non-modulated inputs, using the definition of $\lambda_i^L(t)$ in Equation 3.10 and defining the re-scaled Gaussian function $g(t) := T_{\text{tot}} \lambda^{\text{in}} G(t)$, one can write

$$\int_{-\infty}^{\infty} \mathrm{d}t\ \lambda_i^L(t) \lambda_j^L(t + k) = \int_{-\infty}^{\infty} \mathrm{d}t\ g(t)\, g(t + d + k) \tag{A.13}$$

where $d := T_i - T_j$ is the distance between place fields i and j. Then, using Equation A.13, Q_{ij} can be written (Equation A.12) as a function of the distance d only:

$$Q(d) = \frac{\eta}{T_{\text{tot}}} \sum_{n=-\infty}^{\infty} \int_{-\infty}^{\infty} \mathrm{d}s\, W(s) \int_{-\infty}^{\infty} \mathrm{d}\tau\, \epsilon(\tau) \underbrace{\int_{-\infty}^{\infty} \mathrm{d}t\, g(t) g(t + d - s - \tau - nT_{\text{tot}})}_{g \star g\big|_{d-s-\tau-nT_{\text{tot}}}} + K \tag{A.14}$$

$$\underbrace{\qquad\qquad\qquad\qquad}_{\epsilon * (g \star g)\big|_{d-s-nT_{\text{tot}}}}$$

$$\underbrace{\qquad\qquad\qquad\qquad\qquad\qquad}_{W * (\epsilon * (g \star g))\big|_{d-nT_{\text{tot}}}}$$

$$= \frac{\eta}{T_{\text{tot}}} \sum_{n=-\infty}^{\infty} W * \epsilon * (g \star g)\Big|_{d-nT_{\text{tot}}} + K, \tag{A.15}$$

where $*$ denotes convolution an $\star$ denotes cross-correlation. Finally, defining

$$F^L(d) := \mathcal{L} * (g \star g)\Big|_d, \tag{A.16}$$

with $\mathcal{L} := W * \epsilon$, Equation A.15 can be re-written as

$$Q(d) = \frac{\eta}{T_{\text{tot}}} \sum_{n=-\infty}^{\infty} F^L(d - nT_{\text{tot}}) + K. \tag{A.17}$$

It can be shown that Equation A.17 holds also for the three remaining scenarios: in-phase theta modulation, phase precession, and phase recession, when the function F^L is

appropriately defined. In case of in-phase theta modulation, one derives

$$F^L(d) \approx \mathcal{L} * (g \star g)\Big|_d + \cos(\omega_\lambda d)\ \mathcal{L} * (g_c \star g_c)\Big|_d + \sin(\omega_\lambda d)\ \mathcal{L} * (g_c \star g_s)\Big|_d, \tag{A.18}$$

where $g_c(t) = \cos(\omega_\lambda t) g(t)$, $g_s(t) = \sin(\omega_\lambda t) g(t)$, and the approximation is valid when $\widehat{g}(\omega) \ll 1$ for $\|\omega\| \geq \omega_\lambda/2$, i.e., when the width of the Gaussian is much larger than the period of the modulating sinusoid. Similarly, for phase-precession and phase recession one derives

$$\begin{aligned} F^L(d) \approx \mathcal{L} * (g \star g)\Big|_d + &\quad \cos(\omega_\lambda(1 \pm c)d)\ \mathcal{L} * (g_c \star g_c)\Big|_d \\ + &\quad \sin(\omega_\lambda(1 \pm c)d)\ \mathcal{L} * (g_c \star g_s)\Big|_d, \end{aligned} \tag{A.19}$$

where $\pm$ reads as a minus for phase precession and as a plus for phase recession.

Using Equations A.11 and A.17, the eigenvalues are computed from the continuous Fourier transform of F^L. Assuming that the first CA3 input place field is centered at zero ($T_0 = 0$), recalling that place-fields are uniformly spaced on the track ($\Delta T = T_{\text{tot}}/N$), and defining $F(d) := \sum_{n=-\infty}^{\infty} F^L(d - nT_{\text{tot}})$, I compute the first column $\mathbf{q}$ of the correlation matrix $\mathbf{Q}$ as

$$q_k = Q_{k,0} = Q(T_k - T_0) = Q(k\,T_{\text{tot}}/N) \overset{(A.17)}{=} \frac{\eta}{T_{\text{tot}}} \underbrace{F(k\,T_{\text{tot}}/N)}_{=:\, f_k} + K = \frac{1}{T_{\text{tot}}} f_k + K, \tag{A.20}$$

from which one obtains

$$\tilde{q}_k = \frac{\eta}{T_{\text{tot}}} \tilde{f}_k + \delta_{k0}\, NK. \tag{A.21}$$

To compute $\tilde{f}_k$, I expand the T_{tot}-periodic function F as the Fourier series

$$F(d) = \sum_{l=-\infty}^{\infty} S_l \exp\left(\frac{j\,2\pi l d}{T_{\text{tot}}}\right) \tag{A.22}$$

where the Fourier coefficients $\{S_k\}$ are given by

$$S_k = \frac{1}{T_{\text{tot}}} \int_0^{T_{\text{tot}}} \mathrm{d}t\ F(t) \exp\left(\frac{-j\,2\pi k t}{T_{\text{tot}}}\right) = \frac{1}{T_{\text{tot}}} \int_{-\infty}^{\infty} \mathrm{d}t\ F^L(t) \exp\left(\frac{-j\,2\pi k t}{T_{\text{tot}}}\right) = \frac{1}{T_{\text{tot}}} \widehat{F}^L\left(\frac{2\pi k}{T_{\text{tot}}}\right) \tag{A.23}$$

where $\widehat{F}^L(\omega) := \int_{-\infty}^{\infty} \mathrm{d}t F(t) \exp(-j\omega t)$ is the continuous Fourier transform of F^L. Therefore, one obtains

$$f_k = F\left(\frac{k\,T_{\text{tot}}}{N}\right) \overset{(A.22)}{=} \sum_{l=-\infty}^{\infty} S_l \exp\left(\frac{j\,2\pi l k}{N}\right) \tag{A.24}$$

$$= \sum_{l=-\infty}^{\infty} \sum_{m=0}^{N-1} S_{m-lN} \exp\left(\frac{j\,2\pi(m - lN)k}{N}\right) \tag{A.25}$$

$$= \sum_{m=0}^{N-1} \sum_{l=-\infty}^{\infty} S_{m-lN} \exp\left(\frac{j\,2\pi m k}{N}\right) \underbrace{\exp\left(-j\,2\pi l k\right)}_{1}, \tag{A.26}$$

and, from Equation A.26, using the definition of the DFT, one derives

$$\tilde{f}_k = N \sum_{l=-\infty}^{\infty} S_{k-lN} \overset{(A.23)}{=} \frac{N}{T_{\text{tot}}} \sum_{l=-\infty}^{\infty} \widehat{F}^L\Big(\frac{2\pi(k-lN)}{T_{\text{tot}}}\Big). \tag{A.27}$$

Plugging Equation A.27 into Equation A.21:

$$\tilde{q}_k = \frac{\eta N}{T_{\text{tot}}^2} \sum_{l=-\infty}^{\infty} \widehat{F}^L\Big(\frac{2\pi(k-lN)}{T_{\text{tot}}}\Big) + \delta_{k0}\, NK \tag{A.28}$$

and, assuming that $\widehat{F}^L$ has negligible power at frequencies higher than $N/(2T_{\text{tot}})$, i.e., $\|\widehat{F}^L(\omega)\| \ll 1$ for $\|\omega\| > 2\pi N/T_{\text{tot}}$, one approximates the infinite sum in Equation A.28 by the term $n = 0$:

$$\tilde{q}_k \approx \frac{\eta N}{T_{\text{tot}}^2} \widehat{F}^L\left(\frac{2\pi k}{T_{\text{tot}}}\right) + \delta_{k0}\, NK. \tag{A.29}$$

Finally, plugging Equation A.29 into Equation A.11, one can approximate the eigenvalues by

$$\lambda_k \approx \frac{\eta N}{T_{\text{tot}}^2} \widehat{F}^L\left(\frac{2\pi k}{T_{\text{tot}}}\right) + k_3 + \delta_{k0}\, N(K + k_2) \quad \text{for } k = 0, \ldots, N-1. \tag{A.30}$$

A.2. Model parameters

$L = 1$ m	Length of the track
$v = 0.5$ m/s	Running speed of the rat
$T_{\text{tot}} = 2$ s	Duration of one round of the track
$N = 20$	Number of CA3 input place cells
$\lambda^{\text{in}} = 10$ spikes/s	Average input intensity in one round of the track
$v_0 = 0$ spikes/s	Spontaneous output rate of the CA1 neuron
$\eta = 10^{-3}$	Learning rate
$w^{\text{in}} = \eta$	Amount of synaptic change for input spikes
$w^{\text{out}} = -1.0475\ \eta$	Amount of synaptic change for output spikes
$A_+ = 2.4\ \eta$	Learning window amplitude for LTP
$A_- = \eta$	Learning window amplitude for LTD
$\tau_+ = 10$ ms	Learning window time constant for LTP
$\tau_- = 20$ ms	Learning window time constant for LTD
$\tau_{\text{EPSP}} = 4$ ms	EPSP time constant
$\sigma = 0.2$ s	Place-field Gaussian standard deviation
$f_\lambda = 9.5$ Hz	Frequency of input oscillations
$c = 0.1053$	Compression factor for phase precession / recession

$\widehat{W}(0) = 4.4 \cdot 10^{-6}$ s	Integral of the learning window (derived)
$k_1 = 10^{-2}\,\mathrm{s}^{-1}$	Constant for the learning equation (derived)
$k_2 = -1.01 \cdot 10^{-2}\,\mathrm{s}^{-1}$	Constant for the learning equation (derived)
$k_3 = 1.24 \cdot 10^{-2}\,\mathrm{s}^{-1}$	Constant for the learning equation (derived)
$\Gamma = 2 \cdot 10^{-4}$	Range of the synaptic efficacies at the initial condition
$J_{\max} = 0.4$	Upper saturation boundary for the synaptic efficacies

Bibliography

Abbott LF, Blum KI (1996) Functional Significance of Long-Term Potentiation for Sequence Learning and Prediction. *Cerebral Cortex* 6:406–416.

Abbott LF, Nelson SB (2000) Synaptic plasticity: taming the beast. *Nat. Neurosci.* 3 Suppl:1178–1183.

Ahmed OJ, Mehta MR (2009) The hippocampal rate code: anatomy, physiology and theory. *Trends Neurosci.* 32:329–338.

Allen K, Fuchs EC, Jaschonek H, Bannerman DM, Monyer H (2011) Gap junctions between interneurons are required for normal spatial coding in the hippocampus and short-term spatial memory. *J Neurosci.* 31:6542–6552.

Allen TA, Morris AM, Mattfeld AT, Stark CEL, Fortin NJ (2014) A Sequence of Events Model of Episodic Memory Shows Parallels in Rats and Humans. *Hippocampus* 11:1–11.

Amaral D, Witter MP (1989) The three-dimensional organization of the hippocampal formation: A review of anatomical data. *Neuroscience* 31:571–591.

Anderson MI, Jeffery KJ (2003) Heterogeneous modulation of place cell firing by changes in context. *J. Neurosci.* 23:8827–8835.

Anderson P, Morris R, Amaral D, Bliss T, O'Keefe J (2007) *The Hippocampus Book.*

Baker JL, Olds JL (2007) Theta phase precession emerges from a hybrid computational model of a CA3 place cell. *Cogn Neurodyn* 1:237–248.

Bannerman DM, Sprengel R, Sanderson DJ, McHugh SB, Rawlins JNP, Monyer H, Seeburg PH (2014) Hippocampal synaptic plasticity, spatial memory and anxiety. *Nat. Rev. Neurosci.* 15:181–92.

Barry C, Bush D, O'Keefe J, Burgess N (2012) Models of grid cells and theta oscillations.

Bartos M, Vida I, Jonas P (2007) Synaptic mechanisms of synchronized gamma oscillations in inhibitory interneuron networks. *Nat. Rev. Neurosci.* 8:45–56.

Battaglia FP, Sutherland GR, McNaughton BL (2004) Local sensory cues and place cell directionality: additional evidence of prospective coding in the hippocampus. *J. Neurosci.* 24:4541–4550.

Belluscio MA, Mizuseki K, Schmidt R, Kempter R, Buzsaki G (2012) Cross-Frequency Phase-Phase Coupling between Theta and Gamma Oscillations in the Hippocampus. *J. Neurosci.* 32:423–435.

Benchenane K, Peyrache A, Khamassi M, Tierney PL, Gioanni Y, Battaglia FP, Wiener SI (2010) Coherent Theta Oscillations and Reorganization of Spike Timing in the Hippocampal- Prefrontal Network upon Learning. *Neuron* 66:921–936.

Bi G, Poo MM (1998) Synaptic modifications in cultured hippocampal neurons: Dependence on spike timing, synaptic strength, and postsynaptic cell type. *J. Neurosci.* 18:10464–10472.

Bieri KW, Bobbitt KN, Colgin LL (2014) Slow and Fast Gamma Rhythms Coordinate Different Spatial Coding Modes in Hippocampal Place Cells. *Neuron* 82:670–681.

Bland BH, Konopacki J, Dyck R (2005) Heterogeneity among hippocampal pyramidal neurons revealed by their relations to theta-band oscillation and synchrony. *Exp. Neurol.* 195:458–474.

Bliss TVP, Lomo T (1973) Long-lasting potentiation of synaptic transmission in the dentate area of the anaesthetized rabbit following stimulation of the preforant path. *J. Physiol.)* 232:331–356.

Boccara CN, Sargolini F, Thoresen VyH, Solstad T, Witter MP, Moser EI, Moser MB (2010) Grid cells in pre- and parasubiculum. *Nat. Neurosci.* 13:987–994.

Bose A., Booth V, Recce M (2000) A temporal mechanism for generating the phase precession of hippocampal place cells. *J. Comput. Neurosci.* 9:5–30.

Bostock E, Muller RU, Kubie JL (1991) Experience-dependent modifications of hippocampal place cell firing. *Hippocampus* 1:193–205.

Brandon M, Koenig J, Leutgeb J, Leutgeb S (2014) New and Distinct Hippocampal Place Codes Are Generated in a New Environment during Septal Inactivation. *Neuron* 82:789–796.

Brun VH, Otnaess M, Molden S, Steffenach HA, Witter M, Moser MB, Moser EI (2002) Place Cells and Place Recognition Mantained by Direct Entorhinal-Hippocampal Circuitry. *Science* 296:2243–2246.

Brun VH, Leutgeb S, Wu HQ, Schwarcz R, Witter MP, Moser EI, Moser MB (2008) Impaired Spatial Representation in CA1 after Lesion of Direct Input from Entorhinal Cortex. *Neuron* 57:290–302.

Bullock TH, Buzsaki G, McClune MC (1990) Coherence of compound field potentials reveals discontinuities in the CA1-subiculum of the hippocampus in freely-moving rats. *Neuroscience* 38:609–619.

Burgess CP, Burgess N (2014) Controlling phase noise in oscillatory interference models of grid cell firing. *J. Neurosci.* 34:6224–32.

Burgess N, Barry C, O'Keefe J (2007) An oscillatory interference model of grid cell firing. *Hippocampus* 17:801–812.

Burgess N, OKeefe J (2011) Models of place and grid cell firing and theta rhythmicity. *Curr. Opin. Neurobiol.* 21:734–744.

Buzsáki G (1989) Two-stage model of memory trace formation: A role for 'noisy' brain states. *Neuroscience* 31:551–570.

Buzsáki G (2002) Theta Oscillations in the Hippocampus. *Neuron* 33:325–340.

Buzsáki G, Draguhn A (2004) Neuronal oscillations in cortical networks. *Science* 304:1926–1929.

Buzsáki G (2005) Theta rhythm of navigation: link between path integration and landmark navigation, episodic and semantic memory. *Hippocampus* 15:827–40.

Buzsáki G (2010) Neural Syntax: Cell Assemblies, Synapsembles, and Readers. *Neuron* 68:362–385.

Buzsáki G, Wang XJ (2012) Mechanisms of Gamma Oscillations. *Annu. Rev. Neurosci.* 35:203–225.

Buzsáki G, Moser EI (2013) Memory, navigation and theta rhythm in the hippocampal-entorhinal system. *Nat. Neurosci.* 16:130–8.

Caporale N, Dan Y (2008) Spike timing-dependent plasticity: a Hebbian learning rule. *Annu. Rev. Neurosci.* 31:25–46.

Carr MF, Frank LM (2012) A single microcircuit with multiple functions: state dependent information processing in the hippocampus. *Curr. Opin. Neurobiol.* 22:704–708.

Castro L, Aguiar P (2012) Phase precession through acceleration of local theta rhythm: a biophysical model for the interaction between place cells and local inhibitory Neurons. *J Comp Neurosci* 33:141–150.

Cei A, Girardeau G, Drieu C, Kanbi KE, Zugaro M (2014) Reversed theta sequences of hippocampal cell assemblies during backward travel. *Nat. Neurosci.* 17:719–24.

Chance FS (2012) Hippocampal Phase Precession from Dual Input Components. *J. Neurosci.* 32:16693–16703.

Cheng S (2013) The CRISP theory of hippocampal function in episodic memory. *Frontiers in neural circuits* 7:88.

Cheng S, Frank LM (2008) New experiences enhance coordinated neural activity in the hippocampus. *Neuron* 57:303–13.

Cheng S, Frank LM (2011) The structure of networks that produce the transformation from grid cells to place cells. *Neuroscience* 197:293–306.

Climer JR, Newman EL, Hasselmo ME (2013) Phase coding by grid cells in unconstrained environments: two-dimensional phase precession. *Europ J Neurosci* 38:2526–2541.

Colgin L, T. Denninger, Fyhn, M, Hafting T et al. (2009) Frequency of gamma oscillations routes flow of information in the hippocampus. *Nature* 462:353–357.

Colgin LL (2013) Mechanisms and functions of theta rhythms. *Annu. Rev. Neurosci.* 36:295–312.

Couey JJ, Witoelar A, Zhang SJ, Zheng K, Ye J, Dunn B, Czajkowski R, Moser MB, Moser EI, Roudi Y, Witter MP (2013) Recurrent inhibitory circuitry as a mechanism for grid formation. *Nat. Neurosci.* 16:318–24.

Csicsvari J, Hirase H, Czurkó A, Mamiya A, Buzsáki G (1999) Oscillatory coupling of hippocampal pyramidal cells and interneurons in the behaving Rat. *J. Neurosci.* 19:274–287.

Csicsvari J, Hirase H, Mamiya A, Buzsáki G (2000) Ensemble patterns of hippocampal CA3-CA1 neurons during sharp wave-associated population events. *Neuron* 28:585–594.

Cutsuridis V, Hasselmo M (2012) GABAergic contributions to gating, timing, and phase precession of hippocampal neuronal activity during theta oscillations. *Hippocampus* 22:1597–1621.

Cutsuridis V, Graham B, Cobb S, Vida I (2010) *Hippocampal microcircuits* Springer.

Davidson TJ, Kloosterman F, Wilson MA (2009) Hippocampal Replay of Extended Experience. *Neuron* 63:497–507.

Dayan P, Abbott L (2001) *Theoretical Neuroscience* MIT Press.

de Almeida L, Idiart M, Lisman JE (2009) The input-output transformation of the hippocampal granule cells: from grid cells to place fields. *J. Neurosci.* 29:7504–7512.

Debanne D, Gähwiler BH, Thompson SM (1998) Long-term synaptic plasticity between pairs of individual CA3 pyramidal cells in rat hippocampal slice cultures. *J. Physiol.* 507:237–247.

Deng W, Aimone JB, Gage FH (2010) New neurons and new memories: how does adult hippocampal neurogenesis affect learning and memory? *Nat. Rev. Neurosci.* 11:339–350.

Diba K, Buzsáki G (2008) Hippocampal network dynamics constrain the time lag between pyramidal cells across modified environments. *J Neurosci.* 28:13448–56.

Diekelmann S, Born J (2010) The memory function of sleep. *Nat. Rev. Neurosci.* 11:114–126.

Dombeck D, Harvey C, Tian L, Looger LL, Tank D (2010) Functional imaging of hippocampal place cells at cellular resolution during virtual navigation. *Nat. Neurosci.* 13:1433–1440.

Domnisoru C, Kinkhabwala AA, Tank DW (2013) Membrane potential dynamics of grid cells. *Nature* 495:199–204.

Dragoi G, Harris KD, Buzsáki G (2003) Place representation within hippocampal networks is modified by long-term potentiation. *Neuron* 39:843–853.

Dragoi G, Buzsáki G (2006) Temporal Encoding of Place Sequences by Hippocampal Cell Assemblies. *Neuron* 50:145–157.

Drew LJ, Fusi S, Hen R (2013) Adult neurogenesis in the mammalian hippocampus: why the dentate gyrus? *Learning & memory* 20:710–29.

Dudchenko PA (2004) An overview of the tasks used to test working memory in rodents In *Neuroscience and Biobehavioral Reviews*, Vol. 28, pp. 699–709.

Eggink H, Mertens P, Storm E, Giocomo LM (2014) Hyperpolarization-activated cyclic nucleotide-gated 1 independent grid cell-phase precession in mice. *Hippocampus* 24:249–56.

Ego-Stengel V, Wilson M (2007) Spatial selectivity and phase precession in CA1 interneurons. *Hippocampus* 17:161–174.

Eichenbaum H (2004) Hippocampus: Cognitive processes and neural representations that underlie declarative memory. *Neuron* 44:109–120.

Eichenbaum H, Cohen NJ (2014) Perspective Can We Reconcile the Declarative Memory and Spatial Navigation Views on Hippocampal Function ? *Neuron* 83:764–770.

Ekstrom aD, Meltzer J, McNaughton BL, Barnes Ca (2001) NMDA receptor antagonism blocks experience-dependent expansion of hippocampal "place fields". *Neuron* 31:631–8.

Epsztein J, Brecht M, Lee A (2011) Intracellular Determinants of Hippocampal CA1 Place and Silent Cell Activity in a Novel Environment. *Neuron* 70:109–120.

Etienne AS, Jeffery KJ (2004) Path integration in mammals. *Hippocampus* 14:180–192.

Foster DJ, Wilson MA (2006) Reverse replay of behavioural sequences in hippocampal place cells during the awake state. *Nature* 440:680–683.

Foster DJ, Wilson MA (2007) Hippocampal theta sequences. *Hippocampus* 17:1093–1099.

Frank LM, Brown EN, Wilson MA (2001) A Comparison of the Firing Properties of Putative Excitatory and Inhibitory Neurons From CA1 and the Entorhinal Cortex. *J. Neurophysiol.* 86:2029–2040.

Geisler C, Robbe D, Zugaro M, Sirota A, Buzsaki G (2007) Hippocampal place cell assemblies are speed-controlled oscillators. *Proc. Natl. Acad. Sci. U. S. A.* 104:8149–8154.

Geisler C, Diba K, Pastalkova E, Mizuseki K, Royer S, Buzsaki G (2010) Temporal delays among place cells determine the frequency of population theta oscillations in the hippocampus. *Proc. Natl. Acad. Sci. U. S. A.* 107:7957–7962.

Gerstner W, Kempter R, van Hemmen JL, Wagner H (1996) A neuronal learning rule for sub-millisecond temporal coding. *Nature* 383:76–81.

Gerstner W, Abbott LF (1997) Learning navigational maps through potentiation and modulation of hippocampal place cells. *J. Comput. Neurosci.* 4:79–94.

Gerstner W, Ritz R, van Hemmen JL (1993) Why spikes? Hebbian learning and retrieval of time-resolved excitation patterns. *Biol. Cybern.* 69:503–515.

Gilbert PE, Kesner RP, Lee I (2001) Dissociating hippocampal subregions: A double dissociation between dentate gyrus and CA1. *Hippocampus* 11:626–636.

Giocomo LMM, Moser MB, Moser EI (2011) Computational Models of Grid Cells. *Neuron* 71:589–603.

Girardeau G, Benchenane K, Wiener SI, Buzsáki G, Zugaro MB (2009) Selective suppression of hippocampal ripples impairs spatial memory. *Nat. Neurosci.* 12:1222–1223.

Girardeau G, Zugaro M (2011) Hippocampal ripples and memory consolidation. *Curr. Opin. Neurobiol.* 21:452–459.

Gold JI, Shadlen MN (2007) The neural basis of decision making. *Annu. Rev. Neurosci.* 30:535–574.

Golding NL, Staff NP, Spruston N (2002) Dendritic spikes as a mechanism for cooperative long-term potentiation. *Nature* 418:326–331.

Grossberg S (1980) How does a brain build a cognitive code? *Psychol. Rev.* 87:1–51.

Gundlfinger A, Breustedt J, Sullivan D, Schmitz D (2010) Natural spike trains trigger short- and long lasting dynamics at hippocampal mossy fiber synapses in rodents. *PLoS ONE* 5.

Gupta AS, van der Meer MAA, Touretzky DS, Redish AD (2010) Hippocampal Replay Is Not a Simple Function of Experience. *Neuron* 65:695–705.

Gupta AS, van der Meer MAA, Touretzky DS, Redish AD (2012) Segmentation of spatial experience by hippocampal theta sequences. *Nat. Neurosci.* 15:1032–1039.

Hafting T, Fyhn M, Bonnevie T, Moser MB, Moser EI (2008) Hippocampus-independent phase precession in entorhinal grid cells. *Nature* 453:1248–1253.

Hafting T, Fyhn M, Molden S, Moser MB, Moser EI (2005) Microstructure of a spatial map in the entorhinal cortex. *Nature* 436:801–806.

Hampson RE, Deadwyler SA (1999) Cannabinoids, hippocampal function and memory. *Life Sci.* 65:715–723.

Hansel D, van Vreeswijk C (2012) The mechanism of orientation selectivity in primary visual cortex without a functional map. *J. Neurosci* 32:4049–4064.

Harris EW, Cotman CW (1986) Long-term potentiation of guinea pig mossy fiber responses is not blocked by N-methyl D-aspartate antagonists. *Neurosci. Lett.* 70:132–137.

Harris KD, Henze D, Hirase H, Leinekugel X, Dragoi G, Czurko A, Buzsaki G (2002) Spike train dynamics predicts theta-related phase precession in hippocampal pyramidal cells. *Nature* 417:738–741.

Harris KD, Csicsvari J, Hirase H, Dragoi G, Buzsáki G (2003) Organization of cell assemblies in the hippocampus. *Nature* 424:552–556.

Harvey C, Collman F, Dombeck D, Tank D (2009) Intracellular dynamics of hippocampal place cells during virtual navigation. *Nature* 461:941–946.

Hasselmo ME (1999) Neuromodulation: acetylcholine and memory consolidation. *Trends Cogn. Sci.* 3:351–359.

Hasselmo ME, Bodelón C, Wyble BP (2002) A proposed function for hippocampal theta rhythm: separate phases of encoding and retrieval enhance reversal of prior learning. *Neural Comput.* 14:793–817.

Hasselmo ME (2005) What is the function of hippocampal theta rhythm? - Linking behavioral data to phasic properties of field potential and unit recording data. *Hippocampus* 15:936–949.

Hasselmo ME (2008) Grid cell mechanisms and function: contributions of entorhinal persistent spiking and phase resetting. *Hippocampus* 18:1213–1229.

Hasselmo ME (2012) *How we remember: brain mechanisms of episodic memory* MIT Press.

Haykin S (2009) *Communication Systems* John Wiley & Sons, Inc.

Hebb DO (1949) The organization of behavior: a neuropsychological theory. *Science Education* 44:335.

Hetherington P, Shapiro M (1997) Hippocampal place fields are altered by the removal of single visual cues in a distance-dependent manner. *Behavioural Neuroscience* 111:20–34.

Hill AJ (1978) First occurrence of hippocampal spatial firing in a new environment. *Exp. Neurol.* 62:282–297.

Hopfield JJ (1982) Neural networks and physical systems with emergent collective computational abilities. *Proc. Natl. Acad. Sci. U. S. A.* 79:2554–2558.

Huerta PT, Lisman JE (1995) Bidirectional synaptic plasticity induced by a single burst during cholinergic theta oscillation in CA1 in vitro. *Neuron* 15:1053–1063.

Hunsaker MR, Kesner RP (2008) Evaluating the differential roles of the dorsal dentate gyrus, dorsal CA3, and dorsal CA1 during a temporal ordering for spatial locations task. *Hippocampus* 18:955–964.

Huxter J, Burgess N, O'Keefe J (2003) Independent rate and temporal coding in hippocampal pyramidal cells. *Nature* 425:828–832.

Hyman JM, Wyble BP, Goyal V, Rossi CA, Hasselmo ME (2003) Stimulation in hippocampal region CA1 in behaving rats yields long-term potentiation when delivered to the peak of theta and long-term depression when delivered to the trough. *J. Neurosci.* 23:11725–11731.

Isaac JTR, Buchanan KA, Muller RU, Mellor JR (2009) Hippocampal place cell firing patterns can induce long-term synaptic plasticity in vitro. *J. Neurosci.* 29:6840–6850.

Itskov V, Pastalkova E, Mizuseki K, Buzsaki G, Harris KD (2008) Theta-mediated dynamics of spatial information in hippocampus. *J. Neurosci.* 28:5959–5964.

Jackson J, Redish AD (2007) Network dynamics of hippocampal cell-assemblies resemble multiple spatial maps within single tasks. *Hippocampus* 17:1209–1229.

Jadhav SP, Kemere C, German PW, Frank LM (2012) Awake Hippocampal Sharp-Wave Ripples Support Spatial Memory. *Science* 336:1454–1458.

Jaramillo J, Schmidt R, Kempter R (2014) Modeling inheritance of phase precession in the hippocampal formation. *J. Neurosci.* 34:7715–31.

Jeewajee A, Barry C, O'Keefe J, Burgess N (2008) Grid cells and theta as oscillatory interference: Electrophysiological data from freely moving rats. *Hippocampus* 18:1175–1185.

Jeewajee A, Barry C, Douchamps V, Manson D, Lever C, Burgess N (2014) Theta phase precession of grid and place cell firing in open environments. *Philos. Trans. R Soc. Lond. B Biol. Sci.* 369:20120532.

Jensen O, Lisman JE (1996) Hippocampal CA3 region predicts memory sequences: Accounting for the phase precession of place cells. *Learning Memory* 3:279–287.

Jensen O, Lisman JE (2000) Position reconstruction from an ensemble of hippocampal place cells: Contribution of theta phase coding. *J. Neurophysiol.* 83:2602–2609.

Jezek K, Henriksen EJ, Treves A, Moser EI, Moser MB (2011) Theta-paced flickering between place-cell maps in the hippocampus. *Nature* 478:246–249.

Johnson A, Redish AD (2007) Neural ensembles in CA3 transiently encode paths forward of the animal at a decision point. *J. Neurosci.* 27:12176–12189.

Jones MW, Wilson MA (2005) Phase precession of medial prefrontal cortical activity relative to the hippocampal theta rhythm. *Hippocampus* 15:867–873.

Jung MW, McNaughton BL (1993) Spatial selectivity of unit activity in the hippocampal granular layer. *Hippocampus* 3:165–182.

Kajiwara R, Wouterlood FG, Sah A, Boekel AJ, Baks-Te Bulte LTG, Witter MP (2008) Convergence of entorhinal and CA3 inputs onto pyramidal neurons and interneurons in hippocampal area CA1 - An anatomical study in the rat. *Hippocampus* 18:266–280.

Kamondi A, Acsady L, Wang XJ, Buzsáki G (1998) Theta Oscillations in Somata and Dendrites of Hippocampal Pyramidal Cells In Vivo: Activity-Dependent Phase Precession of Action Potentials. *Hippocampus* 8:244–261.

Kandel ER (2001) The molecular biology of memory storage: a dialogue between genes and synapses. *Science* 294:1030–1038.

Kemp A, Manahan-Vaughan D (2007) Hippocampal long-term depression: master or minion in declarative memory processes? *Trends Neurosci.* 30:111–8.

Kempter R, Gerstner W, Van Hemmen JL, Wagner H (1998) Extracting Oscillations: Neuronal Coincidence Detection with Noisy Periodic Spike Input. *Neural Comput.* 10:1987–2017.

Kempter R, Gerstner W, Van Hemmen JL (1999) Hebbian learning and spiking neurons. *Phys. Rev. E* 59:4498–4514.

Kempter R, Leibold C, Buzsáki G, Diba K, Schmidt R (2012) Quantifying circular-linear associations: Hippocampal phase precession. *J. Neurosci. Methods* 207:113–124.

Kesner RP, Lee I, Gilbert P (2004) A behavioral assessment of hippocampal function based on a subregional analysis. *Rev. Neurosci.* 15:333–351.

Khamassi M, Humphries MD (2012) Integrating cortico-limbic-basal ganglia architectures for learning model-based and model-free navigation strategies. *Frontiers in behavioral neuroscience* 6:79.

Kim SM, Ganguli S, Frank LM (2012) Spatial Information Outflow from the Hippocampal Circuit: Distributed Spatial Coding and Phase Precession in the Subiculum. *J. Neurosci.* 32:11539–11558.

Kitamura T, Pignatelli M, Suh J, Kohara K, Yoshiki A, Abe K, Tonegawa S (2014) Island cells control temporal association memory. *Science* 343:896–901.

Kjelstrup KB, Solstad T, Brun VH, Hafting T, Leutgeb S, Witter MP, Moser EI, Moser MB (2008) Finite scale of spatial representation in the hippocampus. *Science* 321:140–143.

Klausberger T, Magill PJ, Marton LF, Roberts JDB, Cobden PM, Buzsáki G, Somogyi P (2003) Brain-state- and cell-type-specific firing of hippocampal interneurons in vivo. *Nature* 421:844–848.

Kocsis B, Bragin A, Buzsáki G (1999) Interdependence of multiple theta generators in the hippocampus: a partial coherence analysis. *J. Neurosci* 19:6200–6212.

Korotkova T, Fuchs EC, Ponomarenko A, von Engelhardt J, Monyer H (2010) NMDA receptor ablation on parvalbumin-positive interneurons impairs hippocampal synchrony, spatial representations, and working memory. *Neuron* 68:557–69.

Kramis R, Vanderwolf CH, Bland BH (1975) Two types of hippocampal rhythmical slow activity in both the rabbit and the rat: relations to behavior and effects of atropine, diethyl ether, urethane, and pentobarbital. *Exp. Neurol.* 49:58–85.

Lansink CS, Goltstein PM, Lankelma JV, McNaughton BL, Pennartz CMA (2009) Hippocampus leads ventral striatum in replay of place-reward information. *PLoS Biol.* 7.

Lapray D, Lasztoczi B, Lagler M, Viney T, Katona L, Valenti O, Hartwich K, Borhegyi Z, Somogyi P, Klausberger. T (2012) Behavior-dependent specialization of identified hippocampal interneurons. *Nat. Neurosci.* 15:1265–1271.

Lavenex P, Amaral DG (2000) Hippocampal-neocortical interaction: A hierarchy of associativity. *Hippocampus* 10:420–430.

Lee AK, Manns ID, Sakmann B, Brecht M (2006) Whole-Cell Recordings in Freely Moving Rats. *Neuron* 51:399–407.

Lee D, Lin BJ, Lee AK (2012) Hippocampal place fields emerge upon single-cell manipulation of excitability during behavior. *Science* 337:849–53.

Lee I, Kesner RP (2002) Differential contribution of NMDA receptors in hippocampal subregions to spatial working memory. *Nat. Neurosci.* 5:162–168.

Lee I, Rao G, Knierim JJ (2004) A Double Dissociation between Hippocampal Subfields: Differential Time Course of CA3 and CA1 Place Cells for Processing Changed Environments. *Neuron* 42:803–815.

Leibold C, Gundlfinger A, Schmidt R, Thurley K, Schmitz D, Kempter R (2008) Temporal compression mediated by short-term synaptic plasticity. *Proc. Natl. Acad. Sci. U. S. A.* 105:4417–4422.

Lenck-Santini PP, Holmes GL (2008) Altered phase precession and compression of temporal sequences by place cells in epileptic rats. *J. Neurosci.* 28:5053–5062.

Lengyel M, Szatmary Z, Erdi P (2003) Dynamically Detuned Oscillations Account for the Coupled Rate and Temporal Code of Place Cell Firing. *Hippocampus* 13:700–714.

Lengyel M, Huhn Z, Erdi P (2005) Computational theories on the function of theta oscillations. *Biol. Cybern.* 92:393–408.

Leung LS (2011) A model of intracellular theta phase precession dependent on intrinsic subthreshold membrane currents. *J. Neurosci.* 31:12282–12296.

Leutgeb JK, Leutgeb S, Moser MB, Moser EI (2007) Pattern separation in the dentate gyrus and CA3 of the hippocampus. *Science* 315:961–966.

Leutgeb S, Leutgeb JK, Barnes CA, Moser EI, McNaughton, B.L. Moser MB (2005) Independent codes for spatial and episodic memory in hippocampal neuronal ensembles. *Science* 309:619–623.

Lever C, Wills T, Cacucci F, Burgess N, O'Keefe J (2002) Long-term plasticity in hippocampal place-cell representation of environmental geometry. *Nature* 416:90–94.

Levy WB, Steward O (1983) Temporal contiguity requirements for long-term associative potentiation/depression in the hippocampus. *Neuroscience* 8:791–797.

Levy WB (1996) A sequence predicting CA3 is a flexible associator that learns and uses context to solve hippocampal-like tasks. *Hippocampus* 6:579–590.

Li XG, Somogyi P, Ylinen A, Buzsáki G (1994) The hippocampal CA3 network: An in vivo intracellular labeling study. *J. Comp. Neurol.* 339:181–208.

Lisman J, Redish AD (2009) Prediction, sequences and the hippocampus. *Philosophical Transactions of the Royal Society B: Biological Sciences* 364:1193–1201.

Lisman JE, Jensen O (2013) The Theta-Gamma Neural Code. *Neuron* 77:1002–1016.

Lynch MA (2004) Long-Term Potentiation and Memory *Physiol. Rev.* 84:87–136.

MacDonald CJ, Lepage KQ, Eden UT, Eichenbaum H (2011) Hippocampal "time cells" bridge the gap in memory for discontiguous events. *Neuron* 71:737–49.

Magee JC, Cook EP (2000) Somatic EPSP amplitude is independent of synapse location in hippocampal pyramidal neurons. *Nat. Neurosci.* 3:895–903.

Magee JC (2001) Dendritic Mechanisms of Phase Precession in Hippocampal CA1 Pyramidal Neurons. *J. Neurophysiol.* 86:528–532.

Maguire EA, Gadian DG, Johnsrude IS, Good CD, Ashburner J, Frackowiak RS, Frith CD (2000) Navigation-related structural change in the hippocampi of taxi drivers. *Proc. Natl. Acad. Sci. U. S. A.* 97:4398–4403.

Maguire EA, Hassabis D (2011) Role of the hippocampus in imagination and future thinking. *Proc. Natl. Acad. Sci. U. S. A.* 108:E39.

Maier N, Güldenagel M, Söhl G, Siegmund H, Willecke K, Draguhn A (2002) Reduction of high-frequency network oscillations (ripples) and pathological network discharges in hippocampal slices from connexin 36-deficient mice. *J. Physiol.* 541:521–528.

Maier N, Morris G, Schuchmann S, Korotkova T, Ponomarenko A, Böhm C, Wozny C, Schmitz D (2012) Cannabinoids disrupt hippocampal sharp wave-ripples via inhibition of glutamate release. *Hippocampus* 22:1350–62.

Maier N, Nimmrich V, Draguhn A (2003) Cellular and network mechanisms underlying spontaneous sharp wave-ripple complexes in mouse hippocampal slices. *J. Physiol.* 550:873–887.

Malhotra S, Cross RWA, van der Meer MAA (2012) Theta phase precession beyond the hippocampus. *Rev. Neurosci.* 23:39–65.

Markram H, Liibke J, Frotscher M, Sakmann B (1997) Regulation of synaptic efficacy by coincidence of postsynaptic APs and EPSPs. *Science* 275:213–215.

Marr D (1971) Simple memory: a theory for archicortex. *Philos. Trans. R. Soc. Lond. B. Biol. Sci.* 262:23–81.

Martin SJ, Grimwood PD, Morris RG (2000) Synaptic plasticity and memory: an evaluation of the hypothesis. *Annu. Rev. Neurosci.* 23:649–711.

Maurer AP, Cowen SL, Burke SN, Barnes CA, McNaughton BL (2006) Organization of hippocampal cell assemblies based on theta phase precession. *Hippocampus* 16:785–794.

Maurer AP, Cowen SL, Burke SN, Barnes CA, McNaughton BL (2006b) Phase precession in hippocampal interneurons showing strong functional coupling to individual pyramidal cells. *J. Neurosci.* 26:13485–13492.

Maurer A, McNaughton B (2007) Network and intrinsic cellular mechanisms underlying theta phase precession of hippocampal neurons. *Trends Neurosci.* 30:325–333.

Maurer AP, Burke SN, Lipa P, Skaggs WE, Barnes CA (2012) Greater running speeds result in altered hippocampal phase sequence dynamics. *Hippocampus* 22:737–47.

Maviel T, Durkin TP, Menzaghi F, Bontempi B (2004) Sites of neocortical reorganization critical for remote spatial memory. *Science* 305:96–99.

McClelland JL, McNaughton BL, O'Reilly RC (1995) Why there are complementary learning systems in the hippocampus and neocortex: insights from the successes and failures of connectionist models of learning and memory. *Psychol. Rev.* 102:419–457.

McHugh TJ, Blum KI, Tsien JZ, Tonegawa S, Wilson MA (1996) Impaired hippocampal representation of space in CA1-specific NMDAR1 knockout mice. *Cell* 87:1339–1349.

McLelland D, Paulsen O (2009) Neuronal oscillations and the rate-to-phase transform: mechanism, model and mutual information. *J. Physiol.* 587:769–85.

McNaughton B, Morris R (1987) Hippocampal synaptic enhancement and information storage within a distributed memory system. *Trends Neurosci.* 10:408–415.

McNaughton BL, Battaglia FP, Jensen O, Moser EI, Moser MB (2006) Path integration and the neural basis of the 'cognitive map'. *Nature* 7:663–678.

Megias M, Emri Z, Freund TF, Gulyas AI (2001) Total number and distribution of inhibitory and excitatory synapses on hippocampal CA1 pyramidal cells. *Neuroscience* 102:527–540.

Mehta M, Barnes CA, McNaughton BL (1997) Experience-dependent, asymmetric expansion of hippocampal place fields. *Proc. Natl. Acad. Sci. U. S. A.* 94:8918–8921.

Mehta M, Quirk M, Wilson M (2000) Experience-dependent asymmetric shape of hippocampal receptive fields. *Neuron* 25:707–715.

Mehta M, Lee A, Wilson M (2002) Role of experience and oscillations in transforming a rate code into a temporal code. *Nature* 417:741–746.

Melamed O, Gerstner W, Maass W, Tsodyks M, Markram H, Mehta MR, Lee AK, Wilson MA (2004) Coding and learning of behavioral sequences. *Trends Neurosci.* 27:11–15.

Mistry R, Dennis S, Frerking M, Mellor JR (2011) Dentate gyrus granule cell firing patterns can induce mossy fiber long-term potentiation in vitro. *Hippocampus* 21:1157–1168.

Mizuseki K, Sirota A, Pastalkova E, Buzsaki G (2009) Theta Oscillations Provide Temporal Windows for Local Circuit Computation in the Entorhinal-Hippocampal Loop. *Neuron* 64:267–280.

Mizuseki K, Royer S., Diba K., G. B (2012) Activity dynamics and behavioral correlates of CA3 and CA1 hippocampal pyramidal neurons. *Hippocampus* 22:1659–1680.

Moita MAP, Rosis S, Zhou Y, LeDoux JE, Blair HT (2004) Putting fear in its place: remapping of hippocampal place cells during fear conditioning. *J. Neurosci* 24:7015–7023.

Molter C, Yamaguchi Y (2008) Entorhinal theta phase precession sculpts dentate gyrus place fields. *Hippocampus* 18:919–930.

Montgomery SM, Betancur MI, Buzsáki G (2009) Behavior-dependent coordination of multiple theta dipoles in the hippocampus. *J. Neurosci.* 29:1381–1394.

Montgomery SM, Buzsáki G (2007) Gamma oscillations dynamically couple hippocampal CA3 and CA1 regions during memory task performance. *Proc. Natl. Acad. Sci. U. S. A.* 104:14495–14500.

Morris RG, Garrud P, Rawlins JN, O'Keefe J (1982) Place navigation impaired in rats with hippocampal lesions. *Nature* 297:681–683.

Morris R (1984) Developments of a water-maze procedure for studying spatial learning in the rat. *J. Neurosci. Methods* 11:47–60.

Morris RGR, Anderson E, Lynch GSG, Baudry M, Anderson A, Baudry B (1986) Selective impairment of learning and blockade of long term potentiation by an N-methyl-D-aspartate receptor antagonist, APV-5. *Nature* 319:774–776.

Moser E, Moser MB, Andersen P (1993) Synaptic potentiation in the rat dentate gyrus during exploratory learning. *Neuroreport* 5:317–320.

Moser EI, Kropff E, Moser MB (2008) Place cells, grid cells, and the brain's spatial representation system. *Annu. Rev. Neurosci.* 31:69–89.

Müller RU, Kubie JL (1987) The effects of changes in the environment on the spatial firing of hippocampal complex-spike cells. *J. Neurosci.* 7:1951–1968.

Müller RU (1996) A quarter of a century of place cells. *Neuron* 17:813–22.

Müller RU, Stead M, Pach J (1996) The hippocampus as a cognitive graph. *The Journal of general physiology* 107:663–694.

Murray EA (2007) The amygdala, reward and emotion. *Trends Cogn. Sci.* 11:489–497.

Nabavi S, Fox R, Proulx CD, Lin JY, Tsien RY, Malinow R (2014) Engineering a memory with LTD and LTP. *Nature* 511:348–352.

Nakashiba T, Young JZ, McHugh TJ, Buhl DL, Tonegawa S (2008) Transgenic inhibition of synaptic transmission reveals role of CA3 output in hippocampal learning. *Science* 319:1260–1264.

Nakazawa K, Sun L, Quirk M, Rondi-Reig L, Wilson MA, Tonegawa S (2003) Hippocampal CA3 NMDA receptors are crucial for memory acquisition of one-time experience. *Neuron* 38:305–315.

Nakazawa K, McHugh TJ, Wilson MA, Tonegawa S (2004) NMDA receptors, place cells and hippocampal spatial memory. *Nat. Rev. Neurosci.* 5:361–372.

Nakazawa K, Quirk MC, Chitwood Ra, Watanabe M, Yeckel MF, Sun LD, Kato A, Carr Ca, Johnston D, Wilson MA, Tonegawa S (2002) Requirement for hippocampal CA3 NMDA receptors in associative memory recall. *Science* 297:211–218.

Navratilova Z, Giocomo LM, Fellous JM, Hasselmo ME, McNaughton BL (2012) Phase precession and variable spatial scaling in a periodic attractor map model of medial entorhinal grid cells with realistic after-spike dynamics. *Hippocampus* 22:772–789.

Neunuebel JP, Knierim JJ (2014) CA3 retrieves coherent representations from degraded input: Direct evidence for CA3 pattern completion and dentate gyrus pattern separation. *Neuron* 81:416–427.

Nimmrich V, Maier N, Schmitz D, Draguhn A (2005) Induced sharp wave-ripple complexes in the absence of synaptic inhibition in mouse hippocampal slices. *J. Physiol.* 563:663–670.

Niv Y, Joel D, Dayan P (2006) A normative perspective on motivation. *Trends Cogn. Sci.* 10:375–381.

Nunn JA, Graydon FJX, Polkey CE, Morris RG (1999) Differential spatial memory impairment after right temporal lobectomy demonstrated using temporal titration. *Brain* 122:47–59.

O'Keefe J, Dostrovsky J (1971) The hippocampus as a spatial map. Preliminary evidence from unit activity in the freely-moving rat. *Brain Res.* 34:171–175.

O'Keefe J, Nadel L (1978) *The hippocampus as a cognitive map* Oxford: Clarendon Press.

O'Keefe J, Recce ML (1993) Phase relationship between hippocampal place units and the EEG theta rhythm. *Hippocampus* 3:317–330.

O'Keefe J, Burgess N (2005) Dual phase and rate coding in hippocampal place cells: Theoretical significance and relationship to entorhinal grid cells. *Hippocampus* 15:853–866.

O'Mara S (2005) The subiculum: What it does, what it might do, and what neuroanatomy has yet to tell us. *J. Anatomy* 207:271–282.

O'Neill J, Senior T, Csicsvari J (2006) Place-selective firing of CA1 pyramidal cells during sharp wave/ripple network patterns in exploratory behavior. *Neuron* 49:143–155.

Pastalkova E, Itskov Vladimir, Amarasingham Asohan, Buzsaki Gyorgy B (2008) Internally Generated Cell Assembly Sequences in the Rat Hippocampus. *Science* 321:1322–1327.

Pastoll H, Solanka L, van Rossum MCW, Nolan MF (2013) Feedback inhibition enables θ-nested γ oscillations and grid firing fields. *Neuron* 77:141–54.

Petsche H, Stumpf C, Gogolak G (1962) The significance of the rabbit's septum as a relay station between the midbrain and the hippocampus. I. The control of hippocampus arousal activity by the septum cells. *Electroencephalogr. Clin. Neurophysiol.* 14:202–211.

Peyrache A, Khamassi M, Benchenane K, Wiener SI, Battaglia FP (2009) Replay of rule-learning related neural patterns in the prefrontal cortex during sleep. *Nat. Neurosci.* 12:919–926.

Pinsky PF, Rinzel J (1994) Intrinsic and network rhythmogenesis in a reduced traub model for CA3 neurons. *J. Comput. Neurosci.* 1:39–60.

Pitkänen A, Pikkarainen M, Nurminen N, Ylinen A (2000) Reciprocal connections between the amygdala and the hippocampal formation, perirhinal cortex, and postrhinal cortex in rat. A review. *Ann. N. Y. Acad. Sci.* 911:369–391.

Purves D, Augustine G, Fitzpatrick D, et al. (2001) Neuroscience. *Sunderland (MA): Sinauer Associates* .

Ranganathan M, D'Souza DC (2006) The acute effects of cannabinoids on memory in humans: A review. *Psychopharmacology* 188:425–444.

Rasch B, Büchel C, Gais S, Born J (2007) Odor cues during slow-wave sleep prompt declarative memory consolidation. *Science* 315:1426–1429.

Rasch B, Born J (2013) About sleep's role in memory. *Physiol. Rev.* 93:681–766.

Ravassard P, Kees A, Willers B, Ho D, Aharoni D, Cushman J, Aghajan ZM, Mehta MR (2013) Multisensory control of hippocampal spatiotemporal selectivity. *Science* 340:1342–6.

Ray S, Naumann R, Burgalossi A, Tang Q, Schmidt H, Brecht M (2014) Grid-layout and theta-modulation of layer 2 pyramidal neurons in medial entorhinal cortex. *Science* 343:891–6.

Redish AD (1999) *Beyond the cognitive map:* MIT Press.

Redish AD, Battaglia FP, Chawla MK, Ekstrom AD, Gerrard JL, Lipa P, E.S. R, Worley PF, Guzowski JF, McNaughton BL, Barnes CA (2001) Independence of firing correlates of anatomically proximate hippocampal pyramidal cells. *J. Neurosci.* 21:RC134.

Reifenstein ET, Kempter R, Schreiber S, Stemmler MB, Herz AVM (2012) Grid cells in rat entorhinal cortex encode physical space with independent firing fields and phase precession at the single-trial level. *Proc. Natl. Acad. Sci. U. S. A.* 109:6301–6306.

Reifenstein ET, Kempter R, Schreiber S, Stemmler MB, Herz AVM (2013) Single-Trial phase precession analysis in 2-d environments In *Cosyne2013 Abstract*.

Reifenstein ET, Stemmler M, Herz AVM, Kempter R, Schreiber S (2014) Movement dependence and layer specificity of entorhinal phase precession in two-dimensional environments. *PLoS ONE* 9.

Remme MWH, Lengyel M, Gutkin BS (2010) Democracy-independence trade-off in oscillating dendrites and its implications for grid cells. *Neuron* 66:429–437.

Remy S, Spruston N (2007) Dendritic spikes induce single-burst long-term potentiation. *Proc. Natl. Acad. Sci. U. S. A.* 104:17192–17197.

Richter-Levin G, Canevari L, Bliss TVP (1995) Long-term potentiation and glutamate release in the dentate gyrus: Links to spatial learning. *Behav. Brain Res.* 66:37–40.

Robbe D, Montgomery SM, Thome A, Rueda-Orozco PE, McNaughton BL, Buzsaki G (2006) Cannabinoids reveal importance of spike timing coordination in hippocampal function. *Nat. Neurosci.* 9:1526–33.

Robbe D, Buzsaki G (2009) Alteration of theta timescale dynamics of hippocampal place cells by a cannabinoid is associated with memory impairment. *J. Neurosci.* 29:12597–12605.

Rolls ET (1987) Information representation, processing and storage in the brain: analysis at the single neuron level. *The neural and molecular bases of learning* pp. 503–540.

Rolls ET, Kesner RP (2006) A computational theory of hippocampal function, and empirical tests of the theory. *Prog. Neurobiol.* 79:1–48.

Rolls ET, Stringer SM, Elliot T (2006) Entorhinal cortex grid cells can map to hippocampal place cells by competitive learning. *Network (Bristol)* 17:447–465.

Rolls E (2013) The mechanisms for pattern completion and pattern separation in the hippocampus. *Front. Syst. Neurosci.* 7:74.

Royer S, Zemelman B, Losonczy A, Kim J, Chance F, Magee J, Buzsaki G (2012) Control of timing, rates and bursts of hippocampal place cells by dendritic and somatic inhibition. *Nat. Neurosci.* 15:769–775.

Rudoy JD, Voss JL, Westerberg CE, Paller KA (2009) Strengthening individual memories by reactivating them during sleep. *Science* 326:1079.

Sadowski JHLP, Jones MW, Mellor JR (2011) Ripples make waves: binding structured activity and plasticity in hippocampal networks. *Neural Plast.* 2011:960389.

Sakimura K, Kutsuwada T, Ito I, Manabe T, Takayama C, Kushiya E, Yagi T, Aizawa S, Inoue Y, Sugiyama H (1995) Reduced hippocampal LTP and spatial learning in mice lacking NMDA receptor epsilon 1 subunit. *Nature* 373:151–155.

Sakmann B, Neher E (1984) Patch clamp techniques for studying ionic channels in excitable membranes. *Annu. Rev. Physiol.* 46:455–472.

Samsonovich A, McNaughton BL (1997) Path integration and cognitive mapping in a continuous attractor neural network model. *J. Neurosc.* 17:5900–5920.

Sargolini F, Fyhn M, Hafting T, McNaughton BL, Witter MP, Moser MB, Moser EI (2006) Conjunctive representation of position, direction, and velocity in entorhinal cortex. *Science* 312:758–762.

Savelli F, Knierim JJ (2010) Hebbian analysis of the transformation of medial entorhinal grid-cell inputs to hippocampal place fields. *J. Neurophysiol.* 103:3167–3183.

Schlesiger CC, Cannova EA, Mankin BB, Boublil JB, Hales JK, Leutgeb S, Leibold C (2013) The medial entorhinal cortex is required for hippocampal phase precession. *Society for Neuroscience (Abstract)* .

Schmidt R, Diba K, Leibold C, Schmitz D, Buzsaki G, Kempter R (2009) Single-Trial Phase Precession in the Hippocampus. *J. Neurosci.* 29(42):13232–13241.

Schmidt-Hieber C, Häusser M (2013) Cellular mechanisms of spatial navigation in the medial entorhinal cortex. *Nat. Neurosci.* 16:325–331.

Scoville WB, Milner B (1957) Loss of recent memory after bilateral hippocampal lesions. *Journal of neurology, neurosurgery, and psychiatry* 20:11–21.

Sederberg PB, Kahana MJ, Howard MW, Donner EJ, Madsen JR (2003) Theta and gamma oscillations during encoding predict subsequent recall. *J. Neurosci.* 23:10809–14.

Senior TJ, Huxter JR, Allen K, O'Neill J, Csicsvari J (2008) Gamma oscillatory firing reveals distinct populations of pyramidal cells in the CA1 region of the hippocampus. *J. Neurosci.* 28:2274–86.

Shapiro ML, Eichenbaum H (1999) Hippocampus as a memory map: Synaptic plasticity and memory encoding by hippocampal neurons. *Hippocampus* 9:365–384.

Shen J, Barnes CA, McNaughton BL, Skaggs WE, Weaver KL (1997) The effect of aging on experience-dependent plasticity of hippocampal place cells. *J. Neurosci.* 17:6769–6782.

Siapas AG, Lubenov EV, Wilson MA (2005) Prefrontal phase locking to hippocampal theta oscillations. *Neuron* 46:141–151.

Singer W (1993) Synchronization of cortical activity and its putative role in information processing and learning. *Annu. Rev. Physiol.* 55:349–374.

Sjöström PJ, Turrigiano GG, Nelson SB (2001) Rate, timing, and cooperativity jointly determine cortical synaptic plasticity. *Neuron* 32:1149–1164.

Sjöström PJ, Rancz EA, Roth A, Häusser M (2008) Dendritic excitability and synaptic plasticity. *Physiol. Rev.* 88:769–840.

Skaggs WE, McNaughton BL (1996) Replay of neuronal firing sequences in rat hippocampus during sleep following spatial experience. *Science* 271:1870–1873.

Skaggs WE, McNaughton BL, Wilson MA, Barnes CA (1996) Theta phase precession in hippocampal neuronal populations and the compression of temporal sequences. *Hippocampus* 6:149–172.

Solstad T, Moser EI, Einevoll GT (2006) From grid cells to place cells: A mathematical model. *Hippocampus* 16:1026–1032.

Solstad T, Boccara CN, Kropff E, Moser MB, Moser EI (2008) Representation of geometric borders in the entorhinal cortex. *Science* 322:1865–1868.

Song S, Miller KD, Abbott LF (2000) Competitive Hebbian learning through spike-timing-dependent synaptic plasticity. *Nat. Neurosci.* 3:919–926.

Song S, Abbott LF (2001) Cortical development and remapping through spike timing-dependent plasticity. *Neuron* 32:339–350.

Spiers HJ, Maguire EA, Burgess N (2001) Hippocampal amnesia. *Neurocase : case studies in neuropsychology, neuropsychiatry, and behavioural neurology* 7:357–382.

Squire LR (1992) Memory and the hippocampus: a synthesis from findings with rats, monkeys, and humans. *Psychol. Rev.* 99:195–231.

Squire LR, Stark CEL, Clark RE (2004) The medial temporal lobe. *Annu. Rev. Neurosci.* 27:279–306.

Squire LR, Wixted JT (2011) The cognitive neuroscience of human memory since H.M. *Annu. Rev. Neurosci.* 34:259–288.

Stark E, Roux L, Eichler R, Senzai Y, Royer S, Buzsáki G (2014) Pyramidal cell-interneuron interactions underlie hippocampal ripple oscillations. *Neuron* 83:467–480.

Stensola H, Stensola T, Solstad T, Frø land K, Moser MB, Moser EI (2012) The entorhinal grid map is discretized. *Nature* 492:72–8.

Suh J, Rivest AJ, Nakashiba T, Tominaga T, Tonegawa S (2011) Entorhinal Cortex Layer III Input to the Hippocampus Is Crucial for Temporal Association Memory. *Science* 334:1415–1420.

Takahashi M, Nishida H, David Redish A, Lauwereyns J (2014) Theta phase shift in spike timing and modulation of gamma oscillation: a dynamic code for spatial alternation during fixation in rat hippocampal area CA1. *J. Neurophysiol.* 111:1601–14.

Taube JS, Muller RU, Ranck JB (1990) Head-direction cells recorded from the postsubiculum in freely moving rats. II. Effects of environmental manipulations. *J. Neurosci.* 10:436–447.

Terrazas A, Krause M, Lipa P, Gothard KM, Barnes CA, McNaughton BL (2005) Self-Motion and the Hippocampal Spatial Metric. *J. Neurosci.* 25:8085–8096.

Teyler TJ, Rudy JW (2007) The hippocampal indexing theory and episodic memory: Updating the index. *Hippocampus* 17:1158–1169.

Thurley K, Leibold C, Gundlfinger A, Schmitz D, Kempter R (2008) Phase Precession Through Synaptic Facilitation. *Neural Comput.* 20:1285–1324.

Thurley K, Hellmundt F, Leibold C (2013) Phase precession of grid cells in a network model without external pacemaker. *Hippocampus* 23:786–796.

Tolman EC (1948) Cognitive maps in rats and men. *Psychol. Rev.* 55:189–208.

Tort ABL, Komorowski RW, Manns JR, Kopell NJ, Eichenbaum H (2009) Theta-gamma coupling increases during the learning of item-context associations. *Proc. Natl. Acad. Sci. U. S. A.* 106:20942–20947.

Tsodyks M, Sejnowski T (1995) Associative memory and hippocampal place cells. *Int. J. Neural Syst.* 6:81–86.

Tsodyks M, Skaggs W, TJ S, McNaughton BL (1996) Population dynamics and theta rhythm phase precession of hippocampal place cell firing: A spiking neuron model. *Hippocampus* 6:271–280.

Tsodyks MV, Markram H (1997) The neural code between neocortical pyramidal neurons depends on neurotransmitter release probability. *Proc. Natl. Acad. Sci. U. S. A.* 94:719–723.

Tulving E (1972) Episodic and semantic memory. *Organization of Memory* pp. 381–403.

Tulving E (2000) Concepts of memory. *The Oxford handbook of memory Tulving Endel Ed* pp. 33–43.

Tulving E (2002) Episodic memory: From mind to brain. *Annu. Rev. Psychol.* 53:1–25.

Turrigiano GG, Nelson SB (2000) Hebb and homeostasis in neuronal plasticity. *Curr. Opin. Neurobiol.* 10:358–364.

van der Meer MAA, Redish AD (2009) Covert expectation-of-reward in rat ventral striatum at decision points. *Frontiers in integrative neuroscience* 3:1.

van der Meer MAA, Johnson A, Schmitzer-Torbert NC, Redish AD (2010) Triple dissociation of information processing in dorsal striatum, ventral striatum, and hippocampus on a learned spatial decision task. *Neuron* 67:25–32.

van der Meer MAA, Redish AD (2011) Theta phase precession in Rat Ventral Striatum links place and reward information. *J. Neurosci.* 31(8):2843–2854.

van der Meer MAA, Kurth-Nelson Z, Redish AD (2012) Information processing in decision-making systems. *The neuroscientist* 18:342–359.

Vanderwolf CH (1969) Hippocampal electrical activity and voluntary movement in the rat. *Electroencephalogr. Clin. Neurophysiol.* 26:407–418.

Varga C, Golshani P, Soltesz I (2012) Frequency-invariant temporal ordering of interneuronal discharges during hippocampal oscillations in awake mice. *Proc. Natl. Acad. Sci. U. S. A.* 109:2726–2734.

Vida I, Halasy K, Szinyei C, Somogyi P, Buhl EH (1998) Unitary IPSPs evoked by interneurons at the stratum radiatum-stratum lacunosum-moleculare border in the CA1 area of the rat hippocampus in vitro. *J. Physiol.* 506:755–773.

Wagatsuma H, Yamaguchi Y (2007) Neural dynamics of the cognitive map in the hippocampus. *Cognitive Neurodynamics* 1:119–141.

Wallenstein G, Hasselmo M (1997) GABAergic modulation of hippocampal population activity: Sequence learning, place field development, and the phase precession effect. *J. Neurophysiol.* 78:393–408.

Wang ME, Wann EG, Yuan RK, Ramos Álvarez MM, Stead SM, Muzzio Ia (2012) Long-term stabilization of place cell remapping produced by a fearful experience. *J. Neurosci.* 32:15802–14.

Wang XJ (2010) Neurophysiological and computational principles of cortical rhythms in cognition. *Physiol. Rev.* 90:1195–1268.

Weiss C, Bouwmeester H, Power JM, Disterhoft JF (1999) Hippocampal lesions prevent trace eyeblink conditioning in the freely moving rat. *Behav. Brain Res.* 99:123–132.

Whittington M, Traub R, Kopell N, Ermentrout B, Buhl E (2000) Inhibition-based rhythms: experimental and mathematical observations on network dynamics. *Int J Psychophysiol* 38:315–336.

Wierzynski CM, Lubenov EV, Gu M, Siapas AG (2009) State-Dependent Spike-Timing Relationships between Hippocampal and Prefrontal Circuits during Sleep. *Neuron* 61:587–596.

Wilent WB, Nitz DA (2007) Discrete place fields of hippocampal formation interneurons. *J. Neurophysiol.* 97:4152–4161.

Wills TJ, Lever C, Cacucci F, Burgess N, O'Keefe J (2005) Attractor dynamics in the hippocampal representation of the local environment. *Science* 308:873–876.

Wilson MA, McNaughton BL (1993) Dynamics of the hippocampal ensemble code for space. *Science* 261:1055–1058.

Wilson MA, McNaughton BL (1994) Reactivation of hippocampal ensemble memories during sleep. *Science* 265:676–679.

Wittenberg GM, Wang SSH (2006) Malleability of spike-timing-dependent plasticity at the CA3-CA1 synapse. *J. Neurosci.* 26:6610–6617.

Wu Z, Yamaguchi Y (2010) Independence of the unimodal tuning of firing rate from theta phase precession in hippocampal place cells. *Biol. Cybern.* 102:95–107.

Yamaguchi Y, McNaughton B (1998) Non-linear dynamics generating theta phase precession in hippocampal closed circuit and generation of episodic memory In *Proceedings of the fifth international conference on neural information processing.*

Yamaguchi Y (2003) A theory of hippocampal memory based on theta phase precession. *Biol. Cybern.* 89:1–9.

Yamaguchi Y, Sato N, Wagatsuma H, Wu Z, Molter C, Aota Y (2007) A unified view of theta phase coding in the entorhinal hippocampal system. *Curr. Opin. Neurobiol.* 17:197–204.

Ylinen A, Bragin A, Nádasdy Z, Jandó G, Szabó I, Sik A, Buzsáki G (1995) Sharp wave-associated high-frequency oscillation (200 Hz) in the intact hippocampus: network and intracellular mechanisms. *J. Neurosci.* 15:30–46.

Zhang SJ, Ye J, Miao C, Tsao A, Cerniauskas I, Ledergerber D, Moser MB, Moser EI (2013) Optogenetic dissection of entorhinal-hippocampal functional connectivity. *Science* 340:1232627.

Zilli EA, Yoshida M, Tahvildari B, Giocomo LM, Hasselmo ME (2009) Evaluation of the oscillatory interference model of grid cell firing through analysis and measured period variance of some biological oscillators. *PLoS Comput. Biol.* 5.

Zugaro M, Moncondiut L, Buzsaki G (2005) Spike phase precession persists after transient intrahippocampal perturbation. *Nat. Neurosci.* 8:67–71.

Acknowledgements

I would like to take this opportunity to thank all the people that helped develop my thesis project in one way or another. First and foremost, I would like to thank Richard Kempter for his exemplary supervision and teachings. Among many other things, I learned from him the importance of clarity in science, putting students' needs first, and that computational neuroscience should be primarily about understanding biology and interpreting experiments. My two most important collaborators, Robert Schmidt and Tiziano D'Albis, played also a pivotal role in the development of my thesis project. It was an important learning experience to be supervised (by Robert) and to supervise (Tiziano).

I am lucky to have carried out my PhD in a pleasant environment at the ITB and the Bernstein Center for Computational Neuroscience (BCCN). This environment includes the staff, my colleagues, and the scientists of that community. I thank the principal investigators with whom I interacted the most for sharing their knowledge: Susanne Schreiber, Dietmar Schmitz, and Henning Sprekeler. I am also grateful to Hans-Peter Herzel and Peter Hammerstein for introducing me into their exciting fields of research and complementing my training in Neuroscience.

I would like to thank my officemates throughout these years: Jose, for introducing me to the concept of embodiment and the history of cognitive science; Nikolay, for our discussions about complexity in Neuroscience and in life; Martina, for her refreshing views on scientists and normal people; Paula for her help and advice, particularly during my first months at the ITB; Thomas, for helping me out with Linux, Latex, and other computer subtleties. I also thank all of my colleagues from ITB-Neuro (Katha, Janina, Owen, Simon, Roberta, Andre, DJ, Katia, Wei) and from Charite (Claudia, Prateeb, Tugba, Nikolaus) for their support, feedback, and for promoting a friendly atmosphere for our research.

The members of our famous "writing group" (Sinem, Fred, Gundula, Alex, Tomasso, and Joachim) deserve special recognition: thank you for your input, advice, and most of all for your friendship.

Scientific discussions formed an integral part of my development as a researcher. I was fortunate to engage in very interesting and deep discussions with many outstanding people from the Neuroscience community. I particularly would like to thank Matthijs van der Meer, Bruce McNaughton, Carl van Vreeswijk, as well as Farzad Farkooi, Jan H. Schleimer, and Michiel Remme for stimulating discussions and valuable advice for my career.

Many special thanks go to those who helped me get started on my thesis (Jan H. Schleimer) and/or gave me valuable feedback: Tiziano D'Albis, Michiel Remme, Jose Donoso, Fleur Lebhardt, Kay Thurley, and Eric Reifenstein.

Finally, I thank my family for continued support throughout my graduate studies in Germany, and Fleur Lebhardt for being a constant source of motivation.

Selbständigkeitserklärung

Ich erkläre, dass ich die vorliegende Arbeit selbständig und nur unter Verwendung der angegebenen Literatur und Hilfsmittel angefertigt habe. Die Dissertation ist in keinem früheren Promotionsverfahren angenommen oder als ungenügend beurteilt worden. Die dem angestrebten Verfahren zugrundeliegenden Promotionsordnung erkenne ich an.

Berlin, _____ _____

Jorge Jaramillo